Proteomics based approach to understand tissue regeneration

Starfish as a model organism

Catarina de Matos Ferraz Franco

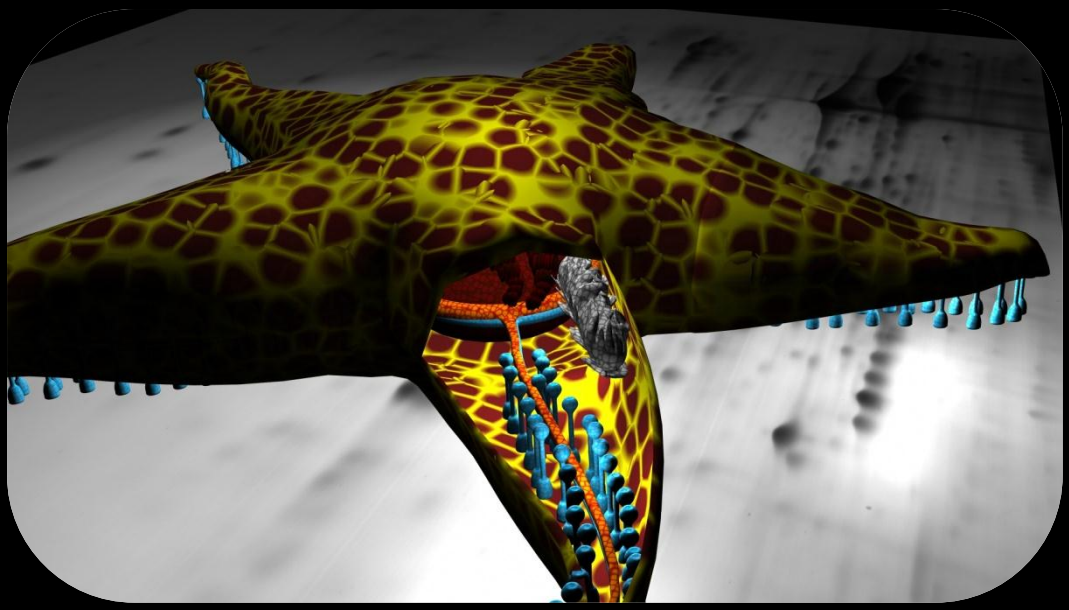

Dissertation presented to obtain the Ph.D degree in Biochemistry

Instituto de Tecnologia Química e Biológica | Universidade Nova de Lisboa

Oeiras,
October, 2011

INSTITUTO
DE TECNOLOGIA
QUÍMICA E BIOLÓGICA
/UNL

Knowledge Creation

Proteomics based approach to understand tissue regeneration

Starfish as a model organism

Catarina de Matos Ferraz Franco

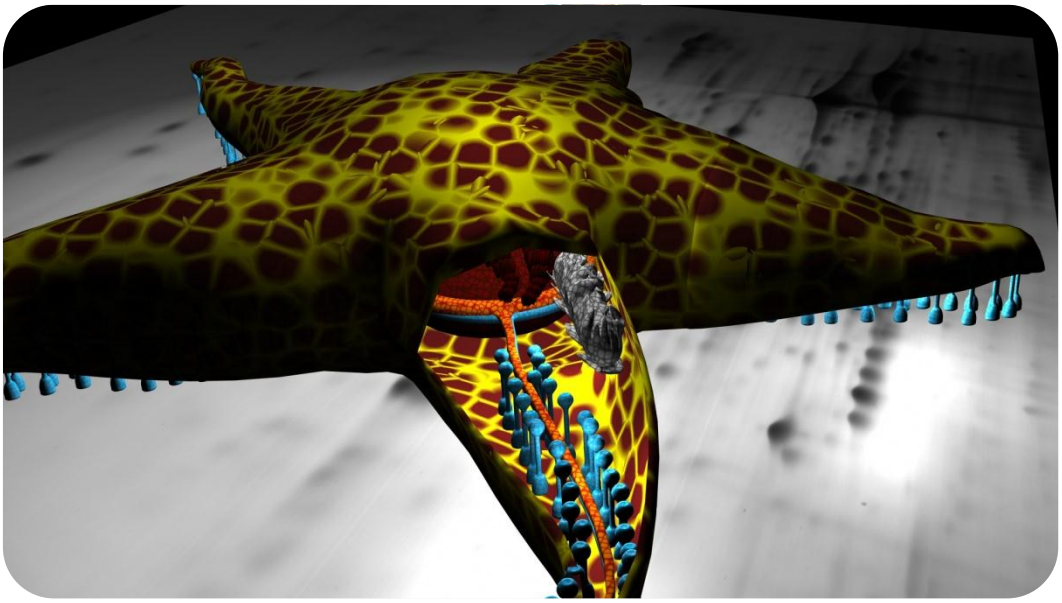

Cover Image: Illustration of the main goal of this thesis. Using proteomic-mass spectrometry approaches towards the characterization and quantification of the proteins expressed in starfish tissues under regeneration and normal conditions. This image was cover of Proteomics, Volume 11, Issue 7. Attribution: Starfish and Proteomics by Catarina Franco.

Dissertation presented to obtain the Ph.D. degree in Biochemistry

Instituto de Tecnologia Química e Biológica | Universidade Nova de Lisboa

Oeiras,
October, 2011

INSTITUTO
DE TECNOLOGIA
QUÍMICA E BIOLÓGICA
/UNL

Knowledge Creation

Proteomics based approach to understand tissue regeneration

Starfish as a model organism

Catarina de Matos Ferraz Franco

Dissertation presented to obtain the Ph.D. degree in Biochemistry

Instituto de Tecnologia Química e Biológica | Universidade Nova de Lisboa

Thesis supervisors: Dr. Ana Varela Coelho and Dr. Romana Santos

The research described in this thesis was performed at Laboratório de Espectrometria de Massa, Instituto de Tecnologia Química e Biológica – Universidade Nova de Lisboa, Oeiras, Portugal.
This work was supported by Fundação para a Ciência e Tecnologia (FCT) through a PhD grant to Catarina Franco (SFRH/BD/29799/2006), a project grant (PTDC/MAR/104058/2008) and through the National Re-equipment Program for "Rede Nacional de Espectrometria de Massa - RNEM" (REDE/1504/RNEM/2005).

Oeiras, Outubro, 2011

Acknowledgments

Agradecimentos

Aos meus pais…

Quadro original de Teresa Matos

Original painting by Teresa Matos

I would like to begin this thesis by the ***foremost important***, the acknowledgment statements, which unfortunately will not make justice to this group of ***V***ery ***I***mportant ***P***eople that have supported me in so very different ways throughout this period of my life and, in one or another way, have made possible the accomplishment of this thesis:

Professora Doutora Ana Varela Coelho

À Professora **Doutora Ana Varela Coelho**, pela orientação e partilha de conhecimentos científicos e amizade. Pela oportunidade de realizar o meu doutoramento numa área que me apaixona. Por toda a sua paciência nos momentos de desespero e por sempre ter acreditado em mim, mesmo durante esses instantes. Por todos estes anos de percurso partilhado, desde a minha licenciatura na Universidade de Évora (2000) até aos dias de hoje (2011), um Obrigado sentido.

Doutora Romana Santos

À **Doutora Romana Santos**, pela orientação e partilha de conhecimentos científicos, e acima de tudo, pela maravilhosa oportunidade de ter "entrado" no mundo dos equinodermes e na apaixonante procura científica do *biomemetismo*, que sem ela nunca teria sido possível embarcar em tamanha aventura. A todos os nossos momentos de cumplicidade e amizade… A todas as conversas e risotas… À palavra amiga em momentos de dúvida e tormento… A tua eterna disponibilidade especialmente nesta fase final de escrita… Obrigado *Ró*…

Dra. Elisabete Pires

À **Dra. Elisabete Pires**, por toda a partilha de conhecimentos na área da espectrometria de massa desde a minha chegada ao laboratório. Por todos aqueles bons momentos de "tem fuga aqui e ali" à frente do HPLC… Mas acima de tudo, Obrigado por todos os momentos que transcendem o passível de ser descrito… A todos as nossas conversas mudas ☺ … A todos os olhares e pensamentos partilhados… Por toda a tua amizade, sorriso e coisas "*axins"*…Obrigado *Beta*…

Doutora Renata Soares

À **Doutora Renata Soares**, por todas as conversas especulativas que, entre muitas outras, transformam as longas viagens diárias para o Laboratório em apetecíveis momentos sorridentes, os quais me fizeram muita falta durante este período de escrita. Obrigado também pelo derradeiro esforço de me leres a tese. Mas principalmente pela tua amizade, carinho, doçura e cumplicidade… Obrigado *Re*…

A todos os meus colegas de Laboratório

A todos aqueles com os quais me cruzei e partilhei caminho, **Gonçalo Costa**, **Gonçalo Graça**, **Marta Mendes**, **Patrícia Alves**, **Sérgio Mota**, **Elsa Lamy**, **Mariana Carvalho**, **Alexandre Campos**, **Duarte Toubarro**, **André Lopes**, **Catarina Pereira**, **Liisa Arike**, **Peter Boross**, **Angela Barreto**, **Sofia Rodrigues**, um grande Obrigado por todos esses momentos partilhados!

A todos aqueles que ainda partilham caminho comigo…Aos da velha guarda, **Elisabete Pires** (Beta), **Conceição Almeida** (Sãozinha); e aos mais recentes **Renata Soares**, **André Almeida**, **Kamila Koci**, **Miguel Ventosa**, **Rui Palhinhas**, **Isabel Marcelino**, **Luís Domingues** e **Joana Martins**… Venham mais aventuras ☺

Elementos de Comissão de Tese

Ao **Professor Mário Barbosa** e **Doutor Pedro Cruz** pelas críticas construtivas e ajuda no programa de trabalhos do meu Doutoramento.

Às Instituições que me apoiaram

Ao **Instituto de Tecnologia Química e Biológica – Universidade Nova de Lisboa**, a minha instituição de acolhimento por ter facultado todas as condições necessárias e indispensáveis à realização do meu Doutoramento. Quero agradecer também todo o apoio do ***ITQB Academics***, especialmente à **Doutora Ana Maria Portocarrero** e **Doutora Fátima Madeira** por toda a paciência com as questões que nos assombram, principalmente na última fase de preparação da tese.

À **Fundação pela Ciência e Tecnologia** (FCT) pelo financiamento da minha bolsa de Doutoramento (SFRH/BD/29799/2006) e projecto (PTDC/MAR/104058/2008) sem os quais seria impossível a concretização do trabalho experimental.

Ao **Aquário Vasco da Gama** pelas magníficas condições de acolhimento das estrelas-do-mar. Um especial agradecimento à **Doutora Fátima Gil** e ao **Miguel Cadete** por darem o apoio necessário à manutenção dos animais.

Doctor Patrick Croves

A special acknowledgment to **Doctor Patrick Croves** for the English abstract revision.

Professor Jens Coorssen

To **Professor Jens Coorssen** I would like to kindly acknowledge the scientific advises, the words of support and enthusiasm about my work, which were of tremendous influence during the last stage of my PhD program and that hopefully, will also have an impact in future projects.

Professor Peter Roepstorff

I would like also to acknowledge **Professor Peter Roepstorff** for the opportunity to be trained at his Laboratory in University of Southern Denmark and especially, for the opportunity to meet such a brilliant and enthusiastic scientific mind and a tremendously kind person that I deeply admire and respect.

A todos os meus Amigos

A todos os meus **Amigos**. Aos que estão presentes no meu dia-a-dia…E aos que guardo num lugar especial do meu coração…**Pedro**, **Isabel**, **Inês**…A todos, um Xi-coração bem apertado.

Um especial obrigado ao Jorge e Márcia pela dedicação e paciência durante a impressão da tese.

À minha família

À minha **Mãe** pelo seu amor incondicional, suas palavras sábias e conhecimentos de outros tempos. Ao meu **Pai** porque sempre me fez acreditar na irreverência e rebeldia. A ambos pelo exemplo de vida e pelo que sou hoje…Obrigado. A toda a minha família obrigado pelas partilhas maravilhosas. Á minha família mais recente, **Gentil**, **Miguel**, **Lourenço**, **"*Vovó*" Palmira**, **"*Vovô*" Santos**… Obrigado pelo constante carinho e preocupação. À **Célia** e ao **Luís** (ou Marisa e André) por me fazerem acreditar que "***Love is in the Air***"… À **Sarinha** e ao **Rosalvo**, que tornam o dia-a-dia uma alegria constante… "*Sabem quem perguntou por vocês?... Ninguém*…☺"… A todos vós, Obrigado…

Ao **Henrique** (*Enrik* ou *Lov*), por todos os momentos de incentivo a continuar a respirar, a relaxar e, a não desistir. Pelas apanhas de mexilhões. Por continuar a acreditar que vou conseguir. Por toda a paciência, principalmente durante o período da escrita da tese. E porque a minha *História* só faz sentido com a tua… Obrigado…

This thesis represents four years of research performed at the Mass Spectrometry Laboratory located in ITQB-UNL, Oeiras, under the supervision of Doutora Ana Varela Coelho and Doutora Romana Santos. The struggles and difficulties of starting a research project from scratch can only be equable with tremendous fun and rewarding experience that one takes advantage from, and that I was fortunate to be part of. With this as a common ground, I would like to use a citation of Professor Oliver Smithies, who won the Nobel Prize in Physiology or Medicine in 2007, and share his point of view about his thesis research, which involved the development of a new method for the measurement of osmotic pressures of protein mixtures:

"Here's my osmotic pressure measurement. And I was rather proud of this method. And I published it with great delight. This paper has a record, you know: nobody ever quoted it. And nobody ever used the method again. And I didn't use the method again. So I have to ask you, what was the point of it all? Well, the answer is really a very serious answer. The answer is I learned to do good science. But it didn't matter what I did when I was learning to do good science. So it doesn't matter what you do when you're doing a thesis, you see. But it's very important that you enjoy it. Because if you don't enjoy it, you won't do a good job and you won't learn science."

Oliver Smithies

Nobel Prize in Physiology or Medicine in 2007

Table of contents

The main objective of this thesis was to use proteomic and mass spectrometry tools to characterize the proteomes of starfish *Marthasterias glacialis* tissues, in particular the radial nerve cord, during arm tip regeneration events. Although the molecular knowledge on echinoderm regeneration potential is nowadays drastically increasing, so far, no proteomic studies were yet conducted. For this reason, this work was divided in two different specific objectives. A first that describes the **proteomes** of starfish tissues known to be involved in the regeneration processes and, a second that uses proteomic tools to identify molecular pathways actively involved in the regeneration of the radial nerve cord after arm-tip ablation.

In **Chapter 2** it is described the proteome of the starfish ***radial nerve cord*** *(RNC)*, a component of echinoderms nervous system, which like in many other regenerating species, has an important role in promoting and inducing regenerative responses, with the peculiarity that itself conserves the intrinsic growth capabilities during adult animal lifespan, allowing it to regenerate upon injury or autotomy of the starfish arms. The proteomes of the **coelomocytes**, also known as echinoderm blood cells, and the **cell free coelomic fluid,** which is the fluid that bathes the internal organs of the starfish, and hence is rich in secreted proteins, were also studied and are described in **Chapter 3**. Some of the results presented in these Chapters were already published in Proteomics (Franco *et al*., 2011A; Franco *et al*., 2011B) and the reprinted versions are presented in **Appendixes 1** and **2**. Two other manuscripts using the data presented in these chapters are under preparation, one that includes an expanded view of the radial nerve cord proteome, where the data collected using two different RNC subcellular fractions allowed to increase the number of the initially published RNC proteins (Franco *et al*., 2011A) to a total of 905 proteins. The second manuscript will include part of the data referring to the characterization of cell free coelomic fluid proteome.

To identify molecular pathways actively involved in the radial nerve cord regeneration process after arm-tip ablation, two different proteomic approaches were used. The first is based on difference gel electrophoresis (DIGE) approach which was conducted on two different radial nerve cord fractions, enriched in soluble and in membrane proteins, at three different time points post arm tip ablation (*PAA*), wound healing at 48h and 13days *PAA*; and tissue re-growth at 10 weeks *PAA*. The data collected from these experiments is described in **Chapter 4** and a manuscript is already prepared and will soon be submitted. Since the results obtained with this work pointed to the importance of post-translational modifications during the early events of arm tip regeneration, a preliminary characterization of protein phosphorylation was performed using a gel based approach and a specific phosphoprotein stain, described in **Chapter 5**. These results will also be included in another manuscript, as soon as validation is performed using the adequate tandem MS approaches for phosphorylation confirmation.

In the final chapter of this thesis, **Chapter 6**, an integrated discussion of all the results is presented together with suggestions for future experimental approaches aiming to increase the knowledge on echinoderms regenerative capabilities.

The list of **references** included in the final pages of this thesis refers to the cited literature in the general introduction (Chapter 1) and discussion (Chapter 6). The literature cited in each chapter is included in the respective reference section.

Please note that in the beginning of each chapter is presented a list of supplementary material that includes experimental data, protein lists or tables containing the results described. The **Supplementary material** can be found in the enclosed CD included in the back cover of this thesis.

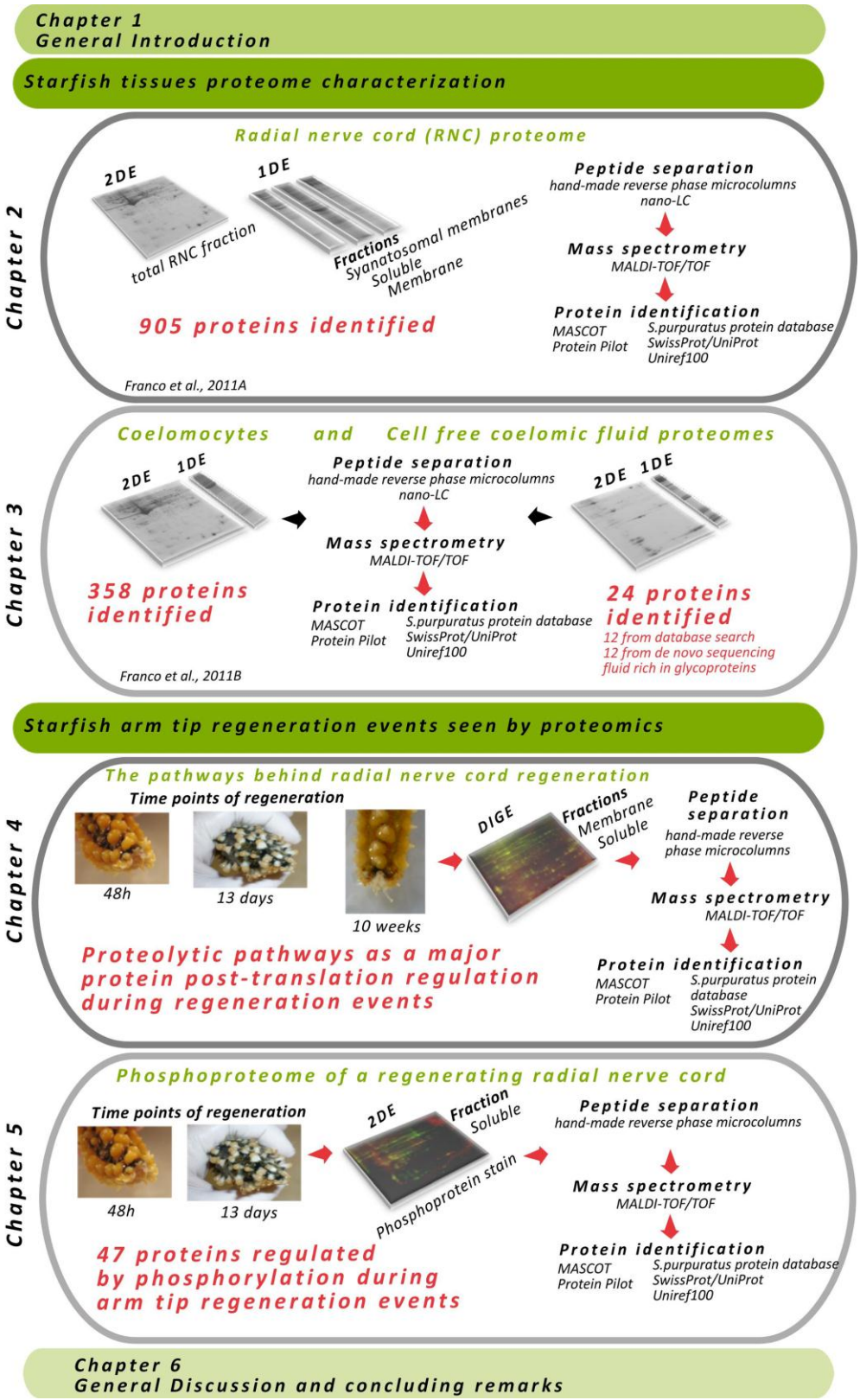
Chapter 1
General Introduction
Starfish tissues proteome characterization
Chapter 2
Radial nerve cord (RNC) proteome
2DE
1DE
total RNC fraction
Fractions
Syanatosomal membranes
Soluble
Membrane
905 proteins identified
Peptide separation
hand-made reverse phase microcolumns
nano-LC
Mass spectrometry
MALDI-TOF/TOF
Protein identification
MASCOT
Protein Pilot
S.purpuratus protein database
SwissProt/UniProt
Uniref100
Franco et al., 2011A
Chapter 3
Coelomocytes and Cell free coelomic fluid proteomes
2DE
1DE
358 proteins identified
Peptide separation
hand-made reverse phase microcolumns
nano-LC
Mass spectrometry
MALDI-TOF/TOF
Protein identification
MASCOT
Protein Pilot
S.purpuratus protein database
SwissProt/UniProt
Uniref100
24 proteins identified
12 from database search
12 from de novo sequencing
fluid rich in glycoproteins
Franco et al., 2011B
Starfish arm tip regeneration events seen by proteomics
Chapter 4
The pathways behind radial nerve cord regeneration
Time points of regeneration
48h
13 days
10 weeks
DIGE
Fractions
Membrane
Soluble
Peptide separation
hand-made reverse phase microcolumns
Mass spectrometry
MALDI-TOF/TOF
Protein identification
MASCOT
Protein Pilot
S.purpuratus protein database
SwissProt/UniProt
Uniref100
Proteolytic pathways as a major protein post-translation regulation during regeneration events
Chapter 5
Phosphoproteome of a regenerating radial nerve cord
Time points of regeneration
48h
13 days
2DE
Fraction
Soluble
Phosphoprotein stain
Peptide separation
hand-made reverse phase microcolumns
Mass spectrometry
MALDI-TOF/TOF
Protein identification
MASCOT
Protein Pilot
S.purpuratus protein database
SwissProt/UniProt
Uniref100
47 proteins regulated by phosphorylation during arm tip regeneration events
Chapter 6
General Discussion and concluding remarks

185/333	Family of proteins expressed in coelomocytes that seem to produce a pathogen-specific immune response
α-CHCA	α-ciano-4-hydroxy-trans-cinnamic acid)
1DE	One dimensional polyacrylamide gel electrophoresis
2DE	Two dimensional polyacrylamide gel electrophoresis
ADP	Adenosine diphosphate
AEBSF	4-(2-Aminoethyl) benzenesulfonyl fluoride hydrochloride
Alk3	Bone morphogenetic protein receptor
AP-1	Activating protein 1 (transcription factor)
AP-2	Activating Protein 2 (transcription factor)
APF	Autotomy-promoting factor
Arp2/3	Actin-related protein 2/3
ATP	Adenosine-5'-triphosphate
BMP	Bone morphogenetic protein
BP	Band pass emission filter
Ca^{2+}	Calcium ion
CaM	Calmodulin
CaMKII	Calmodulin-dependent protein kinase II
CCB	Colloidal Coomassie stain
Cdc42	Cell division control protein 42
cDNA	Complementary DNA
Cecr2	Cat eye syndrome critical region protein 2
CFF	Cell free coelomic fluid
CHAPS	3-[(3-cholamidopropyl)dimethylammonio]-1-propanesulfonate
CID	Collision induced dissociation
CAD	Collision assisted dissociation
CNS	Central nervous system
cra	Member of the ras oncogene family proteins
CSA2	Chonderosarcoma-associated protein 2
Cy2	Cyanine dye 2
Cy3	Cyanine dye 3
Cy5	Cyanine dye 5
CyDyes	Cyanine dyes
DIGE	Difference gel electrophoresis
DNA	Deoxyribonucleic acid
DRG	Dorsal root ganglion
DTE	Dithioerythritol
DTT	Dithiothreitol
ECM	Extra cellular matrix
EDTA	Ethylenediamine tetra acetic acid
EGF	Epidermal growth factor
EMT	Epithelial-mesenchymal transition
EN	Ectoneural nervous system
Erk	Extracellular-signal-regulated kinase
ESI	Electrospray ionization
ESTs	Expressed sequence tags
ETaR	Endothelin-A receptor
FAK	Focal adhesion kinase
FDR	False discovery rate
FGF	Fibroblast growth factor
GAPDH	Glyceraldehyde-3-phosphate dehydrogenase
GAPs	GTPase-activating proteins
GDNF	Glial-cell-line-derived neurotrophic factor
GDP	Guanosine diphosphate
GEFs	Guanine nucleotide exchange factors
Gf	Graphite
GGF	Glial growth factor
GO	Gene ontology
GSK3β	Glycogen-synthase kinase-3β

GSS	Gonad-stimulating substance
GTP	Guanosine triphosphate
GTPase	Guanosine triphosphate hydrolases
H/E(Spl)	Hairy/enhancer of split
HCl	Hydrochloric acid
HEPES	4-(2-hydroxyethyl)-1-piperazineethanesulfonic acid
HN	Hyponeural nervous system
Hsp	Heat-shock protein
IEF	Isoelectric focusing
IGF	Insulin growth factor
IgG	Immunoglobulin G
Il-6	Interleukin-6
ILK	Integrin-linked kinase
JAK	Janus kinase
JNK	C-Jun N-terminal kinase
K^+	Potassium ion
kazal1	Kazal-type serine protease inihibitor 1
kDa	Kilodalton
KLFs	Krueppel-like factors
Lef-1	Lymphoid enhancer-binding factor 1
LIMK	LIM kinase
LPS	Lipopolysaccharides
LuxR	Transcriptional regulator
M	Molecular mass
M	Membrane protein fraction
m/z	Mass-to-charge ratio
MALDI	Matrix-assisted laser desorption/ionization
MAP	Microtubule associated proteins
M_{apar}	Apparent molecular mass
MAPK	Mitogen-activated protein kinase
MASP	(Mannan binding lectin)-associated serine proteases
MBL	Mannan binding lectin
mDIA	Rho GTPase Effector Protein
MET	Mesenchymal-epithelial transition
MFs	Microfilaments
MLCK	Myosin light-chain kinase
MMPs	Matrix-metalloproteinases
M_{pred}	Predicted molecular mass
mRNA	Messenger RNA
MS	Mass spectrometry
MS/MS	Tandem mass spectrometry
Msx1	Msh homeobox 1
MUSK	Muscle-specific kinase
N_2	Molecular nitrogen
Na^+	Sodium ion
nano-LC	Nano flow high-performance liquid chromatography
NEC-2	Neuroendocrine convertase-2
NF-kB	Nuclear factor-κb
NGC	Biomaterial nerve guidance conduits
NGF	Nerve growth factor
NICD	Notch intracellular domain
Nogo	Neurite outgrowth inhibitor receptor
PAA	Post-arm tip ablation
PAK	Serine/Threonine protein kinases
PAR	Partitioning-defective protein family
PCA	Principal component analysis
PGE2	Prostaglandin E2
pI	Isoelectric point
PI3K	Phosphatidylinositol 3-kinase
PIWI	P-element induced wimpy testis
PKA	Protein kinase-A
PKB	Protein kinase-B

PKC	Protein kinase-C
PMF	Peptide mass fingerprint
Prdx	Peroxiredoxin
PTEN	Phosphatase and tensin homolog
PTM	Post-translational modification
Rab	Small GTPase member of the Ras superfamily
Rac	Small GTPase member of the Ras superfamily
Ras	Rat Sarcoma family proteins (small GTPase)
RG	Re-growth
RG RNC	Re-growing radial nerve cord
Rho	Small GTPase member of the Ras superfamily
RNC	Radial nerve cord
RNP	Ribonucleoprotein complexes
ROCK	Rho-associated protein kinase
ROS	Reactive oxygen species
RTK	Receptor tyrosine kinase family
S	Soluble protein fraction
SDS	Sodium dodecyl sulfate
Shh	Sonic hedgehog
SM	Synaptosomal membrane protein fraction
Smurf1	E3 ubiquitin-protein ligase encoding gene
Snail-1	Zinc finger protein SNAI1 (transcription factor)
Snail-2	Zinc finger protein SNAI2 (transcription factor)
SNAP-25	Synaptosomal-associated protein 25
SpBf	Echinoderm homologue gene to the factor B complement component
SpC3	Echinoderm homologue gene to the C3 complement component
SPEC 2C	*Strongylocentrotus purpuratus* calcium-binding protein 2C
SPINK	Pancreatic secretory trypsin inhibitor gene
STAT	Signal Transducer and Activator of Transcription
SUMO	Small Ubiquitin-like Modifier
TAK1	Tgfβ-activated kinase-1
TCA	Trichloroacetic acid
TGF-β	Transforming growth factor-beta superfamily
TOF	Time-of-flight
Trax	Translin-associated factor X
Tris	Tris(hydroxymethyl)aminomethane
tRNA	Transfer RNA
unc	Uncoordinated family member
UPS	Ubiquitin proteasome system
V	Volts
VAMP	Vesicle associated membrane proteins
VEGF	Vascular endothelial growth factor
VGIC	Voltage-gated ion channels
WASP	*Wiskott-Aldrich syndrome protein*
WAVE	*Wiskott-Aldrich syndrome protein (WASP) family verprolin-homologous protein*
WB	Western blot
WH	Wound healing
Zeb	Zinc finger E-box-binding homeobox 2

Abstract

Most echinoderm species share an outstanding capacity for regeneration that is maintained throughout the adult animal lifespan. Regeneration allows these deuterostomes to recover from predation injuries or self-induced arm autotomy, which are known to occur frequently in nature. Although echinoderms are extremely interesting in terms of their phylogenetic proximity to chordates, most areas of echinoderm research have been neglected in recent years. These wonderful animals quickly shifted from being the preferred animal models in the 19^{th}-20^{th} centuries of the pioneer *regenerationists* to scientific oblivion. Other species, for which the possibility of conducting genetic studies became available, are now favored. After the sequencing of an echinoderm species genome, the sea urchin *Strongylocentrotus purpuratus* in 2006, several scientific reports of interesting molecular studies were published. However, since echinoids are the echinoderm class with the least regenerative abilities, this genomic information did not significantly contribute to the field of echinoderm regeneration. Therefore, sequencing of the genomes of other echinoderm classes with high regenerative capabilities, such as crinoids, ophiuroids, asteroids and holothuroids, is still sought.

Even though a lack of genetic information for echinoderms is somewhat discouraging, there are still a set of experimental approaches with tremendous potential that can be applied in the field of echinoderm regeneration. For example, the latest understanding of axonal function and neuronal regeneration events, derived from several *in vitro* and *in vivo* models, highlights the importance of proteolysis, local protein synthesis and a broad range of protein post-translational modifications all occurring without the contribution of differential genome expression. Thus, understanding both normal neuronal function and neuronal regeneration has become a post-genomics problem whose answers rely on experimental approaches such as microarrays to measure mRNA levels, which enable the global quantification of gene expression. However, it is also true that mRNA levels often do not correlate well with protein abundance in the cell because protein levels are determined by complex post-transcriptional processes where every step in the life-cycle of a protein, from its synthesis to its degradation, is subjected to regulation. Two dimensional gel electrophoresis (2DE) allows the separation of the complete set of proteins expressed by a genome, also known as the proteome, isolating each protein in a single region of the gel according to molecular mass and isoelectric points, and whose protein amount can be quantified by densitometry. Mass spectrometry measures mass-to-charge ratios (*m/z*), yielding the information on the molecular mass and fragmentation patterns of peptides derived from proteins. Therefore, proteomic-mass spectrometry methodologies represent a general method for all modifications that change the molecular mass, such as protein post-translational modifications, which determine the protein's activity state, localization, turnover, and interactions with other proteins. Thus, these experimental approaches are more likely to reveal the most reliable and high resolution picture of the cellular molecular events.

Even though proteomic approaches have a promising nature towards characterizing and relative quantifying the proteins being expressed in echinoderm tissues, and more importantly in identifying the molecular pathways responsible for the success of echinoderm regeneration, such approaches have been rarely applied in the field of echinoderm biology. It is within this context that the main objective of this thesis is centered on *using a proteomic based approach to understand echinoderm regenerative potential*. *Marthasterias glacialis,* the common spiny starfish from the Portuguese coast was chosen as the model echinoderm species for the studies due to its remarkable regenerative capabilities. *M. glacialis* like other starfish (Echinodermata, Asteroidea), lacks a cephalic structure, having instead a pentamerous symmetry, with each arm being an anatomical replica of the others. In the case of predation or traumatic injury, the starfish releases the arm(s) by the autotomy plane, located at the base of the arm close to the central disc, and later regenerates a new arm together with all the lost internal organs. Like other starfish species, *M. glacialis* regenerative capabilities allows the survival and regeneration of a new individual if a fifth of the central disk remains attached to the lost arm. At the molecular level, this regeneration capability is

mainly a morphallactic process occurring in the absence of a blastema-like structure as the center of cell proliferation. This regenerative process is more complex and slow, and in *M. glacialis* it can vary from just 15 to 20 weeks to fully regenerate a lost arm tip, or up to several months in the case of an autotomized arm.

This thesis describes the proteomic characterization of the starfish radial nerve cord (Chapter 2). Even though these tissues were considered key drivers of the echinoderm regenerative process, until now, no such proteomic characterizations were performed. To characterize the starfish *Marthasterias glacialis* radial nerve cord (RNC) proteome, a tissue that has a direct contribution as a primary source of regulatory factors, mitogens or morphogens during regeneration, several RNC fractions were analyzed that were enriched in soluble, membrane and synaptosomal membrane proteins. For such characterizations, several proteomic approaches were used: two-dimensional gel electrophoresis (2DE), one-dimensional gel electrophoresis (1DE); an integrated mass spectrometry technique consisting of a set of reversed phase handmade microcolumns and nano flow high-performance liquid chromatography (nano-LC) for the separation of tryptic peptides, which were analyzed with a Matrix-Assisted Laser Desorption/Ionization – Time-of-Flight mass spectrometer (MALDI-TOF/TOF).This resulted in the identification of 905 proteins, validating many of the genes previously predicted to be expressed in the echinoderm nervous system through the analysis of the *Strongylocentrotus purpuratus* genome. Moreover, the identified proteins constitute the first high throughput proteomic evidence of a homology between the echinoderm nervous system and the dorsal nerve cord of chordates. Additionally, it is shown that neuronal transmission in echinoderms relies primarily on chemical synapses in similarity to the synaptic activity of the adult mammal's spinal cord. Several proteins involved in vesicle docking, priming and membrane fusion were identified such as the synaptosomal-associated protein 25 (SNAP-25) and synaptojanin-2-binding protein. Several identified voltage-gated ion channels (VGIC) permeable to potassium (K^+), sodium (Na^+) and calcium (Ca^{2+}), and the absent neuronal gap junctions corroborate the relatedness between the radial nerve cord of echinoderms and spinal cord of chordates, since the synaptic activity of adult mammal spinal cords relies essentially on chemical transmission.

The proteomic characterization both of the coelomocytes, the echinoderm immune cells, and the coelomic fluid, the fluid that bathes the internal organs of the starfish, are also presented in this thesis (Chapter 3). The echinoderm immune cells are known to participate in the immediate response to injury, the wound healing phase, mediation of clotting reactions and the prevention of the disruption of the internal fluid of the starfish. The 2DE/1DE nano-LC MALDI-TOF/TOF approach was also used to characterize the proteome of these cells resulting in the identification of 358 proteins, many of them constituting, to our knowledge, new assignments for echinoderm coelomocytes. The functions of the identified proteins are scrutinized and they highlight the complex and sophisticated pathways of echinoderms innate immune response that seems to rely on several clotting mediators, signaling and antibacterial proteins. The coelomic fluid proteome was characterized using the same set of proteomic approaches and is also described. It appears to be rich in glycoproteins that include a large number of lectin-like proteins, and proteins involved in antimicrobial defense such as a trypsin inhibitor, lysozyme and enolase.

After the characterization of the referred proteomes, the molecular pathways that trigger the amazing intrinsic regenerative ability that leads to a functional re-growth of the nervous system of the starfish *Marthasterias glacialis* were also studied (Chapter 4 and 5) after inducing regeneration by arm-tip amputation. Using a difference gel electrophoresis proteomic approach (DIGE) in combination with a complementary series of gels with different ranges of isoelectric points and two different subcellular nerve fractions, 528 proteins showed an injury correlated variation across the different assay time points of starfish arm-tip regeneration events: wound healing at 48h and 13 days post-arm tip ablation (*PAA*), and radial nerve cord tissue re-growth at 10 weeks *PAA* (Chapter 4). The obtained results indicate that proteolytic pathways modulate the majority of the regenerating RNC resolved proteomes. These proteolytic pathways clearly stand out as major protein post-translation regulator events that modulate protein amounts in specific axonal regions, hence spatially controlling protein functions, affecting cytoskeleton and microtubule regulators, axon guidance molecules and growth cone modulators, protein *de novo*

synthesis machinery, RNA binding and transport, transcription factors, kinases, lipid signaling effectors and proteins with neuroprotective functions. These pathways might also generate positive injury signals through highly regulated proteolytic processes that eventually engage neuronal retrograde transport towards the nucleus, where they mediate the appropriate gene expression modulation. Several signaling proteins were up-regulated, including several small GTPases known to be involved in axon regeneration events in other model organisms and the mediation of several regenerative responses, namely the growth cone cytoskeleton dynamic remodeling. In addition, the high number of proteins identified with an apparent molecular mass above expected suggests functional modulation further induced by post-translational modifications such as conjugation with ubiquitin-like molecules (i.e., SUMO).

Since several references highlight the importance of protein phosphorylation in the early regenerative responses, we also describe a preliminary injury phosphoproteome characterization (Chapter 5). Using a gel based approach and a specific phosphoprotein fluorescent stain, 47 proteins showed injury related phosphorylation dynamics during starfish radial nerve cord wound healing. The results presented in this chapter confirm several of the previously described pathways, which seem to be regulated through phosphorylation and dephosphorylation events. These include cytoskeleton re-organization towards the formation of the neuronal growth cones; membrane rearrangements; actin filaments and microtubule dynamics; mRNA binding and transport; lipid signaling; Notch pathway; calcium activated pathways regulated through calmodulin binding and neuropeptide processing, among others.

The work presented in this thesis hopefully will contribute to an increase in the available molecular knowledge on the echinoderm's amazing regeneration abilities. This set of valuable information should be seen as ground-work for future hypotheses to be tested, a subject that is also speculated in the final chapter of this thesis (Chapter 6). More importantly, I strongly believe that echinoderms can definitely provide us with important missing links that will be a promising way to understand the molecular mechanisms involved in regeneration, which can then be transposed to find regeneration targets to be studied in other organisms, in particular in animals that do not share the same regenerative abilities, namely mammals.

A maioria das espécies de equinodermes possui uma notável capacidade de regeneração, que é mantida durante toda a vida adulta dos animais, permitindo a estes deuterostómios a completa recuperação de lesões provocadas por predação, ou mesmo auto-induzidas, tal como a autotomia do braço, um processo frequentemente observado na natureza. Apesar dos equinodermes estarem filogeneticamente próximos dos cordados, poucos são os estudos recentes com equinodermes em várias áreas de investigação, tendo estes passado de animais modelo em estudos pioneiros na área da regeneração nos séculos XIX e XX, ao esquecimento científico a favor de espécies que se tornaram mais cedo objecto de estudos genéticos.

Com a sequenciação do genoma de uma espécie de ouriço-do-mar em 2006, *Strongylocentrotus purpuratus*, foram publicados vários estudos moleculares em equinodermes. No entanto, uma vez que os equinóides representam a classe de equinodermes com menor capacidade regenerativa, esta informação não foi suficiente para colmatar a falta de estudos moleculares na área da regeneração. Para tal será necessário sequenciar o genoma de representantes de outras classes de equinodermes com maiores capacidades de regeneração, tais como crinoídes, ofiuroídes, asteróides e holoturióides.

No entanto, além da falta de informação ao nível genético, é necessário recorrer a um conjunto de abordagens experimentais mais dirigidas aos produtos de expressão e com potencial para estudar a regeneração nos equinodermes. Por exemplo, estudos recentes sobre a função axonal e eventos de regeneração neuronal destacam a importância da proteólise, síntese local de proteínas, e uma ampla gama de alterações pós-tradução que não reflectem o conteúdo do património genético. Assim, hoje em dia começa a tornar-se evidente que o estudo da função neuronal normal e em regeneração deve ser abordado com recurso a estratégias experimentais pós-genómicas, tais como o uso de **microarrays**, que permitem uma quantificação total da expressão genética. No entanto, sabe-se que os níveis de ARNm não são necessariamente correlacionáveis com a abundância das proteínas na célula, uma vez que estes níveis são muitas vezes regulados por processos de pós-tradução complexos que afectam as diversas etapas do ciclo de vida de uma proteína, desde a sua síntese à sua degradação. A **electroforese bidimensional em gel** (2DE) é uma das técnicas de proteómica mais coesas e robustas, que permite separar as proteínas expressas a partir de um genoma, **o proteoma**. Através desta técnica cada proteína é isolada de acordo com o seu ponto isoeléctrico e massa molecular, ficando concentrada numa região específica de um gel de poliacrilamida, designado por *spot*, e cuja quantidade é mensurável. A **espectrometria de massa** permite calcular valor do rácio entre a massa e carga dos péptidos gerados após a digestão da proteína. Esta informação conjuntamente com o padrão de fragmentação dos mesmos permite identificar a proteína inicialmente isolada por 2DE. Como tal, as técnicas de proteómica-espectrometria de massa representam um método geral para analisar todas as modificações que possam alterar a massa molecular das proteínas, tais como as alterações pós-tradução, que regulam a estado activo de uma proteína, a sua localização, *turnover*, e possíveis interacções com outras proteínas. Por este motivo, estas abordagens experimentais têm o potencial de revelar uma imagem mais fidedigna dos eventos celulares relacionados com a regeneração.

Curiosamente, apesar da natureza promissora desta abordagem para caracterizar e quantificar níveis de expressão proteica nos tecidos dos equinodermes, e mais importante, para identificar as vias moleculares responsáveis pelo sucesso da regeneração dos equinodermes, poucas são as publicações em que a proteómica ou a espectrometria de massa foram aplicadas a estes animais. É neste contexto que se insere o objectivo principal desta tese: usar uma abordagem de proteómica conjugada com a espectrometria de massa para iniciar a compreensão dos mecanismos moleculares responsáveis pelo potencial regenerativo dos equinodermes. A estrela-do-mar *Marthasterias glacialis*, conhecida como estrela-do-mar espinhosa é uma das espécies mais abundantes da costa Portuguesa tendo sito seleccionada como equinoderme modelo para os estudos a realizar devido à sua magnífica capacidade de regeneração. A *M. glacialis,* tal como outras espécies de estrelas-do-mar (Equinodermata,

Asteroidea), não possui uma região cefálica evidenciada apresentando uma simetria pentarradial em que todos os braços são réplicas anatómicas uns dos outros. Numa situação de predação, a estrela-do-mar liberta o braço pelo plano de autotomia localizado perto disco central, regenerando novamente o braço perdido bem como todos os tecidos que o constituem. As capacidades de regeneração desta espécie permitem a sobrevivência e regeneração de um individuo novo, no entanto é necessário que um quinto do disco central se mantenha ligado ao braço perdido. A um nível molecular, esta capacidade de regeneração é maioritariamente um processo morfaláctico ocorrendo na ausência de um *blastema* como centro da proliferação celular. Este processo celular é mais complexo e demorado e na *M. glacialis* pode demorar cerca de 15 a 20 semanas para regenerar completamente a ponta de um braço, ou até vários meses no caso da regeneração completa de um novo braço.

Numa fase inicial do trabalho realizou-se a caracterização dos proteomas de tecidos da estrela-do-mar *Marthasterias glacialis*, nomeadamente do nervo radial (**Capitulo 2**), coelomócitos e do fluido celómico (**Capitulo 3**). A escolha destes tecidos foi fundamentada na relevância do papel que desempenham na indução e promoção das respostas regenerativas, e pelo facto de até à data nenhuma caracterização proteómica destes tecidos tinha sido realizada.

Para caracterizar o proteoma do nervo radial da estrela-do-mar, foram analisadas várias fracções deste tecido, nomeadamente, enriquecidas em proteínas solúveis, membranares ou provenientes de membranas sinaptossomais. Para tal, foram utilizadas diversas abordagens experimentais de proteómica, designadamente, electroforese bidimensional (2DE), electroforese unidimensional (1DE), e separação de péptidos trípticos usando um conjunto de microcolunas artesanais de fase reversa bem como nano-LC, com posterior identificação dos mesmos por MALDI-TOF/TOF. Esta estratégia permitiu identificar 905 proteínas, que validaram muitos dos genes já previstos através da análise do genoma do ouriço-do-mar, *Strongylocentrotus purpuratus*. Para além disto, o conjunto das proteínas identificadas demonstram que o sistema nervoso dos equinodermes depende essencialmente de sinapses químicas, possuindo uma elevada homologia com a espinal medula dos mamíferos. Esta hipótese é fundamentada pela identificação de diversas proteínas envolvidas no processo de fusão de vesículas membranares tais como, a proteína 25 associada a sinaptossomas (SNAP-25), a proteína que se liga à sinaptojamina-2; e ainda diversas proteínas que pertencem à família dos canais iónicos dependentes de voltagem (VGIC) permeáveis ao potássio (K^+), sódio (Na^+) e cálcio (Ca^{2+}). Coincidentemente, a ausência da identificação de proteínas de junções neuronais que parece validar a semelhança do nervo radial com a espinal medula.

Nesta tese é também apresentada a caracterização do proteoma dos coelomócitos, células envolvidas no sistema imunitário dos equinodermes, bem como a do fluido celómico, líquido que banha a cavidade interna do corpo da estrela-do-mar (**Capitulo 3**). Sabe-se que os coelomócitos têm um papel fundamental no processo de cicatrização, mediando reacções de aglomeração e prevenindo a saída do fluido celómico por forma a manter a homeostasia. Para caracterizar o proteoma destas células foi também usada uma abordagem 1DE/2DE e nano-LC MALDI-TOF/TOF que resultou na identificação de 358 proteínas, muitas delas nunca antes atribuídas aos coelomócitos. As funções das proteínas aqui identificadas são discutidas com base nas diversas funções executadas por estas células, detalhando sobre diversas proteínas que participam em vias de sinalização, mediadoras de reacções de aglutinação celular e acção antibacteriana. O proteoma do fluido celómico foi também caracterizado, visto que este é bastante rico em factores secretados pelos coelomócitos e tecidos circundantes. De facto, demonstrou-se ser rico em diversas proteínas semelhantes a lectinas bem como diversas proteínas com função anti-microbiana tais como a lisozima, enolase e um inibidor de tripsina.

Após caracterização dos referidos proteomas, foram estudadas as vias moleculares que desencadeiam a incrível capacidade intrínseca de regeneração dos equinodermes, nomeadamente, as vias envolvidas na regeneração funcional do sistema nervoso da estrela-do-mar *M. glacialis* (**Capítulos 4 e 5**). Para tal a regeneração foi induzida através de amputação da ponta do braço da estrela-do-mar. Foi usada uma abordagem de proteómica

diferencial por electroforese em gel (DIGE), combinando uma série de géis com várias gamas complementares de pontos isoeléctricos, e duas fracções subcelulares do nervo. Os resultados obtidos permitiram correlacionar a variação de cerca de 528 proteínas com vários tempos pós-amputação da ponta do braço da estrela-do-mar. Os tempos seleccionados para o estudo incluem o processo de cicatrização, correspondendo a tecidos recolhidos 48h e 13 dias após a amputação e, regeneração funcional do tecido neuronal, correspondendo à recolha dos mesmos tecidos 10 semanas após amputação (**Capítulo 4**). Os resultados obtidos indicam que as vias de proteólise parecem afectar a maioria do proteoma resolvido, destacando-se claramente como as principais vias de regulação pós-tradução. Estas vias permitem eventualmente a regulação das quantidades de algumas proteínas em regiões específicas dos neurónios, permitindo a regulação espacial das funções das mesmas. As várias proteínas moduladas por proteólise são intervenientes de diversas vias das quais se destacam: regulação do citoesqueleto e microtúbulos, moléculas que orientam o crescimento dos axónios, maquinaria de síntese *de novo* de proteínas, proteínas que se ligam e transportam RNA, factores de transcrição, cinases, e proteínas com funções de neuroprotecção. Outra hipótese para a função das vias de proteólise está relacionada com a produção de sinais de lesão positivos, através de um processo altamente regulado de proteólise, que eventualmente gera fragmentos que ingressam nos sistemas de transporte neuronal retrógrado até ao núcleo, onde posteriormente irão modular a resposta regenerativa adequada. Foram também identificadas várias proteínas com funções de sinalização estando presentes em maiores quantidades no nervo a regenerar, tais como as hidrolases de trifosfato de guanosina (*GTPases*), que se sabem estar envolvidas no processo de regeneração neuronal de outros animais modelo. Além disso, o elevado número de proteínas identificadas com uma massa molecular acima do esperado, sugere modulação funcional induzida por outras modificações pós-tradução tais como a conjugação com moléculas semelhantes à ubiquitina (tais como SUMO).

Uma vez que são várias as referências que também destacam a importância da fosforilação de proteínas nas fases iniciais de regeneração, também se efectuou uma caracterização preliminar do fosfoproteoma associado à fase de cicatrização do nervo radial da estrela-do-mar e que se encontra descrito no **Capitulo 5**. Para a tal foi utilizada uma abordagem baseada em 2DE em combinação com um fluoróforo específico para fosfoproteínas. No total cerca de 47 proteínas demonstraram ser reguladas por fosforilação durante o processo de cicatrização do nervo radial da estrela-do-mar. Muitos dos resultados apresentados neste capítulo confirmam várias das hipóteses descritas no capítulo anterior. Nestas incluem-se vias de regulação do citoesqueleto do cone de crescimento neuronal, regulação da polimerização/despolimerização da actina e microtúbulos, proteínas que se ligam e transportam RNAm; via Notch, vias de sinalização activadas por cálcio entre outras, e que parecem estar também a ser reguladas por eventos de fosforilação/desfosforilação.

Pretende-se que os resultados da presente tese possam ter contribuído para um aumento do conhecimento sobre a capacidade de regeneração dos equinodermes. Mais importante, este conjunto de resultados devem ser vistos como um impulso para testar futuras hipóteses, também estas discutidas no último capítulo desta tese (**Capítulo 6**).

Resumindo, acredito fortemente que a investigação da capacidade de regeneração dos equinodermes nos pode fornecer pistas importantes que ajudarão a compreender melhor os mecanismos moleculares envolvidos na regeneração, conhecimentos estes que poderão ser transpostos para outros organismos que não possuem as mesmas capacidades de regeneração, de forma a tentar encontrar alvos passíveis de manipulação.

CHAPTER 1

GENERAL INTRODUCTION

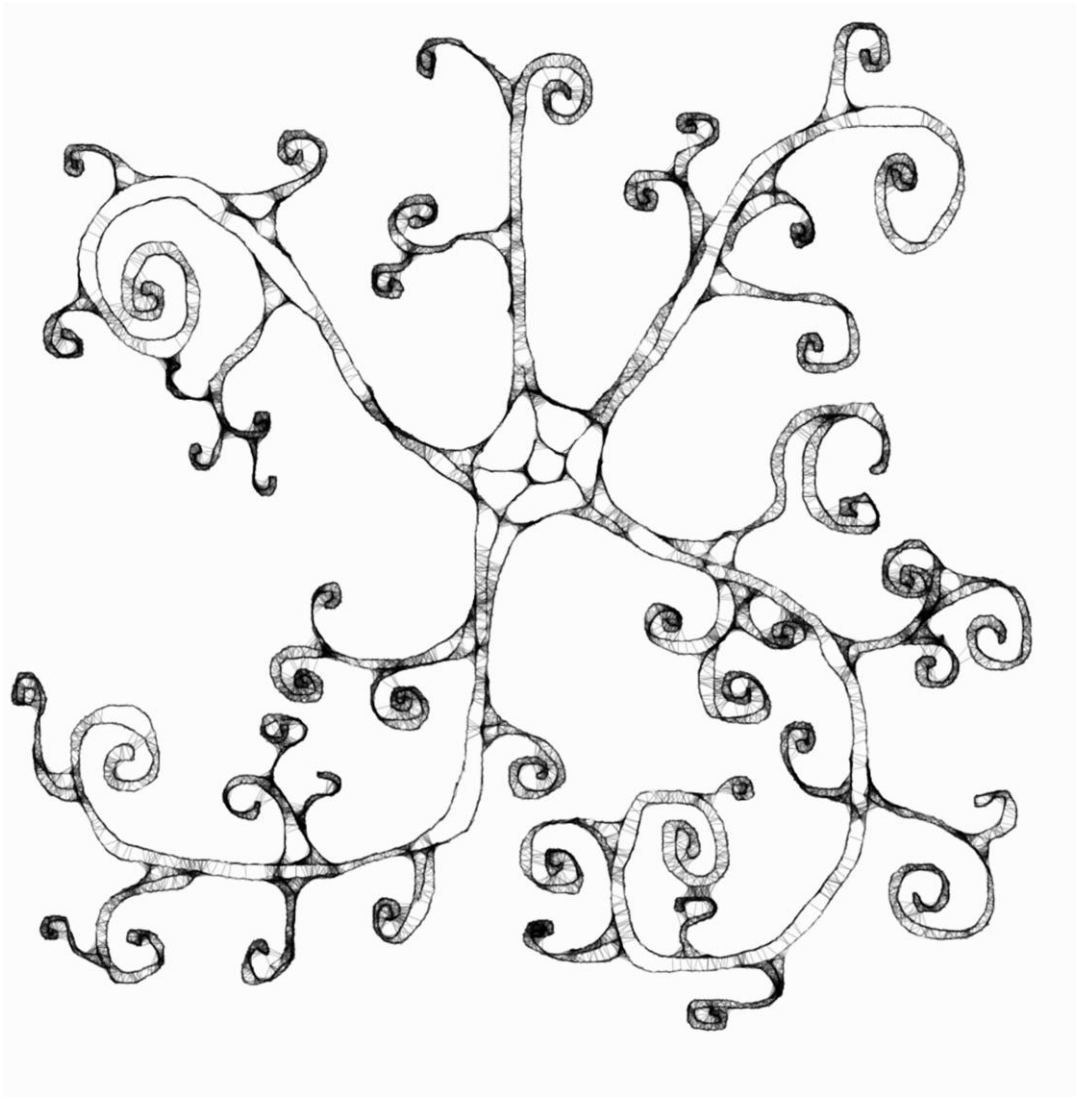

Image: Interpretation of an ophiuroid specie – Euryalina.

"If there were no regeneration there could be no life. If everything regenerated there would be no death. All organisms exist between these two extremes."

Richard Goss (1969)

1.1. The concept of regeneration

The ability of certain animals to regenerate parts of their bodies after loss or injury has long fascinated biologists. Regeneration is a complex cellular process in that, rather than simply forming a scar following injury, the animal forms a new tissue that is very similar to the injured or missing body part. This may involve a set of several different mechanisms, which ultimately will lead to the regrowth or repair of cells, tissues and organs. Regenerative strategies include the **rearrangement of the pre-existing tissue**, the use of **adult somatic stem cells** and **dedifferentiation** (Figure 1.1). The latter involves the processes by which a terminally differentiated cell loses its tissue-specific characteristics and becomes undifferentiated, then, these cells can either re-differentiate into cells of their original type and/or, re-differentiate into cells from a different lineage, also known as **transdifferentiation**.

One of the most elusive questions in regeneration is "where do cells that participate in regeneration come from?" This question can be answered using two distinct types of approaches. The **topographic approach**[1], that describes the physical **localization** of the origin of cells participating in regeneration, which can originate either

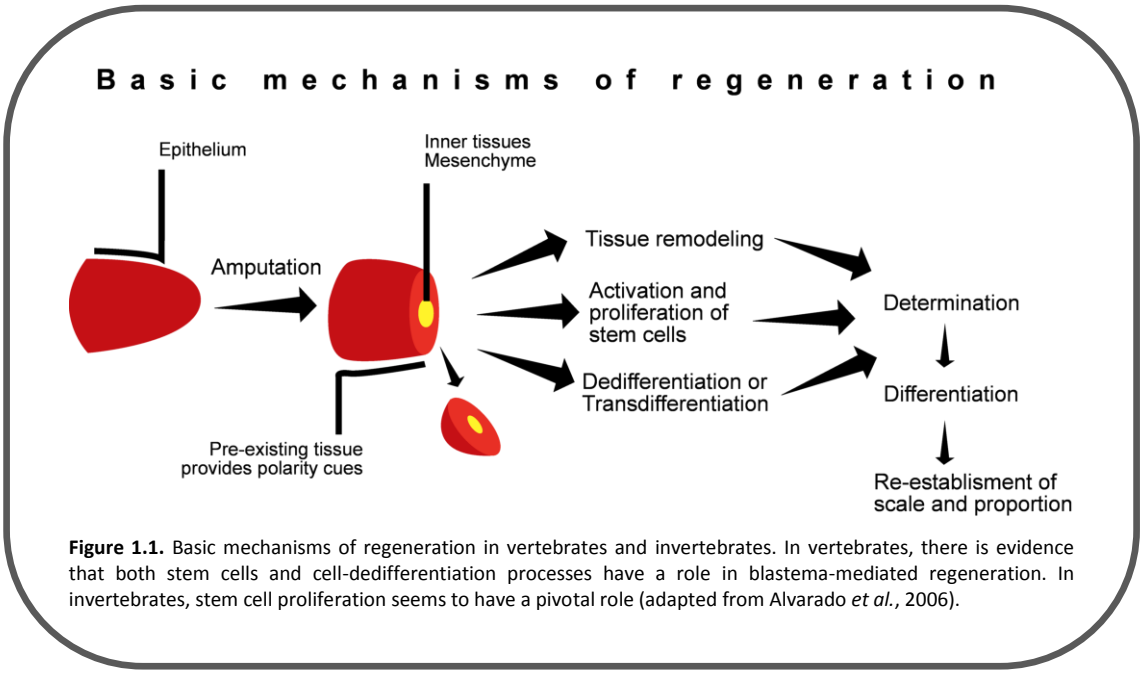

Figure 1.1. Basic mechanisms of regeneration in vertebrates and invertebrates. In vertebrates, there is evidence that both stem cells and cell-dedifferentiation processes have a role in blastema-mediated regeneration. In invertebrates, stem cell proliferation seems to have a pivotal role (adapted from Alvarado *et al.*, 2006).

[1] According to the **topographic approach** the cells responsible for amphibian limb regeneration have a local origin in the vicinity of the plane of amputation; in planaria, the migrating cells that participate in the blastema have a more distant origin; and in liver, the mitotically active cells are not located at the wound surface, but rather scattered throughout the remainder of the body.

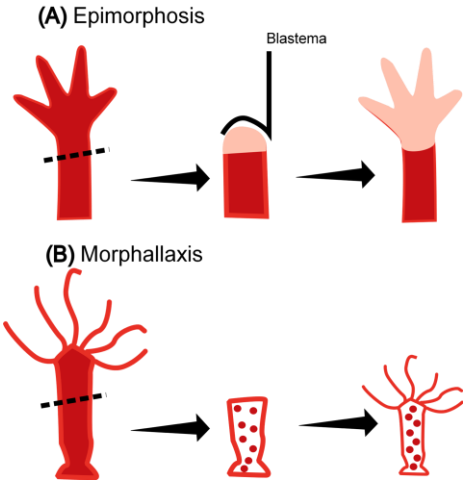

Figure 1.2. Classical examples of regeneration. **(A)** Limb regeneration in amphibians is a representative example of epimorphosis where a mass of undifferentiated cells (blastema) is initially formed after wound healing. These blastema cells then actively proliferate to restore the lost part of the amputated organ. **(B)** Hydra regeneration is categorized as morphallaxis, since there is no blastema; regeneration derives from the direct rearrangement of pre-existing cells in the stump. (adapted from Agata *et al.*, 2007)

locally at the site of damage (amphibian limb regeneration), or from a more distant region (bone marrow-derived stem cells mediated regeneration). The second and more specific approach, describes the **cellular precursors** of regenerating tissues, such as **(1)** dedifferentiation of mature tissue cells to produce immature-like cells which will participate in the regenerative process. In some cases these cells might form cells of a phenotype different from that of the original cells or tissues (transdifferentiation), **(2)** proliferation of the remaining parenchymal cells without dedifferentiation, **(3)** proliferation of stem (progenitor) cells resident in the injured tissue, and **(4)** influx of stem cells originating outside the damaged tissue (Carlson, 2007).

The different variations of regeneration include:

1) **Physiological regeneration**, the natural replacement of extruded or worn-out body parts such as the replacement of blood cells, bone marrow and intestinal mucosa in mammals;

2) **Hypertrophy**, a capacity shared by some internal organs such as the kidneys or liver. In case of tissue removal these organs increase their mass in response to increased functional demand without however, restoration of the initial external form.

3) **Asexual reproduction,** such as fission, can also be seen as a form of regeneration, characterized by the natural subdivision of a single body into one or more parts and, the reorganization of each of the parts into a complete individual.

4) **Reparative regeneration**, the replacement of a **lost** or **damaged** part of the body and can occur at levels from the single cell to major parts of the body such as, the regeneration of the amputated limb or tail of a salamander or, the reconstitution of the entire body of a planarian from a fragment less than 1/200 of the original mass.

Among the several strategies of regeneration, it is the reparative regeneration that has captured more attention in the scientific community due to its promising impact to regenerative medicine (Ambrosio *et al.*, 2010).

For more than a century, and still persisting nowadays, reparative regeneration has been defined as either being an **epimorphic** or **morphallactic** process**,** according to whether or not a blastema is formed after wound healing (Figure 1.2). The concept of **epimorphic regeneration**, was first coined by Thomas Hunt Morgan (1901), and it is characterized by the formation of a blastema that arises through epithelial mesenchymal interactions which contains and expresses intrinsic morphogenetic information.

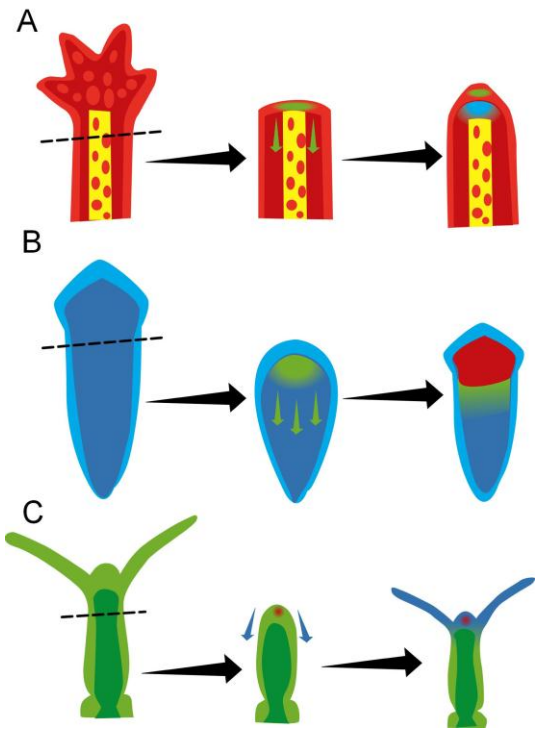

Figure 1.3: Three different regeneration events based on the distalization followed by intercalation concept (**A**, urodeles limb; **B**, planarian; **C**, hydra). In all cases, the most distal portion is formed immediately after amputation (indicated in green in A and B and in red in C) and then intercalary events induce the formation of the intermediate region between the newly formed distal portion and the old proximal portion (green arrows in A and B and blue arrows in C). (adapted from Agata *et al.*, 2007).

According to more recent studies using specific cell markers (Umesono *et al.*, 1997; Agata *et al.*, 1998; Kobayashi *et al.*, 1998; Shibata *et al.*, 1999; Cebrià *et al.*, 2002) and fluorescence activated cell sorter (Ogawa *et al.*, 2002; Hayashi *et al.*, 2006), Agata and colleagues defend that the regeneration phenomena should be reinvestigated at the cellular level and that the classical categories of regeneration must be reconsidered (Agata *et al.*, 2007). These authors suggest that the current categorization leads to a misunderstanding of regeneration, since it might imply that regeneration in different animals may be controlled by different principles, and more importantly, since regeneration cannot actually be divided into these categories. Also according to Agata *et al*., a theory that unifies the concept of regeneration is sought, and it is suggested that it might rely on concepts such as "distalization" and "intercalation" since all processes are governed by the control of positional information (Agata *et al.*, 2007). In summary, the distal portion of the body is formed immediately after wound healing around the cut surface, a step called **distalization**, and interaction of the newly formed distal portion and the remaining proximal portion may induce reorganization of positional information and lost tissues are then intercalatively generated to restore the original structures, **intercalation** (Figure 1.3). Such concept describes regeneration events from invertebrates to vertebrates. However, the **tissues** acquiring distal characteristics and **cells** participating in the regeneration of lost tissues **vary** among **different animals** and **different regeneration systems.**

1.2. Molecules and pathways that organize cells

Multicellular organisms exist in one of the two types of cellular arrangements, **epithelial** or **mesenchymal**. Epithelial–mesenchymal transition is an indispensable mechanism during **morphogenesis**, as without mesenchymal cells, tissues and organs will never be formed (Thiery *et al.*, 2006). The interactions that govern such conversions, **epithelial-mesenchymal transition, EMT** or the opposite **mesenchymal-epithelial transition, MET** (Figure 1.4); are processes that are central to many aspects of **embryonic morphogenesis** and **adult tissue repair**, as well as a number of **diseases** such as cancer (Baum *et al.*, 2008). To understand cellular interactions and subsequent molecular pathways that govern such shifts during regenerative processes would be most useful, since they may be in the basis of failed regenerative processes such as the origin of cells that contribute to fibrotic tissue scarring (epithelial or otherwise) (Margadant *et al.*, 2010) creating an environment not permissive for regeneration to occur. Such cellular conversions require the coordinated changes of many families of molecules that govern **cell-cell adhesion**, **cellular polarity**, and **invasive cell motility**.

1.2.1. Changes in cell-cell adhesion: Cadherin switching

In order for an epithelial sheet to produce individual mesenchymal cells, cell-cell adhesions (adherens junctions, desmosomes, and tight junctions) that are localized in the lateral domain near the apical surface and establish the apical polarity of the epithelium, must be disrupted. The principal transmembrane proteins that mediate cell-cell adhesions are members of the **cadherin superfamily** (Stepniak *et al.*, 2009). **E-cadherin** and **N-cadherin** interact through their extracellular IgG domains with cadherins-like molecules on adjacent cells. One of the characteristics of EMT is the "cadherin switching", in which often the epithelia that express E-cadherin will downregulate its expression, and express different cadherins, such as N-cadherin (Christofori *et al.*, 2003) thus, promoting motility. However, cadherin switching is not sufficient to bring about a complete EMT alone (Maeda *et al.*, 2005). Cadherin expression and function are regulated through a number of transcription factors that are central to most EMTs, such as **Snail-1**, **Snail-2**, **Zeb1**, **Zeb2**, **Twist**, and **E2A** (de Craene, 2005). At the post-transcription level, the E-cadherin protein is ubiquitinated by the E3-ligase, which targets **E-cadherin to the proteasome** (Fujita *et al.*, 2002). Its turnover at the membrane is regulated by either caveolae-dependent endocytosis or clathrin dependent endocytosis (Bryant, 2004), and p120-catenin prevents endocytosis of E-cadherin at the membrane (Xiao *et al.*, 2007). E-cadherin function can also be disrupted by **matrix metalloproteases**, which degrade its extracellular domain (Egeblad *et al.*, 2002). Some or all of these mechanisms may occur during an EMT to disrupt cell-cell adhesion.

1.2.2. Changes in the cell-ECM adhesion

Cell-ECM adhesion is mediated principally by **integrins**, which are transmembrane proteins composed of two non-covalently linked subunits, α and β, which bind to ECM components such as **fibronectin**, **laminin**, and **collagen**. The cytoplasmic domain of integrins can also link to the cytoskeleton and interact with intracellular signaling molecules. Altering the way that a cell interacts with the ECM is determinant in EMTs, however, the miss-expression of integrin subunits is not sufficient for a successful EMT *in vitro* or *in vivo* (Valles *et al.*, 1996; Carroll *et al.*, 1998). Most integrins can cycle between high and low affinity states, governed at integrin cytoplasmic tail (Hood *et al.*, 2002). In addition to integrin activation, the "clustering" of integrins on the cell surface also affects the overall strength of integrin-ECM interactions, a process known as **avidity**, which can be activated by **chemokines**, and is dependent on **RhoA** and **phosphatidylinositol 3' kinase** (PI3K) activity (Hood *et al.*, 2002).

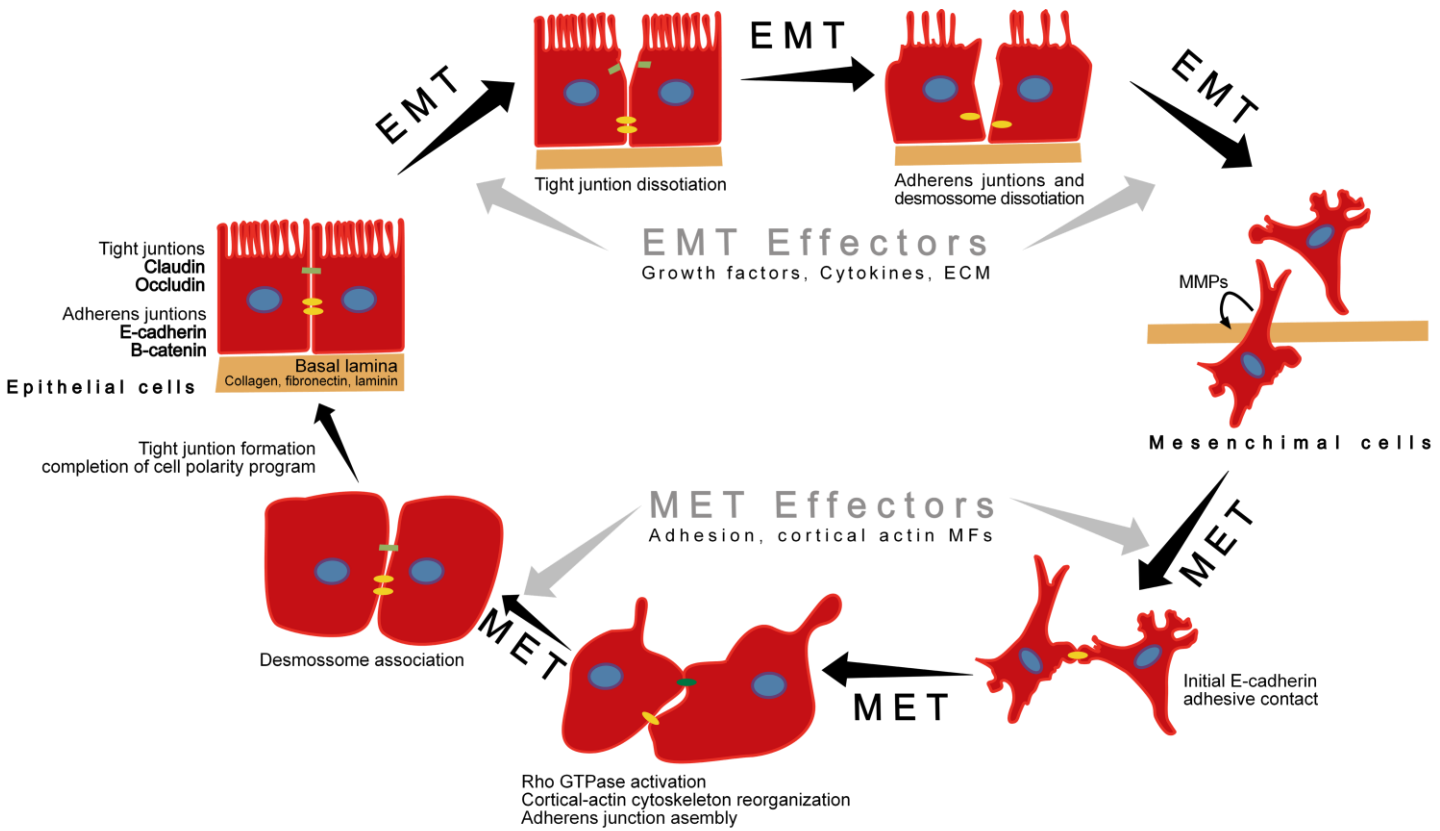

Figure 1.4. The cycle of epithelial-mesenchymal transition. The diagram shows the cycle of events during which epithelial cells are transformed into mesenchymal cells and *vice versa*. The different stages during EMT and the reverse process MET are regulated by effectors of EMT and MET, which influence each other. Important events during the progression of EMT and MET, including the regulation of the tight junctions and the adherens junctions, are indicated. **E-cadherin**, epithelial cadherin; **ECM**, extracellular matrix; **MFs**, microfilaments; **MMPs**, matrix-metalloproteases. (Figure based on Thiery *et al*., 2006).

1.2.3. Changes in cell polarity

Cellular polarity is defined by the distinct arrangement of cytoskeleton elements and organelles in epithelial *versus* mesenchymal cells. While epithelial polarity is characterized by cell-cell junctions found near the apical-lateral domain (non-adhesive surface), and a basal lamina (adhesive surface) opposite to the apical surface, the mesenchymal cells do not have apical/basal polarity. Instead, mesenchymal cells have a front-end/back-end polarity, with actin-rich lamellipodia and Golgi localized at the leading edge (Hay, 2005). Molecules that establish cell polarity include **Cdc42**, **PAK1**, **PI3K**, **PTEN**, **Rac**, **Rho**, and the **PAR proteins** (Moreno-Bueno *et al.*, 2008; McCaffrey *et al.*, 2009). It is known that changes in cell polarity help to promote an EMT such as seen in mammary epithelial cells, where the activated TGF-β receptor II causes Par6 to activate the E3 ubiquitin ligase Smurf1, which then targets RhoA to the proteasome. The **loss of RhoA** activity results in the **loss of cell-cell adhesion and epithelial cell polarity** (Ozdamar *et al.*, 2005).

Many of the same polarity (**Crumbs**, **PAR**, and **Scribble complexes**), structural (**actin**, **microtubules**), and regulatory molecules (**Cdc42**, **Rac1**, **RhoA**) that govern epithelial polarity are also central to cell motility (Nelson, 2009). These molecules also govern the migration of the mesenchymal cells away from the epithelium, a process in which they need to become motile. It was also found that many mesenchymal cells express the intermediate filament **vimentin** which may be responsible for several aspects of the EMT phenotype (Mendez *et al.*, 2010).

1.2.4. Invasion of the basal lamina: One of the many roles of proteolysis

The basal lamina stabilizes the epithelium and it is a barrier to migratory cells (Erickson, 1987) that consist of ECM components such as collagen type IV, fibronectin, and laminin. The emerging mesenchymal cells must penetrate a basal lamina and one of the mechanisms that these cells use is the production of enzymes that degrade it. Such molecules include the **plasminogen activator**, a protease that is associated with a number of EMTs such as neural crest migration (Erickson *et al.*, 1987), and the formation of cardiac cushion cells during heart morphogenesis (McGuire, 1993). **Type II serine protease** (Jung *et al.*, 2007) and **matrix-metalloproteases** (MMPs) are also important for many EMTs (Duong *et al.*, 2004).

1.2.5. EMT transcription factors

At the basis of every EMT or MET program are the transcription factors that regulate the gene expression required for these cellular transitions. This is performed by directly repressing cell adhesion and epithelial polarity molecules, and by upregulating genes required for cell motility and basal lamina invasion. Amongst the most important transcription factors are Snail, Zeb, and LEF/TCF. The activity of the transcription factors is also regulated at the protein level, including translational control, protein stability (targeting to the proteasome) (Zhou *et al.*, 2004; Wang *et al.*, 2009), and nuclear localization (Yamashita *et al.*, 2004). Curiously it has been shown that non-coding RNAs are emerging as important regulators of EMTs (Ma *et al.*, 2010).

1.2.6. Ligand-receptor signaling pathways

The initiation of an EMT or MET is an event tightly regulated during development and tissue regeneration because misregulation of such pathways would be of catastrophic nature to the cellular organization and to the organism itself. A variety of external and internal signaling mechanisms coordinate the complex events of the EMT which can be induced by either **diffusible signaling** molecules or **ECM components**. While the activation of a single signaling pathway can be sufficient for an EMT, in most cases an EMT or MET is initiated by multiple signaling

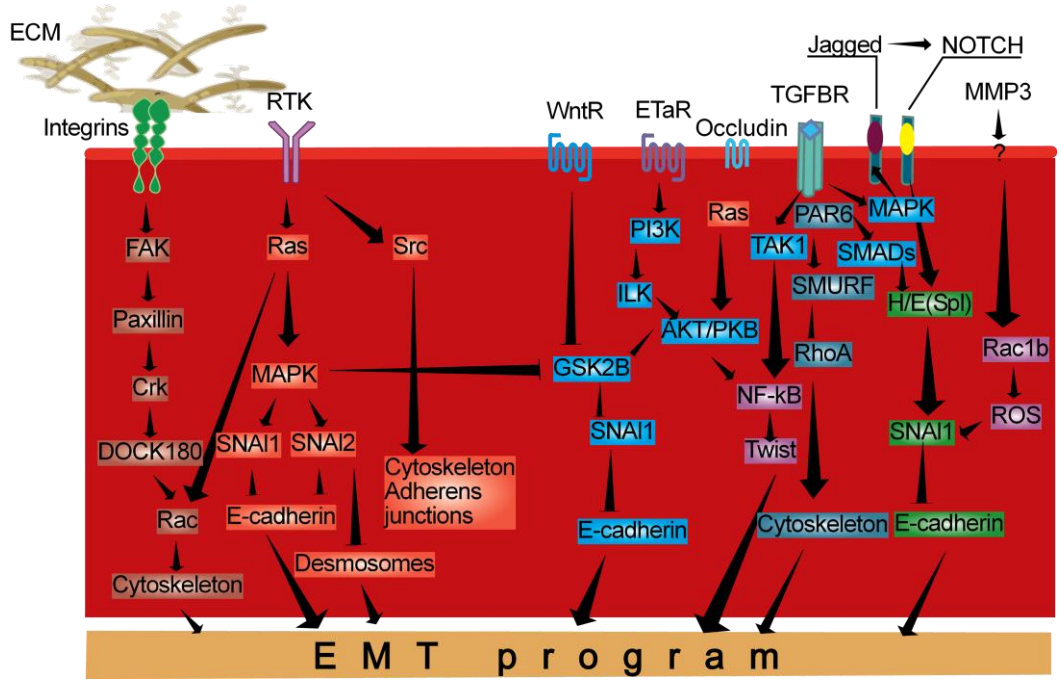

Figure 1.5. Overview of the molecular networks that regulate EMT. Illustration of the crosstalk of some of the signaling pathways that are activated by regulators of EMT. **ECM**, extracellular matrix **ETaR**, endothelin-A receptor; **FAK**, focal adhesion kinase; **GSK3β**, glycogen-synthase kinase-3β; **H/E(Spl)**, hairy/enhancer of split; **ILK**, integrin-linked kinase; **MAPK**, mitogen-activated protein kinase; **NF-κB**, nuclear factor-κB; **PAR6**, partitioning-defective protein-6; **PI3K**, phosphatidylinositol 3-kinase; **PKB**, protein kinase-B; **ROS**, reactive oxygen species; **TAK1**, TGFβ-activated kinase-1; **TGFβR**, TGFβ receptor; **WntR**, Wnt receptor. (Figure based on Thiery *et al.*, 2006).

pathways (Figure 1.5) acting in concert which may include one or more of the five most important ligand-receptor signaling pathways namely ,**TGF-β**, **Wnt**, **RTK**, **Notch**, and **Hedgehog**.

The **transforming growth factor-beta (TGF-β) superfamily** includes TGF-β, activin, and the bone morphogenetic protein (BMP) families. These ligands operate through receptor serine/threonine kinases to activate a variety of signaling molecules including **Smads**, **MAPK**, **PI3K**, and **ILK**. Most of the EMTs studied to date are induced in part, or solely, by TGF-β superfamily members (Zavadil *et al.*, 2005). One of the immediate impacts of TGF-β signaling is to immediately change epithelial cell polarity, for example, in a TGF-β induced EMT of mammary epithelial cells, TGF-β receptor II (TGF-βR) directly phosphorylates the polarity protein, Par6, leading to the dissolution of tight junctions (Ozdamar *et al.*, 2005). TGF-β signaling also regulates gene expression through the phosphorylation and activation of Smads, which are important co-factors in the stimulation of an EMT (Roberts, 2006). Furthermore, TGF-βR I directly binds to and activates PI3K (Yi *et al.*, 2005), which in turn activates **ILK** and downstream pathways. ILK is capable of orchestrating most of the major events in an EMT (inducible by TGF-β signaling), including the loss of cell-cell adhesion, interacting directly with growth factor receptors (TGF-β, Wnt, or RTK), integrins, the actin cytoskeleton, PI3K, and focal adhesion complexes (Delcommenne *et al.*, 1998), and promote invasion across the basal lamina through the up-regulation of MMPs (Gustavson *et al.*, 2004).

Many EMTs or METs are also regulated by **Wnt signaling**. Wnts signal through seven-pass transmembrane proteins of the Frizzled family, which activates G-proteins and PI3K, inhibits GSK-3b, and promotes nuclear β-catenin signaling (Logan *et al*., 1999).

The **receptor tyrosine kinase (RTK) family** of receptors and the **growth factors**[2] that activate them also regulate EMTs or METs. Ligand binding promotes RTK dimerization and activation of the intracellular kinase domains by auto-phosphorylation of tyrosine residues. These phosphotyrosines act as docking sites for intracellular signaling molecules, which can activate signaling cascades such as **Ras/MAPK**, **PI3K/Akt**, **JAK/STAT**, or **ILK**.

The **Notch signaling family** also regulates EMTs. When the Notch receptor is activated by its ligand Delta, an intracellular portion of the Notch receptor ligand is cleaved and transported to the nucleus where it regulates target genes (Timmerman *et al.*, 2004).

Other signaling pathways that activate EMTs include **inflammatory signaling** molecules such as interleukin-6 (Il-6, inflammatory and immune response) (Sullivan *et al.*, 2009); **lipid hormones** such as prostaglandin E2 (PGE2) (Dohadwala, 2006); **ROS species** which can activate EMTs by PKC and MAPK signaling (Wu, 2006); and **hypoxia** (Dunwoodie, 2009). In addition to diffusible signaling molecules, **extracellular matrix molecules** also regulate EMTs or METs in which integrin signaling appears to be important in this process (Zuk *et al.*, 1994) and involves ILK mediated activation of NF-kB, Snail-1, and Lef-1 (Medici *et al.*, 2010). Other ECM components that regulate EMTs include hyaluronan (Camenisch, 2002), the gamma-2 chain of laminin 5 (Koshikawa *et al.*, 2000), periostin (Ruan *et al.*, 2009), and podoplanin (Martin-Villar *et al.*, 2006).

[2] such as Fibroblast Growth Factor (FGF) (Ciruna *et al.*, 2001); Epidermal Growth Factor (EGF) (Lu *et al.* 2003); Insulin Growth Factor (IGF) (Irie *et al.* 2005) and Vascular Endothelial Growth Factor (VEGF) (Wanami *et al.* 2008).

1.3. Animal models in regeneration

"It can be shown, I think, with some probability that the forming organism is of such a kind that we can better understand its action when we consider it as a whole and not simply as the sum of a vast number of smaller elements"

Thomas Hunt Morgan
Nobel Prize in Physiology or Medicine in 1933

The first scientific observation of regeneration was reported in 1712 by René-Antoine Ferchault de Réaumur, who made a detailed description of crayfish limb regeneration. At that time, Réaumur hypothesized that the regenerating limbs arose from the expansion of tiny preformed limbs that resided inside crayfish exoskeleton (Okada, 1996) (Figure 1.6).

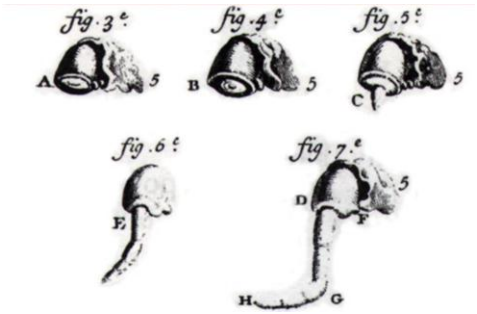

Figure 1.6: Réaumur's drawings illustrating the successive stages of limb regeneration in the crayfish (Adapted from Okada, 1996).

Nowadays, our perception of regeneration has changed and considerably evolved. However, we are still distant from the necessary knowledge to eventually manipulate and control regenerative properties.

Virtually all species from protozoa to humans have the capacity to regenerate, but the extent of their regenerative ability varies greatly. Planaria, starfish and some worms can regenerate most of their body, whereas many other species are able to regenerate only parts of specific tissues (Figure 1.7). Understanding the modes and mechanisms that are involved in regeneration of diverse systems is potentially advantageous for biomedicine, for instance, the knowledge on why does a specific regenerative process takes place in a particular organism and does not, in others, could provide new pathways to stimulate regeneration if the adequate endogenous pathways are unavailable.

Across metazoan, animals have been chosen to study regeneration according to the available genetic tools. The currently vastly studied models include in the invertebrates **hydra**, **planarians** and **ascidians**; and the vertebrates **newts**, **axolotls**, **frogs**, **zebrafish**, **chicks** and **mice** (Table 1.1).

1.3.1. Hydra

Hydra was one of the first animals in which regeneration was formerly described (Lenhoff *et al.*, 1744). In this species, the loss of essential tissues such as the head is prevented by regeneration. Within the first few hours after decapitation, regeneration proceeds without detectable proliferation (Holstein *et al.*, 1991) instead; it causes cells in the gastric column to undergo determination and differentiation to replace the missing head (Wolpert *et al.*,

Table 1.1. Genetic tools used in regeneration model systems research (adapted from Alvarado, 2006).

Group	Species	Regenerative capacities	Microarray	Trangenesis	Knockout/ knock down	Genome sequences
Invertebrates	Hydra	All tissues and organs	No	Yes	RNA*i*	No
	Planarians	All tissues and organs	Yes	No	RNA*i*	Yes
	Ascidians	All tissues and organs	Yes	Yes	Morpholinos	Yes
Vertebrates	Newts	Limbs, tails, heart, lens, spinal cord, brain, jaw, retina, hair cells of the inner ear	Yes	Yes	Morpholinos	No
	Axolotls	Limbs, tails, heart, spinal cord, brain	Yes	Yes	Morpholinos	No
	Frogs	Pré-metamorphic limbs, tail, retina, lens, hair cells of the inner ear	Yes	Yes	Morpholinos	Yes
	Zebrafish	Fins, tail, heart, liver, spinal cord, hair cells of the inner ear, lateral line	Yes	Yes	Morpholinos, mutagenesis	Yes
	Chicks	Hair cells of the inner ear	Yes	Yes	Morpholinos	Yes
	Mice	Liver, digit tips	Yes	Yes	Mutagenesis, homologous recombination	Yes

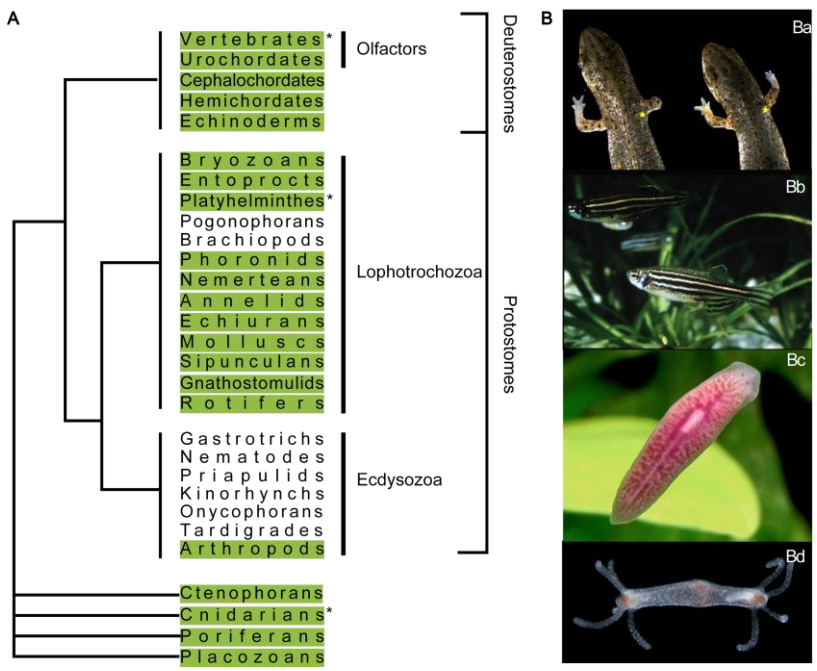

Figure 1.7. The phylogenetic distribution of regeneration across metazoan and model species in the field of regeneration. **(A)** The phylogenetic distribution of regeneration in multicellular organisms (taxa that contains animals that regenerate are highlighted in green; taxa that contain the conventional model organisms to study regeneration are highlight with *). **(B)** Examples of organisms that are currently being investigated to determine the molecular basis of regeneration. Ba, Newt; Bb, Zebrafish; Bc, Planarian; Bd, Hydra. (Figure adapted from Alvarado, 2006).

1971). Another interesting property of hydra is its ability to re-form an animal from dissociated cells (Hobmayer *et al.*, 2000). Studies on hydra biology use both transgenesis (Miljkovic *et al.*, 2002) and RNA*i* (Table 1.1). Several genes have been implicated in the regulation of polarity in hydra and include key regulators of development, such as Hox genes (Schummer *et al.*, 1992), *brachyury* (Technau *et al.*, 1999) and *goosecois* (Broun *et al.*, 1999). Components of developmentally related signaling pathways have also been identified, such as Wnt and its antagonist, *dickkopf* (Guder *et al.*, 2006). RNA*i* studies have shown that silencing of the evolutionarily conserved serine protease gene *kazal1* indicated that there is a role in the suppression of excessive autophagy, as well in cell survival after amputation (Chera *et al.*, 2006). Further studies indicated that these functions are consistent with the observed phenotype in mice mutated in the genes coding for serine peptidase inhibitor *SPINK1* and *SPINK3* (Chera *et al.*, 2006).

1.3.2. Planarians

Planarians have also been classical models for regeneration over more than 100 years (Reddien *et al.*, 2004) (Figure 1.8). Unlike hydras, planarians regenerate the missing body parts by first assembling the blastema, which arises from the proliferation of pre-existing somatic stem cells known as neoblasts. The blastema is constituted by an outer epithelia layer that covers the mesodermally derived tissue. It represents a canonical **epithelial-mesenchymal interaction**. Recently, RNA*i* was used to screen over 1000 genes, which uncovered over 240 genes having relation with regeneration processes (Reddien *et al.*, 2005), such as genes encoding for FKB-like immunophilin, chonderosarcoma-associated protein 2 (CSA2), nucleostemin and SMAD4 (Reddien *et al.*, 2005a). The function of the proteins responsible for regulating the production of stem-cell progeny, the PIWI family proteins, were described for the first time in planarians (Reddien *et al.*, 2005b), and are known also to be expressed in the mouse testis, which are needed for the completion of spermatogenesis (Deng *et al.*, 2002).

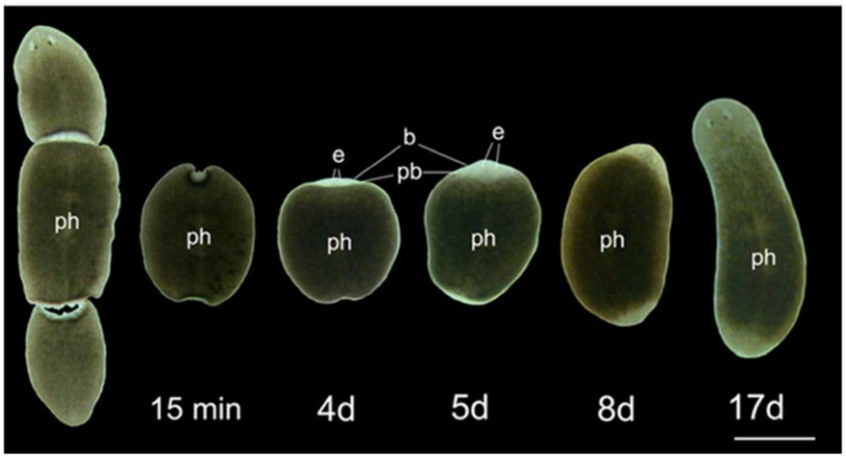

Figure 1.8. Anterior and posterior regeneration in the planarian *Schmidtea mediterranea* after a transverse cut, at 19˚C. In the first few days of regeneration, a white blastema (b) is formed made up of undifferentiated cells, and at 3-4 days of regeneration small eyespots (e) appear in the anterior blastema (4 d). Following their initial appearance in the blastema, the eyespots grow to their normal size by aggregation of newly differentiated cells (5 d, 8 d). Also, the brain has regenerated in the anterior part and pigment cells start to be visible in the blastema region. In the posterior part, the missing organs, such as the ventral nerve cords and the digestive system have been reformed. After some weeks of regeneration, the planarian is fully regenerated, although smaller than the original organism (17 d). Remodeling of the existing tissue has occurred, e.g. the size of the pharynx has been adjusted to the dimensions of the new organism. Growth of the planarian will occur upon feeding. **b**, blastema; **e**, eyes; **d**, days; **pb**, post-blastema; **ph**, pharynx. Scalebar: 4mm. (Taken from Handberg-Thorsager *et al.*, 2008).

1.3.3. Amphibians

Regeneration in **amphibians** is mediated by terminally differentiated cells at the site of amputation that re-differentiate to form the lost parts (transdifferentiation), and also by undifferentiated stem cells (Morrison *et al.*, 2006). In mammals, the cell transdifferentiation processes are restricted to endothelial cells of pancreas and Schwann cells of the peripheral nervous system (Hao *et al.*, 2006). Among the vertebrates, urodele amphibians, such as newt, are considered to be the champions of regeneration, as they can regenerate limbs, tail, brain, spinal cord, hair cells, lens and retina, jaws and heart (Tsonis, 2000). Even though traditional genetics are not available, tools such as ESTs and transgenesis in newts, salamanders and axolotl are available (Sobkow *et al.*, 2006) which already allowed a tremendous understanding of the regulatory pathways involved in amphibian regeneration. **Limb regeneration** in newts and axolotls requires the formation of a blastema (Figure 1.9). After amputation, the wound is covered by a specialized epithelium that provides signals to the underlying cells of the stump to dedifferentiate and/or maintain cell proliferation. A nerve dependent regeneration process then takes place with the release of nerve trophic factors, for which the glial growth factor (GGF) and transferrin have been proposed as possible candidate factors (Kiffmeyer *et al.*, 1991). Among other suspected cell-proliferation and regeneration-inducing factors for the blastema are the fibroblast growth factor like molecules (FGFs) and their receptors (FGFRs) which stimulate the expression of *Shh* (sonic hedgehog), *Msx1*, and *Fgf10*, and the concomitant production of new limb structures (Yokoyama *et al.*, 2001). In opposition to the transdifferentiation pathways undertaken in limb regeneration, **tail regeneration** in amphibians, which offers a model for spinal cord regeneration, is mainly stem cell derived. In salamanders, the ependymal cells that line the central canal of the spinal cord are considered to be central nervous system (CNS) stem cells, and have also been shown to participate in the regeneration of the spinal cord. Furthermore, the ependymal cells migrate to the surrounding tissues during tail regeneration and form cartilage and muscle, thereby switching from ectodermal to mesodermal lineages (Echeverri *et al.*, 2002). It has been shown that expression of the bone morphogenetic protein (BMP) receptor *Alk3* and expression of *Msx1* results in regeneration of all tail tissues during the developmental stages of *Xenopus*. On the contrary, expression of a constitutively active Notch intracellular domain (NICD) resulted in imperfect muscle regeneration. This indicated that BMP acts upstream of Notch, and that it exerts an independent effect on muscle regeneration. When both Notch and BMP signaling are inhibited at regeneration-permissive stages, the complete inhibition of tail regeneration is observed (Beck *et al.*, 2003).

Figure 1.9. Regeneration of the forelimb in a newt after amputation at distal or proximal sites. The original limb is shown at the top and the regenerated limb at the bottom of the image. (Taken from Brockes, 1997).

1.3.4. Vertebrates

Zebrafish is also an excellent model to study regeneration in lower vertebrates (Woods *et al.*, 2005). These animals are easy to maintain in the laboratory, their developmental time is short and genetic screens have produced numerous mutants, including some that affect regeneration; they have a sequenced genome and a wide range of available genetic tools (microarray analyses; transgenesis and knock-down technology using morpholinos; chemical mutagenesis and small molecule screens have provided both developmental and regeneration mutants) (Peterson *et al.*, 2000). **Fin regeneration** in fish shares a number of responses with limb regeneration in amphibians (Figure 1.10) (wound epithelium, blastema formation and response to retinoic acid) (White *et al.*, 1994). Genetic screens have also identified unexpected regeneration regulators in fish. For example, *nbl* (no blastema), was found to encode heat-shock protein 60 (Hsp60). Its expression is increased in blastema cells and its dysfunction, due to mutation, affects mitochondria and leads to apoptosis (Makino *et al.*, 2005).

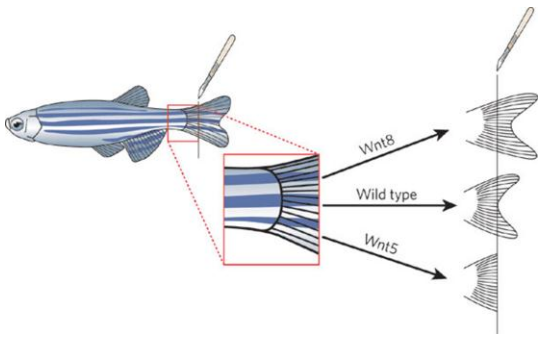

Figure 1.10. Zebrafish tail-fin regeneration is an excellent model for studying regeneration, and several factors that modulate regeneration have been found in this system. After the distal tail fin has been removed, a blastema forms near the wound. The fin typically regenerates to a normal wild-type size. However, if the canonical Wnt-mediated signaling pathway is activated by Wnt8, cell proliferation increases in the regenerating fin (although the size of the regenerating fin eventually becomes equivalent to that of a wild-type fin). By contrast, activation of the non-canonical Wnt-mediated signaling pathway by Wnt5 suppresses regeneration. (taken from Zon, 2008).

Studies of the regenerative capacities of **mammals** have focused primarily on the role of stem cells (somatic, fetal and embryonic) in tissue repair since there is a continuous renewal of tissues as part of homeostasis. This is achieved primarily by the activities of multipotent stem cells that reside in the renewing tissues. Mammals' digestive system has a remarkable regenerative ability. Even though amputation of the intestine does not trigger its regeneration, it has been extensively studied as a paradigm for tissue turnover and proliferation of stem cells in the epithelium that lines the small intestine. In contrast, partial amputation of liver does induce the remaining lobes of the liver to enlarge and replace the missing mass of the organ. However, this is achieved through the proliferation of all mature cell types comprising the intact liver, in a specific order, without apparent dedifferentiation or transdifferentiation. Even though there are evidences of olfactory-neuron regeneration in mammals, and the generation of new neurons in the adult mammalian brain, these animals fail to have the same regenerative potential as amphibians and other animals. Attempts to induce regeneration after spinal-cord injury have mainly focused on the use of **growth factors** and **adhesion molecules** that are capable of modulating the induction of axonal growth, such as Nogo (Buchli *et al.*, 2005), FGF (Klimaschewski *et al.*, 2004), and integrin (Condic, 2001). However, so far these attempts have failed to induce complete regeneration of CNS tissues. Numerous experiments have shown that adult or embryonic stem cells can repopulate sites of damage in tissues that include the heart, brain and retina, nevertheless, further research studies are needed until the complexity of stem-cell regulatory systems and the tissues and organs they differentiate into is completely unraveled.

1.4. Echinoderms

Echinoderms are among the more bizarre products of metazoan evolution. Although they are radially symmetrical as adults, they begin the development as bilaterally symmetrical embryos and larvae (Figure 1.11). They are considered to lack a head and a brain (Jefferies *et al.*, 1996), yet they apparently evolved from deuterostome ancestors that probably had both (Nielsen, 1995). Echinoderms together with urochordates, cephalochordates and hemichordates are the only invertebrate deuterostomes. This close relationship, established using morphological, embryological and fossil data, has been reaffirmed in molecular studies (Blair *et al.*, 2005). The currently accepted phylogenetic relationship groups together the phylum Echinodermata with the phylum Hemichordata and places these as sister groups of the phylum Chordata which contains the Urochordata (tunicates), Cephalochordata and the Vertebrata (Figure 1.12) (García-Arrarás *et al.*, 2010).

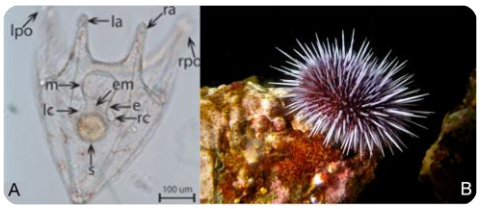

Figure 1.11. Larvae and adult sea urchin *Strongylocentrotus purpuratus*. **A)** Stage I: four arm stage larvae with bilateral symmetry; lpo, left postoral arm; la, left anterolateral arm; ra, right anterolateral arm; rpo, right postoral arm; m, mouth; lc, left coelom; em, esophageal muscles; e, esophagus; rc, right coelom; s, stomach. B) adult sea urchin with pentaradiate symmetry. (**A** adapted from Smith *et al.*, 2008 and B adapted from http://marissamarinescience.synthasite.com/purple-sea-urchin.php).

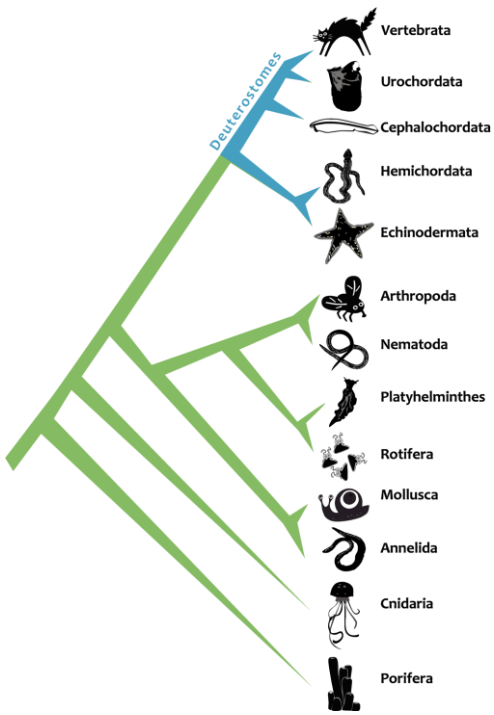

Figure 1.12. Phylogenic tree with the relationship between Echinodermata and the other phyla. Adapted from García-Arrarás *et al*., 2010.

Echinoderms possess a suite of distinctive and unique morphological characteristics (Figure 1.13): the water vascular system, an organ system involved in locomotion, respiration, sensation and feeding; a mineralized endoskeleton with a characteristic porous microstructure; and a central nervous system that lies perpendicular to the gut (Nielsen, 1995).

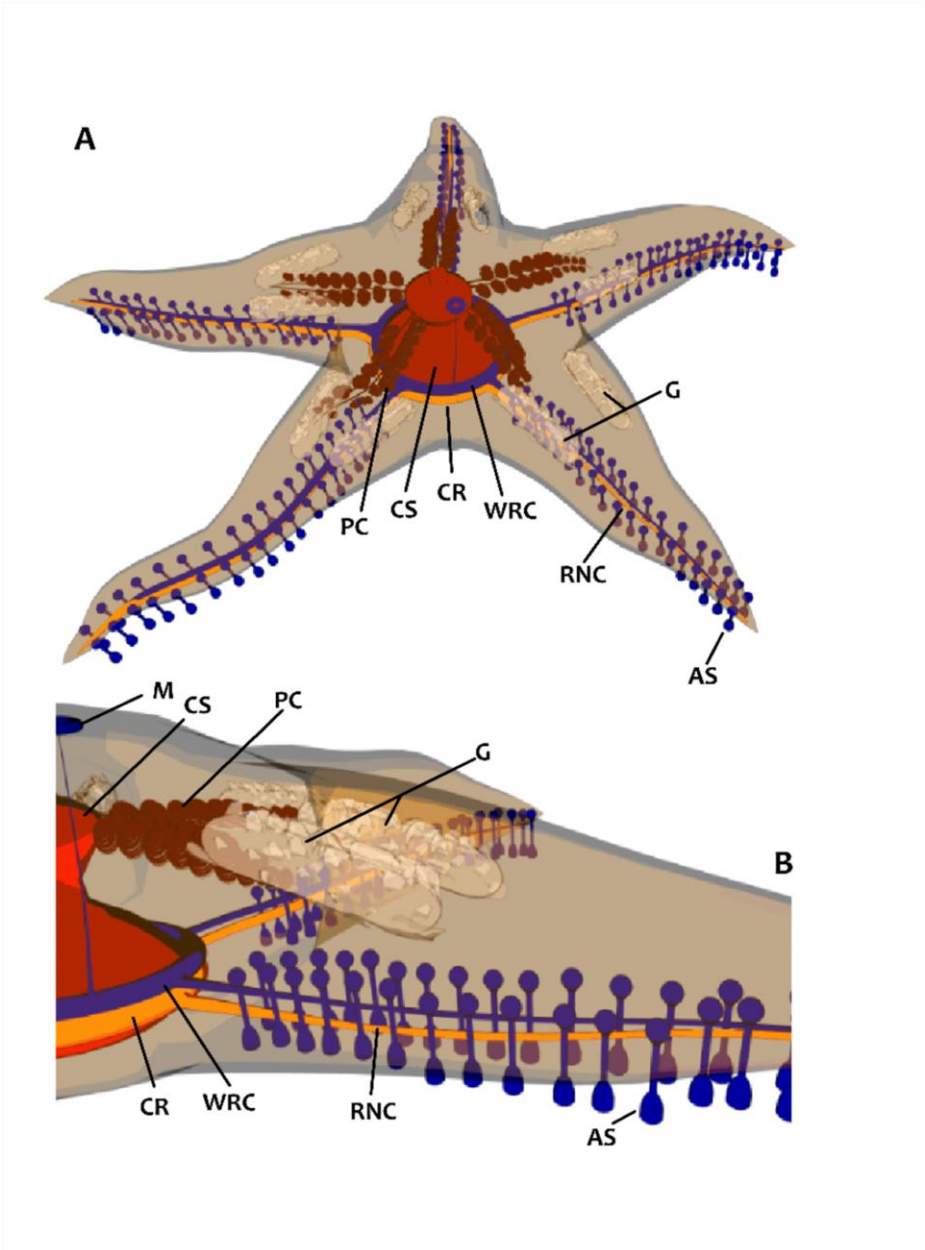

Figure 1.13. Simplified diagram of the anatomical organization of the adult starfish. Starfish as all echinoderms have a radial symmetry, which means that each arm has an exact replica of all internal organs. **A**, top view of an adult starfish (aboral side), and **B,** lateral view of one starfish arm showing the organizational relationship between the internal organs. **Nervous system**: CR, circumoral nerve ring; RNC, radial nerve cord. **Digestive system:** CS, cardiac stomach; PC, pyloric caeca. **Water vascular system**: WRC, water ring canal; AS, ambulacrary system with tube feet; M, madreporite (controls entry of water into the water vascular system). **Reproductive system**: G, gonads. Figure adapted from Franco *et al.*, 2011A.

1.4.1. Regeneration in echinoderms

"Echinoderms provide unique models for studying regeneration, while the peculiar anatomical and physiological situation of their nervous system, including its lack of centralization, makes them particularly amenable for approaching this problem from a neurobiological perspective. Furthermore, the key phylogenetic position of echinoderms in relation to invertebrate chordates and vertebrates makes the occurrence and prospective roles of neurally derived factors in repair and regenerative processes in this phylum a matter of even more interest and significance."

(Thorndyke et al., 2001)

One of the most striking aspects of echinoderm biology and also one of the most widely recognized is their outstanding capacity for regeneration. Regeneration in echinoderms serves a wide range of biological purposes such as the reconstruction of external parts (spines, pedicellariae and tube feet) and internal organs (gonads, gut, whole visceral mass, nervous system) that are often subjected to predation or amputation, self-induced or traumatic, allowing the complete functional regrowth of lost parts. Also, regeneration developed as part of a program of asexual reproduction and hence it offers tremendous potential as a cloning strategy. In some species, such as the starfish from the *Linckia* genus, the autotomized arms may regenerate to produce a completely new adult (Cuenot, 1948) (Figure 1.14). This ability undoubtedly depends upon a remarkable histogenetic and morphogenetic plasticity that allows the expression of new developmental programs (or re-expression of old ones) at all life stages including the adult. In terms of the cellular strategies involved in regeneration events, echinoderms seem to employ both epimorphic and/or morphallactic processes according to species and injury type. Typical epimorphic processes, with blastema formation, appear to be employed in situations where regeneration is widely predicted, rapid and effective. This is the case of the regeneration of the long and fragile arms of both crinoids and ophiuroids after autotomy (Carnevali *et al.*, 2001; Bonasoro *et al.*, 2001). In contrast, morphallactic regeneration seems to be a more complex and slower process, which tends to follow traumatic mutilations, such as seen in the regeneration of starfish arm tip (Mladenov *et al.*, 1989; Moss *et al.*, 1998). In this case amputation is not a predictable event and the regenerative mechanisms imply phenomena of substantial rearrangement of the "old" structures.

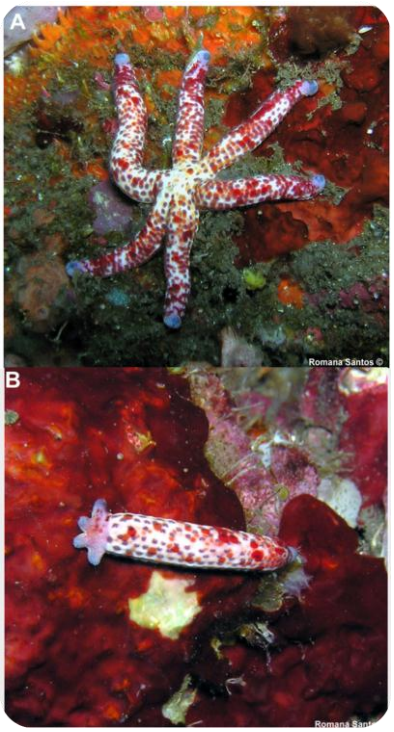

Figure 1.14: Tropical starfish *Linckia multiflora*. **A**, adult specimen and **B**, regenerating starfish from an autotomized arm. (Images borrowed with kind permission from Romana Santos).

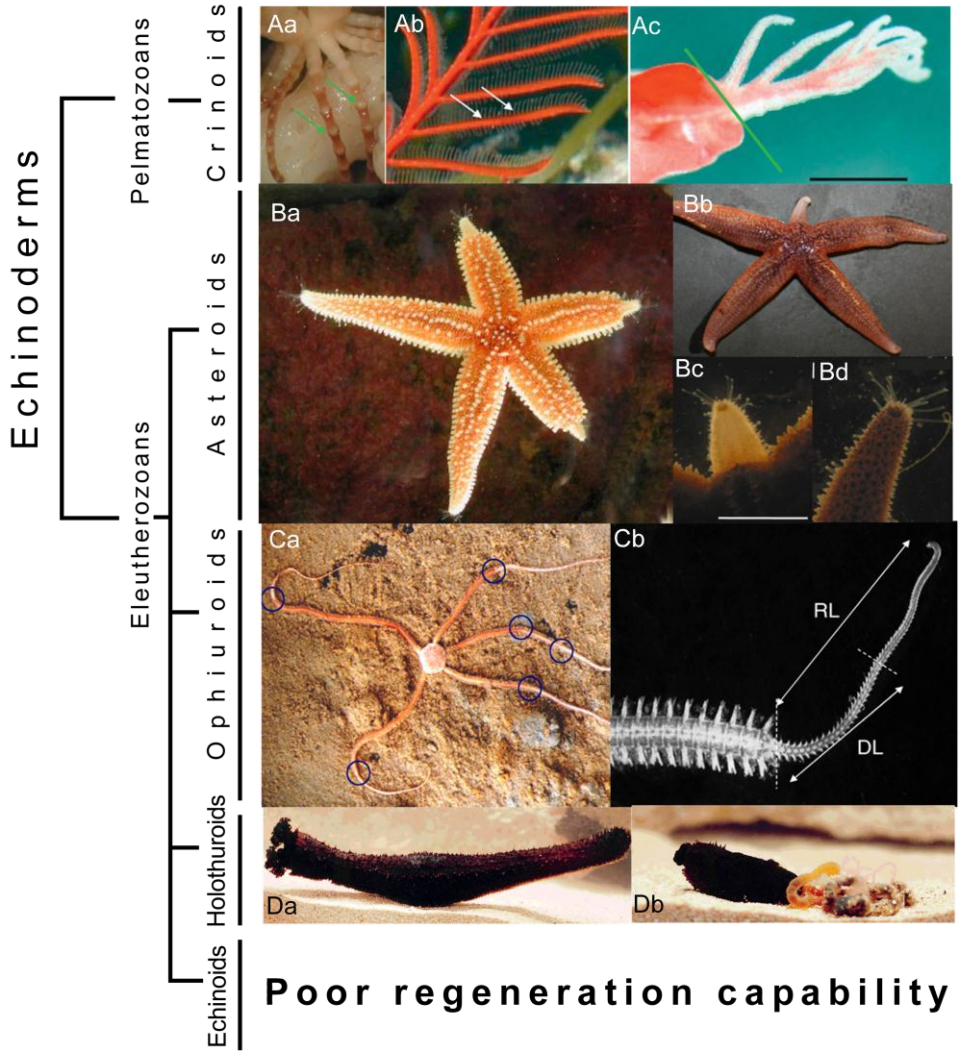

Figure 1.15. Examples of echinoderm species that have been used to study regeneration. **A** Crinoid *Antedon mediterranea*; Aa, Photographic detail of the aboral appendices (cirri and arrows), frequently subjected to amputation/regeneration; Ab, Photographic detail of the lateral branching of the arms (pinnulae and arrows) which are preferential sites of regeneration; Ac, Stereomicroscopic view of a regenerating arm (2 weeks post-amputation) Bar=1mm (images taken from Carnevali *et al.*, 2010). **B** Asteroid *Asterias rubens*; Ba, starfish regenerating tree arm tips (image taken from Dupont *et al.*, 2007); Bb, Starfish regenerating an entire arm from the amputation plane; Bc, early regenerated arm less pigmented that an intact arm of the same animal (Bd) (Images taken from Hernroth *et al.*, 2010). **C**, Ophiuroid *Amphiura filiformis*, Ca, a brittlestar with six scars that indicate sites of regeneration (image taken from Dupont *et al.*, 2007); Cb, brittlestar with a new arm extended in length and clearly distinguishable from the older stump. The demarcation between the proximal differentiated part (with ossicles, podia and spines) and the distal undifferentiated part is indicated by a dotted line. DL, differentiated length; RL, regenerated length (image taken from Dupont *et al.*, 2006). **D**, Holothuroid *Holothuria glaberrima*; sea cucumber specimen shown before (Da) and after (Db) evisceration. The organs to be regenerated include the intestine, hemal system, one respiratory tree, and gonads (images taken from García-Arrarás *et al.*, 1999).

Echinoderm regeneration ability has long been appreciated amongst several biologists and was the main reason why these animals were considered to be favorite models for the pioneer *regenerationists* in the 19th and early 20th centuries. However, echinoderms were left to scientific oblivion in favor of species for whose the possibility of conducting genetic studies became early available. Nowadays echinoderms have been slowly recovering for such neglect, and there are already several scientific reports of interesting regeneration related studies in several species of echinoderm classes such as crinoids, ophiuroids, asteroids and holothuroids (Figure 1.15) (for review see Carnevali, 2006). Regeneration also occurs in echinoids, but is less spectacular in terms of extend and degree of capacities and only few examples have been investigated so far (Bonasoro *et al.*, 2004; Dubois *et al.*, 2001). Curiously, the only echinoderm to have its genome sequenced is the sea urchin *Strongylocentrotus purpuratus* (consortium, 2006) and thus, even though a great homology is expected with other echinoderm species, this has for certain hampered classical genetic studies using these animals as models for regeneration. Nevertheless, recent research demonstrated that echinoderms do have the potential as viable and tractable models for molecular research on regeneration. For example, as described in a letter to editor, Dupont and Thorndyke (Dupont *et al.*, 2007) highlight the involvement of the bone morphogenic protein/transforming growth factor-β (BMP/TGFβ)-signaling pathway in both ophiuroids and crinoids (Bannister *et al.*, 2005; Patruno *et al.*, 2002; Patruno *et al.*, 2003), the HOX-signaling pathway in brittlestars and starfish (Thorndyke *et al.*, 2001b; Ikuta, 2011) and the Ependymin pathway in the sea cucumber (Suàrez-Castillo *et al.*, 2004) and more recently, the identification of an increased expression of homologs genes to survivin and mortalin during sea cucumber visceral regeneration (Mashanov *et al.*, 2010). These molecules are known to be implicated in mitosis and apoptosis, allowing the proper balance of cell division and death. Studies using the sea cucumber, an echinoderm capable of regenerating its viscera allowed also to find ***1)*** a Wnt homologue (WNT-9) overexpressed during the regenerative process (Ortiz-Pineda *et al.*, 2009); ***2)*** to perceive the importance of ECM-integrin interactions during regeneration (Cabrera-Serrano *et al.*, 2004) and ***3)*** to understand that significant changes in ECM content occur during intestine regeneration and that the onset of these changes is correlated to the proteolytic activities of MMPs (Quinones *et al.*, 2002), similarly to the described events in other regenerating animal models.

1.4.1.1. Wound healing, coelomocytes and echinoderm immune responses

It has been commonly described for several echinoderm species that the primary response to amputation is a rapid muscular contraction (Moss *et al.*, 1998) (Figure 1.16) with subsequent healing mediated by **coelomocytes**, which migrate to the injury site where they prevent bleeding by clotting (Smith, 1981), modulate extracellular matrix (Tanney *et al.*, 1998) and limit the invasion of pathogens (Pinsino *et al.*, 2007; Carnevali *et al.*, 2001; Holm *et al.*, 2008). Several authors suggest

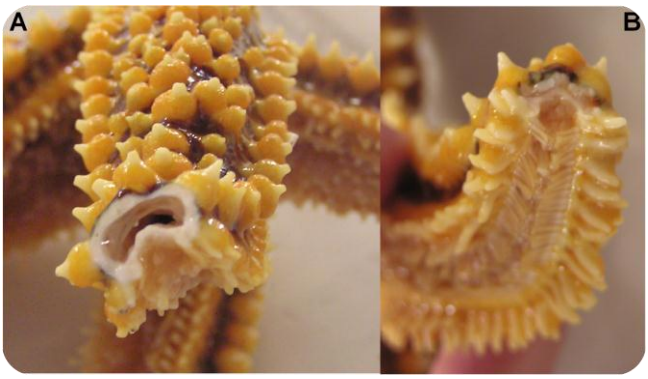

Figure 1.16. Wound healing after arm tip ablation of the starfish *Marthasterias glacialis*. **A**, immediately after wound infliction and **B,** 24 h post arm tip ablation, where it is possible to observe a strong muscular contraction to close the wound (Pictures from Catarina Franco, unpublished).

coelomocytes as sources for the regenerating tissues (Carnevali *et al.*, 1993; Rinkevich *et al.*, 2009), however, regeneration studies on various echinoderms report an initial accumulation of these cells, but not of proliferation beneath the wound epidermis (Moss *et al.*, 1998; Mladenov *et al.*, 1989; Hernroth *et al.*, 2010).

The **coelomocytes** (Figure 1.17), also called invertebrate blood cells, are recognized as the main cellular component of the echinoderm immune system and participate in functions similar to their counterparts in vertebrates, namely, coagulation, immunological defense and oxygen transport (Cavey *et al.*, 1994; Roch, 1996). In echinoderms, the coelomocytes occupy the perivisceral coelomic cavities, such as the water-vascular and haemal systems as well as the connective tissue and tissues of various organs (Muños-Chápuli *et al.*, 2005). Although the origin of coelomocytes in echinoderms is not well known, the majority of the available reports suggest that the hematopoietic source of these cells most probably derive from the coelomic epithelium (Chia, 1996) and also from the axial organ, a complex and elongated mass of tissue that represents the common junction of the circulatory system (Millott, 1969) and the Tiedemann body. These tissues showed an increased cell proliferation which reflected the increased number of coelomocytes upon response to lipopolysaccharide (LPS) (Holm *et al.*, 2008).

Figure 1.17. Live coelomocytes from the sea urchin, *Paracentrotus lividus*. **A,** petaloid phagocyte; **B,** red spherule cell; **C**, colorless spherule cell; **D**, vibratile cell. Scale bar = 5 microns. (Image taken from Matranga *et al.*, 2005).

All echinoderm classes are provided with several different categories of coelomocytes which can be divided according to their morphology, physiology and function (Table 1.2). However, a considerable discrepancy in a common nomenclature is still observed in several reports that describe the same or similar cell types present in different species or classes (Penn, 1979; Vanden Bossche *et al.*, 1976; Kaneshiro *et al.*, 1980; Ramírez-Gómez *et al.*, 2010). In starfish, in particular in *Asterias rubens*, four different morphotypes have been described with phagocytes being the dominant type (Pinsino *et al.*, 2007 and 2008). Amebocytes are responsible for phagocytosis of foreign particulate material, in which lysosomal enzymes, including lipase, peroxidase and serine protease, are constitutively present (Glinski *et al.*, 2000). Both phagocytic amebocytes and spherule cells appear to be involved in cell clumping and the formation of capsules around ingested parasites (Glinski *et al.*, 2000).

Coelomocytes are suspended in a fluid medium, also called coelomic fluid, which bathes echinoderms internal organs. This fluid (CFF, cell free coelomic fluid) has a composition similar to sea water in terms of minor dissolved salts and other minerals, but however, is loaded with proteins secreted either by coelomocytes or by surrounding tissues, essential for encapsulation of invasive material and clotting reactions and thus, are involved in cell-free (humoral) immune responses (Glinski *et al.*, 2000). Currently there are two different views concerning the type of immune responses elicited by echinoderms. The first defends that echinoderms, as all invertebrates, possess a highly sophisticated immune system that is however, entirely innate and composed of a simpler complement system and a large set of antimicrobial peptides and proteins (Smith *et al.*, 2011). The second theory proposes that both the humoral and cellular responses of echinoderms resembles those of the immune system of vertebrates which includes two sub-populations of coelomocytes that strongly resemble the adherent cells (mammalian B lymphocytes), and non-adherent cells (mammalian T lymphocytes) (Brillouet *et al.*, 1981; Leclerc *et al.*, 1992) and an antibody factor that shows homologies with human Kappa-like proteins (Leclerc, 2000; Leclerc *et al.*, 2011) with a

molecular mass of 120-130 kDa with four subunits of 30 kDa each (Delmotte *et al.*, 1986). This last hypothesis suggests that the conventional immune system comprised by *innate* and *adaptive* responses, developed at this point of evolution thus, positioning echinoderms in a strategic and interesting node of the evolution of the immune system. Moreover, it is widely accepted that echinoderms have a simpler complement system, a large set of lectin genes and a number of antimicrobial peptides.

Several of the humoral factors present in the coelomic fluid, essential for the immobilization, phagocytosis and encapsulation or lysis of the invasive microorganisms are already described and characterized. These include a lectin-like family of proteins, which according to the analysis of the sea urchin genome, are composed of over 100 small C-type lectins, 400 mosaic proteins with lectin domains and 34 galectins. Additionally, a few pentraxins and fucolectins (Multerer *et al.*, 2004), perforins and vitellogenin have also been described and are involved in adhesion between the cells surrounding and microorganisms (Leclerc, 2000). Several other molecules have been also characterized and include a 220 kDa agglutinating factor thought to be involved in coagulation of coelomocytes (Canicatti *et al.*, 1991); a cytokine similar to interleukin-1 (Prendergast *et al.*, 1970; Beck *et al.*, 1991) and interleukin-2 (Beck *et al.*, 1989) and homologue proteins of the vertebrate complement system, such as the SpC3 an homologue of C3 complement component (Al-Sharif *et al.*, 1998) and SpBf an homologue of factor B (Smith *et al.*, 1998). Several antimicrobial molecules have also been detected, such as the two recently characterized cysteine-rich AMPs, called strongylocins, which are peptides crucial for the antimicrobial activity (Li *et al.*, 2008); steroidal glycosides or saponins (Andersson *et al.*, 1989); polyhydroxylated sterols (Andersson *et al.*, 1989); naphtoquinone pigments such as echinochrome A (Kuwahara *et al.*, 2009). Lysozymes, which are known for their antibacterial activity, have also been identified which may synergistically provide effective defense against bacterial infections (Canicatti *et al.*, 1989).

Table 1.2. Summary of coelomocyte types reported for echinoderm classes. ***E***: Echinoidea, ***H,*** Holothuroidea, ***A,*** Asteroidea, ***C***, Crinoidea, ***O***, Ophiuroidea.

Coelomocyte type	Present in class	Role	References
Discoidal cell	E, H	Phagocytosis, clotting, encapsulation, chemotaxis, opsonisation, graft rejection	(Coteur *et al.*, 2002; de Faria *et al.*, 2008; Eliseikina *et al.*, 2002; Endean, 1966; Matranga, 2005; Ramirez-Gomez *et al.*, 2010; Smith *et al.*, 2006)
Polygonal cell	E		
Small phagocyte	E, H		
Amebocytes /Phagocytes	E, H, A, C, O		
Colored spherule	E, H, C	Antibacterial activity	(de Faria *et al.*, 2008; Endean, 1966; Smith *et al.*,2006)
Lymphocyte	E, H, A	Progenitor cells	(Coteur *et al.*, 2002; Eliseikina *et al.*, 2002; Endean, 1966; Ramirez-Gomez *et al.*, 2010; Xing *et al.*, 2008)
Vibratile	E, H, A, O	Coelomic fluid movement, clotting	(de Faria *et al.*, 2008; Eliseikina *et al.*, 2002; Endean, 1966; Matranga *et al.*, 2005; Pinsino *et al.*, 2008; Ramirez-Gomez *et al.*, 2010; Smith *et al.*, 2006; Xing *et al.*, 2008)
Crystal cells	H	Osmoregulation	(Eliseikina *et al.*, 2002; Endean, 1966; Ramirez-Gomez *et al.*, 2010; Xing *et al.*,2008
Hemocytes	H, A, O	Oxygen transport	(Eliseikina *et al.*, 2002; Endean, 1966; Pinsino *et al.*, 2008)

(Adapted from Ramírez-Gómez *et al.*, 2010)

1.4.1.2. Echinoderms nervous system and regeneration

1.4.1.2.1. Echinoderms have nerve-dependent regeneration events

In a wide number of zoological groups it has been shown that the presence of the nervous system is necessary for the success of regeneration due to the presence of neurotrophic substances such as the candidates' fibroblast growth factor-2, glial growth factor, substance P and transferrin (Goldfrab, 1909; Brokes *et al.*, 1984).

In the early 1900´s this subject was not of consensus among echinoderm scientists, with several researchers claiming that the nervous system was necessary for regeneration to occur (King, 1898; Prizibram *et al.*, 1901; Valentine *et al.*, 1926) as for others claimed that regeneration occurred without the intervention of the nervous system (Goldfarb *et al.*, 1909; Schapiro, 1914). It was not until Huet performed irradiation experiments in **asteroids** that it was proven that the action of the radial nerve cord was needed throughout the whole course of regeneration, and that it did not occur if the radial nerve cord was removed prior to injury (Huet, 1975).

In **crinoids** blastema-driven arm regeneration, the nervous system acts as an important source/vehicle for the different types of non-neuronal migratory cells, responsible for the regenerative processes, including stem neoblast-like elements (amoebocytes), phagocytes and granule cells (Carnevali *et al.*, 1997). The nervous system also acts as a primary source of regulatory factors involved in the regenerative processes of the neural tissue itself, and also to a larger extent, in the development and regrowth of all other structures (Thorndyke *et al.*, 2000). In **holothurians**, the crucial involvement of the nervous system is also evident in regeneration and complete recovery of functional integrity of the viscera (García-Arrarás *et al.*, 1991).

In both vertebrates and invertebrates, the specific role of the nervous system in regeneration usually implies also its direct contribution as a primary source of regulatory factors, mitogens or morphogens. Several of these factors have already been identified and characterized in echinoderms and include neurotransmitters, such as, monoamines like dopamine, noradrenaline (norepinephrine), and serotonin (Thorndyke *et al.*, 2001). A variety of neuropeptides have also been extensively characterized such as cholecystokinin, substance-P, and RFamide-like factors, identified with immunological methods. More importantly, native peptides such as SALMFamides 1 and 2 (S1 and S2), SGYSVLYamide, GFSKLYFamide, FPVGRVHRFamide, holokinins 1 and 2, stichopin, NGIWYamide, autotomy-promoting factor (APF), and gonad-stimulating substance (GSS) have also been found. Finally, also several growth-factor-like molecules such as the transforming growth factor β (TGF-β), basic fibroblast growth factor (FGF-2), and nerve growth factor (NGF), were identified on the basis of immunological probes using heterologous antisera (for complete review see Thorndyke *et al.*, 2001).

1.4.1.2.2. The morphology of an unusual nervous system and its regeneration features

The echinoderms present a neural organization that distinguishes them from other deuterostomes (chordates and hemichordates) as they exhibit a number of unusual or unique features that have not been reported for other metazoans (Cobb, 1995) (Figure 1.18). Although in the adult echinoderm, the nervous system does not present a cephalized region, the neural net is far from being simple. The recent analysis of the ultrastructure of the circumoral nerve ring and the radial nerve cord of a sea cucumber species (Mashanov *et al.*, 2006), demystified several misconceptions of echinoderm neuronal physiology, such as the absence of glial cells (Stubbs *et al.*, 1995), and the idea that chemical synapses are extremely scarce in the echinoderm nervous system (Byrne, 1994). Some of the most important features of the morphology of echinoderms nervous system are here summarized:

Echinoderms nervous system is composed by a motor system constituted by a profound or **hyponeural nature (HN)**, represented by the nerves of Lange and the lateral nerves which are related with the movement of the tube feet, spines, pedicellariae and test. The hyponeural nerves are separated by a thin connective tissue layer from

the oral or **ectoneural nervous system (EN),** but remain connected via short neural bridges that are composed of nerve cell perikaria (Mashanov *et al.*, 2006). The EN nervous system is of sensory nature and it is constituted by a pentagonal nervous ring, the circumoral nerve ring, which surrounds the oral cavity, (Smith, 1936; Smith, 1965; Ruppert *et al.*, 1994), from which derive five radial nerve cords. Each **radial nerve cord (RNC)** traverses the arm through its oral side and across its longitudinal axe (Huet, 1975).

The whole HN and EN components of the RNC are epithelial tubes with a thick neuroepithelium at one side. A thin ciliated non-neuronal epithelium complements the neuroepithelium to form a tube, thereby enclosing the epineural and hyponeural canals. The whole of the EN and HN subsystems is separated from the surrounding tissue by a continuous basal lamina. The nerve ring, the EN and HN parts of the radial nerves are all neuroepithelia composed of supporting cells (glial cells) and neurons.

According to ultrastructural characters, three types of neurons were identified in the radial nerve cord of a sea cucumber (Mashanov *et al.*, 2006): **(1)** putative primary sensory neurons, whose cilium protrudes into hyponeural canal; **(2)** non-ciliated neurons with swollen rough endoplasmic reticulum cisternae; **(3)** and monociliated neurons that are embedded in the trunk of nerve fibers. The neurons can be found in the periphery of both HN and EN components with the central portion, or neuropile, made up of nerve fibers. Different types of synapses occur in the neuropile area and they meet all morphological criteria of classical chemical synapses.

Innervation of organs occurs by peripheral nerves that emerge from the RNCs. In the extremities of the arms, the RNCs are connected with the pigmented eye spots, the only specialized sensory organs identified, with the exception of dispersed sensory cells within the epidermis that function as primary sensory receptors of light, contact, and chemical stimuli (Yoshida *et al.*, 1966). The integrity of the radial nerves and the circumoral nerve ring was shown to be essential for the coordination of tube feet, controlling the movement of starfish.

As previously stated, one of the frequent misconceptions related with echinoderm central nervous system is that it has long been seen as being absent of glial cells. This might be derived from the fact that standard commercially available antibodies failed to unambiguously immunolocalize these cells in echinoderm nervous system (Mashanov *et al.*, 2010). However, it was previously shown that non-neuronal cells of the starfish and sea cucumber nervous system are capable of producing the so called Reissner´s substance (Mashanov *et al.*, 2009; Viehweg *et al.*, 1998), which in vertebrates is known to be secreted by a phylogenetically conserved secretory radial glial cell subtype (Lichtenfeld *et al.*, 1999). Encouraged by these results, Mashanov and colleagues produced two novel monoclonal antibodies that specifically recognized echinoderm glial cells (Mashanov *et al.*, 2010) that in combination with epifluorescence, confocal and electron microscopy allowed to describe the echinoderm glial features for the first time. According to this study echinoderm glia shares striking similarities with the radial glia of chordates and the basic features include: ***(a)*** an elongated shape; ***(b)*** long radial process; ***(c)*** short lateral protrusions branching from the main processes and penetrating into the surrounding neuropile, ***(d)*** prominent orderly oriented bundles of intermediate filaments, and ***(e)*** ability to produce Reissner´s substance. Radial glia account for the majority of glia cells in echinoderms and constitutes more than half of the total cell population in the radial nerve cord and about 45% in the circumoral nerve ring. The difference in glial cell number between those regions is significant, suggesting structural specialization within the seemingly simple echinoderm nervous system.

Concerning the centralization of echinoderms nervous system there are currently two different viewpoints; **(A)** one that states that the circumoral nerve ring and the immediately adjacent nerve cords act as control centers that drive behavior of the entire animal (Smith, 1966) and; **(B)** the widely accepted hypothesis that the echinoderm nervous system is not centralized, and that the radial nerve ring merely serves to connect the radial

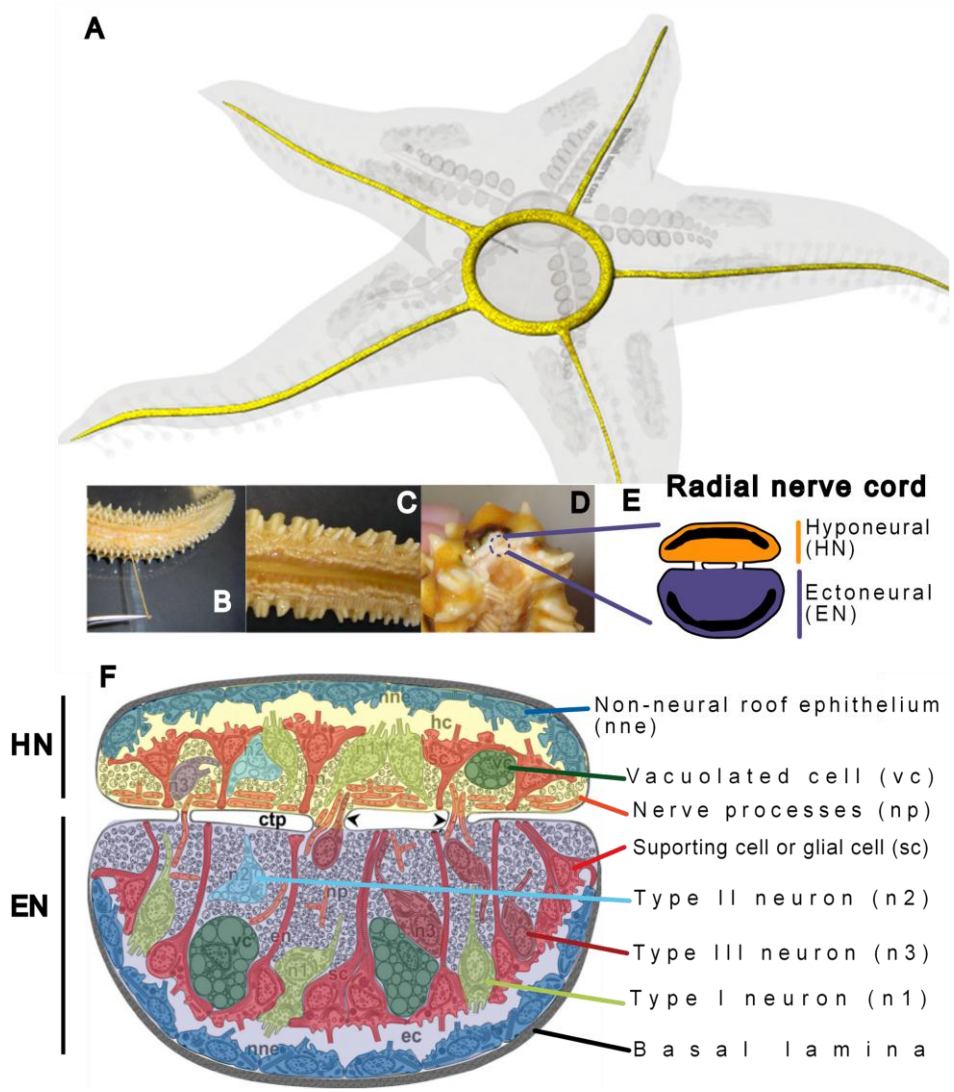

Figure 1.18. Structure of the radial nerve cord of an echinoderm. **A**, General representation of starfish nervous system; **B,** Radial nerve cord being extracted from the radial canal localized on the oral side of the starfish body. **C,** Detailed picture of the radial canal; **D,** Picture of a transverse cut through the arm tip of the radial nerve cord with the radial nerve details highlighted in E; **E**, Higher magnification of the circled area in C showing the organization of the hyponeural and ectoneural nerve bands in the radial nerve cord. **F**, Schematic reconstruction of a transverse section through the radial nerve cord (adapted from Mashanov *et al.*, 2006), arrowheads show the short nerves that connect the ectoneural and hyponeural subsystems. *bl*, basal lamina; *ctp*, connective tissue partition; *ec*, ectoneural canal; *en*, ectoneural band of the RNC; *hc*, hyponeural canal; *hn*, hyponeural band of the RNC; *nne*, non-neural epithelium; *np*, nerve processes; *n1*, type I neuron; *n2*, type II neuron; *n3*, type III neuron; *sc*, supporting cell or glial cell; *vc*, vauolated cell.

nerve cords together and to mediate the interaction between them. According to holothurians nervous system ultrastructure, the cellular composition and histological organization are identical between the ectoneural ring and cords (Mashanov *et al.*, 2006) favoring the decentralization theory.

Mashanov and co-workers also described the cellular events that take place during regeneration of radial nerve cord of the sea cucumber using light and transmission electron microscopy (Mashanov *et al.*, 2008) providing a great understanding of time graded cellular events. According to this highly detailed report, shortly after lesion, it is possible to observe an extensive nerve fiber degeneration and neuronal apoptosis detectable in both ectoneural and hyponeural neuroepithelia that persist, to a varying extent, for the entire duration of the experiment. This was later confirmed using TUNEL assay in another species of sea cucumber (Miguel-Ruiz *et al.*, 2009). It is postulated by these authors that apoptotic events are recapitulating the known embryonic developmental process of overproducing neurons, that will eventually be discarded, as it is observed during embryonic development in vertebrates, where about half of the neurons that are formed in the spinal cord undergo apoptosis (Oppenheim, 1991). The gap created in the sea cucumber nerve cord is rapidly bridged, at first by connective tissue that became covered by the regenerating coelomic epithelium and subsequently by regenerating nerve tissue. On both sides of the wound, the ectoneural and hyponeural components of the injured RNC form separate tubular rudiments, with the epithelial walls composed by dedifferentiated glial cells, capable of mitotic division, and also some nerve fibers and occasional neuronal perikarya. The authors further suggest that the glial cells play a crucial role in regeneration by both providing the necessary guiding scaffold support and, by producing new neurons. Another highlighted mechanism of injured radial nerve regeneration involves the proliferation and migration of the existing perikarya. Finally, the anterior and posterior regenerating nerves grow towards one another and eventually fuse to restore nerve continuity. The gliocytes and accumulated nerve cells in the site of injury go through a process of re-differentiation making the fully regenerated RNC indistinguishable from the intact cord at a histological level. The authors further conclude that echinoderms regenerating features are shared with vertebrates which also can regenerate and include:

A) The regeneration permissive environment of the radial nerve cord, in which both the intact and regenerating nervous tissues contain no myelin;
B) The absent glial scar;
C) Echinoderm neuroepithelia is supported also by glial cells;
D) The important function enrolled by glial cells providing both new nerve and glial cells and also providing a guided migration to newly forming neurons.

1.4.1.2.3. The genomic view of an echinoderm nervous system

The analysis of the sea urchin genome allowed an unprecedented glimpse into echinoderms nervous system (Burke *et al.*, 2006). This genomic data allowed the identification of several homologues of genes involved in neurogenesis. This was of extreme importance because shared and/or missing components and pathways have the potential of revealing how metazoan neurogenic gene regulatory networks have been shaped by evolution to produce the vertebrate nervous system. Furthermore, the several classes of orthologue genes allowed to further shape in detail the complexity of echinoderms nervous system, and were the ultimate prove for long contradicting questions concerning the biology of neuronal transmission in echinoderms:

1) Several genes required for synapse formation and function were identified (neuroligin; β-neurexin; agrin; MUSK; thrombopondin), as also genes encoding for proteins necessary for neurotransmitter synthesis and transport;
2) A large family of G-protein coupled receptors were identified including rhodopsin-type receptors, metabotropic glutamate-like receptors and secretin receptor-like proteins;

3) Genes coding for both gap junction proteins (connexins and pannexins) and also cannabinoid, lysophospholipid and melanocortin receptors were not identified;
4) Several G-protein coupled peptide receptors and precursors for several neuropeptides and peptide hormones were identified, that include insulin and IGF family;
5) Identification of a neurotrophin-like and Trk receptors indicates that these neuronal signaling systems are not exclusive to chordates;
6) The expression of a set of retinal genes in the tube feet, which are non-ocular structures, provide new understanding in how these animals perceive light, suggesting that these structures function also as photosensory organs.

1.4.1.3. Starfish arm tip regeneration events

The morphological events of starfish arm regeneration have been extensively studied and characterized in several asteroid species such as *Asterias rubens* (Moss *et al.*, 1998; Hernroth *et al.*, 2010), *Leptasterias hexactis* (Mladenov *et al.*, 1989) and *Asterias rollestoni* (Tingjun *et al.*, 2011). Even though it has been recognized that the mechanisms of cellular/tissue regeneration can be much more flexible than the reductive dichotomic view (morphallaxis *vs* epimorphosis), that can somehow overlap (Carnevali *et al.*, 2001), in starfish, the morphallactic process of regeneration seems to be the main motor of tissue replacement and regrowth due to the absence of a blastema-like structure formation as the center of cell proliferation. This is so whether the ablation site is traumatic or in the natural autotomy plane (Mladenov *et al.*, 1989; Moss *et al.,* 1998). In contrast with other echinoderms, starfish have only a single autotomy plane for each arm (Wilkie, 2001); located at the base of the arm, close to the central disc, which causes a relatively large wound when the arm is sacrificed. The morphallactic regenerative process has been characterized has being slower when compared with the epimorphosis of ophiuroids and crinoids, with no sign of particular increase in cell proliferation at the site of regeneration (Mladenov *et al.*, 1989; Moss *et al.*, 1998; Carnevali, 2006; Carnevali *et al.*, 2009). It is only during the latter stage of arm tip re-growth that is observed an increased proliferation, both in the adjacent tissues, such as the coelomic epithelium (Mladenov *et al.*, 1989) and the growing tip itself (Moss *et al.*, 1998). Recent research using lipofuscin and DNA damage markers in regenerating tissues indicates that the "new" arms do not form from aging cells but rather from physiological young cells, more likely originated from progenitor/stem cells recruited from more distant and different tissues such as, the **coelomic epithelium**, which showed a mitogenic response in both wound healing and the subsequent regeneration; and the **pyloric caeca** (Hernroth *et al.*, 2010), in which the authors consider that the large mitotic cells observed might also be originated in the coelomic epithelium which is also one of the three layers that constitutes the gut of Asteroidea. Based on these recent findings, authors propose a new working hypothesis for the morphallactic process of arm regeneration in starfish which include four phases: **(1)** wound healing with the accumulation of coelomocytes, **(2)** migration of distant non-aging cells of mixed origin, including the pyloric caeca and coelomic epithelium, **(3)** proliferation in these organs to compensate for cell loss, and finally **(4)** local proliferation in the regenerating arm (Hernroth *et al.*, 2010).

Of consensual agreement to both authors (Hernroth *et al.*, 2010; Moss *et al.*, 1998) are the time events of the different stages of arm re-growth of *Asterias rubens*: A wound healing phase during the first week after injury, with increased cellular proliferation in distal organs including the coelomic epithelium and pyloric caeca; early regeneration phase up to 5 weeks, with increased cellular proliferation and the subsequent arm re-growth stage, with already a high degree of differentiation with even the eyespots being visible at approximately 10 weeks (Hernroth *et al.*, 2010) and with a pronounced cellular proliferation in regenerating tissues and a decline in distal organs. This is in agreement with morphallactic-like hypothesis for the regeneration in starfish, where a mixed population is proposed to migrate to the injury site, as there is a lack of blastema formation (Mladenov *et al*., 1989; Moss *et al*., 1998).

1.4.1.4. Molecular insights of echinoderm regeneration

Although in the past years most of regeneration studies on echinoderms have investigated the histological and cellular aspects, more recently, echinoderm scientists have focused their attention on candidate genes (Bannister *et al.*, 2005; Patruno *et al.*, 2002; Patruno *et al.*, 2003; Thorndyke *et al.*, 2001b; Ikuta, 2011) and development processes associated with signaling pathways, whose functions were deduced from studies on other model organisms (Martini *et al.*, 1988; Henry *et al.*, 1996; Michlopoulos *et al.*, 1997; Wu *et al.*, 2000; Buonanno *et al.*, 2001; Raya *et al.*, 2003; Jadlowiec *et al.*, 2004; Karhadkar *et al.*, 2004; Harada *et al.*, 2005; Stoick-Cooper *et al.*, 2007). This was of extreme importance to evaluate if the pathways in question shared equal importance in echinoderm regeneration events and thus, have been conserved throughout evolution. However, since echinoderms have such extraordinary regeneration capacities that are not shared with the majority of chordates, there is a high probability that they also do not share some of the responsible pathways. For such discoveries, unbiased experimental procedures are of extreme importance, and already were successful in describing some additional target genes associated with regenerative process (Santiago *et al.*, 2000; Suarez-Castillo *et al.*, 2004; Sun *et al.*, 2005; Rojas-Cartagena *et al.*, 2007) even if having an insufficient genome-wide profiling information.

So far only a limited amount of research has been undertaken on large scale gene expression profiles. The few conducted studies were mainly centered in understanding expression profiles of gene activity during intestinal regeneration in the sea cucumber (Rojas-Cartagena *et al.*, 2007; Ortiz-Pineda *et al.*, 2009; Sun *et al.*, 2011). In the study conducted by Sun and colleagues (Sun *et al.*, 2011), high throughput 454 cDNA sequencing was used to compare the transcripts of both uninjured and injured sea cucumbers. These authors state that during regeneration, the mRNA levels of hundreds of genes were significantly different from baseline levels of the control animals. Altogether, 324 and 80 genes were significantly up-regulated and down-regulated, respectively. Many of the transcriptional differences correlated with organogenesis and cellular process and were similar to the differential expressed genes of other species, such as the salamander (Monaghan *et al.*, 2009). The differently expressed genes included **genes associated with development**, such as **Hox genes**, which were also found to be over expressed in a different sea cucumber species during intestinal regeneration (Ortiz-Pineda *et al.*, 2009) and are known to be involved in the regeneration process of axolotl, newt regenerating limbs (Beauchemin *et al.*, 2004; Gardiner *et al.*, 1996), hydra (Schummer *et al.*, 1992), rat liver (Mizuta) and zebrafish fin (Thummel *et al.*, 2007). The **BMP family proteins** (bone morphogenic proteins) were also found to be differently expressed in the sea cucumber (Ortiz-Pineda *et al.*, 2009; Sun *et al.*, 2011). These important growth factors are known to be involved in the regulation of bone formation and growth in zebrafish fin regeneration (Smith *et al.*, 2006), tail and limbs regeneration in *Xenopus sp*. tadpoles (Beck *et al.*, 2006), axolotl limb skeletal regeneration (Satoh *et al.*, 2010), planarian axis pattern establishment during regeneration (Molina *et al.*, 2007; Reddien *et al.*, 2007), and gastrointestinal and skin development in vertebrate (Batts *et al.*, 2006; Owens *et al.*, 2008). **Krueppel-like factors** (KLFs) were also found to have an important role during sea cucumber intestinal and body wall regeneration. These factors are members of the zinc-finger family of transcription factors capable of binding GC-rich sequences that regulate a diverse array of developmental events and cellular processes, such as maintenance of stem cells, epithelial barrier formation, control of cell proliferation, skeletal and smooth muscle development, intestinal cell development, and retinal neuronal regeneration (Swamynathan, 2010). Several differentially expressed **ECM-associated genes** were also identified and include the proteins, collagen and laminin, also identified in sea cucumber *H. glaberrima* (Quinones *et al.*, 2002), and the metalloproteinase MMP14 that has been directly associated with ECM remodeling during regeneration. Several **cytoskeleton-associated genes** were found to be differently regulated, in which authors correlated this observation with events of muscle dedifferentiation processes as previously described (Monaghan *et al.*, 2009). Interestingly, several genes that might be responsible for **epigenetic reprogramming** during regeneration have also been identified and include genes encoding for proteins responsible for chromatin remodeling, DNA methylation, transcriptional regulation, and histone modification. In the gene expression profile experiments conducted by Ortiz-Pineda and colleagues, also a **Wnt**

homologue (WNT-9) was overexpressed in the regenerating intestine during the first two weeks of regeneration (Ortiz-Pineda *et al.*, 2009). Wnt pathways have been increasingly associated with regenerative phenomena. Wnt was found to be involved in blastema formation of the regenerating limbs of anuran tadpoles (Yokoyama *et al.*, 2007) and in lens regeneration in newts (Hayashi *et al.*, 2006). In mammals, Wnt has been studied in bone (Kim *et al.*, 2007), hair follicle (Ito *et al.*, 2007) and deer antler regeneration (Mount *et al.*, 2006) among others. In planaria, Wnt is necessary for proper brain pattern formation (Kobayashi *et al.*, 2007) and B-catenin for antero-posterior axis formation during regeneration (Gurley *et al.*, 2008).

1.4.1.5. Echinoderms and proteomics

Homology-driven proteomics allows the characterization of proteomes from organisms with unsequenced genomes, since if both analyzed unknown proteins and reference proteins from unrelated species belong to conserved protein families, a few identical peptides fragmented in MS/MS experiments might enable their direct cross-species identification by conventional database searching means (Junqueira *et al.*, 2008). However, so far only few **proteomic characterizations** of echinoderm tissues were performed, such as the characterization of the proteome and phosphoproteome of test and spine (Mann *et al.*, 2008; Mann *et al.*, 2010); the characterization of the protein components from the mature ovary of the sea urchin (Sewell *et al.*, 2008) and proteome of the developing tooth of the sea urchin (Alvares *et al.*, 2007). Also, few **differential proteomics** were performed on different echinoderm research areas or using echinoderm as model organisms such as, the characterization of the immune responses mediated by echinoderms coelomocytes (Dheilly *et al.*, 2009 and 2011); the identification of proteins exhibiting turnover and phosphorylation dynamics during sea urchin egg activation (Roux *et al.*, 2008) and dissecting the mechanism of Ca^{2+}-triggered membrane fusion on sea urchins oocytes (Furber *et al.*, 2010). Nevertheless, unbiased proteomic approaches were not yet applied to study echinoderms regeneration events, a field in which I hope to contribute with proteomics-derived knowledge that hopefully will lead to a better understanding of molecular pathways behind echinoderm regeneration events.

1.4.1.6. The model: Starfish Marthasterias glacialis

Marthasterias glacialis (Linné, 1758) (spiny starfish), is an asteroid echinoderm, a group that has demonstrated to play one of the most influential roles in benthic ecosystems on a variety of scales (Verling *et al.*, 2003). Its range extends from the north of Finland (*glacialis* means icy, frozen, or glacial; also referring to the water conditions it prefers) across the Mediterranean Sea and the Adriatic Sea to the Guinean Gulf (Mortensen, 1927). This starfish can be found in extreme low water to about 200 m in a variety of habitats from sheltered muddy sites to wave exposed rock faces. *M. glacialis* is a major predator of marine animals, including other echinoderms such as sea urchins (Savy, 1987), with mussels being the preferred prey. This starfish species can attain 70 cm in diameter, however is commonly found with 25-30 cm. Each arm bears three longitudinal

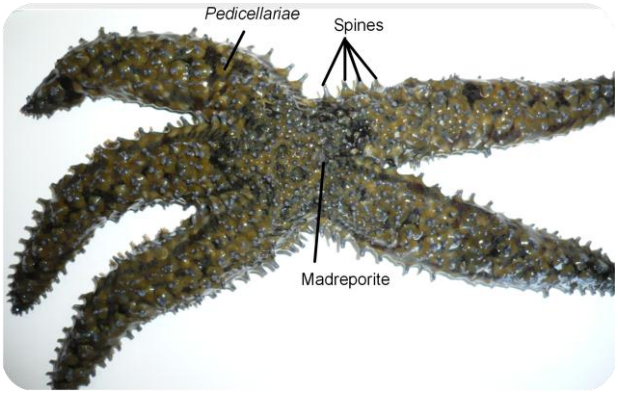

Figure 1.19. *Marthasterias glacialis* with some morphological features highlighted.

rows of spike-like spines surrounded by large cushions of pedicellariae with smaller spines scattered between these rows (Figure 1.19). The animals show a variation in color from dirty brown to greenish-grey.

During the period 1940–1950s, this species received great attention, mainly due to its asterosaponins (Minale *et al.*, 1982). Nowadays, *M. glacialis* allowed to characterize cytotoxic carotenoids (Ferreres *et al.*, 2010); the nature of mutable collagenous tissues of echinoderms (Santos *et al*., 2005); the identification of novel neuropeptides (Yun *et al.*, 2007) and the anti-adhesive glycoproteins present in starfish mucus (Bavington *et al.*, 2004) amongst several other scientific reports.

M. glacialis is one of the most commonly seen starfish species in the Portuguese coast. There were several other reasons for choosing this echinoderm species as model for the conducted studies, ***1)*** this starfish is easy to collect since it can be found abundantly in exposed rock surfaces in Estoril coast, especially during winter time; ***2)*** it is easy to maintain in a controlled aquarium environment and; ***3)*** like other starfish species, *M. glacialis* remarkable regenerative capabilities allows the survival and regeneration of a new individual if a fifth of the central disk remains attached to the lost arm. At the molecular level, this regeneration capability is mainly a morphallactic process occurring in the absence of a blastema-like structure. Since this regenerative process is more complex and slow, in *M. glacialis* it can vary from just 15 to 20 weeks to fully regenerate a lost arm tip, or up to several months in the case of an autotomized arm.

1.5. Proteomics

All cellular processes involve proteins, and therefore their characterization has drawn an exponential interest over the years. Initially this was performed by targeted approaches, such as western blot or microscopy. Although a great number of cellular processes were unraveled, often these approaches open only a narrow window of the complexity of processes occurring simultaneously. For these reasons, unbiased high throughput approaches are of extreme importance. A great breakthrough in this direction was the development of **microarrays**, which enable the global quantification of gene expression. However, it is also true that mRNA levels often do not correlate well with protein abundance in the cell. This is because protein levels are determined by complex post-transcriptional processes, where every step in the life-cycle of a protein, from its synthesis to its degradation, is subject to regulatory input (Mann *et al.*, 2003). Furthermore, the central role of covalent protein modifications, such as phosphorylation, acetylation, and glycosylation in cellular physiology as signals in information processing or, as marks mediating protein associations is becoming increasingly appreciated (Mann *et al.*, 2003). These modifications can also guide assembly of proteins into large macromolecular machines or instruct their localization to different organelles. Among different possible approaches to study proteins, proteomics-mass spectrometry based approaches is increasingly being used to understand these processes.

The simplest definition of *proteome* was first introduced by the geneticist Marc Wilkins stating that the **proteome** is comprised by the complete set of "**proteins expressed by a given genome**" (Wilkins *et al.*, 1996). Although this date does not mark the birth of proteomics, since SDS electrophoresis for the separation of proteins was first introduced in 1970s (Laemmli, 1970), it is definitely a landmark of the blooming of the proteomics era, with the introduction of soft ionization techniques such as **matrix-assisted laser desorption ionization (MALDI)** (Karas *et al.*, 1985) or **electrospray (ESI) ionization** (Fenn *et al.*, 1989) (Figure 1.20) into the field of mass spectrometry allowing to determine **mass-to-charge ratio** (*m/*z) of biological molecules including proteins; preceded with the

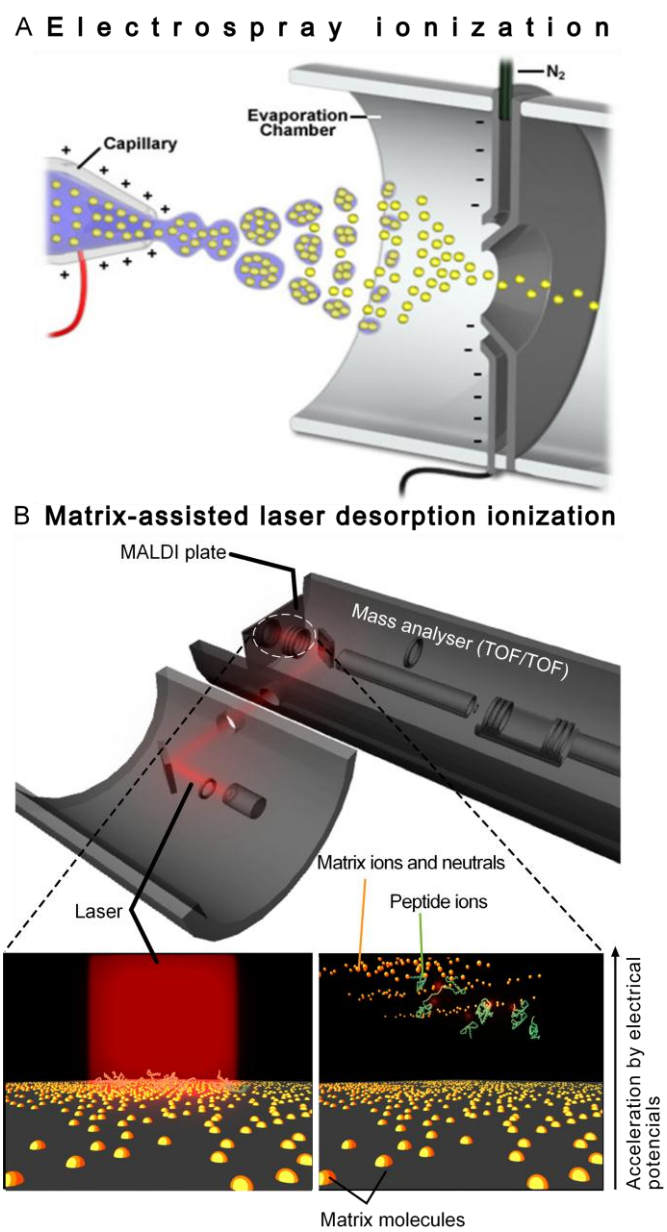

Figure 1.20. Soft ionization modes in biological mass spectrometry. Mass spectrometers consist of three parts: an **ionization source**, responsible for converting analyte molecules into gas-phase ions; a **mass analyzer** that separates ions according to their *m/z* and an ***ion detector*** (Yates, 2000). Under soft ionization technologies, such as electrospray ionization (ESI) or matrix-assisted laser desorption ionization (MALDI), it is possible to maintain covalent bonds enabling the analysis of large molecules, such as protein and peptides. **A**, electrospray ionization involves the generation of peptide ions from aqueous solution. The solution containing the sample passes through a needle subjected to a high voltage. The solution stream is ejected from the needle orifice as a spray of droplets. The solvent is eliminated from the droplets by a heated capillary or an inert gas. Solutions with acidic pH favor protonation of the N-terminal amines and histidine nitrogens, and peptide fragmentation is facilitated when the peptide ions are positively charged. Thus, ESI protocols commonly include acidification steps prior to peptide ion analysis in the mass analyzer (Lim *et al.*, 2004). **B,** In MALDI, peptides are co-crystallized with a UV absorbing matrix that transfers the energy of the laser to the biomolecules promoting desorption into the gas-phase and ionization (Zhu *et al.*, 2003).

introduction of mass spectrometry-based methods for protein identification such as **peptide mass fingerprint** (Henzel *et al.*, 1993; James *et al.*, 1993; Pappin *et al.*, 1993; Yates *et al.*, 1993) or **tandem mass spectrometry** to obtain sequence information from fragmented peptides (Roepstorff, 1984) (**BOX 1.1**).

Nowadays proteomic experimental approaches have expanded from the classical identification of all the proteins in a given tissue to include **1) functional proteomics,** the quantification and identification of the **differently expressed** proteins among distinct conditions; **2)** the identification of **protein-protein interactions** and **3)** the

BOX 1.1. Peptide mass fingerprint and tandem mass spectrometry for peptide sequencing. Peptide Mass Fingerprinting (PMF) is a strategy used to identify proteins by matching their constituent fragment masses (peptide masses) to the theoretical peptide masses generated from a protein or DNA database and is most suitable for the identification of proteins from species for which complete genome sequences are available. The first step in PMF is that an intact, unknown protein is cleaved with a proteolytic enzyme to generate peptides. A PMF database search is usually employed following MALDI TOF mass analysis. The premise of PMF is that every unique protein will have a unique set of peptides and hence unique peptide masses. Identification is accomplished by matching the observed peptide masses to the theoretical masses derived from a sequence database. PMF identification relies on observing a large number of peptides, 5+, from the same protein at high mass accuracy. This technique does well with 2D gel spots where the protein purity is high. PMF protein identification can run into difficulties with complex mixtures of proteins. PMF for the identification of proteins became quite popular in early 90´s due to the introduction of a MALDI TOF instrument capable of 50 ppm mass accuracy that made PMF routine (Mann *et al.*, 1993; Henzel *et al.*, 1993).

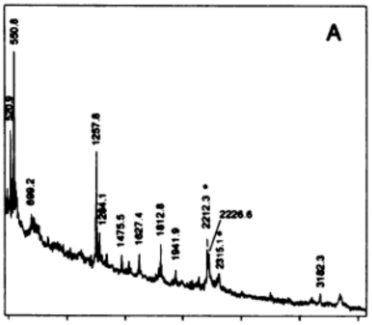

MALDI mass spectra of *in situ* tryptic digestion cysteine synthase A (image taken from Henzel *et al.*, 1993)

Peptide sequencing by tandem mass spectrometry is based upon the random cleavage of the peptide bonds between adjacent amino-acid residues in a peptide sequence achieved by collision-induced dissociation (CID). The accepted nomenclature for fragment ions was first proposed by Roepstorff and Fohlman (Roepstorff, 1984), and the types of fragment ions observed in an MS/MS spectrum depend on many factors. If this charge is retained on the N-terminal fragment, the ion is classed as either a, b or c. If this charge is retained on the C terminal, the ion type is either x, y or z. The number in subscript indicates the number of residues in the fragment.

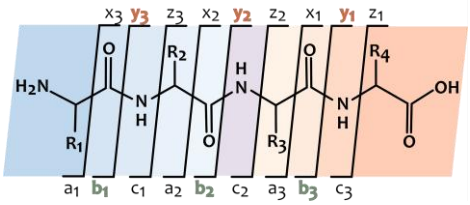

Peptide fragmentation annotation using the scheme of Roepstorff *et al.*, (1984).

Using a MALDI-TOF/TOF with collision gas (CID or CAD) all ion series can be seen and can be accompanied by composition dependent satellites due to loss of ammonia or water. However, usually the most abundant fragment ion types observed are a, b, and y.

The **peptide sequence tag approach** is used to identify proteins based on their fragmentation spectra. Briefly, a couple of masses are extracted from the spectrum in order to obtain the peptide sequence tag, which is a unique identifier of a specific peptide and can be used to find it in a database containing all possible peptide sequences (Mann *et al.*, 1994).

In case of unassigned peptides, it is often useful to use tandem mass information to discover or confirm the presence of post-translational modifications and also to identify new proteins through *de novo* sequencing strategies (Steen *et al.*, 2004).

characterization of proteins **post-translational modifications (Table 1.3)**, which are covalent processing events that change the properties of a protein either by proteolytic cleavage or by addition of a modifying group to one or more amino acids (Mann *et al.*, 2003).Generally, in such studies proteins are extracted from tissues and then separated using a set of complementary approaches, such as **two-dimensional polyacrylamide gel electrophoresis** (2DE) **or gel free based approaches** prior to mass spectrometry. Although nowadays there is still an active discussion on the *pros* and *cons* of the main approaches to follow in the Proteomics field, 2DE is still one of main approaches used in proteomics. This sound and mature methodology is still the target of constant method optimizations that increase the number of protein to be analyzed, *i.e.*, by improving protein extraction yields from tissues (Butt *et al.*, 2005); increasing protein detection sensitivity (Harris *et al.*, 2007) and improving the solubilization of traditionally difficult samples such as membrane proteins, acidic or basic proteins; low abundance, amongst others (Churchward *et al.*, 2007). 2DE enables the separation of complex mixtures of proteins in an isolated gel spot according to their isoelectric point (*pI*) (1^{st} dimension) and molecular mass (*M*) (2^{nd} dimension), and just from **one single analysis** it provides the information on **protein charge**, **abundance**, **localization**, **isoforms** and **post-translational modifications**. This is in contrast with gel-free based approaches such as liquid chromatography-tandem mass spectrometry based methods, which performs analysis on peptides consequently losing information on *M*, *pI* and protein isoforms.

Depending on the gel size and *pH* gradient used in the first dimension, 2DE can resolve more than 5000 proteins simultaneously (Görg *et al.*, 2004) however, it is the subsequent choice of protein detection method; such as colloidal Coomassie, fluorescent dyes or reactive fluorophores; that will determine the limit of detection and the

Table 1.3. Some common and important post-translational modifications (adapted from Mann *et al.*, 2003)

PTM type	ΔMass (Da)*	Stability**	Function and notes
Phosphorylation pTyr pSer, pThr	 +80 +80	 +++ +/++	Reversible, activation/inactivation of enzyme activity, modulation of molecular interactions, signaling
Acetylation	+42	+++	Protein stability, protection of N-terminus. Regulation of protein-DNA interactions (histones)
Methylation	+14	+++	Regulation of gene expression
Acylation, fatty acid modification Farnesyl Myristoyl Palmitoyl Etc.	 +204 +210 +238	 +++ +++ +/++	Cellular localization and targeting signals, membrane tethering, mediator of protein-protein interactions
Glycosylation *N*-linked O-linked	 >800 203. >800	 +/++ +/++	 Excreted proteins, cell-cell recognition/signaling *O*-GlcNac, reversible, regulatory functions
GPI anchor	>1000	++	Glycosylphophatidylinositol (GPI) anchor. Membrane tethering of enzyme receptors, mainly to outer leaflet of plasma membrane
Hydroxyproline	+16	+++	Protein stability and protein-ligand interactions
Sulfation (sTyr)	+80	+	Modulator of protein-protein and receptor-ligand interactions
Disulfide bond formation	-2	++	Intra- and intermolecular crosslink, protein stability
Deamination	+1	+++	Possible regulator of protein-ligand and protein-protein interactions, and also a common chemical artifact
Pyroglutamic acid	-17	+++	Protein stability, blocked N-terminus
Ubiquitination	>1000	+/++	Destruction signal. After tryptic digestion, ubiquitination site is modified with the Gly-Gly dipeptide
Nitration of tyrosine	+45	+/++	Oxidative damage during inflammation

* A more comprehensive list of PTM Δmass values can be found at http://www.abrf.org/index.cmf/dm.home

** Stability: + labile in tandem mass spectrometry, ++ moderately stable, +++ stable.

linear dynamic range of the detectable proteins (for a complete review on protein detection methods see Gauci *et al.*, 2010). Furthermore, specific protein stains can be used to detect protein post-translational modifications such as Pro-Q Diamond for phosphoproteins or Pro-Q Emerald for glycoproteins, which can later be confirmed using the appropriate mass spectrometry methodologies (Mann *et al.*, 2003).

1.5.1. Proteomics approaches to study neuronal regeneration events

The fact that neurons exhibit an extremely polarized morphology (*i.e.*, in some species the axons can extend up to one meter from neuron cell body) implies the high complex nature of the intracellular signaling pathways within the nervous system. The synaptic machinery itself is thought to be composed of more than a thousand interacting proteins that include diverse signaling pathways, several protein post-translational modifications and highly sophisticated intracellular transport systems (Grant *et al.*, 2005). Further challenges arise if the axon is separated from the neuron soma through an injury, an event that needs to be efficiently communicated back to the nucleus, in order to initiate the proper regenerative response. Two different types of communication events are initiated with an injury, which occur as temporally graded signals. They are categorized as ***injury negative signals***, and include the cessation of the membrane action potentials and the interruption of the normal supply of transported molecules along the axon, and; the ***injury positive signals*** that include a vast range of synthesized proteins and activated/modified molecules at the injury site, that further engage the retrograde transport system to travel back to the cell soma in order to modulate changes in transcription and translation patterns to induce the regenerative response (Figure 1.21) (reviewed in Abe *et al.*, 2008; Rishal *et al.*, 2010; Snider *et al.*, 2002).

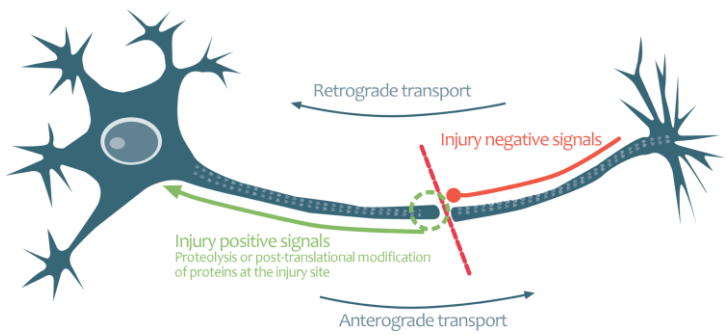

Figure 1.21. Different modalities of retrograde injury signaling. Negative signals include the loss of electrophysiological signal and the loss of constitutive trophic factors. Positive injury signals include the formation of *de novo* or modified molecules at the injury site that will further travels to neuronal soma as injury signals.

As it is well known, some neurons retain the ability to functionally regenerate and extend axons in case of an injury, as the case for certain neurons in the peripheral nervous system (PNS) of mammals. Dorsal root ganglion (DRG) neurons are an elegant mammalian PNS model that allowed proving that the signals elicited at the injury site have the capacity to increase the intrinsic growth ability of neurons (positive injury signals). This phenomenon is referred to as “conditioning lesion” and it is based on the fact the DRG neurons possess two axonal branches, a peripheral axon that regenerates when injured and a centrally projecting axon that does not regenerate following injury. Nevertheless, if an injury is inflicted in the peripheral branch prior to injury to the central branch, these last (normally, not regenerating axons) can re-grow normally (Richardson *et al.*, 1984).

Some nervous systems present a complete inability of neurons to regrow across a lesion site, which is the case of the adult mammalian central nervous system (CNS), due to the inhibitory nature of the neuronal environment, the loss of the intrinsic growth capacity concomitant with nervous system differentiation and the inappropriate immune responses. Several efforts have been made to identify the inhibitory factors present in the

environment, which include the glial scar (for reviews see Silver *et al.*, 2004; Tang *et al.*, 2003) and molecules such as Nogo, myelin-associated glycoprotein (Schwab, 2004; Llorens *et al.*, 2011) among several others (Yiu *et al.*, 2006).

Nowadays, **proteomic-mass spectrometry** based approaches are increasingly being used in the field of regeneration to determine both basic and clinical differential protein expression, protein-protein interactions and post-translational modifications. In the field of nerve regeneration, these approaches are being recognized as extremely useful because changes in axons after injury often occur without the contribution of transcriptional events in the cell body, and frequently involve proteolysis, local axonal protein synthesis and a broad range of post-translational modifications (reviewed in Sun *et al.*, 2010).There are several examples of successful case studies using proteomic approaches that have led to great breakthroughs. One example is the elegant study using *Lymnaea* (snail) neurons in culture and 2DE-MS approaches, which allowed the discovery of a calpain generated proteolytic fragment of an intermediate filament that sterically hinders the dephosphorylation of a positive injury signal (phosphorylated Erk) during its retrograde transport journey back to the cell body (Perlson *et al.*, 2004; 2005 and 2006). Other examples of molecular events involved in neuronal regeneration revealed by proteomics are summarized in Figure 1.22.

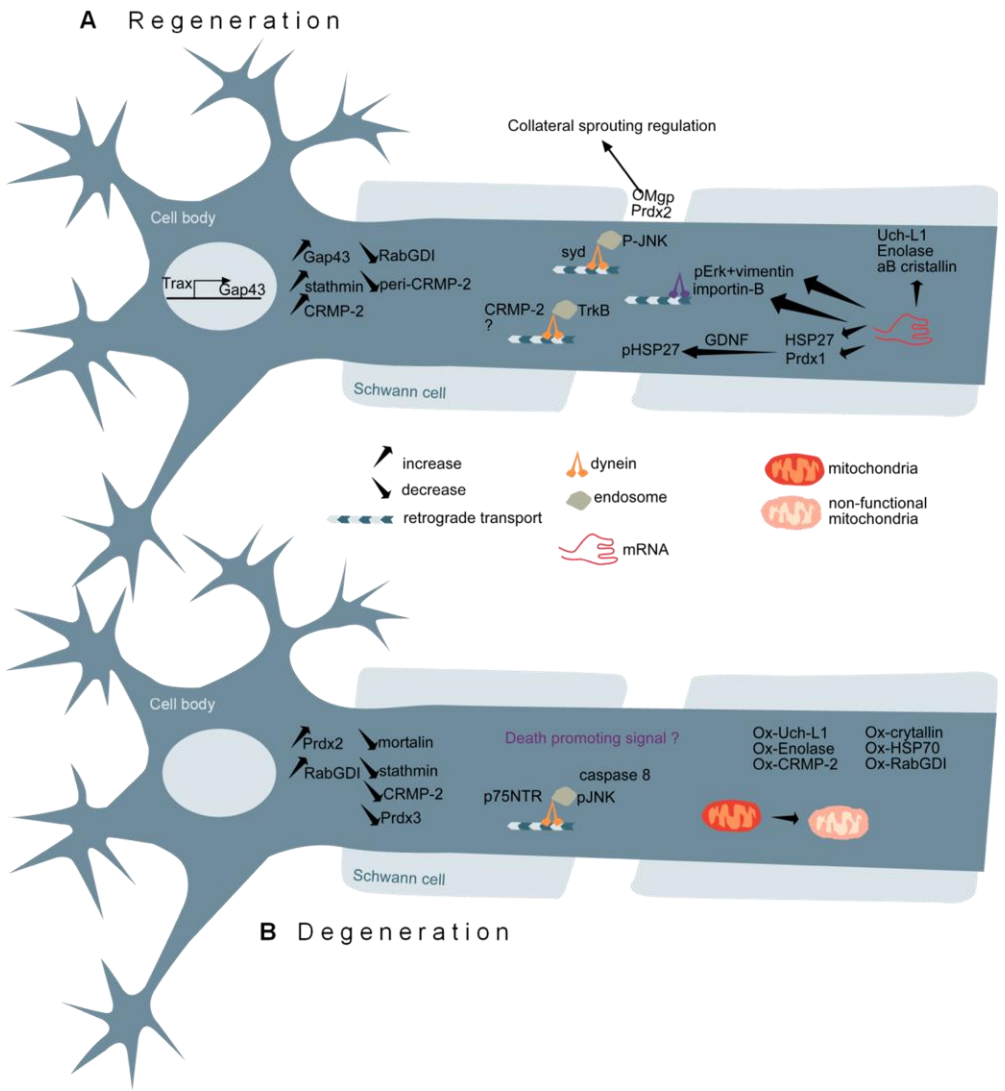

Figure 1.22. Molecular events involved in neuronal regeneration and degeneration as revealed by proteomics studies. A correlation emerges between axonal regeneration and degeneration: most proteins mediating regeneration are found to be either modified (and thus possibly malfunctioning) or reduced in degeneration. **A**, multiple molecular events contribute to regeneration. Elevation in protein levels of growth cone-enriched protein such as stathmin, GAP-43, and CRMP-2 enhances axonal outgrowth. The retrograde transport of several positive axonal injury signaling complexes plays a role in initiating the regeneration response. Chaperones (cristallin and HSP27) and antioxidant proteins (Prdx2) also contribute to axonal regeneration and collateral sprouting. **B,** proteins involved in promoting regeneration appear to be modified by oxidation, indicative of their possible malfunction during degeneration. Retrograde transport of a specific death signal and mitochondrial dysfunction also contribute to degeneration. *p*, phospho(…); *GDNF*, glial cell-derived neurotrophc factor; *GAPDH*, glyceraldehydes-3-phosphate dehydrogenase; *Prdx*, peroxiredoxin; *Trax*, translin-associated factor X (adapted from Sun *et al.*, 2010).

1.6 THESIS AIMS

The **general aim** of this thesis was to use **proteomics-mass spectrometry based approaches** to understand **regeneration events** triggered on starfish upon **arm tip-ablation**.

The **specific aims** include:

1. Proteome characterization of *M. glacialis* organs involved in the regeneration process, namely:
    a. **radial nerve cord (Chapter 2)**
    b. **coelomic fluid** and **coelomocytes (Chapter 3)**.

2. Understand the molecular **pathways responsible for radial nerve cord regeneration** by the identification and characterization of the radial nerve proteins that show an **injury correlated variation** during two distinct stages or arm tip regeneration events: **wound healing** and tissue **re-growth (Chapter 4);**

3. Perform a **preliminary characterization of phosphorylation dynamics** of radial nerve cord proteins during the immediate response to injury events (wound healing) **(Chapter 5)**.

CHAPTER 2

RADIAL NERVE CORD PROTEOME CHARACTERIZATION

CATARINA FERRAZ FRANCO[1], ROMANA SANTOS[1,2], ANA VARELA COELHO[1]

1: Instituto de Tecnologia Química e Biológica, Universidade Nova de Lisboa, Oeiras, Portugal;

2: Unidade de Investigação em Ciências Orais e Biomédicas, Faculdade de Medicina Dentária, Universidade de Lisboa, Portugal.

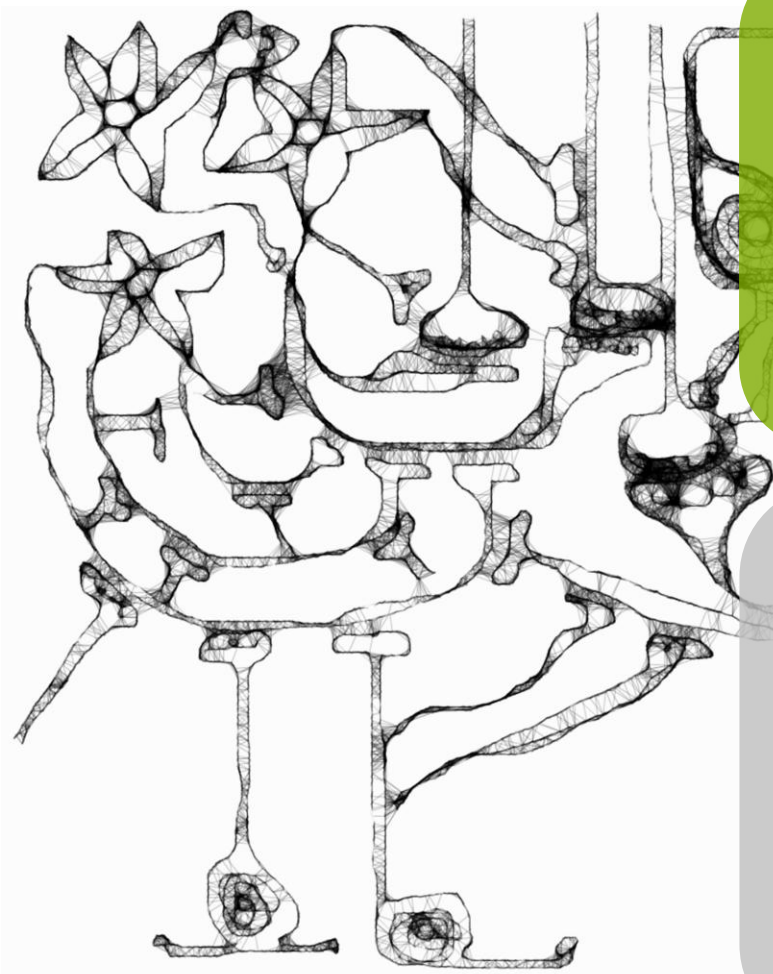

Image: Interpretation of starfish synapses.

PUBLICATIONS CONTAINING EXPERIMENTAL DATA PRESENTED IN THIS CHAPTER

Franco C., Santos R., Coelho A.V. (2011) Exploring the proteome of an echinoderm nervous system: 2DE of the Starfish radial nerve cord and the synaptosomal membranes subproteome. *Proteomics*. 11, 1359-1364. (Appendix 1)

Franco, C., Santos, R., Coelho, A.V. (2011) Expanded view of an echinoderm CNS proteome: The missing piece in the complex puzzle of deuterostome CNS evolution. Manuscript drafted. Journal to be defined.

AUTHORS CONTRIBUTION

Franco C.(CF), Santos R. (RS) and Coelho A.V (AVC) were responsible for the conception and design of the experiments. Tissue collection, optimization of protein separation protocols, 2DE experiments, 1DE experiments, nano-LC separation of peptides, MALDI-TOF/TOF data acquisition, protein identification, annotation, data analysis and interpretation were performed by **CF**. **CF** wrote the manuscript published in Proteomics and the draft of the manuscript "Expanded view of an echinoderm nervous system proteome: The missing piece in the complex puzzle of deuterostome CNS evolution" and RS and AVC revised them critically.

Supplementary material containing experimental data described in this chapter*

Supplementary table 2.1: *Non-redundant protein list* resulting from protein clustering and parsimony analysis of the identified proteins in *2DE* experiments of the radial nerve cord extracts from the starfish *Marthasterias glacialis*, identified by MALDI-TOF/TOF-MS. The table includes identified protein clusters, pathway analysis, MASCOT/ProteinPilot identification scores, sequence coverage, accession numbers, 2DE spot ID, sequences of the fragmented peptides and BLASTp results for unknown/uncharacterized and *S. purpuratus* proteins. Complete information on all identified spots per stage of protein identification is present in Supplementary data 2.2.

Supplementary data 2.2: Sequence and peptide information of all the proteins identified in the radial nerve cord of *M. glacialis* using the protein identification workflow described in materials and methods. Protein identification data are organized in three different spreadsheets according to the Protein identification Stages. To enable a more comprehensive reading of the tables, images of the 2DE gel annotated with the spots identified per protein identification stage are also shown.

Supplementary table 2.3: Protein clustering and parsimony analysis of the identified proteins in 1DE experiments of the synaptosomal enriched fraction of the radial nerve cord of *M. glacialis*. The table includes identified protein clusters, pathway analysis, ProteinPilot identification scores, sequence coverage, accession numbers, sequences of the fragmented peptides and BLASTp results for unknown/uncharacterized and *S. purpuratus* proteins. Complete information on all identified proteins per 1DE band is present in Supplementary data 2.4.

***Supplementary data 2.4*:** Sequence and peptide information of all the proteins identified in the synaptosomal enriched fraction of the radial nerve cord of *M. glacialis*. Protein identification data is organized in different spreadsheets per replicate.

Supplementary data 2.5: Sequence and peptide information of all the proteins identified in the 1D-nano-LC MALDI-TOF/TOF analysis of *M. glacialis* radial nerve cord soluble proteins.

***Supplementary data 2.6*:** Sequence and peptide information of all the proteins identified in the 1D-nano-LC MALDI-TOF/TOF analysis of *M. glacialis* radial nerve cord membrane proteins.

***Supplementary table 2.7*:** Non-redundant protein list resulting of all the identified proteins in the starfish radial nerve cord protein fractions with the correspondent GO annotations according to biological process, molecular function and cellular component.

* Please see enclosed CD to access the supplementary material

SUMMARY | RADIAL NERVE CORD PROTEOME CHARACTERIZATION

Efforts in determining the evolutionary origin of chordate central nervous system (CNS) has led scientists to look at their closest invertebrate deuterostome relatives, the echinoderms. Several morphological approaches have generated many hypotheses but ultimately been unable to decipher the homology of deuterostome CNS. This morphological information should be integrated with genomic, proteomic and expression profiling data of different deuterostomes in order to draw new theories on the evolution of the brain and origins of behavior. However, echinoderms current knowledge based on genomic, transcriptomic and proteomic data is still far behind when comparing with other organisms, which may have hindered the postulation of new theories and hypotheses related with CNS evolution throughout the deuterostome clade.

In this chapter is described the first extensive proteomic characterization of the radial nerve cord of an echinoderm, the starfish *Marthasterias glacialis*. This was achieved using gel based approaches (both 1D and 2D SDS PAGE) in combination with mass spectrometry to characterize the intact radial nerve cord and several fractions enriched in radial nerve cord soluble, membrane and synaptosomal membrane proteins.

The identified proteins constitute the first high throughput evidence of an homology between the echinoderm nervous system and the dorsal nerve cord of chordates. Additionally it is shown that neuronal transmission in echinoderms relies primarily on chemical synapses in similarity to the synaptic activity in adult mammal's spinal cord.

2.1. INTRODUCTION

Can echinoderms be alternative models for neurobiology? Why taking the chance in these poorly studied animals?

Despite the phylogenetic proximity with vertebrates, the echinoderms nervous system is probably the least well studied among all metazoans. Nevertheless echinoderms have been recently recognized as important models to explore the basic mechanisms of the regeneration phenomenon and its molecular aspects (Thorndyke *et al.*, 2001A; Thorndyke *et al.*, 2001B; Dupont *et al.*, 2007) due to their spectacular regenerative ability, employed to completely reconstruct body appendages, including the radial nerve cord among other organs.

Despite several morphological studies which revealed the essential neuroanatomy of starfish nervous system, using histology, ultrastructure and immunohistochemistry with antibodies against specific neurotransmitters and regulatory peptides[3], there is still

[3] Cobb *et al.*, 1970; Elphick *et al.*, 1991; García-Arrarás *et al.*, 1991; Hyman *et al.*, 1955; Martinéz *et al.*, 1993; Martínez *et al.*,

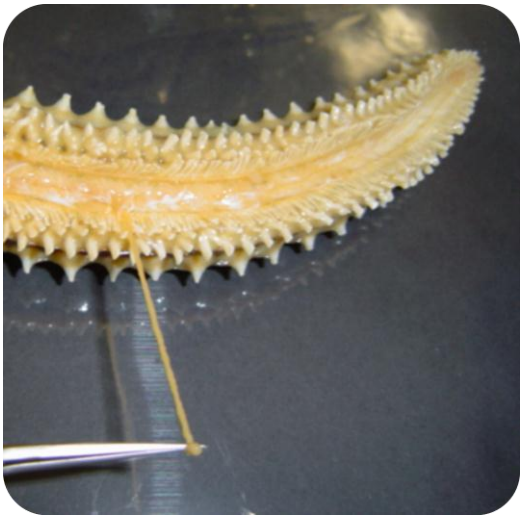

Figure 2.1: Starfish radial nerve cord extraction. Two radial nerve cords were collected per animal simply by pulling with a pair of tweezers from the extremity of the arm tip, on the oral side of the starfish.

a lack of studies providing large-scale identification of proteins involved in the molecular neuroarchitecture of the starfish nervous system.

Data on echinoderms is slowly increasing, but it is still far behind the knowledge available for other organisms. With the sequencing of the purple sea urchin *Strongylocentrotus purpuratus* genome in 2006 (Consortium, 2006), new doors were opened to investigate the functions of many predicted genes common to other animals. However, since then, the few proteomic studies performed on echinoderm tissues validated only a minority of the genome predicted protein sequences (Mann *et al*., 2008; Swell *et al*., 2008), still prevailing the need to verify this rich source of information. This genomic data allowed already an unprecedented glance into the molecular basis of the poorly understood echinoderm nervous system, by the identification of several homologues of genes involved in neurogenesis. This is of extreme importance because shared and/or missing components and pathways have the potential of revealing how metazoan neurogenic gene regulatory networks have been shaped by evolution to produce the vertebrate nervous system (Burke *et al*., 2006). Nevertheless, genomic information is limited to search for absent genes and cannot identify the echinoderm nervous system proteins being expressed, and therefore should be complemented by comparative proteomic studies.

The present chapter aims to contribute to increase the knowledge on the molecular mechanisms of echinoderms nervous system, by performing the first extensive proteomic characterization of the radial nerve cord from the starfish *Marthasterias glacialis*. The identified proteins further represent a strong impulse to overcome some of the obstacles that have prevented conventional neurobiological approaches in echinoderms, and can be used as a starting point for future studies and also to elucidate the role of this organism as a model animal. Altogether, 905 different proteins were identified across the several subcellular enriched fractions analyzed by different proteomic approaches. Protein functions are here speculated based on existing annotations, and hence, should be seen as targets to validate neuronal functions within echinoderms nervous system.

2.2. MATERIALS AND METHODS

2.2.1. Starfish radial nerve cord extraction

Several adult specimens of the starfish *Marthasterias glacialis* (Linné, 1758) were collected at low tide on the west coast of Portugal (Estoril, Cascais). The animals were transported to "Vasco da Gama" Aquarium (Dafundo, Oeiras) where they were kept in open-circuit tanks with re-circulating sea water at 15°C and 33 ‰. They were fed *ad libitum* with a diet of mussels collected weekly at the same site. Animals used for the experiments had similar sizes, with radius ranging from 10 to 13 cm, measured from the largest arm tip to the center of the oral disc. Two radial nerve cords were collected per animal as previously described (Moss *et*

1994; Martínez *et al*., 1996; Mladenov *et al*., 1989; Moore *et al*., 1993; Moss *et al*., 1994; Moss *et al*., 1998; Newman *et al*., 1994; Newman *et al*., 1995A; Newman *et al*., 1995B; Smith 1966; Cobb *et al*., 1967; Cobb *et al*., 1989; García-Arrarás *et al*., 2001

al., 1998) (Figure 2.1). The extracted radial nerve cords were conserved at -80°C until further use.

2.2.2. Radial nerve cord total protein fraction

For protein extraction, approximately 30 mg of starfish total radial nerve cord (RNC) were mixed with 100 µL of 2DE solubilization buffer (Table 2.1) containing a protease inhibitor cocktail (AEBSF, E-64, bestatin, leupetin, aprotinin and sodium EDTA, Sigma). After homogenization at 4°C for 30 min, the sample was centrifuged at 10.000 x *g* for 15 min at 4°C. The pellet was discarded and the supernatant was used for the proteome analysis. The protein concentration was determined using 2D Quant Kit ™ (GE Healthcare).

2.2.3. Membrane and soluble protein fractions

To achieve the best protein extraction yield and reproducibility, the tissue was disrupted by automated frozen disruption methodology as previously described (Butt *et al*., 2006). Briefly, 100 mg of the deep frozen radial nerve cord (in liquid N_2) was placed in a previously chilled teflon sample chamber containing 4 stainless steel beads (5 mm diameter). The chamber was placed in a Mikro-Dismembrator (Sartorius) and set to 3000 *rpm* for 60s. Enriched fractions of membrane and soluble proteins were obtained as previously described (Butt *et al*., 2006) with minor alterations. To avoid sample loss, the resulting powder (still in a deep frozen state) was resuspended with vigorous agitation for 3 minutes, in hypotonic lysis Buffer (2x) supplemented with protease, kinase and phosphatase inhibitors (20 mM HEPES, pH 7.4; Complete protease inhibitor cocktail; 4µM cantharidin; 4µM staurosporine and 1 mM sodium orthovanadate) inside the teflon chamber. After removal of cellular debris and insoluble material (100 x *g*; 10min; 4°C), the total cellular membranes (***M***) were collected from the homogenate by ultracentrifugation at 55.000 *rpm*, 3h, 4°C using an Optima-Max E Ultracentrifuge with the TLS-55 rotor (Beckman-Coulter). The membranes were gently washed in ice-cold 1x PBS also supplemented with protease, kinase and phosphatase inhibitors (Complete protease inhibitor cocktail; Cantharidin 2µM; Staurosporine 2µM and sodium orthovanadate 0.5 mM, Sigma). In order to collect the washed membranes, another ultracentrifugation step was performed. Supernatants containing the total soluble proteins (***S***) were precipitated with trichloroacetic acid (TCA) 10% (w/v), β-mercaptoethanol 0.07% (v/v) and the protein pellet washed with ice-cold acetone with 0.7% (v/v) β-Mercaptoethanol for complete removal of the TCA.

Both membrane and soluble protein enriched fractions were frozen at -80°C until further analysis.

Table 2.1: IEF optimized conditions for the radial nerve cord total protein extract. Abbreviations: S&H, step and hold; G, gradient.

Conditions	**IEF Strips length**							
	7cm				**11 cm**			
Protein solubilization buffer	8 M Urea, 2M thiourea, 2 % (w/v) CHAPS, 60 mM DTE				8 M Urea, 2M thiourea, 2 % (w/v) CHAPS, 60 mM DTE			
pH range	3-10 L				3-11 NL			
Ampholyte buffer used; final concentration % (v/v)	3-10 L; 1% (v/v)				3-11 NL; 1% (v/v)			
Total protein loaded (µg)	100				400			
IEF program	Voltage (v)	Voltage mode	Time (h:min)	V.h	Voltage (v)	Voltage mode	Time (h:min)	V.h
	150	S&H	2:00	300	100	S&H	1:30	150
	300	S&H	2:00	600	250	S&H	1:00	250
	1000	S&H	1:30	1500	1000	S&H	1:30	1500
	3000	G	1:00	1500	2500	S&H	1:00	2500
	3000	S&H	4:00	12000	4000	G	0:30	1000
	Total		10:30	15900	4000	S&H	4:40	18600
					Total		10:15	24000

2.2.4. Synaptosomal membranes protein fraction

The synaptosomal membranes fraction was isolated as previously described (Singh *et al*., 2009; Dunah *et al*., 2001), with minor adaptations to starfish nervous tissue. Briefly, approximately 40 mg of a radial nerve cord was homogenized in ice-cold TEVP buffer (10 mM Tris-HCl pH 7.4; 5 mM NaF; 1 mM Na_3VO_4; 1 mM EGTA) containing 320 mM sucrose and a protease inhibitor cocktail. The homogenate was centrifuged at 1000 x *g* for 10 min to remove nuclei and large debris. The obtained supernatant was centrifuged at 10.000 x *g* for 20 min in order to obtain a crude synaptosomal fraction which was subsequently lysed by hypo-osmotic shock and centrifuged at 25.000 x *g* for 30 min to pellet

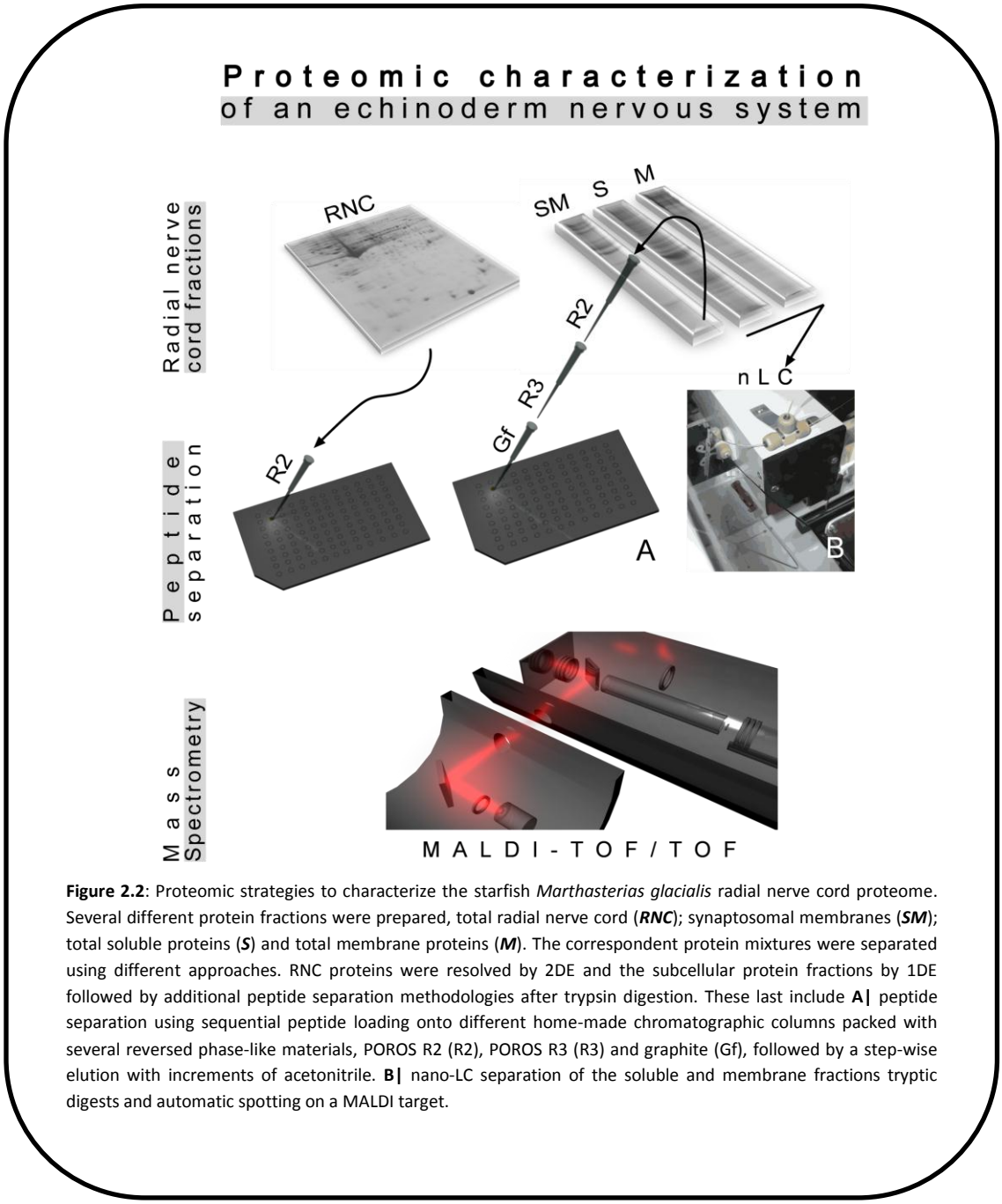

Figure 2.2: Proteomic strategies to characterize the starfish *Marthasterias glacialis* radial nerve cord proteome. Several different protein fractions were prepared, total radial nerve cord (***RNC***); synaptosomal membranes (***SM***); total soluble proteins (***S***) and total membrane proteins (***M***). The correspondent protein mixtures were separated using different approaches. RNC proteins were resolved by 2DE and the subcellular protein fractions by 1DE followed by additional peptide separation methodologies after trypsin digestion. These last include **A|** peptide separation using sequential peptide loading onto different home-made chromatographic columns packed with several reversed phase-like materials, POROS R2 (R2), POROS R3 (R3) and graphite (Gf), followed by a step-wise elution with increments of acetonitrile. **B|** nano-LC separation of the soluble and membrane fractions tryptic digests and automatic spotting on a MALDI target.

the synaptosomal membrane fraction (***SM***).

2.2.5. Protein separation

2.2.5.1. 1D SDS-PAGE

The subcellular fractions obtained by the procedures described above (soluble, membrane and synaptosomal membrane fractions) were solubilized in a buffer containing SDS (1 %, w/v) and DTT (50 mM) and heated up to 60°C for 10 min. The three subcellular fractions were then diluted to 0.5% (w/v) SDS using deionized water and incubated in the 1DE sample buffer (62.5 mM Tris-HCl pH 6.8; 20% (v/v) glycerol and traces of bromophenol blue). The protein concentration was determined using 2D Quant Kit ™ (GE Healthcare). For protein separation, 10% and 12.5% (w/v) acrylamide 7 cm gels were used, loaded with 25 µg total protein per lane. Gels were then stained with colloidal Coomassie (Neuhoff *et al*., 1988). Briefly, after fixing the proteins in the gels for 18h with a solution of 50% (v/v) ethanol, 3% (v/v) phosphoric acid, gels were pre-incubated for 1h with 34% (v/v) methanol containing 3% (v/v) phosphoric acid and 17% (w/v) ammonium sulphate. Coomassie Blue G-250 (Sigma) was then added [0.35% (w/v)] to the previous solution and staining of the gels continued for 100h more. Prior to image acquisition, gels were washed with deionized water to remove background stain.

2.2.5.2. 2D SDS PAGE

1st dimension: For the isoelectric focusing (IEF) of the radial nerve cord total protein extract, Immobiline DryStrips (GE Healthcare) with lengths of 7 and 11 cm (pH gradients of 3-10 *linear* and 3-11 *non linear*, respectively) were used. The IEF conditions were thoroughly optimized for both conditions in order to allow complete focusing of the proteins. **Table 1** summarizes the optimized conditions for each of the two types of strips used for IEF.

2nd dimension: Strips from IEF were equilibrated in a two-step process with a buffer (50mM Tris-HCl pH 8.8, 6M urea, 30 % (v/v) glycerol, 2 % (w/v) SDS, 0.002 % (w/v) bromophenol blue) containing either 2% (w/v) DTE or 4% (w/v) iodoacetamide. Protein separation in the second dimension was performed in 24 cm SDS-PAGE gels (12.5% (w/v) acrylamide) each containing two 11 cm IEF strips, or in 7cm SDS-PAGE gels (12.5% (w/v) acrylamide) for the smaller IEF strips. Electrophoresis was carried out at 38 mA/gel in the running buffer (25 mM Tris, pH 8.8; 192 mM glycine, and 0.1% (w/v) SDS) until the bromophenol blue reached the bottom of the gel. Proteins were visualized by staining the gels with colloidal Coomassie staining (Neuhoff *et al*., 1988).

***2D gel image analysis*:** Stained gels were scanned using a densitometer (LabScan, GE Healthcare). Gel image analysis was performed using the ImageMaster Platinum software (version 5.0; GE Healthcare). The spots selected for protein identification were present in five of the ten 2D gels analyzed and had a relative spot volume (% vol.) above 0.05 %.

2.2.6. In-gel tryptic digestion

The previously excised gel spots and bands were washed with 50% (v/v) acetonitrile (ACN) to remove stain traces, dehydrated with ACN and vacuum-dryed. Afterwards, gel plugs were digested as previously described (Santos *et al*., 2009). Briefly, modified trypsin (6.7 ng/µL in 50mM ammonium bicarbonate) was added to the dried gel plugs and incubated at 37°C overnight. The obtained supernatant was recovered and gel plugs were further incubated with sufficient volume of 5% (v/v) formic acid and ACN in order to extract higher molecular mass peptides. The recovered supernatant was pooled with the first digest, vacuum-dried and resuspended in 5% (v/v) formic acid prior to mass spectrometry analysis.

2.2.7. Tryptic peptides purification, concentration and separation

2.2.7.1. Handmade microcolumns

Desalting and concentration of the acidified supernatants containing the tryptic peptides was carried out with chromatographic microcolumns using GELoader tips packed with different affinity materials according to the complexity of the tryptic peptide mixture. Tryptic peptides from the RNC 2DE gel spots were directly eluted from POROS R2 (Applied Biosystems) microcolumns (20 µm bead size) onto the MALDI plate using 0.5 µl of 5 mg/ml α-CHCA (α-ciano-4-

hydroxy-trans-cinnamic acid) in 50% (v/v) ACN with 2.5% (v/v) formic acid and air-dried. For the SM tryptic digests obtained from 1D gel bands, a step-wise elution was preferred using microcolumns packed with POROS R2, R3 (20 µm bead size) and graphite powder (Larsen *et al*., 2002; Gobon *et al*., 1999) using increasing ACN concentrations (30, 40 and 50% with 2.5% (v/v) formic acid).

2.2.7.2. Nano-LC separation of the peptides

Peptides from the 1D digested bands from ***S*** and ***M*** fractions were injected in a C18 reversed phase nano-LC column (EASY-Column, 10cm, ID 75µm; Proxeon Biosystems) and separated using a Proxeon Easy-nLC (Proxeon Biosystems). Peptides were eluted at a flow rate of 300nL/min using the following gradient: 5-10% (v/v) of solvent B for 4min, 10-50% (v/v) for 19 min and 50-100% (v/v) for 4 min (Solvent B: Acetonitrile, 0.5% (v/v) formic acid; Solvent A: 0.5% (v/v) formic acid). The obtained fractions (20s) were mixed with a solution of 5 mg/mL α-CHCA in 50% (v/v) ACN, 2.5 % (v/v) formic acid and deposited onto a LC-MALDI target plate (72 spots per gel band) using an online SunCollect automatic spotting system (SunChrom). Both pre-column and analytical column were equilibrated with 5% (v/v) of solvent B before analyzing the next sample.

2.2.8. MALDI-TOF/TOF analysis

Tandem mass spectrometry was performed using a MALDI-TOF/TOF 4800 plus mass spectrometer (Applied Biosystems). The mass spectrometer was externally calibrated using des-Arg-Bradykinin (904.468 Da), angiotensin 1 (1296.685 Da), Glu-Fibrinopeptide B (1570.677 Da), ACTH (1-17) (2093.087 Da), and ACTH (18-39) (2465.199) (4700 Calibration Mix, Applied Biosystems). Each reflector MS spectrum was collected in a result-independent acquisition mode, typically using 1000 laser shots per spectra and a fixed laser intensity of 3500V. The fifteen strongest precursors were selected for MS/MS, the weakest precursors being fragmented first. MS/MS analyses were performed using CID (Collision Induced Dissociation) assisted with air, with a collision energy of 1 kV and a gas pressure of 1 x 10^6 torr. Two thousand laser shots were collected

BOX 2.1| Search parameters

MASCOT (version 2.2; Matrix Science, Boston, MA) searches were performed without taxonomical restrictions, a minimum mass accuracy of 30 ppm for the parent ions, an error of 0.3 Da for the fragments, one missed cleavage in peptide masses, and carbamidomethylation of Cys and oxidation of Met as fixed and variable amino acid modifications, respectively.

ProteinPilot (Protein Pilot software version 3.0, revision 114732; Applied Biosystems, USA) searches were performed without taxonomic restrictions and search parameters were set as follows: enzyme, trypsin; Cys alkylation, iodoacetamide; special factor, gel-based ID; and ID focus, biological modification and amino acid substitution.

BOX 2.2| Protein sequence databases information

[A] Purple sea urchin *Strongylocentrotus purpuratus* predicted database (42.420 entries; December 2006; ftp://ftp.ncbi.nih.gov/genomes/StrongylocentrotuS_purpuratus/protein;

[B] Uniprot/SwissProt database (release 2010_04; 11.134.468 entries);

[C] Non-redundant protein database Uniref100 (release 2010_06; 10.246.365 entries).

[D] Uniprot/SwissProt database (release 2011_01; 566.840 sequences; 203.332.110 residues)

[E] Non-redundant protein database Uniref100 (release 2011_01; 11.659.891 clusters)

BOX 2.3| Data deposition on public repositories

Protein identification files derived from MASCOT were converted to mzML files using PRIDE Converter tool (Barsnes *et al*., 2009) and are available in the PRIDE database (Vizcaíno *et al*., 2009).

Project ID: Radial nerve cord proteome characterization
Accession number: 15331

for each MS/MS spectrum using a fixed laser intensity of 4500V.

2.2.9. Protein identification

2.2.9.1. Protein identification workflow for 2DE spots

Since *M. glacialis* does not have a specific protein database derived from genome, or other specific source(s) of information, in order to maximize the number of identifications to be obtained from the experimental data, two different search algorithms were used in a "3 step" protein identification workflow, (see BOX 2.1 for details on the search parameters used) together with several different protein sequence databases (See BOX 2.2 for details on the databases), briefly:

***Stage 1*:** All spectra were submitted for search using the software MASCOT against the three different protein databases (A-C) (BOX 2.2). A combined analysis of PMF (Peptide Mass Fingerprint) and tandem mass (MS/MS) was performed using the search parameters

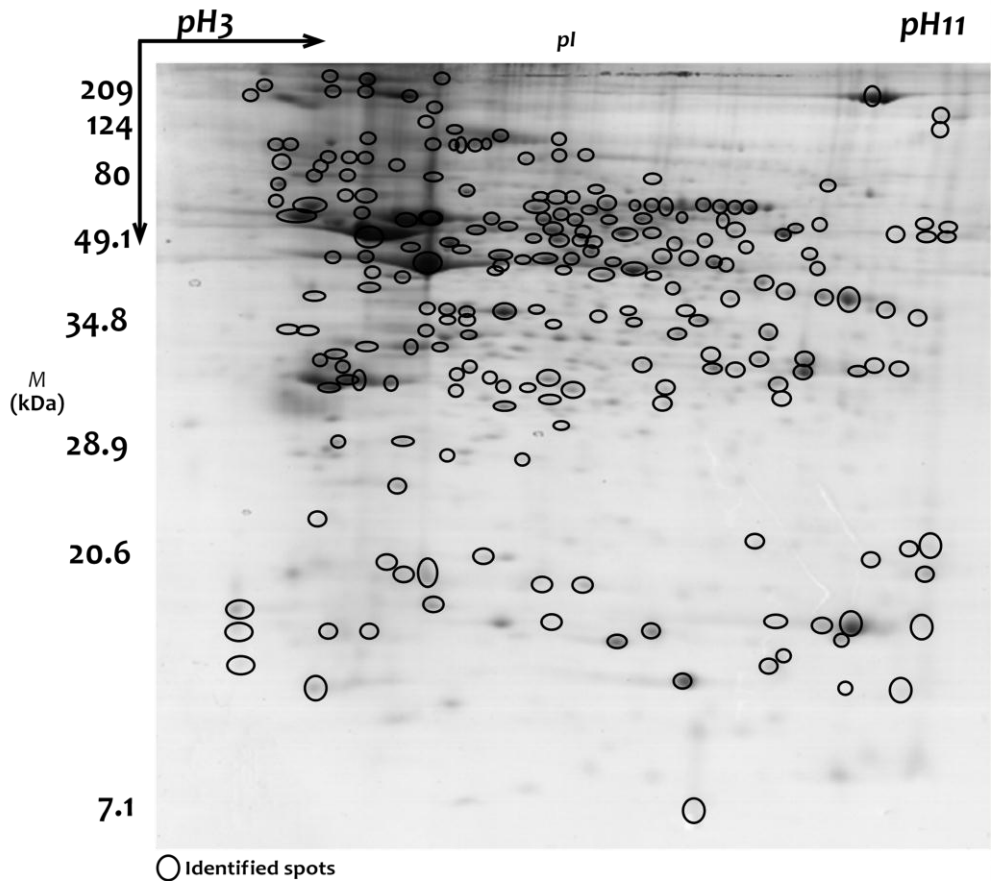

Figure 2.3: 2DE SDS-PAGE gel of the starfish *M. glacialis* RNC: Starfish radial nerve cord proteins were separated according their isoelectric point using non-linear 3-11 pH IEF strips (11cm). For second dimension 12.5 % SDS PAGE were used to separate proteins according their molecular masses *(M)*. Black circles indicate identified protein spots.

defined in BOX 2.1. The identified proteins using database A joined with B were only considered if a protein score above 69 (p<0.05) was obtained; and peptides were only considered if individual ions scores were above 39 (p<0.05). When using database C, successful identifications were only considered if the protein score was above 81 (p<0.05); and peptides were only considered if individual ions scores were above 50 (p<0.05).

Stage 2: Proteins without a successful identification in stage 1 were further processed with ProteinPilot software and searched against database A joined with B (search parameters are defined in BOX 2.1). Identified proteins were selected if their unused score was above a false discovery rate (FDR) of 1%. Furthermore, identified proteins were only considered if having at least one peptide with 95% confidence.

Stage 3: Proteins with good quality MS/MS spectra but without a successful identification in stage 2 were further processed using ProteinPilot and searched against database C. Protein identifications were considered if the described thresholds were achieved (FDR<1%; at least one peptide with 95% confidence). Protein identifications with only one peptide with 95% confidence were further validated using Peaks Studio 4.5 software (Bioinformatic Solutions) by auto *de-novo* sequencing of the MS/MS spectra combined with manual inspection of the assigned sequence. Quality criteria for manual confirmation of MS/MS spectra were the assignment of major peaks, occurrence of uninterrupted y- or b-ion series at least with 3 consecutive amino acids and the presence of a2/b2 ion pairs.

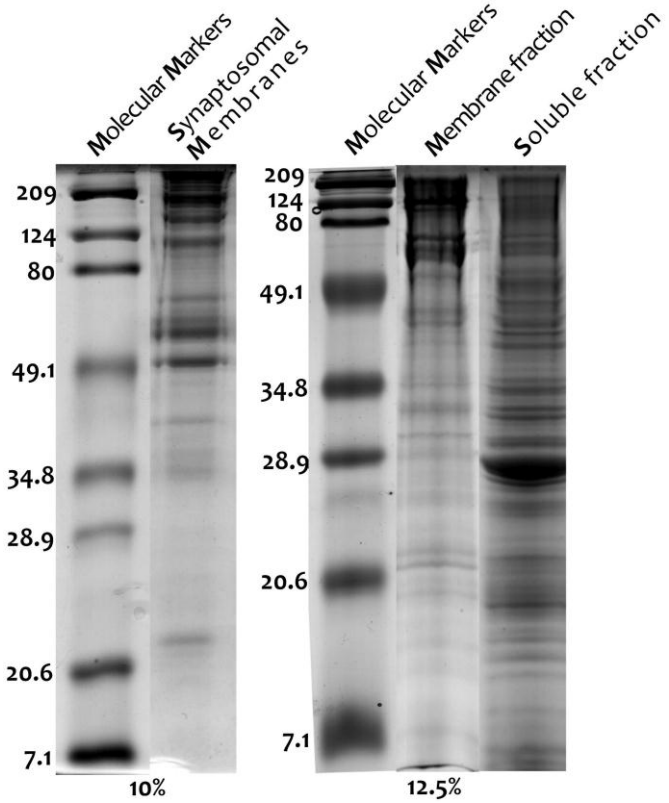

Figure 2.4: Radial nerve cord protein enriched fractions separated according *M* in 1DE SDS PAGE gels. An acrylamide concentration of 10 and 12.5% (w/v) was used for synaptosomal membranes and soluble/membrane fractions, respectively.

2.2.9.2. Protein identification workflow for 1DE bands

2.2.9.2.1. Synaptosomal membranes protein fraction

The collected spectra (5435 MS/MS spectra) were processed with ProteinPilot using LC mode against database A joined with B. The FDR was determined individually for each 1DE band using PSPEP algorithm from ProteinPilot software. Identified proteins were selected if the protein unused score was within a false discovery rate of 1% and if having at least 1 peptide with 99% confidence or if having two peptides: one peptide with 95% confidence and at least one other with confidence above 50%.

2.2.9.2.2. Soluble and membrane protein fractions

The collected spectra (6479 and 3619 for the soluble and membrane fraction, respectively) were processed in ProteinPilot and MASCOT using LC modes (or MS/MS ions search) against newer versions of the previously described proteins databases (BOX 2.2, database A joined with D, and E). Identified peptides and inferred proteins were selected if having a significant homology MASCOT score (p<0.05) or, if having a ProteinPilot unused score above 1.5 and at least 1 peptide with 95% confidence. The FDR was determined using the original and reversed protein databases merged together. The established thresholds are above the limit to attain a FDR of 1%.

2.2.10. BLASTp and GO annotation of the identified proteins

Uncharacterized/unknown proteins and all *S. purpuratus* proteins were further submitted to protein-protein BLAST searches (BLASTp) against SwissProt database search using Basic Local Alignment Search tool available at NCBI web site (http://blast.ncbi.nlm.nih.gov/) through BLAST2GO java application (http://www.blast2go.de), a research tool designed with the main purpose of enabling GO based data mining on sequence data for which no GO annotation is available (BLASTp minimal Expectation value set to < $1x10^{-3}$). Identified proteins were further annotated with the GO categories using both STRAP software (Bhatia *et al*., 2009) and BLAST2GO annotation tools.

2.3. RESULTS

2.3.1. 2DE protein map of Marthasterias glacialis radial nerve cord

To characterize the starfish radial nerve cord (RNC) proteome ten 2DE gels were run corresponding to ten biological replicates. After gel image analysis approximately 403 spots were detected per 2DE gel. Among the detected spots 339 were compliant with the criteria described in *Material and Methods* and thus, were further excised and processed for protein identification by mass spectrometry. The RNC 2DE annotated reference gel is available via the WORLD-2DPAGE Portal displaying also relevant information on all identified spots including protein identification data at http://world-2dpage.expasy.org/repository/0024/ (Figure 2.3). Using the two identification algorithms and the selected protein databases 286 spots were successfully identified (Supplementary table 2.1 and Supplementary data 2.2) representing 84% of the selected spots. This high yield of protein identification was only possible due to the applied protein identification workflow consisting of a combination of different databases and search algorithms (Figure 2.5A).

2.3.2. The extra mile in starfish nerve cord proteome characterization: analysis of subcellular enriched fractions of the radial nerve cord

Since proteomic analysis of whole tissues is often disadvantageous for the study of low abundance proteins, a nerve subcellular fractionation was performed in order to obtain an enriched fraction in synaptosomal membrane proteins, total cytosolic proteins (soluble fraction) and total membrane proteins (membrane fraction). All three enriched protein fractions were separated using 1DE (Figure 2.4) and for peptides resulting from the digestion of the SM sliced lanes were separated either using homemade microcolumns packed with different materials and stepwise elution using increments of ACN, for the synaptosomal enriched fractions or, using a nano-LC system and a MALDI plate spotter, for the soluble and membrane enriched fractions.

In the synaptosomal membrane proteins enriched fraction 158 proteins were identified, of which 34 were unique (Supplementary table 2.3 and Supplementary data 2.4; Figure 2.5B, E).

A substantial increase on the number of identified radial nerve cord proteins was achieved when using the Proxeon Easy-nLC (Proxeon Biosystems, Odense, Denmark) coupled to a MALDI spotter to separate the tryptic peptides from the soluble and membrane proteins enriched fractions, prior to MALDI-TOF/TOF mass spectrometry. In fact, within 491 and 321 different proteins identified in the soluble and membrane fractions, 343 and 193, respectively, were new assignments (Figure 2.5 C, D, E) (Supplementary data 2.5 and 2.6.

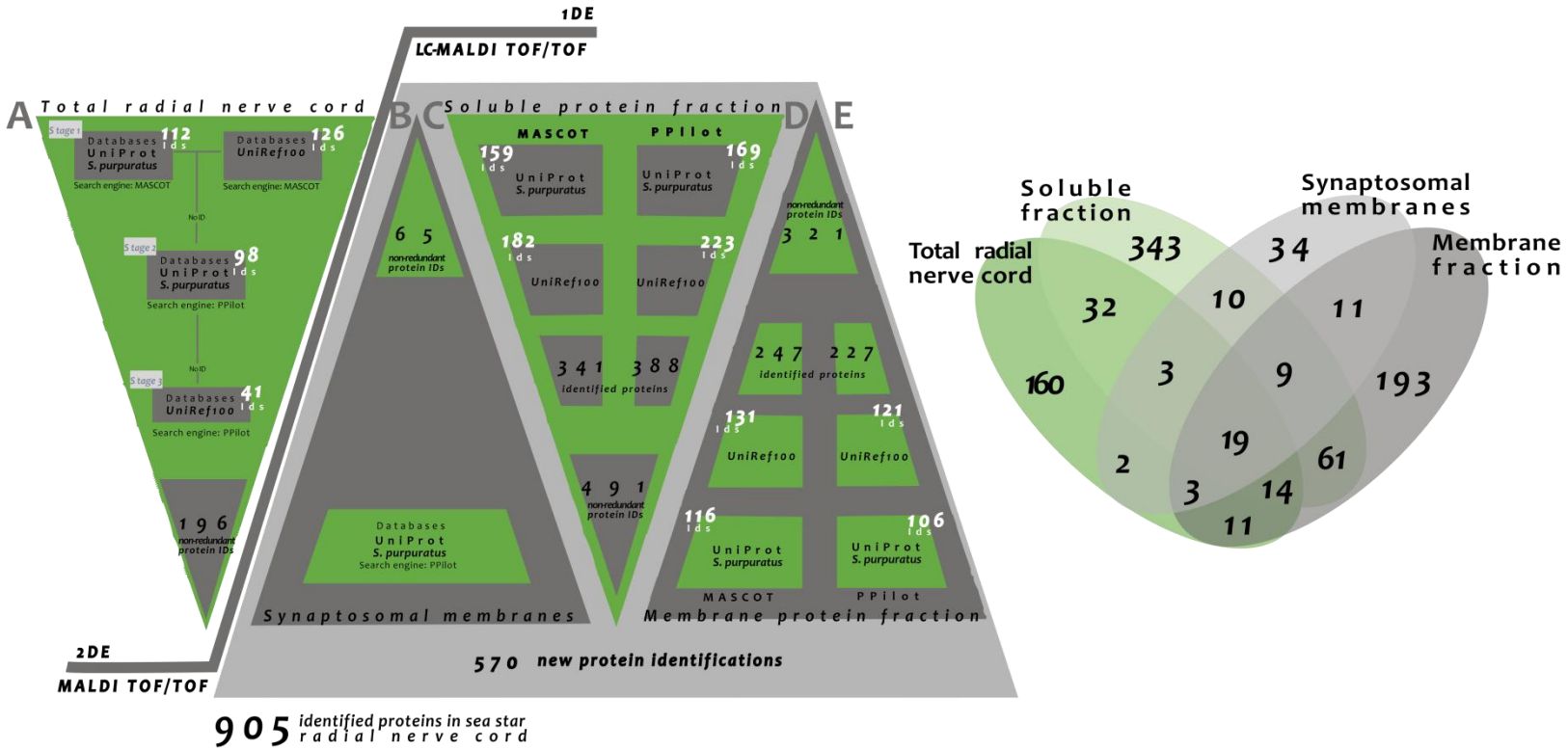

Figure 2.5: Number of identified proteins in each protein fraction using two different search algorithms and three different protein databases. **A|** In the 2DE analysis of the total radial nerve cord proteins, searches using MASCOT resulted in the identification of 112 proteins in the UniProt/*S. purpuratus* databases and 126 proteins in the UniRef100 protein database. Searches with ProteinPilot combining UniProt/*S. purpuratus* and UniRef100 databases produced 139 protein identifications. Altogether, approximately 196 non-redundant protein identifications were obtained (Supplementary table 2.1). **B|** In the 1DE analysis of the synaptosomal membrane proteins enriched fraction, searches using ProteinPilot software resulted in the identification of 65 non-redundant proteins. **C, D|** In the 1DE analysis of the soluble and membrane proteins enriched fractions, searches performed with MASCOT enabled the identification of 341 proteins (159 in UniProt/*S. purpuratus* and 182 in Uniref100 databases) and 247 proteins (116 in UniProt/*S. purpuratus* and 131 in Uniref100 databases), respectively. As for searches with Protein Pilot, 388 proteins were identified in the soluble fraction (165 UniProt/*S. purpuratus* and 223 in Uniref100 databases respectively) and 227 proteins in the membrane fraction (106 UniProt/*S. purpuratus* and 121 in Uniref100 databases respectively) (Supplementary data 2.5 and 2.6). **E|** Number of common and unique identified proteins within all the analyzed radial nerve cord fractions. The complete list of the identified proteins is presented in Supplementary table 2.7.

The different proteomic approaches and the several subcellular proteins enriched fractions employed to characterize the proteome of the starfish nervous system allowed the identification of 905 different proteins. However, only 19 proteins are common to all the assayed protein fractions highlighting the importance of the proteomic characterization of several subcellular components to achieve a complementary and also, confirmatory list of proteins (Supplementary table 2.7) (Figure 2.5E). Since only a limited number of starfish proteins are deposited on the available protein sequence databases, the present study is a homology driven proteomic characterization of *M. glacialis* radial nerve cord. Not surprisingly, the sea urchin *S. purpuratus* is the species having a higher number of homologous protein sequences (99 homologies found). Interestingly, it was followed by *Homo sapiens* (Supplementary table 2.7) with 38 homologies found.

Since for the majority of the identified proteins gene ontology annotations are not yet available, BLAST2GO software was used to fully annotate the identified proteins according to three independent sets of GO: biological function; molecular function and cellular component (Figure 2.6) (Supplementary table 2.7).

The comparison of the subcellular location of the identified synaptosomal membrane (SM) proteins with the proteins identified in the remaining RNC protein enriched fractions showed that although the SM fractionation procedure was originally optimized for mammalian nerve tissues, it was also effective on echinoderms nerve tissues. As shown in Figure 2.6, among the identified proteins there is enrichment in synapse proteins for the SM fraction and also a depletion of several cytoskeleton proteins. Other GO categories distribution across the different fractions also show that the fractionation in soluble and membrane proteins was effective in generating different subsets of the radial nerve cord proteome, which allowed to circumvent the systematic identification of high abundant proteins, thus further increasing the number of different proteins identified in the radial nerve cord (Figure 2.6).

2.4. DISCUSSION

2.4.1. Starfish radial nerve cord proteins highlight the functional complexity of echinoderm nervous system and narrows the distance from chordate CNS

The possible homology between the echinoderm nervous system and chordate central nervous system (CNS) is neither new nor consensual (Hagg *et al*., 2005A; Nielsen *et al*., 2006; Hagg *et al*., 2005B). It is still an issue of great debate since the major approaches to support this hypothesis rely mainly on information provided by comparative anatomy and morphological studies. In an effort to further clarify this persisting question, the biological functions of the identified proteins in starfish radial nerve cord were compared with the proteins reported for the spinal cord of a vertebrate (Gil-Dones *et al*., 2009) (Figure 2.7). At a first glimpse, this analysis reveals a surprising homology between the biological functions of the proteins identified in both nervous systems, the starfish radial nerve cord and the rat spinal cord. Nevertheless, in order to draw new theories on CNS evolution within the deuterostome clade, new experimental approaches are needed, which may include specific protein pull downs or the depletion of the most abundant proteins to further identify low abundance proteins in the echinoderm nervous system.

A comprehensive look into the identified proteins and how they correlate with neuronal functions in the radial nerve cord of the starfish is here discussed and will further clarify the functional similarities found with other nervous systems (complete annotation of the identified proteins is presented in Supplementary table 2.7):

2.4.2. Neuronal transmission in echinoderms

2.4.2.1. Neuronal transport systems

Several proteins with functions related with endocytosis/exocytosis, motor proteins, microtubule and cytoskeleton modulators, were identified in the starfish radial nerve cord, narrowing the distance between the neuroarchitecture of echinoderms and other well characterized nervous systems. Among the identified proteins is clathrin heavy chain, one of the

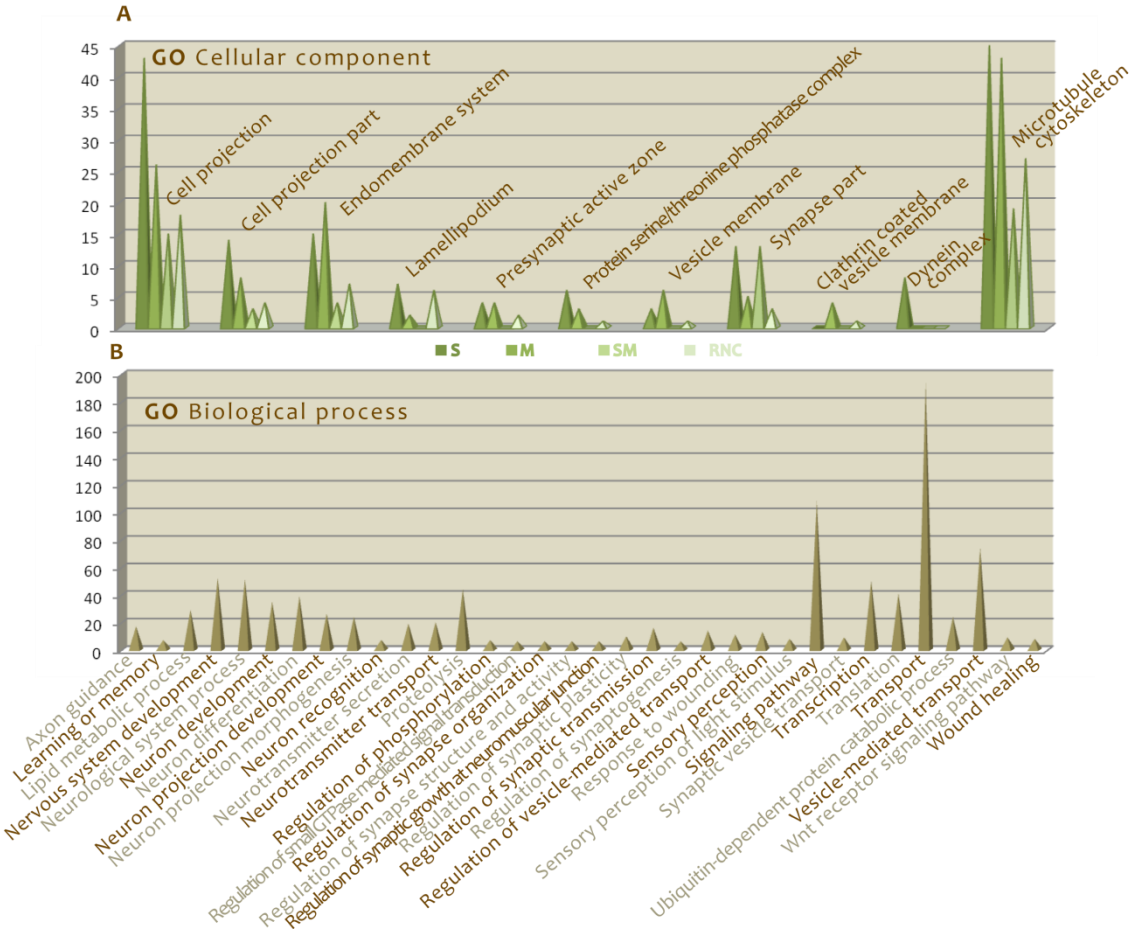

Figure 2.6: Gene Ontology annotations of the identified starfish *Marthasterias glacialis* radial nerve cord proteins. GO annotations were retrieved from BLAST2GO software and are displayed according to two different categories **A| Cellular component**; **B| Biological process**. For the complete set of radial nerve cord proteins GO annotations see Supplementary table 2.7. Abbreviations: **S**, Soluble proteins fraction; **M**, Membrane proteins fraction; **SM**, Synaptosomal membrane proteins fraction; **RNC**, total radial nerve cord proteins.

major constituent of coated pit vesicles, along with several other clathrin binding proteins responsible for coat assembly (adaptor-related protein complex sigma 1 subunit). Proteins known to be involved in intracellular protein transport were also highly represented, such as ras-related proteins rab-2a and rab-10; transmembrane emp24 domain trafficking protein 2; adp-ribosylation factor and adaptor-related protein complex sigma 1 subunit among others. Several motor proteins from the dynein motor complex were also present namely, dynein light chain, dynein heavy chain and dynein light chain roadblock- type 1. Other motor proteins like a kinesin-like protein and proteins belonging to the dynein activation complex were also identified in the starfish radial nerve cord. These last proteins are important for the vesicular transport of molecules (i.e., neurotransmitters, transcription factors, newly synthesized proteins) from the neuron soma to the synaptic axon terminal (anterograde transport) or in the opposite direction (retrograde transport) carrying them along microtubule and cytoskeleton tracks (Stiess *et al*., 2010). These motor proteins-based transport systems are determinant not only for the normal neuronal function, but also for the efficient modulation of genome expression due to the polarized morphology of neurons (Perlson *et al*., 2004).

2.4.2.2. Membrane potential towards electrical signaling

In this proteomic characterization evidences of membrane potentials generated by K^+, Ca^{2+} and Na^+ channels were found since proteins such as Na^+/K^+ alpha 1 polypeptide, Na^+/K^+ antiporter, the voltage-gated potassium channel btb poz domain-containing protein kctd16, K^+ uptake trk family protein, potassium channel subfamily t member 1, and also several calcium dependent proteins, *i.e.*, calcium-binding protein 39 and calmodulin, were identified. Neurons rely on voltage-gated ion channels (VGIC) permeable to potassium (K^+), sodium (Na^+) and calcium (Ca^{2+}) in order to generate and transmit electrical signals that, when reaching the axonal terminal will culminate in the release of neurotransmitters. Although several VGIC proteins are predicted in the *S. purpuratus* genome (Burke *et al*., 2006), up to date, this proteomic characterization constitutes the first report of their presence in echinoderm nervous system.

2.4.2.3. Chemical synapses and neurotransmitter release

Neurotransmitter mediated release depends on several classes of molecules that temporally coordinate a cascade of events which include targeting the synaptic vesicles to the pre-synaptic membrane, their calcium-dependent fusion and exocytosis to release the neurotransmitters into the synaptic cleft (Kennedy *et al*., 2011). Several classes of these important proteins are also encoded in *S. purpuratus* genome (Burke *et al*., 2006) and were also identified for the first time in the radial nerve cord of an echinoderm in this proteomic characterization.

Several Rab GTPases, a multigene family that mediates targeting of intracellular vesicles to membranes and thus are involved in the targeting of synaptic vesicles,

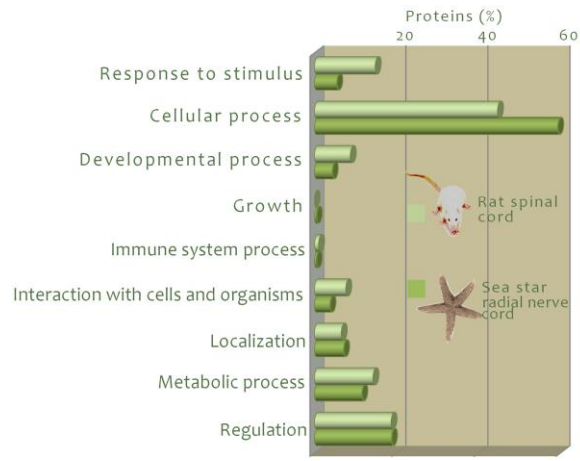

Figure 2.7: Comparative analysis of the biological function distributions of proteins identified in the radial nerve cord of an echinoderm, the starfish *Marthasterias glacialis* and the proteins reported for the spinal cord proteome of a vertebrate, the wistar rat *Rattus norvegicus* (Gil-Dones *et al*., 2009).

were identified also in the starfish radial nerve cord such as, GDP dissociation inhibitor 1, which in vertebrates is predominantly present in the brain and neural/sensory tissues; and ras-related proteins, such as ara-4, rab-10, rab-2a, rab-37, rab-8a, rap-1b and rab-3D. This last small GTPase is the major isoform that binds to synaptic vesicles.

Also involved in the synaptic vesicle membrane fusion events are the transient intermembrane interactions between vesicle associated membrane proteins (VAMP) and the target membrane proteins SNAP-25, and syntaxin (Weber *et al*., 1998; Coorssen, 2008). *S. purpuratus* appears to have single-copy genes for VAMP, SNAP-25 and syntaxin homologues (Burke *et al*., 2006). In this study we identified in the radial nerve cord an homologue of *Drosophila* SNAP-25 protein, which has 63% identity with *S. purpuratus* predicted SNAP-25. Moreover, the homologous of sea urchin VAMP protein was also identified as well as several proteins that bind to syntaxin (such as Rab-11A and spectrin). One protein homologue to the human protein lin-7 homolog A was also identified, which is a protein known to be involved in the localization of synaptic vesicles at synapses. Synaptotagmins are vesicle anchored proteins that bind to phospholipids in the presence of calcium, triggering membrane fusion. One isoform of the rat synaptojanin-2-binding protein was also identified in starfish radial nerve cord, that shares 37% identity with the sea urchin hypothetical synaptojanin.

A vesicle-fusing ATPase was also identified, which is involved in vesicle-mediated transport and is a cellular component of the dendritic shaft and postsynaptic density. Other proteins involved in protein trafficking and transport among different compartments, as well as clathrin, one of the major proteins of the synaptic vesicle, were also identified.

Electrical synapses (or neuronal gap junctions) are relatively simple compared to chemical ones and enable rapid impulse propagation (Zoidl *et al*., 2002). However, these proteins appear to be encoded by distinct gene families unequally distributed among different animal phyla (Hervé *et al*., 2005). BLAST searches within the genome of the purple sea urchin failed to find representative genes of any of these proteins (Burke *et al*., 2006) and in agreement, in this study no Gap junction proteins were identified, which can be one more piece of evidence to support the relatedness between the radial nerve cord of echinoderms and spinal cord of chordates, since the synaptic activity of adult mammal spinal cords relies essentially on chemical transmission.

Calcium is one of the most important cellular second messengers, and similarly to other neuronal systems it seems to also exert fundamental functions in neuronal activity of the echinoderms nervous system. As examples, calpain, a calcium-dependent cysteine-type protease essential for cytoskeleton remodeling and indispensable for axonal growth cone formation (Spira *et al*., 2001), was identified, together with several proteins whose functions are modulated by calcium binding, namely, EF hand family protein, FK506-binding protein, calnexin, hippocalcin-like 1, calmodulin, echinoderm microtubule associated protein like 1, neurocalcin-delta, calreticulin, among others.

2.4.2.4. Neurogenesis and regeneration

One of the most interesting echinoderm capabilities is their amazing ability to fully regenerate body parts upon a traumatic injury, a natural trait also extended to their nervous system (Thorndyke *et al*., 2001A; Thorndyke *et al*., 2001B; Dupont *et al*., 2007), although far from being understood. Regeneration is seen at some point to be a recapitulation of the embryogenic pathways. Several proteins involved in neurogenesis with functions of axonal guidance, dendrite morphogenesis and neuron growth have been identified namely, proprotein convertase subtilisin kexin type 2, beta-tubulin at 60d, netrin 1, peptidylglycine alpha-amidating monooxygenase, ubiquitin c, uncoordinated family member (unc-44), vasodilator-stimulated phosphoprotein, guanine nucleotide binding protein q polypeptide, calreticulin, dihydropyrimidinase and protein enabled. Several proteins belonging to the *Wnt* signaling pathway, described as involved in the regeneration of the thickened wound epithelia in the ophiuroid *Amphiura filiformis* (Rychel *et al*., 2009), were also identified, namely, bromodomain containing 7, casein kinase beta polypeptide, casein kinase II alpha subunit, GTPase_rho, PHD finger protein, ras-related c3 botulinum toxin substrate 1 (rho small GTP binding

protein rac1), serine threonine-protein phosphatase 2a catalytic subunit alpha isoform and survival of motor neuron protein-interacting protein 1.

2.4.2.5. Sensory perception

Echinoderms lack evident light-sensitive organs, however, they respond to light, photoperiod and lunar cycles. Several proteins responsible for sensory perception were identified, accentuating the functional complexity of echinoderms nervous system. These include guanine nucleotide binding protein beta polypeptide 1, member ras oncogene isoform cra a, mitogen-activated protein kinase 1, odorant receptor, ornithine aminotransferase (gyrate atrophy), quinone oxidoreductase, retinol dehydrogenase 8 (all-trans) and the intermediate filament protein ON3.

2.5. CONCLUDING REMARKS

In summary, the many newly identified proteins in the radial nerve cord of the starfish *M. glacialis* are of extreme importance and highlight the potential of echinoderms as models to study CNS itself and its regeneration ability. The use of these animals as model systems, given their simpler morphology, easy manipulation and complex nervous system, can be a promising way to understand the molecular mechanisms involved in regeneration, which can then be transposed to find regeneration targets to be studied in other model organisms, namely mammals.

2.6. ACKNOWLEDGMENTS

This work was supported by Fundação para a Ciência e Tecnologia through a PhD grant to Catarina Franco (SFRH/BD/29799/2006), a research contract by the Ciência 2008 program to Romana Santos, a project grant (PTDC/MAR/104058/2008) and through the National Re-equipment Program for "Rede Nacional de Espectrometria de Massa - RNEM" (REDE/1504/RNEM/2005). We also acknowledge Dr. Patrick Flammang for scientific advice, Vasco da Gama Aquarium (Dafundo, Oeiras, Portugal), namely Dr. Fátima Gil and Miguel Cadete, for starfish maintenance, Henrique Braga for the help with mussels collection and Dr. Renata Soares for paper revision. Acknowledgements are extended to Daniel Ettlin (Thermo UNICAM, Portugal) and Dr. Erik Verschuuren (Proxeon, Denmark) for providing the Nano-HPLC (Proxeon) and Gûnes Barka (SunChrom) for providing the automatic Spotter.

2.7. REFERENCES

Barsnes, H., Vizcaino, J. A., Eidhammer, I., Martens, L. PRIDE converter: making proteomics data-sharing easy. Nat. Biotechnol. 2009, 27, 598–599.

Bhatia, V.N., Perlman, D.H., Costello, C.E., McComb, M.E. Software Tool for Researching Annotations of Proteins: Open-Source Protein Annotation Software with Data Visualization. Anal Chem. 2009, Oct 19. [Epub ahead of print]

Burke, R. D., Angerer, L M., Elphick, M. R., Humphrey, G. W., Yagushi, S., Kiyama, T., Liang, S., Mu, X., Agca, C., Klein, W. H., Brandhorst, B. P., Rowe, M., Wilson, K., Churcher, A. M., Taylor, J. S., Chen, N., Murray, G., Wang, D., Mellott, D., Olinski, R., Hallböök, F., Thorndyke, M. C. A genomic view of the sea urchin nervous system. Developmental Biology. 2006, 300, 434-460.

Butt R. H.; Coorssen J. R. Pre-extraction Sample Handling by Automated Frozen Disruption Significantly Improves Subsequent Proteomic Analyses. J Proteome Res. 2006, 5, 437-448.

Cobb, J. L.S. The significance of the radial nerve cords in asteroids and echinoids. Z. Zellforsch. 1970, 108, 457-474.

Cobb, J.L. S., Laverack, M. S. Neuromuscular systems in echinoderms. Symp. Zool. Soc. Lond. 1967, 20, 25-51.

Cobb, J.L. S., Moore, A. Studies on the integration of sensory information by the nervous system of the brittlerstar *Ophiura ophiura*. Mar. Behav. Physiol. 1989, 14, 211-222.

Consortium, Sea Urchin Sequencing. The genome of the sea urchin *Strongylocentrutus purp*uratus. Science. 2006, 10, 941-952.

Coorssen, J.R. (2008) Synaptic Proteins and Regulated Exocytosis. In: Encyclopedia of Neuroscience. Binder, M.D.; Hirokawa, N.; Windhorst, U. (Eds.) Springer, Heidelberg.

Dunah, A. W., Standaert, D. G. Dopamine D1 receptor-dependent trafficking of striatal NMDA glutamate receptors to the postsynaptic membrane. The journal of Neuroscience. 2001, 21, 5546-5558.

Dupont, S., Thorndyke, M. Bridging the regeneration gap: insights from echinoderm models. Nature Reviews Genetics. 2007, 8.

Elphick, M. R., Price, D. A., Lee, T. D., Thorndyke, M. C. The SALMFamides: a new family of neuropeptides isolated from an echinoderm. Proc. R. Soc. Lond. 1991, 243, 121-127.

Emes, R., Pocklington, A., Anderson, C., Bayes, A., Collins, M., Vickers, C., Croning, M., Malik, B., Choudhary, J., Armstrong, J., Grant, S. Evolutionary expansion and anatomical specialization of synapse proteome complexity. *Nature Neuroscience.* 2008, 11, 799-806.

García-Arrarás, J. E., Enamorado-Ayala, I., Torres-Avillán, I., Riviera, V. FMRFamide-like immunoreactivity in cells and fibers of the holothurian nervous system. Neurosci. Lett. 1991, 132, 199-202.

García-Arrarás, J. E., Rojas-Soto, M., Jimenez, L. B., Diaz-Miranda, L. The enteric nervous system of echinoderms: unexpected complexity revealed by neurochemical analysis. J. Exp. Biol. 2001, 204, 865-873.

Gil-Dones, F., Alonso-Orgaz, S., Avila, G., Martin-Rojas, T., Moral-Darde, V., Barroso, G., Vivanco, F., Scott-Taylor, J., Barderas M.G. An optimal protocol to analyze the rat spinal cord proteome. Biomarker Insights. 2009, 4, 135-164.

Gobon, J., Nordhoff, E., Migorodskaya, E., Ekman, R., Roepstorff, P. Sample purification and preparation technique based on nano-scale reversed-phase columns for the sensitive analysis of complex peptide mixtures by matrix-assisted laser desorption/ionization mass spectrometry. Journal of Mass Spectrometry. 1999, 34, 105-116.

Hagg, E.S. Echinoderm rudiments, rudimentary bilaterians, and the origin of the chordate CNS. Evol and Develop. 2005A, 7:4, 280-281.

Hagg, E.S. Reply to Nielsen. Evol and Develop. 2005B, 8:1, 3-5.

Hervé, J.C., Phelan, P., Bruzzone, R., White, T.W. Connexins, innexins and pannexins: Bridging the communication gap. Bioch Biophis Acta. 2005, 1719, 3-5.

Hyman, L. H. The Invertebrates: Echinodermata. New York : McGraw-Hill, 1955, 4.

Kennedy, M.J., Ehlers, M.D. (2011) Mechanisms and function of dentritic exocytosis. Neuron. 69, 856-875.

Koyama, T., Noguchi, K., Aniya, Y., Sakanashi, M. Analysis of annticoagulant action of placinin, a cew anticoagulant peptide isolated from the starfish *Acanthaster planci*, in the blood coagulation cascade. Gen Pharmacol. 1998, 31, 277-282.

Larsen, M. R., Cordwell, S. J., Roepstorff, P. Graphite powder as an alternative or supplement to reversed-phase material for desalting and concentration of peptide mixtures prior to matrix-assisted laser desorption/ionization-mass spectrometry. Proteomics. 2002, 2, 1277-1287.

Mann, K., Poutka, A. J., Mann, M. The sea urchin (*Strongylocentrotus purpuratus*) test and spine proteomes. Proteome Science. 2008, 6, epub.

Martinéz, A., López, J., Montuenga, L., Villaró, A. C. Regulatory peptides in gut endocrine cells and nerves in the starfish *Marthasterias glacialis*. Cell Tissue Res. 1993, 271, 375-380.

Martínez, A., Riveros-Moreno, V., Polak, J. M., Moncada, S., Sesma, P. Nitric oxide (NO) synthase immunoreactivity in the starfish *Marthasterias glacialis*. Cell Tissue Res. 1994, 275, 599-603.

Martínez, A., Unsworth, E. J., Cuttitta, F. Adrenomedullin-like immunoreactivity in the nervous system of the starfish *Marthasterias glacialis*. Cell Tissue Res. 1996, 283, 169-172.

Mladenov, P. V., Bisgrove, B., Aostra, S., Burke, R. D. Mechanisms of arm tip regeneration on the sea star *Lepasterias hexactis.* Roux´s Arch. Devl. Biol. 1989, 198, 19-28.

Moore, S. J., Thorndyke, M. C. Immunocytochemical mapping of the novel echinoderm neuropeptide SALMFamide 1 (S1) in the starfish *Asterias rubens*. Cell Tissue Res. 1993, 274, 605-618.

Moss, C., Burke, R. D., Thorndyke, M. C. Immuno-cytochemical localisation of the echinoderm neuropeptide GFNSALMFamide (S1) and serotonin in the larvae of the starfish *Pisaster ochraceus* and *Asterias rubens*. J. Mar. Biol. Ass. 1994, 74, 61-71.

Moss, C., Hunter, A., Thorndyke, M. Patterns of bromodeoxyuridine incorporation and neuropeptide immunoreactivity during arm regeneration in the starfish *Asterias rubens*. Phil. Trans. R. Soc. Lond. 1998, 353, 421-436.

Neuhoff, V., Harold, N., Ehrhardt, W. Improved staining of proteins in polyacrylamide gels including isoelectric focusing gels with clear background at nanogram sensitivity using Coomassie Brilliant Blue G-250 and R-250. Electrophoresis. 1988, 9, 255-262.

Newman, S. J., Elphick, M. R., Thorndyke, M. C. Tissue distribution of the SALMFamide neuropeptides S1 and S2 in the starfish *Asterias rubens* using novel monoclonal and poly-clonal antibodies. I. Nervous and locomotory systems. Proc. R. Soc. Lond. 1995A, 261, 139-145.

Newman, S. J., Elphick, M. R., Thorndyke, M. C. Tissue distribution of the SALMFamide neuropeptides S1 and S2 in the starfish *Asterias rubens* using novel monoclonal and poly-clonal antibodies. II. Digestive system. Proc. R. Soc. Lond. 1995B, 261, 187-192.

Newman, S. J., Thorndyke, M. C. Localisation of gamma aminobutyric acid (GABA)-like immunoreactivity in the echinoderm *Asterias rubens*. Cell Tissue Res. 1994, 278, 177-185.

Nielsen, C. Homology of echinoderm radial nerve cords and the chordate neural tube???. Evol and Develop. 2006, 8:1, 1-2.

Perlson, E., Medzihradszky, K.F., Darula, Z., Munno, D.W., Syed, N.I., Burlingame, A.L., Fainzilber, M. (2004) Differential Proteomics Reveals Multiple Components in Retrogradely Transported Axoplasm After Nerve Injury. *Molecular and cellular proteomics*. 3, 510-520.

Ryan, T., Grant, S. The origin and evolution of synapses. *Nature Reviews Neuroscience.* 2009, 10, 701-712.

Rychel, A.L., Swalla, B.J. (2009) Regeneration in Hemichordates and Echinoderms. In Stem cells in marine organisms. Springer Netherlands. Baruch Rinkevich and Valeria Matranga (eds), 245-265.

Sahara, H., Hanashima, S., Yamazaki, T., Takahashi, S., Sugawara, F., Ohtani, S., Ishikawa, M. Anti-tumor effect of chemically synthetized sulfolips based on sea urchin's natural sulphonoquinovosylmonoacylglycerols. Jpn. J. cancer Res. 2002, 93, 85-92.

Sahara, H., Ishikawa, M., Takahashi, T., Ohtani, S., Sato, N., Gasa, S., Akino, T., Kikuchi, K. In vivo anti-tumor effect of 3´-sulphonoquinovosyl1'-monoacylglyceride isolated from a sea urchin (*Strongylocentrotus intermedius*) intestine. Br. J. Cancer. 1997, 75, 324-332.

Santos, R., Costa, G. C., Franco, C. F., Alves, P. G., Flammang, P., Coelho, A. V. First Insights into the biochemistry of the tube foot adhesive from the sea urchin *Parentrotus lividus* (Echinoidea, Echinodermata). Marine Biotechnology. 2009, 11, 686-698.

Singh, O. V., Yaster, M., Xu, J., Guan, Y., Guan, X., Dharmarajan, A. M., Raja, S. N., Zeitlin, P. L., Tao, Y. Proteome of synaptosome-associated proteins in spinal cord dorsal horn after peripheral nerve injury. Proteomics. 2009, 9, 1241-1253.

Smith, J. E. The form and function of the nervous system. Phy. R. A. Boolootian. New York : Interscience, 1966, 503-512.

Spira, M.E., Oren, R., Dormann, A., Ilouz, N., Lev, S. (2001) Calcium, Protease activation, and cytoskeleton remodeling underlie growth cone formation and neuronal regeneration. Cellular and Molecular Neurobiology. 21, 591-604.

Stiess, M., Bradke, F. (2010) Neuronal polarization: The cytoskeleton leads the way. Develop Neurobiol. 71, 430-444.

Swell, M. A., Eriksen, S., Middleditch, M. J. Identification of protein components from the mature ovary of the sea urchin *Evechinus chloroticus* (Echinodermata: Echinoidea). Proteomics. 2008, 8, 2531-2542.

Thorndyke, M., Carnevali, C. Regeneration neurohormones and growth factors in echinoderms. Can J Zool. 2001B, 79, 1171-1208.

Thorndyke, M.C., Patruno, M., Moos, C., Beesley, P. Cellular and molecular bases of arm regeneration in brittlestars in Prc 10th Int Echinoderm Conf, Dunedin, 2000. AA Balkema, Rotterdam. Barker M. 2001A, 323-326.

Vizcaíno JA, Côté R, Reisinger F, Foster JM, Mueller M, Rameseder J, Hermjakob H, Martens L. A guide to the Proteomics Identifications Database proteomics data repository. Proteomics. 2009. 9, 4276-4283.

Wang, W., Hong, J., Lee, C. O., Im, K. S., Choi, J. S., Jung, J. H. Cytotoxic stereols and saponins from the starfish *Certonardoa semiregukar*is. J. Nat Prod. 2004, 67, 584-591.

Weber, T., Zemelman, B.V., McNew, J.A., Westermann, B., Gmachl, M., Parlati, F., Söllner, T.H., Rothman, J.E. (1998) SNAREpins: minimal machinery for membrane fusion. Cell. 92(6), 759-772.

Zoidl, G., Dermietzel, R. On the search for the electrical synapse: a glimpse at the future. Cell Tissue Res. 2002, 310, 137-142.

CHAPTER 3

COELOMIC FLUID AND COELOMOCYTES PROTEOME CHARACTERIZATION

CATARINA FERRAZ FRANCO[1], ROMANA SANTOS[1,2], ANA VARELA COELHO[1]

1: Instituto de Tecnologia Química e Biológica, Universidade Nova de Lisboa, Oeiras, Portugal;

2: Unidade de Investigação em Ciências Orais e Biomédicas, Faculdade de Medicina Dentária, Universidade de Lisboa, Portugal.

PUBLICATIONS CONTAINING EXPERIMENTAL DATA PRESENTED IN THIS CHAPTER*

Franco C., Santos R., Coelho A.V. (2011) Proteome characterization of sea star coelomocytes - the innate immune effector cells of echinoderms Proteomics. 11(17), 3587-3592. (Appendix 2)

*NOTE: The results obtained in the proteomic characterization of the cell free coelomic fluid here described are preliminary and future work needs to be done for further publication

AUTHORS CONTRIBUTION

Franco C. (CF), Santos R. (RS) and Coelho A.V (AVC) were responsible for the conception and design of the experiments. Coelomic fluid collection and preparation, optimization of protein separation protocols, 2DE experiments, 1DE experiments, nano-LC separation of peptides, MALDI-TOF/TOF data acquisition, protein identification, annotation, pathway analysis and data interpretation were performed by CF. CF wrote the manuscript published in Proteomics and RS, AVC revised it critically.

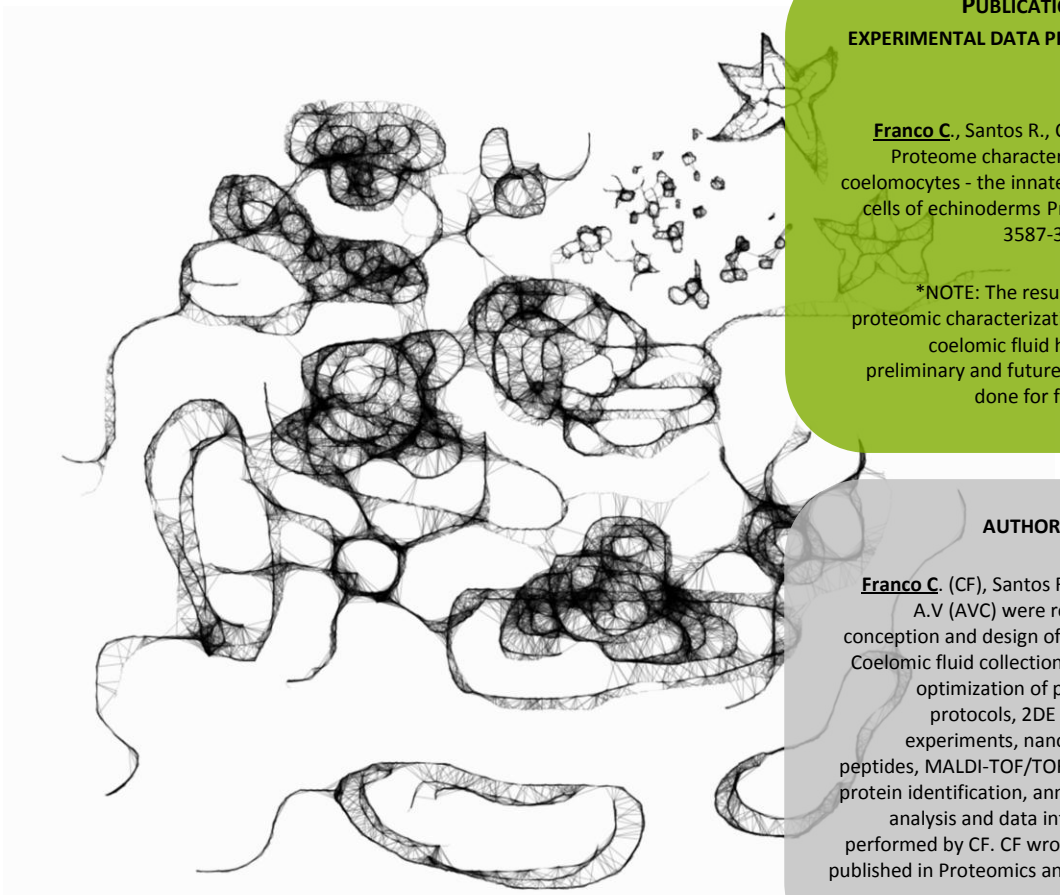

Image: Interpretation of starfish coelomocytes.

CHAPTER 3

COELOMIC FLUID AND COELOMOCYTES PROTEOME CHARACTERIZATION

Supplementary material containing experimental data described in this chapter*

COELOMOCYTES PROTEOME CHARACTERIZATION

Supplementary data 3.1: *Sequence and peptide information* of all proteins identified in starfish *Marthasterias glacialis* coelomocytes *2DE* gels using the protein identification workflow herein described. Protein identification data are organized in four different spreadsheets according to the *Protein Identification Stages*.

Supplementary data 3.2: *Sequence and peptide information* of all proteins identified in *1DE*-nano-LC MALDI-TOF/TOF analysis of *M. glacialis* coelomocytes.

Supplementary table 3.3: *Non-redundant protein list* resulting from protein clustering and parsimony analysis of the identified proteins in 1DE nano-LC- MALDI-TOF/TOF-MS and 2DE-MALDI-TOF/TOF-MS experiments of *M. glacialis coelomocytes*. The table includes identified protein clusters, pathway analysis, MASCOT/ProteinPilot identification scores, sequence coverage, accession numbers, 2DE spot/1DE lane ID, sequences of the fragmented peptides and BLASTp results for unknown/uncharacterized and *S. purpuratus* proteins.

CELL FREE COELOMIC FLUID PROTEOME CHARACTERIZATION

Supplementary data 3.4**:** *Sequence and peptide information* of all proteins identified in *M. glacialis cell free coelomic fluid (CFF) 2DE* gels using MASCOT for protein identification and PEAKS Studio for *de novo* sequencing of unidentified peptides. Annotated *MS/MS* spectra of *de novo* sequenced peptides are also presented.

Supplementary data 3.5: *Sequence and peptide information* of all proteins identified in *1DE*-nano-LC MALDI-TOF/TOF analysis of *M. glacialis* CFF proteome.

Supplementary table 3.6**:** *Non-redundant protein list* of the identified proteins the *CFF* derived from both 1DE nano-LC- MALDI-TOF/TOF-MS and 2DE-MALDI-TOF/TOF-MS experiments. GO annotations according to biological process, molecular function and cellular component for all the identified proteins is also presented.

Supplementary figure 3.1: *Cluster analysis of the CFF 2DE spots* peptide mass fingerprints (PMF) performed with SPECLUST in order to identify groups of similar spots. Random coelomocytes PMF were also included as decoys to evaluate CFF proteins similarity with other distinct proteomes.

* Please see enclosed CD to access the supplementary material

SUMMARY| COELOMIC FLUID PROTEOME CHARACTERIZATION

Starfish coelomic fluid is in contact with all internal organs, carrying a multitude of secreted molecules and a large population of circulating cells, the coelomocytes. Since echinoderms lack an acquired immune system, the circulatory coelomocytes mediate the innate immunity, being key players in clotting reactions, phagocytosis, encapsulation, nodule formation and secretion of antibacterial and antifungal proteins. These cells are also known to have an important role in the first stage of regeneration, *i.e*. wound closure, necessary to prevent body fluid balance disruption and to limit the invasion of pathogens.

This chapter focuses on the proteome characterization of these multi-tasked cells, the coelomocytes, and the cell free coelomic fluid, which is rich in factors secreted by these circulating cells. Both proteome characterizations were achieved using a combination of 1D SDS PAGE gels, nano-LC-MS/MS or 2D SDS PAGE gels for protein separation, and MALDI-TOF/TOF mass spectrometry analysis for protein identification.

To our knowledge, the present work represents the first comprehensive list of starfish coelomocyte proteins. Some of the secreted proteins into the coelomic fluid were also identified, the majority being glycoproteins, such as lectins and fibrinogen like molecules. Evidences of new pathways that have not yet been assigned to echinoderms coelomocytes are described as well, constituting a valuable resource to stimulate future studies on the function of these proteins and pathways and evaluate their similarity with vertebrate immune cells.

3.1. INTRODUCTION

Similarly to other invertebrates, echinoderms lack an acquired immune system and therefore do not express the lymphoid antibody producers' cell line responsible for the existence of immunoglobulins in vertebrates. Nevertheless, they have a very well developed nonspecific and nonadaptive immune response that shows similarities to higher vertebrate innate immunity. This response is mediated by the circulatory cells that occupy the perivisceral coelomic cavities - coelomocytes, which are key players in clotting reactions, phagocytosis, oxygen transport, synthesis and secretion of antibacterial and antifungal proteins (Cavey *et al*., 1994; Gross *et al*., 1999; Haug *et al*., 2010) namely, hemolysins, agglutinins and lectins (Gross *et al*., 1999; Cervello *et al*., 1996; Tahseen *et al*., 2009).

With the characterization of cDNA sequences from the purple sea urchin *Strongylocentrotus purpuratus,* evidences of homologies in the innate immune responses within the deuterostome lineage were revealed, in which echinoderms and vertebrates are included (Al-Sharif *et al*., 1998). Sea urchins were shown to possess proteins homologous to the vertebrate C3 and factor B complement system components, called *SpC3* and *SpBf*, respectively (Al-Sharif *et al*., 1998; Smith *et al*., 1998). These two proteins act together to promote opsonization of foreign cells and particles in sea urchins and subsequent destruction by the coelomocytes (Smith *et al*., 1998). The level of complexity of echinoderm immune responses has been further demonstrated by the identification of several differently expressed proteins in sea urchins coelomic fluid upon bacterial challenge.

These include the 185/333 proteins, which seem to be tailored to produce a pathogen-specific immune response, as well as apextrin and calreticulin that seem to be involved in the sequestration or inactivation of bacteria (Dheilly *et al*., 2009; Nair *et al*., 2005; Dheilly *et al*., 2011). Other examples of immune system associated molecules identified in echinoderms include serine protease inhibitors and scavenger receptors (SRCRs) (for review Smith *et al.*, 2011).

In starfish, coelomocytes have been reported to respond to trauma stress, having an important role in wound closure, which is the first stage of regeneration. This is done by a rapid and massive accumulation of coelomocytes at the wound site, which plugs and heals the wound, helping to maintain homeostasis, thus preventing the loss of body fluids and limiting the invasion of pathogens (Pinsino *et al*.,2007; Carnevali *et al*., 2001; Holm *et al*., 2008). At the molecular level, enhanced expression of profilin transcripts in coelomocytes has demonstrated the immune response of echinoderms to minimal injury (Smith *et al*., 1992).

In order to initiate the proper immune response mediated by coelomocytes, intercellular communication events must be effective, and since coelomocytes are dispersed in the coelomic fluid, soluble factors are determinant to initiate the necessary cellular cascade of events. Proteins and peptides are common signaling molecules, influencing cell growth, proliferation and survival. In echinoderms these molecules, namely neurotransmitters (eg. monoamines like dopamine and serotonin), neuropeptides (eg. substance P; SALFamide 1 and 2) and nerve derived growth factors (eg. transforming growth factors-TGF-β, bone morphogenetic protein-BMP, nerve growth factor-NGF, fibroblast growth factors-FGF-2) have been shown to be secreted by the radial nerve cord or by circulating coelomocytes into the coelomic fluid (Carnevali *et al*., 1998; Patruno *et al*., 2001).

Among the characterized coelomic fluid proteins are those that are involved in the echinoderm immune responses, that include agglutination factors such as amassin, which promotes clot formation through coelomocytes cross-linking (Hillier *et al.,* 2003); and a wide variety of lectins, which play important functions in foreign cells recognition by binding mono- and disaccharides present in the surface of pathogens, causing a direct activation of the complement system (Ikeda *et al*., 1987). Analysis of purple sea urchin genome shows genes encoding more than 100 small C-type lectins, over 400 mosaic proteins with lectin domains and 34 galectins (Smith *et al*., 2011) in addition to a few pentraxins and fucolectins (Multerer *et al.*, 2004). Numerous C-type lectins have been characterized in several echinoderm species, such as echinoidin (Multerer *et al.*, 2004) and echinonectin (Alliegro *et al.,* 1988) but essentially from a functional and biochemical point of view, and hence, proteomic approaches may bring useful information on new echinoderm lectins or on other new proteins with opsonin and agglutin functions, important for echinoderms immune response.

Amongst the invertebrate animal models, the class Echinoidea of the phylum Echinodermata has one of the most studied non-vertebrate immune system. However, the molecular basis of echinoderm immune systems has been advancing through the generation of basically two types of information, the publication of the purple sea urchin genome that provided an unprecedented insight into the echinoid immune repertoire (consortium, 2006; Rast *et al*., 2006) and the identification of the genes being expressed (macroarray technology) in coelomocytes upon immunological challenge with bacterial lipopolysaccharides (Ramírez-Gómez *et al*., 2009; Nair *et al*., 2005). To date, only a few proteomic studies aiming to identify the proteins present in coelomocytes and differently expressed upon an immunologic challenge have been conducted (Dheilly *et al*., 2009 and 2011), and so far, no high throughput proteomic characterization of coelomocytes or of proteins secreted to the coelomic fluid has been performed.

Here we present the first high throughput proteomic characterization of coelomocytes and cell free coelomic fluid from the starfish *Marthasterias glacialis*. The combination of 1D and 2D SDS-PAGE gels and mass spectrometry (MALDI-TOF/TOF) allowed the identification of 358 coelomocyte proteins and 47 proteins present in the cell-free coelomic fluid. Many of the identified proteins constitute new assignments for

Figure 3.1: Coelomic fluid collection. The starfish epidermis is punctured with a needle and the coelomic fluid is drained by gravity or is collected using a syringe with anticoagulant to prevent coelomocyte clotting formation.

proliferation and regeneration. Also, several lectin-like proteins were identified in *M. glacialis* coelomic fluid together with the identification of a protein homologous to ficolin, which may be involved in the activation of the lectin complement pathway. Several other proteins that might have important functions in echinoderm immunity machinery that had never been described in the coelomic fluid were also identified.

In summary, the obtained results represent the most complete comprehensive list of starfish coelomocyte proteins available at present, thus constituting a valuable resource for future research on the function of these newly assigned molecules in immune response of echinoderms.

echinoderms and belong to molecular pathways, to date not reported for this Phylum. Among these are pathways involved in cytoskeleton dynamic reorganization, regulation of cell adhesion, regulation of cell division cycle and apoptosis, signal transduction, regulation of trafficking/migration of immune cells and calcium mediated adhesion during inflammation, vesicular protein secretion, regulation of cellular

3.2. MATERIALS AND METHODS

3.2.1. Starfish coelomic fluid collection

Several adult specimens of both genders of the starfish *Marthasterias glacialis* (Linné, 1758) were collected at low tide on the west coast of Portugal (Estoril, Cascais). Animals were transported to "Vasco da Gama"

Table 3.1: IEF optimized conditions for the starfish coelomocytes and cell free coelomic fluid.

	CELL FREE COELOMIC FLUID				COELOMOCYTES			
Protein solubilization buffer	8 M Urea, 2M thiourea, 2 % (w/v) CHAPS, 60 mM DTE				8 M Urea, 2M thiourea, 2 % (w/v) CHAPS, 60 mM DTE			
pH range; IEF Strip length	3-11 NL; 7cm				3-11 NL; 11cm			
IPG Buffer used; final concentration % (v/v)	IPG Buffer 3-11 NL; 1% (v/v)				IPG Buffer 3-11 NL; 1% (v/v)			
Total protein loaded (µg)	100				400			
IEF program	Voltage (v)	Voltage mode	Time (h:min)	V.h	Voltage (v)	Voltage mode	Time (h:min)	V.h
	100	S&H	1:30	150	100	S&H	1:30	150
	250	S&H	1:00	250	250	S&H	1:00	250
	1000	S&H	1:30	1500	1000	S&H	1:30	1500
	2500	S&H	1:00	2500	2500	S&H	1:00	2500
	4000	G	0:30	1000	4000	G	0:30	1000
	4000	S&H	2:24	9600	4000	S&H	4:40	18600
	Total		07:54	15000	Total		10:15	24000

Aquarium (Dafundo, Oeiras) where they were kept in open-circuit tanks with re-circulating seawater at 15°C and 33‰. They were fed *ad libitum* with a diet of mussels collected weekly at the same site. Animals used in the experiments had similar sizes, with radius ranging from 10 to 13 cm, measured from the largest arm tip to the center of the oral disc.

The internal fluid of the starfish, the coelomic fluid, was collected by puncturing the animal epidermis at the arm tip with a needle and collecting the fluid by gravity into an ice cold recipient containing a protease inhibitor cocktail to prevent endogenous proteolysis (Figure 3.1). Then, low speed centrifugation was used in order to separate the coelomic fluid in two fractions, the coelomocytes and the cell-free coelomic fluid.

The number of coelomocytes present in *M. glacialis* coelomic fluid was also determined, however it had to be collected using a syringe with an anticoagulant to avoid clotting (1.2 ml pediatric syringes, S-Mono Vet Starsted and 20Gx 1(1/2)' hypodermic needle, S-Mono Vet needle, Starsted) (Figure 3.1). Cells were then counted using a Burker chamber. For the proteomic experiments, pelleted coelomocytes were flash frozen in liquid N_2 and stored at -80°C until further processing.

3.2.2. Cell free coelomic fluid protein extraction

The total protein from the supernatant, corresponding to cell free coelomic fluid (CFF), was precipitated using trichloroacetic acid (TCA) 10% (w/v), β-mercaptoethanol 0.07% (v/v) for 1h on ice. The protein pellet was then washed with ice cold acetone with 0.7% (v/v) β-Mercaptoethanol for three times for complete removal of the TCA. After centrifugation, the precipitated and washed CFF protein extract was resuspended in 1D sample buffer (Laemmli, 1970) or in 2D solubilization buffer (Table 3.1) supplemented with a complete protease inhibitor cocktail (Sigma). The total protein concentration was determined using 2D Quant Kit ™ (GE Healthcare).

3.2.3. Coelomocytes total protein extraction

The deep frozen coelomocytes were then mechanically disrupted as previously described (Butt *et al*., 2006). Briefly, 50 mg of the deep frozen cells were placed in a previously chilled teflon sample chamber containing 4 stainless steel beads (5 mm diameter). The chamber was placed in a Mikro-Dismembrator (Sartorius) and set to 3000 *rpm* for 60s. The resulting powder was resuspended in the previously mentioned buffers. After the removal of cellular debris by low speed centrifugation, the total protein concentration was determined as described for CFF.

3.2.4. Protein separation

3.2.4.1. 1D SDS PAGE

For 1DE protein separation, 7cm 12.5% (w/v) acrylamide gels were used, loaded with 25 µg total protein per lane and stained with colloidal Coomassie (Neuhoff *et al.*, 1998). Then, gel lanes were sliced for *in*-gel digestion.

3.2.4.2. 2D SDS PAGE

2DE was performed using an IPGphor system (GE Healthcare) in which 7 and 11cm pH 3-11 *non linear* Immobiline DryStrip were loaded, respectively, with 100 and 400 µg total protein of the CFF and coelomocytes protein extracts. Isoelectric focusing was thoroughly optimized in order to obtain optimal protein resolution despite high salt content of samples. Table 3.1 summarizes the optimized conditions used for isoelectric focusing.

After a two-step equilibration of the strips for reduction and alkylation, the second dimension was performed in an Ettan DaltSix (GE Healthcare) using 24 cm 12.5% acrylamide gels, each containing two IEF strips. Gels were stained with colloidal Coomassie (Neuhoff *et al.*, 1998), scanned with LabScan (GE Healthcare) and analyzed with Progenesis SameSpots (version 3.3; NonLinear Dynamics).

3.2.5. In-gel tryptic digestion

The excised gel spots and bands were washed and digested with trypsin as previously described in Chapter 2.

3.2.6. Tryptic peptides desalting and separation

3.2.6.1. 2DE spots

The tryptic digests from the 2D gel spots were desalted and concentrated on homemade chromatographic microcolumns using GELoader tips packed with POROS R2 (20 µm bead size) and directly eluted onto the MALDI plate using 0.5µl of 5 mg/ml α-CHCA in 50% (v/v) ACN with 2.5% (v/v) of formic acid.

3.2.6.2. 1DE bands

Peptides from the 1D digested bands were further fractionated by nano-LC and spotted directly into a MALDI plate as previously described in Chapter 2.

3.2.7. MALDI-TOF/TOF analysis

Tandem mass spectrometry was performed using the same conditions as described in Chapter 2.

BOX 3.1| Search parameters

MASCOT (version 2.2; Matrix Science, Boston, MA) searches were performed with a minimum mass accuracy of 30 ppm for the parent ions, an error of 0.3 Da for the fragments, one missed cleavage in peptide masses, and carbamidomethylation of Cys and oxidation of Met as fixed and variable amino acid modifications, respectively.

ProteinPilot (Protein Pilot software version 3.0, revision 114732; Applied Biosystems, USA) searches were performed without taxonomic restrictions and search parameters were set as follows: enzyme, trypsin; Cys alkylation, iodoacetamide; special factor, gel-based ID; and ID focus, biological modification and amino acid substitution.

BOX 3.2| Protein sequence databases information

[A] Purple sea urchin *Strongylocentrotus purpuratus* predicted database (42.420 entries; December 2006; ftp://ftp.ncbi.nih.gov/genomes/StrongylocentrotuS_purpuratus/protein;

[B] Uniprot/SwissProt database (release 2010_04; 11.134.468 entries);

[C] non-redundant protein database Uniref100 (release 2010_06; 10.246.365 entries).

BOX 3.3| Data deposition on public repositories

Protein identification files derived from MASCOT were converted to mzML files using PRIDE Converter tool (Barsnes *et al.*, 2009) and are available in the PRIDE database (Vizcaíno *et al.*, 2009).

Project ID: Coelomocytes
Accession number: 15332/15334
Username: review04162
Password: 2aZMhe^d

3.2.8. Protein identification, annotation and pathway analysis

3.2.8.1. Coelomocytes 2DE spots protein identification workflow

In order to overcome the lack of a complete starfish genome information, which impairs the success of protein identification, two different search algorithms, MOWSE and Paragon (see details on BOX 3.1), and several different protein databases were used (see details on BOX 3.2) in a "4 stage" protein identification workflow (Figure 3.2). Protein identification files derived from MASCOT are available in the PRIDE database (see BOX 3.3 for details).

Stage 1: All spectra were submitted for search using MASCOT algorithm against database **A** joined with **B** (BOX 3.2). A combined analysis of PMF (Peptide Mass Fingerprint) and tandem mass (MS/MS) was performed. The identified proteins were only considered if a protein significant score above 69 was obtained (p<0.05); and peptides were only considered if individual ions scores were above 39 [ion score>39 indicates identity or extensive homology (p<0.05)].

Stage 2: Proteins without a successful identification in stage 2 were further processed ProteinPilot algorithm and searched against database **A** joined with **B**. Proteins were only considered if having at least one peptide with 99% confidence (p<0.01) or if having two peptides: one with 95% confidence (p<0.05) and at least a second with confidence above 50%.

Stage 3: Proteins without a successful identification in stage 1 and 2 were further processed using MASCOT algorithm against database **C**. A combined analysis of PMF (Peptide Mass Fingerprint) and tandem mass (MS/MS) was also performed. Successful identifications were only considered if protein significant score was above 81 (p<0.05); and peptides were only considered if individual ions

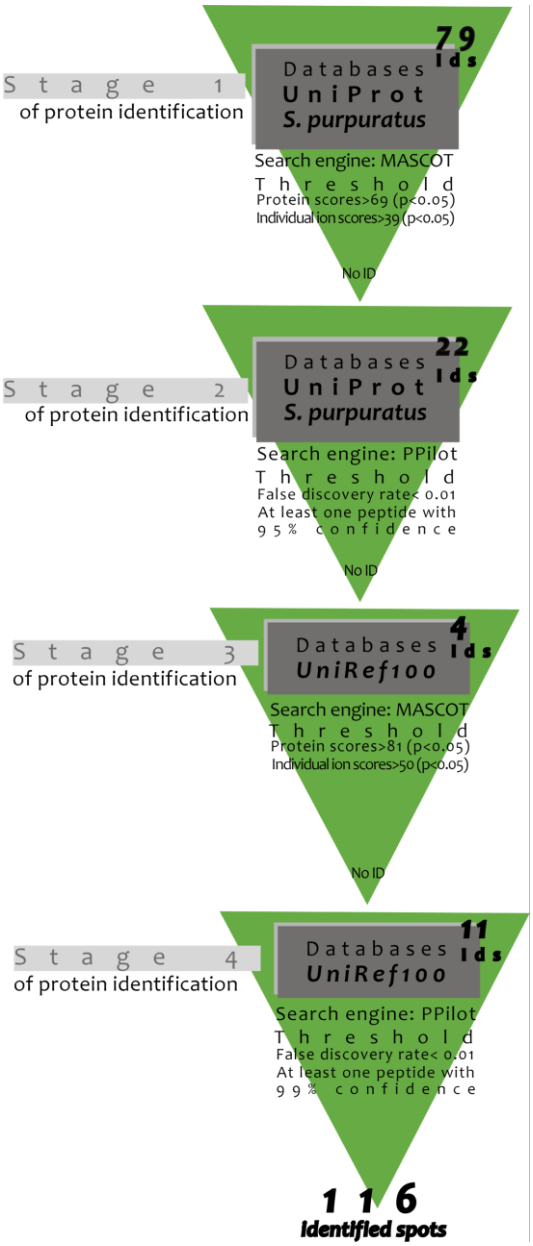

Figure 3.2: **Coelomocytes 2DE protein identification workflow.** Schematic representation of the protein identification workflow using two search engines (MASCOT®, ProteinPilot®) and four protein databases (see BOX 3.2 for details).

scores were above 50 [ion score>50 indicates identity or extensive homology (p<0.05)].

Stage 4: Proteins without a successful identification from stage 3 were further processed ProteinPilot algorithm and searched against database **C**. Proteins were only considered if having at least one peptide with 99% confidence (p<0.01) or if having two peptides: one with 95% confidence (p<0.05) and at least a second with confidence above 50%.

3.2.8.2. Cell free coelomic fluid 2DE spots protein identification workflow

All tandem mass spectra were searched with MASCOT against all described protein databases A-C (BOX 3.2). Proteins were only accepted if confirmatory identifications were obtained (identified in more than one protein database) and if having scores above the defined thresholds (p<0.05). Since only a reduced number of spots had successful protein identification, all the MS/MS spectra from the collected 2DE spots were subjected to *de novo* sequencing in an additional characterization effort to deduce peptide sequences from the obtained tandem mass spectra.

3.2.8.3. De novo sequencing of coelomic fluid proteins

The PEAKS Studio 5.2 software (Bioinformatics Solutions) was used for automated *de novo* sequencing. This was followed by manual confirmation of the sequences generated. The *de novo* sequencing parameters used included a parent and fragment-mass error tolerance of 30 ppm and 0.3 Da, respectively; trypsin as the protease with one maximum missed cleavage allowed; partial modification of cysteine (carbamidomethyl-cysteine) and methionine (oxidized). Critical inspection of the automated generated MS/MS spectra annotation was performed based on the most abundant peptide fragments 'b-ions and y-ions', the less abundant peptide fragments 'a-ions', the neutral losses of

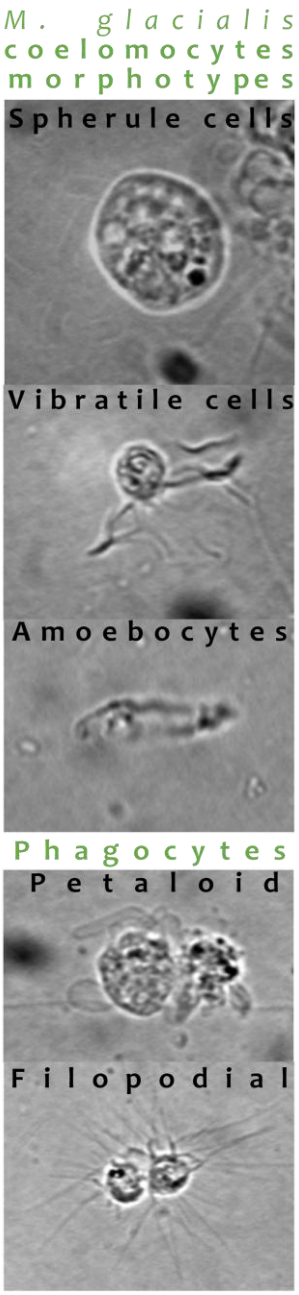

Figure 3.3: *Marthasterias glacialis* coelomocytes: Based on the morphological features presented by the cells circulating in *M. glacialis* coelomic fluid, 4 types of coelomocytes were identified using optical microscopy: spherule and vibratile cells, amoebocytes and phagocytes (petaloid and filopodial).

water for b-ions and y-ions, as well as the immonium ions.

3.2.9. Protein identification workflow of the nano-LC experiments

All spectra (4135 and 5328 for the coelomocytes and cell-free coelomic fluid, respectively) were processed with ProteinPilot using LC mode against database **A** and **B**. The false discovery rate (FDR) was determined individually for each 1DE band using PSPEP algorithm from ProteinPilot software using the reversed and original database joined together. Identified proteins were selected if the protein unused score was within a FDR of 1% and if having at least 1 peptide with 99% confidence or if having two peptides: one with 95% confidence and at least a second with confidence above 50%.

3.2.10. BLASTp searches and protein annotation

Uncharacterized/unknown proteins and all *S. purpuratus* proteins were further submitted to protein-protein BLASTp searches against SwissProt database using Basic Local Alignment Search tool available at NCBI web site (http://blast.ncbi.nlm.nih.gov/). STRAP software (Bhatia *et al*., 2009) was used to fully annotate the identified proteins using the UniProt gene ontology information on biological function, subcellular location and molecular functions. A pathway analysis using DAVID functional annotation tools (http://david.abcc.ncifcrf.gov/home.jsp) (Da Wei Huang *et al*., 2009) was also performed, obtaining a more comprehensive overview of the relevant functions enrolled by the coelomocytes. Cell-free coelomic fluid proteins were also annotated with gene ontologies using BLAST2GO web resource (http://www.blast2go.org/), however since a reduced number of proteins were identified in the coelomic fluid, no pathway analysis was performed.

3.3. RESULTS

3.3.1. Coelomocytes

Although the several types of coelomocytes where not individually analysed in our proteome characterization, a previous observation of the collected coelomocytes from *M. glacialis* was performed using light microscopy. On the basis of their morphological features 4 types of coelomocytes were recognized in the coelomic fluid: spherule and vibratile cells, amoebocytes and phagocytes (petaloid and filopodial) (Figure 3.3).

The determination of the number of coelomocytes present in *M. glacialis* coelomic fluid was performed using a Burker chamber with cells counted under a light microscope. The results showed that *M. glacialis* coelomic fluid has a population of coelomocytes comprised between 1-2 x 10^6 cell/ml, which is in the range of the values reported for the starfish *Asterias rubens* (Pinsino *et al*., 2007).

To characterize the proteome of *M. glacialis* immune cells, the coelomocytes from five biological replicates were collected by low speed centrifugation of the coelomic fluid (Figure 3.4). Then, five 2D gels were run and the detected spots were only selected for protein identification if they were present consistently in all of the analyzed 2D gels. The selected spots from the coelomocytes 2D gels were processed for protein identification by mass spectrometry and altogether, more than 85% of the coelomocytes selected spots (104), had successful protein identification (Supplementary data 3.1). This was only which was possible using a protein identification workflow that combined different databases and search algorithms. Detailed information on the number of identified proteins in each step of the protein identification

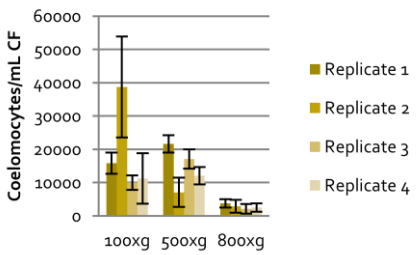

Figure 3.4: Coelomocyte collection optimization. The number of coelomocytes present in the coelomic fluid was determined prior and after the low speed centrifugation step. Centrifugation at 800 x *g* (10 min, 4°C) was enough to ensure the collection of 99.6 % of the total number of coelomocytes present in the coelomic fluid.

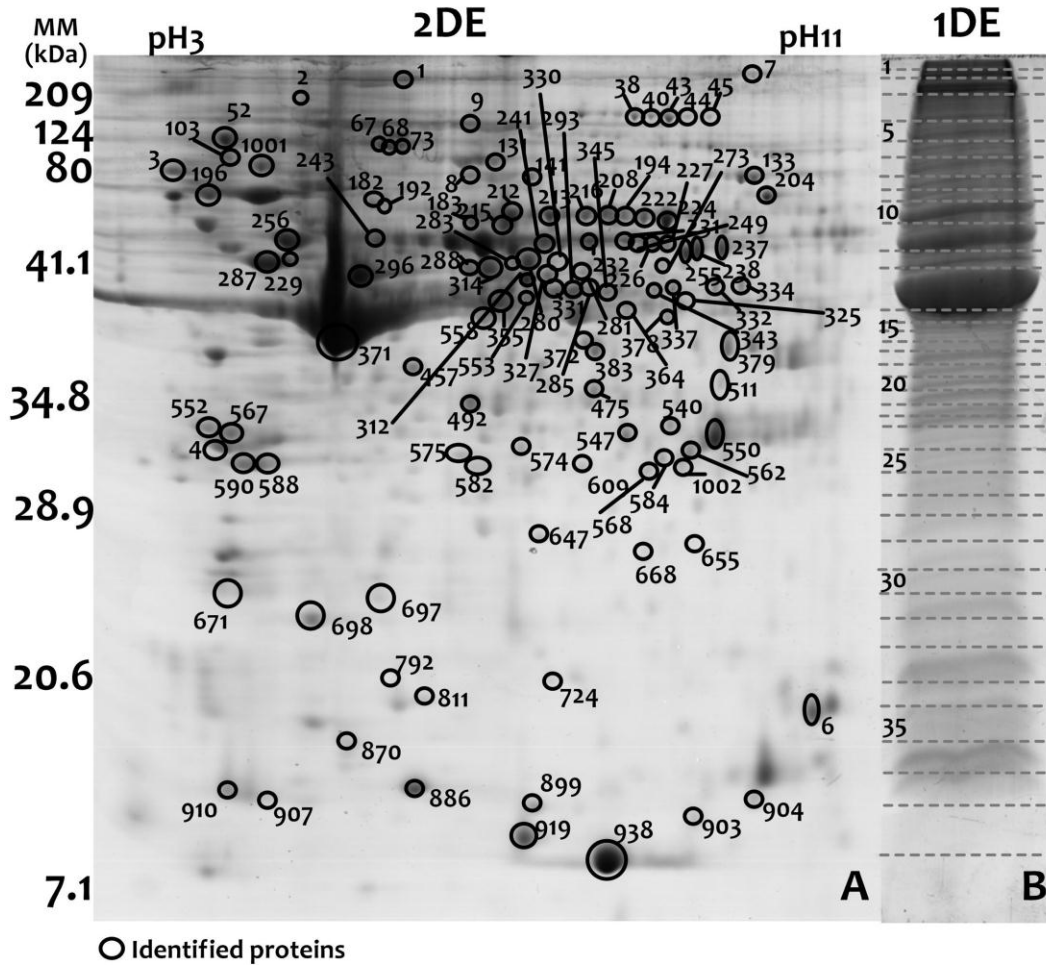

Figure 3.5: Gel separation of protein extract of the starfish *M. glacialis* coelomocytes by 2D **(A)** and 1D **(B)** electrophoresis. Black circles indicate spots with protein identification compliant with the specified criteria.
The fully annotated gel images and correspondent list of identified proteins are available in the Supplementary data 3.1 and 3.2.

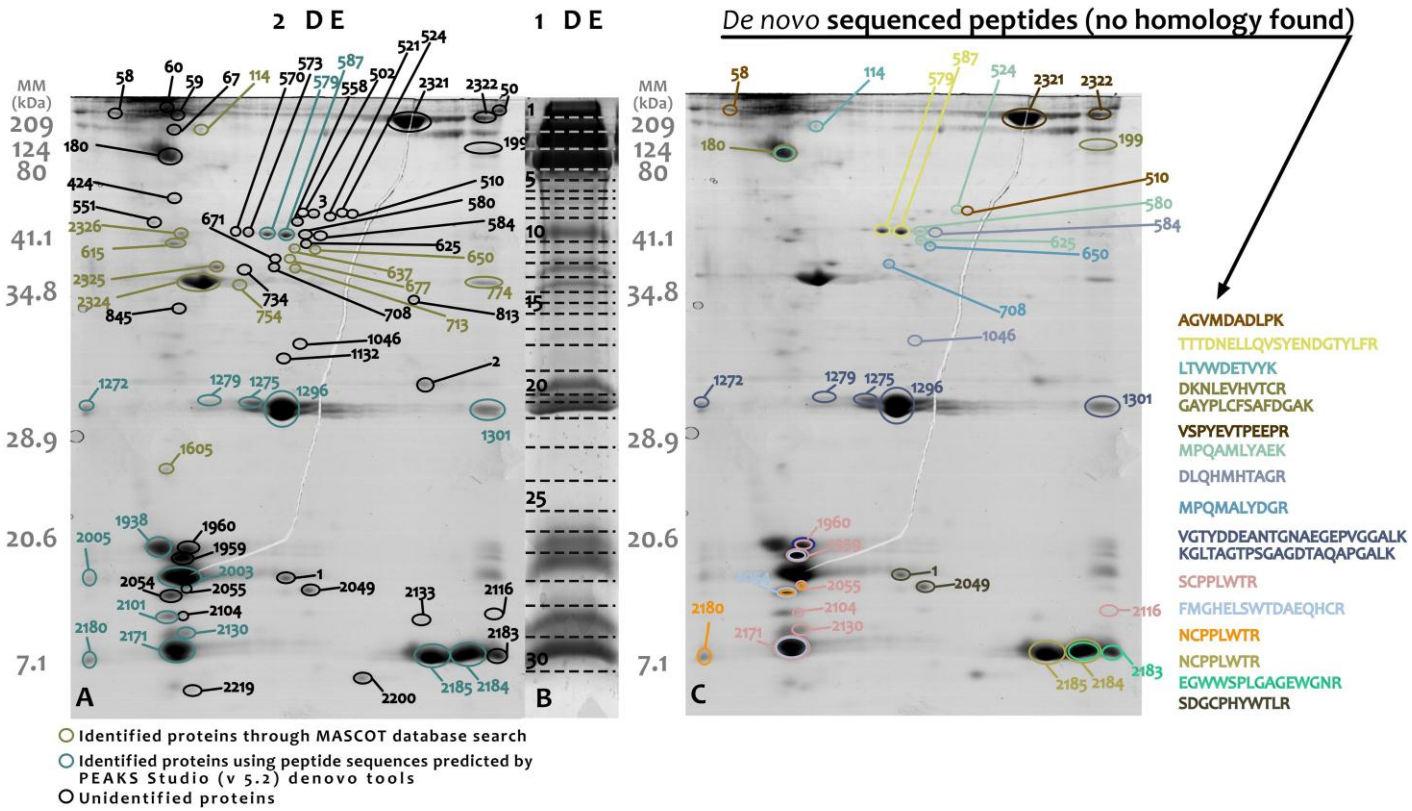

Figure 3.6: Gel separation of protein extract of the starfish *M. glacialis* cell free coelomic fluid. **A|** Fully annotated 2DE gel images with the identified proteins by MASCOT search or *de novo* sequencing; the complete protein and peptide information is available in the Supplementary data 3.4. **B|** Cell free coelomic fluid total protein separation by 1DE; the complete list of CFF proteins identified by 1D nano-LC MALDI-TOF/TOF is presented in Supplementary table 3.6. **C|** *De novo* sequenced peptides present in more than one 2DE CFF gel spot and that show no significant homology with any available protein database. The determined peptide sequences are presented on the right hand side.

workflow is given in Figure 3.2. The coelomocytes and cell free coelomic fluid reference 2D maps with the correspondent identified spots is also shown in Figure 3.5 and 3.6.

As in each 1D band (Figure 3.5B) there is a high rate of protein co-migration, an extra separation at the peptide level was performed. This was achieved by injecting each band digest in a nano-flow HPLC coupled to a MALDI plate spotter. The peptides for each 1D band were separated in one chromatographic run and the obtained 72 fractions per gel band were applied onto the MALDI sample plate. This approach, followed by database search using independent data for each band, allowed the identification of approximately 6 proteins per band, from which were derived a total of 242 proteins with an estimated FDR of 1% (Supplementary data 3.2).

The combination of two techniques for protein separation (1D SDS-PAGE coupled with nano-LC and 2D SDS-PAGE) followed by MALDI-TOF/TOF mass spectrometry allowed the identification of 358 proteins (116 proteins from 2D proteome and 242 proteins from 1D-nano-LC proteome), many of them constituting, to our knowledge, new assignments for echinoderm coelomocytes. Also, some of the proteins were identified in more than one 2D spot, indicating the presence of possible post-translational modifications or different protein isoforms that should be further investigated in order to obtain a more complete annotation of the coelomocytes proteome. Since only a few starfish proteins are deposited on the available protein sequence databases (1438 results for Asteroidea in UniProt; of which only 58 are curated sequences), the present study is a homology driven proteomic characterization. As expected, a high number of identified proteins were homologous to other echinoderm proteins deposited on the searched protein databases (30%). However, several of the identified proteins from the starfish coelomocytes shared homology with proteins from other organisms (i.e., Chordata 34%; Nematode and Annelida 9%; Arthropoda 6%; Bacteria 6%), in some of the cases with only one identified peptide. This suggests the presence of novel forms of the proteins predicted in the sea urchin genome, which need to be further validated, thus highlighting the urgent need to increase the available information on genomes/proteomes from echinoderm species.

3.3.2. Cell free coelomic fluid

For the CFF proteome characterization ten 2DE gels were performed and analyzed towards spot selection for protein identification. As seen in Figure 3.6, the CFF proteome is, by far, less complex in terms of the number of detected proteins (little over 200 detected protein spots). It is possible to see seven intense protein spots (or groups of spots), localized at masses of approximately 200 (spot 2321), 80 (spot 180), 34 (spot 2324) 30 (spot 1296), 20 (spot 2003) and 7 kDa (spots 2185, 2184, 2171) (Figure 3.6). Although several protein databases were used, the rate of CFF protein identification was substantially lower compared to coelomocytes. For instance, from the referred intense protein spots, only one was successfully identified through database search (spot 2324, actin). Over 120 gel spots were removed (in triplicate) and processed for protein identification, of which only 10% were successfully assigned to protein when searched against the described protein databases (Supplementary data 3.4). Since the unidentified tandem mass spectra were consistently of good quality (i.e. with a high *signal/noise* ratio and even fragments distributed across the mass range), they were further processed by automated *de novo* sequencing using PEAKS Studio software (version 5.2). Only peptide sequences that presented a PEAKS *de novo* confidence above 50% were selected for further manual sequence confirmation. A list of over 300 peptides (Supplementary data 3.4) was then inspected for peptide sequences common to more than one 2DE spot and further reduced to a final list of 29 peptides having the above described characteristics (Table 3.2). These peptide sequences were then submitted to BLAST searches at the NCBI site (http://blast.ncbi.nlm.nih.gov/) using the algorithm PSI-BLAST with the parameters adjusted to enable short sequences search. This strategy allowed the identification of 12 peptides sequences homologous to known protein families, many belonging to the lectin protein family (Supplementary data 3.4): echinonectin (Figure 3.7B), serum lectin P35, spEchinoidin (Figure 3.7C), bothrojaracin, lectin HeEL-1 and coagulation factor 5/8 (Figure 3.7D). Also, a group of two spots (579, 587) had a considerable homology

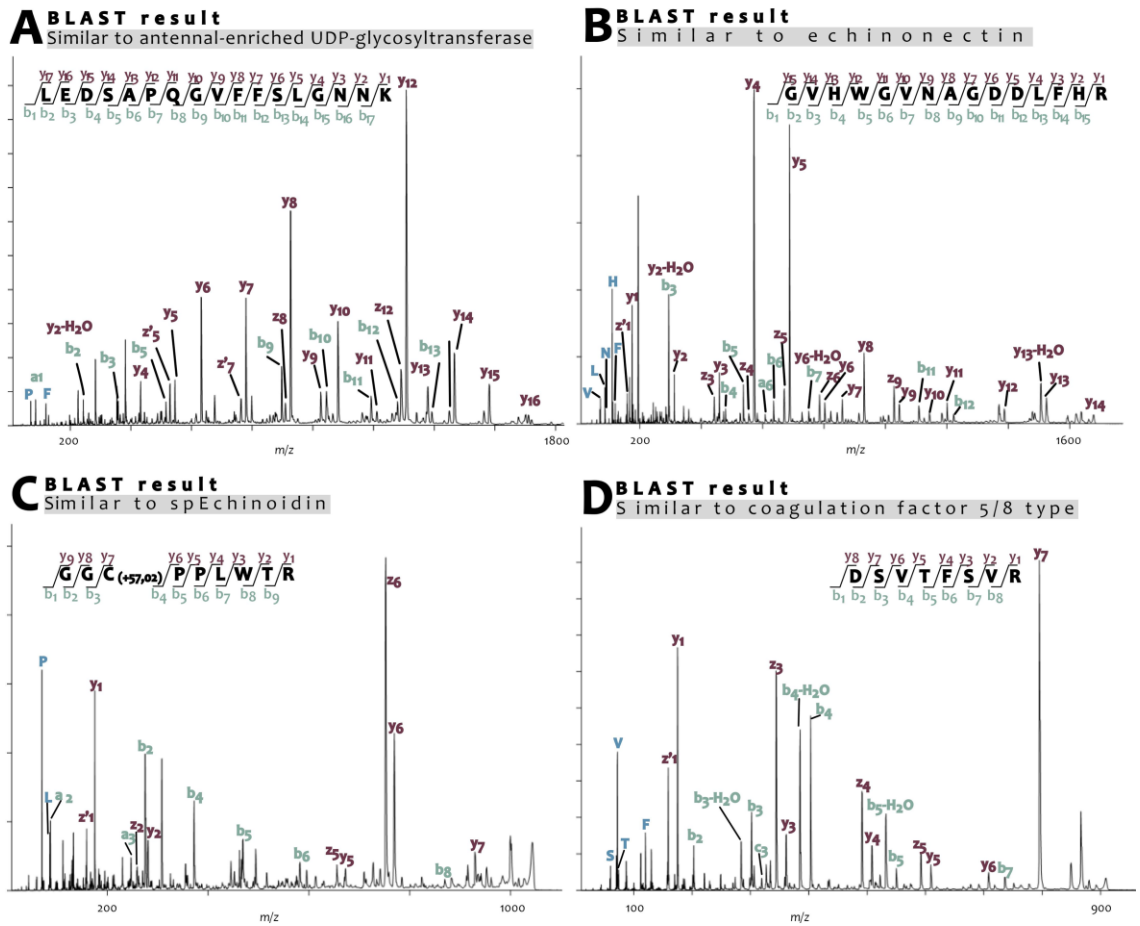

Figure 3.7: Examples of peptide sequences inferred from the tandem mass spectra using the *de novo* sequencing tools of PEAKS Studio v. 5.2. The most abundant peptide fragments 'b-ions and y-ions', the less abundant peptide fragments 'a-ions', the neutral losses of water for b-ions and y-ions, as well as the immonium ions were utilized to develop confident and complete peptide sequences *de novo* from MS/MS spectra.

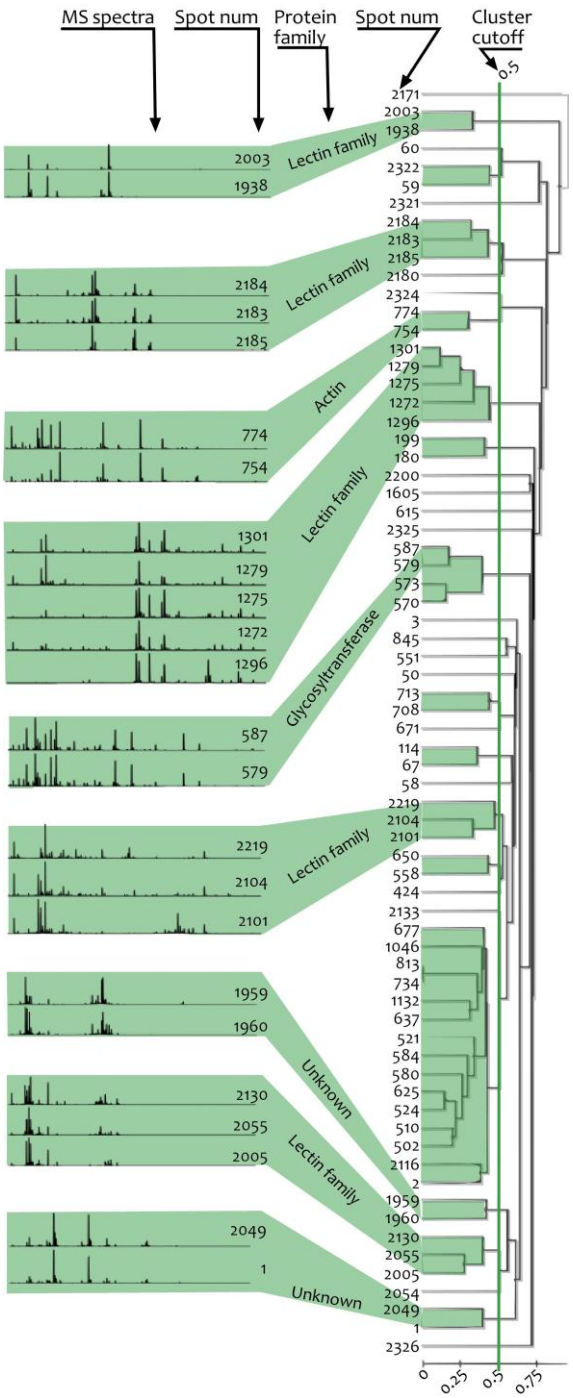

Figure 3.8: Peptide mass fingerprint similarities between cell-free coelomic fluid proteins. The analyzed MS spectra were grouped in 34 different clusters (0.5 cluster cut-off) according to the number of similar *m/z* peaks (i.e. mass differences within 0.5 Da). Some of the clustered groups share either the same protein identification derived from MASCOT search or, identical *de novo* peptide sequences predicted by PEAKS Studio software (Table 3.2; Supplementary data 3.4). Clustered spectra are highlighted in green.

TABLE 3.2

Cell-free coelomic fluid proteins identified through BLAST search of the *de novo* predicted peptide sequences. All peptides represented here appear consistently in more than one 2DE spot, indicating the presence of protein post-translational modifications or protein isoforms. *De novo* sequences were submitted to PSI BLAST and the information on the homologies found are presented (*accession number and #name of the protein with the homologous peptide; +number of identic residues and $gaps in the matched sequences). &For the *de novo* sequenced peptides matched to an hypothetical protein, an extra *BLASTp* search was performed. For the complete list of *de novo* sequenced peptides see Supplementary data 3.4.

Spots	*de novo* predicted peptide sequence	*m/z*	PEAKS Studio de novo score (%)	PSI BLAST				Sequence of the query peptide	*BLASTp*[&]
				Query accession*	Query name[#]	Identity[+]	Gaps[$]		
2324/754	**VGC(+57,02)SDESGPSLVHR**	1499,68	71/57	AEE87267.1	beta-actin	10/10 (100%)	0/10 (0%)	DESGPSLVHR	-
1272/1279	**GGVWGVNANDNLYYR**	1697,82	58/59	XP_002602245.1	hypothetical protein BRAFLDRAFT_76934 [Branchiostoma floridae]	11/14 (79%)	0/14 (0%)	GVWGVNANDNLYYR	ref|XP_789788.2|similar to echinonectin, partial [Strongylocentrotus purpuratus]/Expect = 3e-17
1272/1275/ 1296/1301	**GVHWGVNAGDDLFHR**	1679,82	78/83/74/79	XP_002602245.1	hypothetical protein BRAFLDRAFT_76934 [Branchiostoma floridae]	11/15 (73%)	1/15 (7%)	GVWGVNANDNLYYR	ref|XP_789788.2|similar to echinonectin, partial [Strongylocentrotus purpuratus]/Expect = 3e-18
1272/1275/ 1301	**DVVWGVNSADKLFYR**	1768,88	71/79/69	XP_002597862.1	hypothetical protein BRAFLDRAFT_105468 [Branchiostoma floridae]	10/13 (77%)	0/13 (0%)	GVWGVNANDNLYYR	ref|XP_780554.2 similar to serum lectin P35 [Strongylocentrotus purpuratus]/Expect = 4e-21
1272/1275/ 1301/1279/ 1296	**APGEAGSPAGTSWQNLPGR**	1852,91	50/78/65/59/6 5	gi|260821203	hypothetical protein BRAFLDRAFT_87403 [Branchiostoma floridae]	10/15 (67%)	0/15 (0%)	AGSPAGTSWQNLPG R	gb|ABY28359.1|tachylectin-like protein [Branchiostoma belcheri tsingtauense] /Expect = 4e-81
579/587	**KATVGNEALFR**	1205,69	89/90	AEF23433.1	glycosyl transferase family 2	8/8 (100%)	0/8 (0%)	VGNEALFR	-
579/587	**LEDSAPQGVFFSLGNNK**	1822,95	82/83	XP_969004.1	similar to antennal-enriched UDP-glycosyltransferase	12/15 (80%)	1/15 (7%)	DSAPQGAVYFSLGSN	-
1938/2005/ 2003	**KSWQDAEDHC(+57,02)R**	1431,62	59/53/57	XP_001185502.1	similar to snEchinoidin, partial [Strongylocentrotus	7/8 (88%)	0/8 (0%)	WQDAEDHC	-
1938/2003	**AEC(+57,02)PPHWTC(+57,0 2)YLGSC(+57,02)YR**	2056,91	64/61	Q56EB0	Bothrojaracin subunit beta	11/16 (69%)	0/16 (0%)	ADCPPDWSSYEGSCY R	ref|XP_001177433.1 similar to spEchinoidin [Strongylocentrotus purpuratus] / Expect = 3e-14
2130/2171	**GGC(+57,02)PPLWTR**	1043,50	75/76	XP_001199883.1	similar to spEchinoidin [Strongylocentrotus purpuratus]	7/7 (100%)	0/7 (0%)	GCPPLWT	-
2171/2180	**GAPDNSGSNEDC(+57,02)VD FLPR**	1949,81	74/66	XP_790805.2	similar to secreted lectin homolog; HeEL-1	10/13 (77%)	0/13 (0%)	GQPDNAGNNEDCV	-
2180/2185/ 2184	**DSVTFSVR**	910,45	90/79/86	YP_004219647.1	coagulation factor 5/8 type domain protein	7/8 (88%)	0/8 (0%)	DNVTFSVR	-

with a glycosyltransferase peptide (Figure 3.7A). Furthermore, many of the *de novo* sequenced peptides were consistently present in more than one 2DE spot, indicating the presence of protein post-translation modifications or protein different isoforms (Table 3.2).

For the remaining *de novo* predicted peptide sequences (17 different peptides), and according to BLAST results, no homologies were found with known protein families, and hence may constitute non-conserved portions of the protein sequences and/or novel starfish cell-free coelomic fluid proteins (Figure 3.6C; Supplementary data 3.4).

To further clarify the presence of the same protein in different 2D spots due to PTMs or isoforms, a cluster analysis of the 2DE spots peptide mass fingerprints was performed using the web interface, SPECLUST (http://bioinfo.thep.lu.se/speclust.html) (Alm *et al*., 2006) in order to group mass spectra according to their similarities. To improve statistical relevance of the results, peptide mass fingerprint spectra from randomly chosen coelomocytes proteins were also included as decoys in the cluster analysis. This analysis organized the majority of the CFF and coelomocyte proteins in different similarity clusters with the exception of cytoskeletal and constitutive proteins that are present in both proteomes (Supplementary figure 3.1). Apart from these exceptions, not only the cluster analysis indicated that CFF proteins are unique to this tissue but also revealed 34 major groups (cut-off score of 0.5) of 2DE spots which have similar peptide mass fingerprint spectra (Figure 3.8).

In the 1D-nano-LC MALDI-TOF/TOF CFF proteomic characterization, the same 10% of success in protein identification was observed, with a total identification of 29 proteins, which were mainly new assignments since they were not identified in the 2DE proteome characterization (Supplementary data 3.5).

Altogether, these results reinforce the hypothesis that the complexity of this proteome might be related with the presence of several PTM (*i.e*., glycosylation) other than the number of different proteins or, the presence of novel starfish coelomic fluid proteins with low homology with other echinoderm species.

3.4. DISCUSSION

A functional overview of the identified proteins in *M. glacialis* coelomocytes and cell free coelomic fluid clearly highlights the multiple roles of this fluid in the biology of echinoderms. Furthermore, the newly identified proteins provide preliminary evidence for several undescribed molecular pathways.

The complete non-redundant list of all identified proteins in coelomocytes (2DE and 1DE/nano-LC MALDI-TOF/TOF proteomes) and cell-free coelomic fluid (2DE and 1DE/nano-LC MALDI-TOF/TOF proteomes plus proteins inferred by *de novo* sequenced peptides), together with the correspondent annotations and/or spectra are available in the Supplementary tables 3.3 e 3.6.

A comprehensive overview into the identified proteins and how they correlate with coelomocytes and coelomic fluid functions in the starfish biology is discussed below.

3.4.1. Coelomocytes proteome

3.4.1.1. Cytoskeleton regulation and cellular adhesion related proteins

Asterias rubens coelomic fluid phagocytic cell population (a dendritic-like coelomocyte phenotype) can perform a rapid morphological transition from petaloid to filopodial shape (Pinsino *et al*., 2007). In order for a cell to move and change shape, its cytoskeleton must undergo rearrangements that involve breaking down and reforming filaments. Evidences of two major pathways involved in these events were found through several identified proteins. The first is the integrin signaling pathway, which is triggered when integrins in the cell membrane bind to extracellular matrix components causing downstream events such as actin reorganization and activation of MAPK and other signaling cascades (Yoo *et al*., 2008). The second pathway involves regulation by Rho GTPase, a family of key regulatory molecules that link surface receptors to the organization of the actin cytoskeleton. Also several proteins which play a role in the regulation of cell adhesion and cytoskeleton organization were found: profilin, (previously reported as being associated with changes in cell shape in the sea urchin coelomocytes

(Smith *et al*., 1992), ezrin; alpha-parvin, filamin A and C, several actin binding and capping proteins, clathrin-associated proteins and linker proteins.

3.4.1.2. Signaling, cellular regulation and proliferation related proteins

As coelomocytes secrete a number of regulating factors into the coelomic fluid, the pathways that lie at the base of these important biological events, like vesicular protein secretion mediated by G-protein receptor activated pathways, were also represented through several identified proteins namely: clathrin heavy chain, AP-1 complex subunit mu, AP-2 complex subunit sigma and ras-related protein Rab-11A. Moreover, several Ca^{2+} binding proteins, such as calmodulin, calpain, calreticulin and gelsolin were identified indicating that like in other immune cells, calcium intracellular concentration is also an important second messenger in signaling events of echinoderm coelomocytes (Vig *et al*., 2009). Other regulatory proteins such as, cell division cycle and apoptosis regulator protein 1 LIM, senescent cell antigen-like-containing domain protein 2 and Rho-related GTP-binding protein RhoB were also found. Cell proliferation is tightly regulated by exposure to serum, growth factors, survival factors and other cues from the cellular environment. This was shown to be the case also for the starfish coelomocytes (Cavey *et al*., 1994; Patruno *et al*., 2001; Carnevali *et al*., 1998). Several RAS family proteins and growth factors were also identified in this study, such as several Ras-related proteins (e.g., Rab-10, Rab-6A, Rab-7A) and the growth factor receptor-bound protein 2-B; LIM and senescent cell antigen-like-containing protein and the pre–B cell colony-enhancing factor.

3.4.1.3. Regeneration related proteins

Coelomocytes are involved in very early stages of regeneration namely in the wound healing phase (Coteur *et al*., 2002), and the *wnt* genes have already been described as being involved in the formation of thickened wound epithelia that is vital for regeneration in ophiuroid *Amphiura filiformis* (Dupont *et al*., 2007). Several proteins belonging to this pathway were also identified in the present study, namely, cAMP-dependent histone kinase and guanine nucleotide-binding protein subunit beta-1.

3.4.2. Coelomic fluid proteome

The coelomic fluid is the fluid that baths the internal organs of echinoderms and in which coelomocytes are suspended, being extremely rich in secreted factors, which mediate important anti-pathogen functions, and also other signaling proteins. Several biochemical and functional studies of individual molecules extracted from CFF (Haug *et al*., 2010; Cervello *et al*., 1996) have been performed, revealing that different coelomic fluid proteins have different impacts on cell viability, adhesion and antimicrobial effects (Holm *et al*., 2010) which further highlights the importance of using proteomic tools for protein identification or *de novo* peptide sequencing. Although some proteomic studies were already conducted using echinoderms coelomocytes (Dheilly *et al*., 2009 and 2011), so far, there is no available report on the 2D proteome of cell-free coelomic fluid (secreted factors). Hence, the present study constitutes the first coelomic fluid soluble proteins proteomic characterization.

3.4.2.1. Lectins and the complement pathway

Lectins are a large heterogeneous group of soluble or membrane proteins and glycoproteins that bind mono and disaccharides (Kilpatrick, 2002), being capable of agglutinating cells and/or precipitating glycoconjugates (Goldstein *et al*., 1980). In marine invertebrates, lectins have been thought to participate in the immune response by inducing bacterial agglutination or by acting as opsonins to enhance phagocytosis by coelomocytes (Bayne, 1990). Together with ficolins, also identified in the CFF (1DE nano-LC experiment; Supplementary data 3.5), the several identified lectins may play an important function in activating the lectin pathway of lytic complement system in the starfish innate immunity (see BOX 3.4). For this reason, novel peptide sequences may be important tools to design new experiments aiming to elucidate the role of lectins in complement activation in echinoderms.

The fact that lectins belong to a heterogeneous protein family (sea urchin genome presents over 500 different genes coding for lectin family proteins) and bind different saccharides, may have hindered the direct identification via protein database searches. Therefore, future proteomics studies should include an extra

glucosidase digestion step to remove mono, di or oligosaccharides bound to lectins prior to MALDI-TOF/TOF mass spectrometry.

Another important fact that strengthens the hypothesis of glycosylation as an important protein PTM in the modulation of echinoderm immunity is the presence of a glycoprotein from the glycosyltransferase family (spots 587, 589) in the starfish cell-free coelomic fluid (also identified by *de novo* sequencing; Supplementary data 3.4). In fact, glycosyltransferases are known to be involved in the glycosylation events of several proteins (reviewed in Lairson *et al*., 2008) whose function in echinoderm innate immunity needs to be further clarified.

3.4.2.2. Antimicrobial defense

During host-pathogen interaction secreted proteases serve important roles in parasitic metabolism and the host families of protease inhibitors play an important role in immunity by inactivating and clearing protease virulence factors or parasites. In echinoderms, a trypsin inhibitor from the starfish *Asterias forbesi* coelomic fluid has been previously isolated and characterized (Marcum, 1987) as well as, several kazal-type serine proteinase inhibitors cDNA sequences that have been reported to be expressed during immunological insult with lipopolysaccharides (LPS) (Ramírez-Gomez *et al*., 2009). In this proteomic characterization several proteins with known antibacterial activity were also identified in the starfish cell free coelomic fluid, including homologous proteins to bovine pancreatic trypsin inhibitor, lysozyme (previously reported on *S. purpuratus* coelomic fluid, Shimizu *et al*., 1999) and enolase. Although enolase is best known for its metabolic function, it is a multifunctional enzyme that has been reported to promote the activation of plasminogen on the surface of leukocytes promoting degradation of extracellular matrices (fibrolytic activity) towards cellular migration (López-Alemany *et al*., 2003) necessary in any inflammatory response, and hence may serve the same purpose in echinoderm immunity.

In this starfish cell-free coelomic fluid proteome, a protein homologous to fibrinogen was also identified which might be responsible for the formation of

Box 3.4| Innate immunity complement system: the lectin pathway

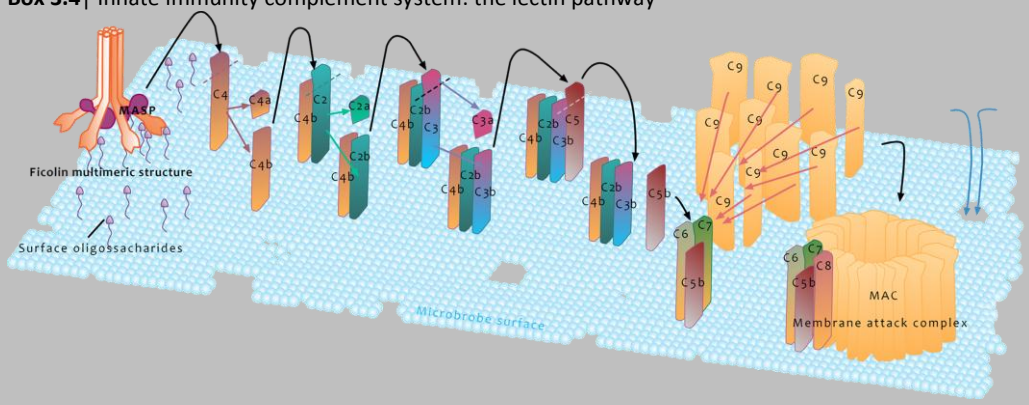

The lectin pathway is initiated by binding of the ficolin-MASP-2 complex [i.e., MBL (mannan binding lectin)-associated serine proteases)] to oligosaccharides on the surface of microbes. The ligand binding induces the activation of the MASP with subsequent cleavage of C2 and C4 in the generation of C3 convertase (CabC2b). The cleavage of the complement component C3 generates the anaphylactic and antimicrobial peptide C3a and the opsonin C3b.The cascade of events progresses then to the activation of C5 convertase (C4bC2bC3b) which will cleave C5 to release the potent anaphylactic peptide C5a and C5b. C5b then initiates the assembly of the internal activation steps of C6-C9 leading to the formation of the membrane attack complex (MAC). The MAC forms pores in the cell membrane, leading to complement mediated cytolysis (reviewed in Thomsen, 2011).

coelomocytes cloths. Fibrinogen is a secreted glycoprotein that when cleaved by thrombin (converted to fibrin) exposes the *N*-terminal polymerization sites responsible for the formation of the clots. Fibrinogen ESTs have already been identified in the coelomocytes of both sea urchins and sea cucumbers (Ramírez-Gómez *et al.*, 2009; Terwilliger *et al*., 2006; Nair *et al*., 2005).

3.4.2.3. Other CFF proteins

Since the coelomic fluid is the fluid that baths all internal organs of echinoderms, its function is not only restricted to immunity, acting also as an important cellular communication vehicle. Several proteins whose function may be related with cellular communication events or other biological functions were also identified in this proteomic characterization and may be interesting targets for future studies. Among these are: cytoskeletal proteins that have important functions in cellular and leukocyte adhesion such as erzin and gelsolin; the calcium-binding protein SPEC 2C, known to accumulate during larval development and metamorphosis of *S. purpuratus*; the microtubule modulator protein Echinoderm microtubule-associated protein-like 2, the signal transduction proteins teneurin, and circularly permutated Ras protein 2. Interestingly, a protein homologous with glycoprotein tenascin was also identified in the coelomic fluid. This extracellular protein plays an important function in axon guidance during neuron migration as well as in axons during development and neuronal regeneration and may be one of the secreted molecules responsible for the outstanding intrinsic neuronal growth capacity of echinoderms.

3.5. CONCLUDING REMARKS

The present study constitutes the first high throughput proteomic characterization of echinoderm coelomic fluid circulating cells, coelomocytes, and soluble secreted proteins. The newly identified coelomocyte proteins provide evidence for several unreported signaling pathways, eventually responsible for the diverse functions enrolled by these cells. The identified proteins in the coelomic fluid highlight the complex and sophisticated pathways of echinoderms innate immune response which seems to rely on several signaling proteins, clotting mediators and antibacterial proteins.

Contrary to our expectations, no homologous proteins of the vertebrate complement system were identified; however, several secreted lectins were present in the coelomic fluid, constituting the most abundant protein family in this fluid. Although further characterization of these sugar binding proteins is needed to elucidate their roles in starfish immunity, it is possible that they function together with ficolin, also identified in the starfish CFF, to induce the lectin pathway that leads to the activation of the complement system.

To extend this proteomic characterization, new methodologies for preparation of coelomocyte subcellular fractions and enrichment of low abundant proteins or depletion of abundant proteins will need to be developed. Also, the characterization of cell-free coelomic fluid proteins (secreted factors) PTMs will further elucidate how the described pathways and coelomocytes communication events are being regulated. Finally, this comprehensive list of proteins is of extreme importance as a ground-work for future studies aiming to clarify the homology with vertebrate immune cells or discover the pathways responsible for coelomocytes functions during starfish regeneration events.

3.6. ACKNOWLEDGMENTS

This work was supported by Fundação para a Ciência e Tecnologia through a PhD grant to Catarina Franco (SFRH/BD/29799/2006), a research contract by the Ciência 2008 program to Romana Santos, a project grant (PTDC/MAR/104058/2008) and through the National Re-equipment Program for "Rede Nacional de Espectrometria de Massa - RNEM" (REDE/1504/RNEM/2005). We also acknowledge Vasco da Gama Aquarium (Dafundo, Oeiras, Portugal), namely Dr. Fátima Gil and Miguel Cadete, for starfish maintenance. Acknowledgements are extended to

Daniel Ettlin (Thermo UNICAM, Portugal) and Dr. Erik Verschuuren (Proxeon, Denmark) for providing the Nano-HPLC (Proxeon) and Gûnes Barka (SunChrom) for providing the automatic Spotter.

3.7. REFERENCES

Alliegro, M.C., Ettensohn, C.A., Burdsal C.A. (1988) Echinonectin: a new embryonic substrate adhesion protein. J Cell Biol. 107, 2319-2327.

Alm, R., Johansson, P., Hjernø, K., Emanuelsson, C., Ringnér, M., Häkkinen, J. (2006) Detection and identification of protein isoforms using cluster analysis of MALDI-MS mass spectra. J Proteome Res. 5(4),785-792.

Al-Sharif, W. Z., J. O. Sunyer, J. D. Lambris, and L. C. Smith. Sea urchin coelomocytes specifically express a homologue of the complement component C3. J. Immunol. 1998, 160, 2983-2997.

Barsnes, H., Vizcaino, J. A., Eidhammer, I., Martens, L. PRIDE converter: making proteomics data-sharing easy. Nat. Biotechnol. 2009, 27, 598–599.

Bayne, C.J. (1990) Pagocytosis and non-self recognition in invertebrates. Bioscience. 40, 723-731.

Bhatia, V.N., Perlman, D.H., Costello, C.E., McComb, M.E. Software Tool for Researching Annotations of Proteins: Open-Source Protein Annotation Software with Data Visualization. Anal. Chem. 2009, 81, 9819–9823.

Butt, R. H.; Coorssen, J. R. Pre-extraction Sample Handling by Automated Frozen Disruption Significantly Improves Subsequent Proteomic Analyses. J Proteome Res. 2006, 5, 437-448.

Carnevali, C.; Bonasoro, F.; Welsch, U.; Thorndyke, M. C. Arm regeneration and growth factors in crinoids. San Francisco: Mooi and Telford, 1998, 145-150.

Carnevali. C.; Bonasoro, F. Microscopic overview of crinoid regeneration. Microsc Reasearch Tecnhiq. 2001, 55, 403-426.

Cavey, M.J.; Märkel, K. In F.W. Harrison and F.S. Chia (eds.). Microscopic anatomy of invertebrates. Vol 14:Echinodermata. Wiley-Liss, New York. 1994,169-245.

Cervello, M.; Arizza, V.; Cammarata, M.; Matranga, V.; Parrinello, N. Properties of sea urchin coelomocytes agglutinins. Italian Journal Zool. 1996, 63, 353-356.

Consortium, Sea Urchin Sequencing. The genome of the sea urchin *Strongylocentrutus purpuratus*. Science. 2006, 10, 941-952.

Coteur, G.; DeBecker, G.; Warnau, M.; Jangoux, M.; Dubois, P. Differentiation of immune cells challenged by bacteria in the common European starfish, *Asterias Rubens* (Echinodermata). Europ Journal of Cell Biol. 2002, 81, 413-418.

Da Wei Huang, D.W., Sherman, B.T., Lempicki, R.A. Systematic and integrative analysis of large genelists using DAVID bioinformatics resources. Nat Protocols. 2009, 4, 44-57.

Dheilly, N. M., Haynes, P.A., Bove, U., Nair, S.V., Raftos, D.A. Comparative proteomic analysis of a sea urchin (*Heliocidaris erythrogramma*) antibacterial response revealed the involvement of apextrin and calreticulin. Journal of Invertebrate Pathology. 2011, 106, 223-229.

Dheilly, N. M., Nair, S.V., Smith, L.C., Raftos, D.A. Highly Variable Immune-Response Proteins (185/333) from the Sea Urchin, *Strongylocentrotus purpuratus*: Proteomic Analysis Identifies Diversity within and between Individuals. The Journal of Immunology. 2009, 182, 2203-2212.

Dupont, S., Thorndyke, M. Bridging the regeneration gap: insights from echinoderm models. Nature Reviews Genetics. 2007, 8.

Goldstein, I.J., Hughes, R.C., Monsigny M., Osawa, T., Sharon, N. (1980) What should be called a lectin? Nature. 285, 66.

Gross, P.S.; Al-Sharif, W.Z.; Clow, L.A.; Smith, L.C. Echinoderm immunity and the evolution of the complement system. Developmental and comparative immunology. 1999, 23, 429-442.

Haug, C.L.T.; Stensvag, K. Antimicrobial peptides in echinoderms. Invertebrate Survival Journal. 2010, 7, 132-140.

Hillier, B.J., Vacquier, V.D. (2003) Amassin, an olfactomedin protein, mediates the massive intercellular adhesion of sea urchin coelomocytes. J Cell Biology. 160, 597-604.

Holm, K., Voronkina, I., Sharlaimova, N., Thorndyke, M., Henroth, B. (2010) Functional properties of proteins from the coelomic fluid of the wounded sea star *Asterias rubens* (L). Journal of Invertebrate Pathology. 105, 197-199.

Holm, K.; Dupont, S.; Sköld, H.; Stenius, A.; Thorndyke, M.; Hernroth, B. Induced cell proliferation in putative hematopietic tissues of the sea star, *Asterias rubens*. The Journal Exp Biol. 2008, 211, 2551-2558.

Ikeda, K., Sannoh, T., Kawasaki, N., Kawasaki, T., Yamashina, I. (1987) Serum lectin with known structure activates complement through the classical pathway. J Biol Chem. 262, 7451-7454.

Kilpatrick, D.C. (2002) Animal lectins: a historical introduction and overview. Biochem Biophys Acta. 1572, 187-197.

Laemmli, U.K. Cleavage of structural proteins during the assembly of the head of bacteriophage T4. Nature. 1970, 227, 680-685.

Lairson, L.L., Henrissat, B., Davies, G.J., Withers, S.G. (2008) Glycosyltransferases: Structures, Functions, and Mechanisms. Ann Reviews Biochem. 77, 521-555.

López-Alemany, R., Longstaff, C., Hawley, S., Mirshahi, M., Fábregas, P., Jardí, M., Merton, E., Miles, L.A., Félez, J. (2003) Inhibition of cell surface mediated plasminogen activation by a monoclonal antibody against α-Enolase. American Journal of Hematology. 72, 234-242.

Marcum, J.A. (1987) A trypsin inhibitor from the coelomic fluid of the sea star *Asterias forbesi*. Biol Bull. 172, 357-361.

Multerer, K.A., Smith, L.C. (2004) Two cDNA sequences from the purple sea urchin, *Strongylocentrotus purpuratus*, conding mosaic proteins with domains found in factor H, factor I and complement components C6 and C7. Immunogenetics. 59, 89-106.

Nair, S.V., Del Valle, H., Gross, P.S., Terwilliger, D.P., Smith, L.C. (2005) Macroarray analysis of coelomocyte gene expression in response to LPS in the sea urchin. Identification of unexpected immune diversity in an invertebrate. Physiol Genomics. 22, 33-47.

Neuhoff, V., Harold, N., Ehrhardt, W. Improved staining of proteins in polyacrylamide gels including isoelectric focusing gels with clear background at nanogram sensitivity using Coomassie Brilliant Blue G-250 and R-250. Electrophoresis. 1988, 9, 255-262.

Patruno, M., Thorndyke, M.C., Carnevali, M.D.C., Bonasoro, F., Beesley, P.W. (2001) Growth factors, heat-shock proteins and regeneration in echinoderms. J Exp Biol. 204, 843-848.

Pinsino, A.; Thorndyke, M.; Matranga, V. Coelomocytes and post-traumatic response in the common sea star Asterias rubens. Cell stress & chaperones. 2007, 12, 331-341.

Ramírez-Gómez, F., Ortiz-Pineda, P.A., Rivera-Cardona, G., García-Arrarás, J.E. (2009) LPS-induced genes in intestinal tissue of the sea cucumber *Holothuria glaberrima*. PLoS One. 4(7), e6178.

Rast, J.P., Smith, L.C., Loza- Coll, M., Hibino, T., Litman, G.W. (2006) Genomic insights into the immune system of the sea urchin. Science. 314, 952-956.

Shimizu, M., Kohno, S., Kagawa, H., Ichise, N. (1999) Lytic activity and biochemical properties of lysozyme in the coelomic fluid of the sea urchin *Strongylocentrotus intermedius*. J Invertebrate Pathol. 73, 214-222.

Smith, C.L.; Shih, C.S.; Dachenhausen, G. Coelomocytes express SpBf, a homologue of factor B, the second component in the sea urchin complement system. J. Immunol. 1998, 161, 6784-6793.

Smith, L. C., R. J. Britten, and E. H. Davidson. SpCoel1, a sea urchin profilin gene expressed specifically in coelomocytes in response to injury. Mol. Biol. Cell. 1992, 3, 403-414.

Smith, L.C., Gosh, J., Buckley, K.M., Clow, L.A., Dheilly, N., Haug, T., Henson, J.H., Li, C., Man, L., Majeske, A, J., Matranga, V., Nair, S., Rast, J.P., Raftos, D.A., Roth, M., Sacchi, S., Schrankel, C.S., Stesvag, K. (2011) Echinoderm immunity. In: Invertebrate Immunuty. Söderhall, K. (eds). Springer Verlag.

Tahseen, Q. Coelomocytes: Biology and possible immune functions in invertebrates with special remarkes on nematodes. Internation Journal Zool. 2009, 1-13.

Terwilliger, D.P., Buckley, K.M., Mehta, D., Moorjani, P.G., Smith, L.C. (2006) Unexpected diversity displayed by the immune cells of the purple sea urchin, *Strongylocentrotus purpuratus*. Physiol Genomics. 26, 134-144.

Thomsen, T., Schlosser, A., Holmskov, U., Sorensen, G.L. (2011) Ficolins and FIBCD1: Soluble and membrane pattern recognition molecules with acetyl group selectivity. Molecular Immunology. 48, 369-381.

Vig, M., Kinet, J.P. Calcium signaling in immune cells. *Nature Immunology.* 2009, 10, 21-27.

Vizcaíno JA, Côté R, Reisinger F, Foster JM, Mueller M, Rameseder J, Hermjakob H, Martens L. A guide to the Proteomics Identifications Database proteomics data repository. Proteomics. 2009. 9, 4276-4283.

Yoo, Y., Guan, J.L. (2008) Integrin Signaling Through Focal Adhesion Kinase. In: LaFlamme, S.E., Kowalczyk, A.P. (eds.) Cell Junctions: Adhesion, Development, and Disease. Wiley-VCH Verlag GmbH & Co. KGaA, Weinheim, Germany.

THE PROTEOLYTIC PATHWAYS BEHIND REGENERATION

PROTEOMICS REVEALS THE IMPACT OF PROTEOLYSIS DURING STARFISH NERVOUS SYSTEM FUNCTIONAL REGENERATION

CATARINA FERRAZ FRANCO[1], ROMANA SANTOS[1,2], ANA VARELA COELHO[1]

1: Instituto de Tecnologia Química e Biológica, Universidade Nova de Lisboa, Oeiras, Portugal;

2: Unidade de Investigação em Ciências Orais e Biomédicas, Faculdade de Medicina Dentária, Universidade de Lisboa, Portugal.

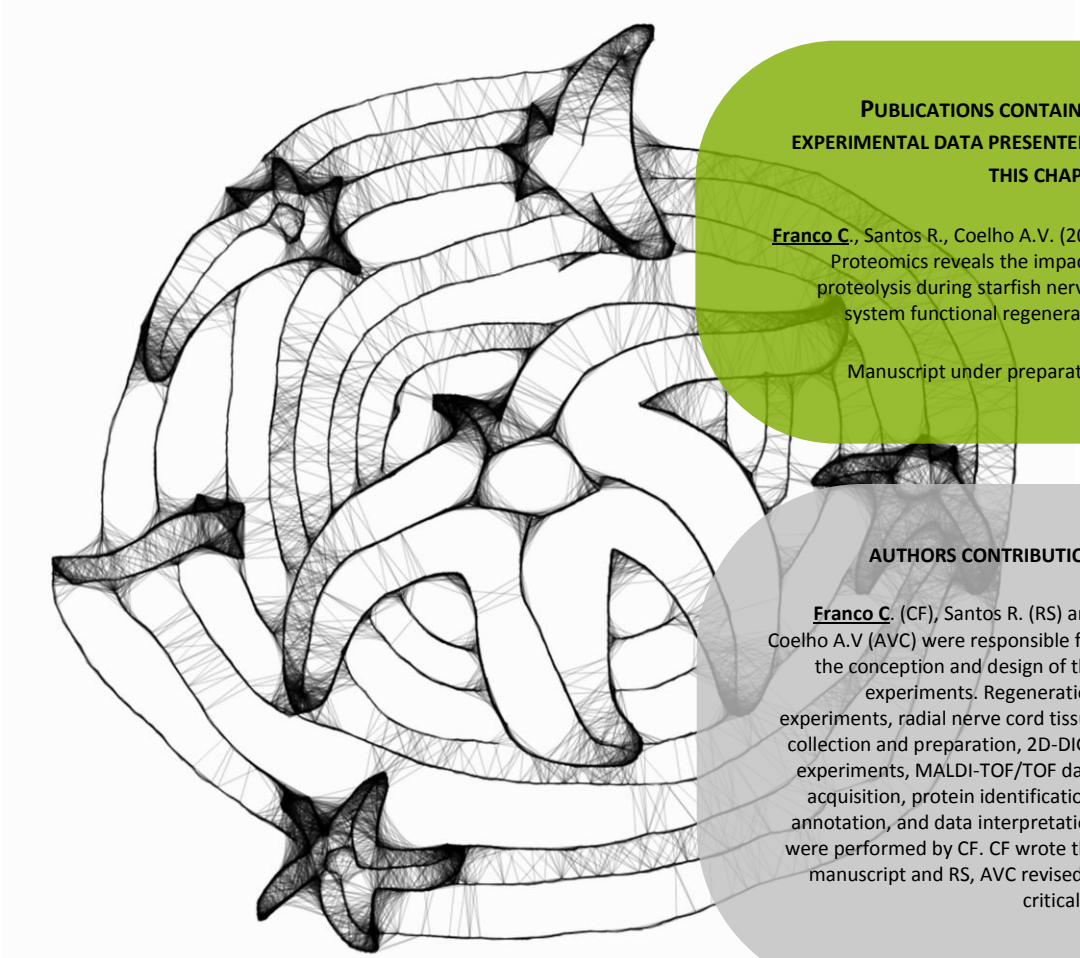

PUBLICATIONS CONTAINING EXPERIMENTAL DATA PRESENTED IN THIS CHAPTER

Franco C., Santos R., Coelho A.V. (2011) Proteomics reveals the impact of proteolysis during starfish nervous system functional regeneration

Manuscript under preparation.

AUTHORS CONTRIBUTION

Franco C. (CF), Santos R. (RS) and Coelho A.V (AVC) were responsible for the conception and design of the experiments. Regeneration experiments, radial nerve cord tissue collection and preparation, 2D-DIGE experiments, MALDI-TOF/TOF data acquisition, protein identification, annotation, and data interpretation were performed by CF. CF wrote the manuscript and RS, AVC revised it critically.

Image: Starfish regenerating.

CHAPTER 4

THE PROTEOLYTIC PATHWAYS BEHIND REGENERATION

PROTEOMICS REVEALS THE IMPACT OF PROTEOLYSIS DURING STARFISH NERVOUS SYSTEM FUNCTIONAL REGENERATION

Supplementary material containing experimental data described in this chapter*

WOUND HEALING (48H AND 13DAYS POST-ARM TIP ABLATION)

Supplementary table 4.1: List of all the identified peptides and proteins associated with *Marthasterias glacialis* radial nerve cord wound healing events in both soluble and membrane enriched fractions using both search engines and several protein sequence databases.

Supplementary table 4.2: List of all proteins identified in both soluble and membrane enriched fractions of *M. glacialis* wound healing radial nerve cord containing the information on mass shift; *pI* shift; proteolytic status (fragment or substrate); general protein functions; and respective gene ontology annotations.

TISSUE RE-GROWTH (10 WEEKS POST-ARM TIP ABLATION)

Supplementary table 4.3: List of all the identified peptides and proteins associated with *M. glacialis* radial nerve cord re-growth events in both soluble and membrane enriched fractions using both search engines and several protein sequence databases.

Supplementary table 4.4: List of all proteins identified in both soluble and membrane enriched fractions of *M. glacialis* re-growing radial nerve cord containing the information on mass shift; *pI* shift; proteolytic status (fragment or substrate); general protein functions; and respective gene ontology annotations.

* Please see enclosed CD to access the supplementary material

SUMMARY | THE PROTEOLYTIC PATHWAYS BEHIND REGENERATION

The molecular pathways that trigger the amazing intrinsic regenerative ability that leads to a functional re-growth of echinoderms nervous system are still unknown. In order to approach this subject, a 2D-DIGE proteomics strategy was used, in combination with a complementary series of gels with different *pI* ranges and two different subcellular protein enriched fractions from the starfish *Marthasterias glacialis* (Echinodermata, Asteroidea) radial nerve cord.
Within the 7329 total resolved spots, 944 showed differences associated with arm tip regeneration process [wound healing (WH): 48h; 13 days post arm tip ablation; and functional radial nerve cord re-growth (RG): 10 weeks post arm tip ablation]. Tandem mass spectrometry and protein identification using two search engines and three different protein sequence databases allowed the identification of 528 proteins in both soluble and membrane proteins enriched fractions throughout the assayed time points. Several functional classes of proteins known to be involved in axon regeneration events in other model organisms, such as chordates, were identified for the first time in echinoderm nervous system regeneration events and more importantly, were found to be regulated at a post-translational level through proteolytic pathways. The several pathways that seem to be regulated by proteolysis include cytoskeleton and microtubule regulators, axon guidance molecules and growth cone modulators, protein *de novo* synthesis machinery, RNA binding and transport, transcription factors, kinases, lipid signaling effectors and proteins with neuroprotective functions. Also, several proteins with no previous association with neuronal regeneration were identified and are pointed out as interesting molecules for future studies further highlighting the importance of the contribution that these deuterostomes can add to the field of neuroregeneration. In addition, the high number of proteins identified with an apparent molecular mass above the expected, suggests functional modulation further induced by other post-translational modifications such as conjugation with ubiquitin-like molecules, which might further modulate neuronal regeneration events, an interesting hypothesis that clearly deserves future research.

4.1. INTRODUCTION

Nowadays, the problematic of tissue regeneration gains emphasis, particularly in mammalian tissues that present a reduced ability to recover from traumatic injury. This is the case of the adult mammalian central nervous system (CNS) in which the response to injury consists of inflammation and scar tissue formation, with neurons being unable to regrow across the lesion site due to the inhibitory nature of the neuronal environment and the loss of the intrinsic growth capacity concomitant with nervous system differentiation. Several efforts have been made to identify these inhibitory factors, which include the formation of the glial scar (for reviews see Silver *et al.*, 2004; Tang, 2003) and molecules such as *Nogo*, myelin-associated glycoproteins (Schwab, 2004; Llorens *et al.*, 2011) among several others (Yiu *et al.*, 2006).

Particular interest arose from a specific class of proteases, the matrix metalloproteinases (MMPs), since they are capable of degrading the protein core of several neuronal growth-inhibitory molecules such as chondritin sulfate proteoglycans (CSPGs), *Nogo* and tenascin-C (for review see Pizzi *et al.*, 2007) and thus facilitate nervous tissue remodeling and regeneration. The MMP family of enzymes includes at least 20 different zinc-dependent endopeptidases (Shapiro, 1998) which can either be secreted from cells or be anchored to the plasma membrane. MMP-like proteases have been found in insects, crustaceans, mussels, sea cucumbers (Quiñones *et al.*, 2002) and vertebrates (see review Mannello *et al.*, 2005). These proteases were first reported has being associated with the metamorphosis of tadpole tails (Gross *et al.*, 1962). However, after years of intense studies using several animal tissues, their importance in other catabolic activities have been confirmed, namely in remodeling events that include bone formation, mammary development, blood-vessel remodeling, inflammation, wound healing and neuronal regeneration (for the role of MMPs in tissue remodeling see review Page-McCaw *et al.*, 2007). Initially MMPs were thought to function mainly as enzymes that degrade structural components of the extracellular matrix (ECM) creating a more fluid microenvironment ideal for cells to migrate. Nowadays it is known that the roles of MMPs-driven proteolysis are wider, being involved in: ***1)*** the production of specific substrate-cleavage fragments with independent biological activity that have potent chemoattractive effects (eg. recruiting a variety of progenitor and stem

BOX 4.1| Calpain activation upon axotomy

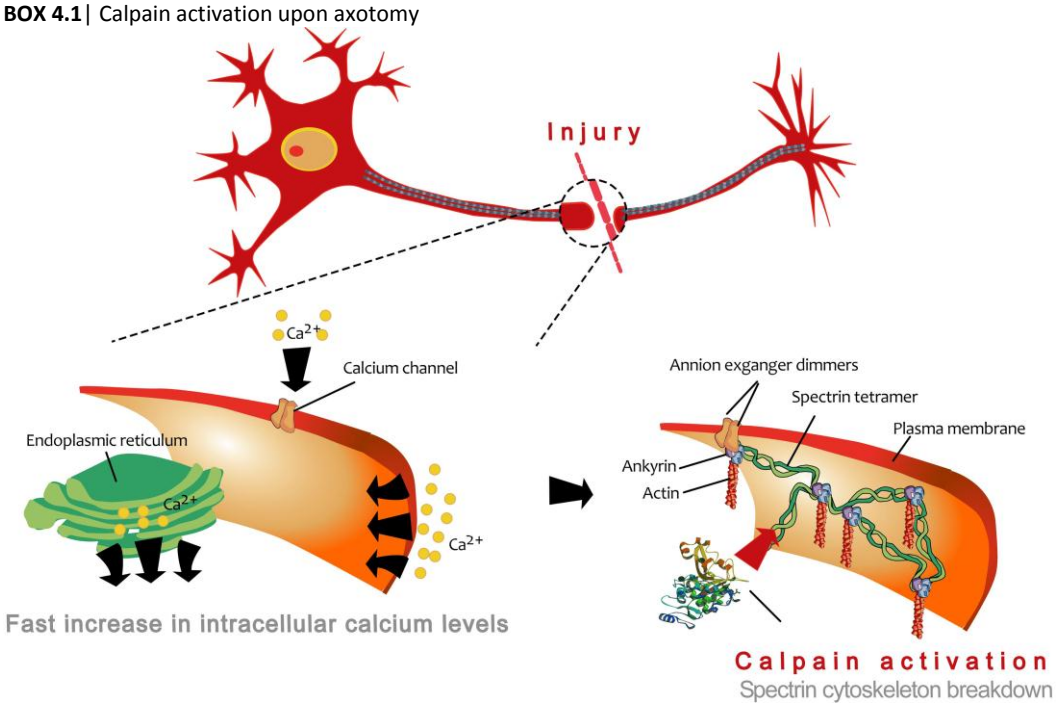

After axotomy, intracellular calcium concentration rises rapidly at the site of transection, with the level reaching more than 1 mM. This increase in calcium can be attributed to the sudden influx of calcium ions into the axoplasm through ruptured membrane, the opening of voltage-gated calcium channels or the inversion of Na^{+}/Ca^{2+} exchanger. The newly-formed growth cone always arises from the area where calcium concentration is elevated. The transient elevation of calcium then causes the activation of calcium-dependent proteases, such as calpain, which in turn carry out the process of protein degradation necessary for successful regeneration, that include proteolysis of the submembrane cytoskeletal component spectrin, and the newly synthesized vimentin molecules whose fragments will enable the transport of phosphorylated Erk along with importin β1.

cells *in vitro*) (Agrawal *et al.*, 2010); ***2)*** the regulation of tissue architecture through effects on ECM intercellular junctions (Page-McGaw *et al.*, 2007); ***3)*** the direct or indirect activation, deactivation or modification of molecules signaling activity (Streuli, 1999); ***4)*** the regulation of the dynamic interactions of neurite outgrowth through chemorepulsion or chemoattraction (Pizzi *et al.*, 2007); and ***5)*** the promotion of axonal regeneration by facilitating an increase in growth factors levels present in the extracellular environment (Lee *et al.*, 2001).

The efficacy of MMPs in promoting a growth-permissive environment has been further tested using a PEGylated fibrinogen hydrogel embedded with different MMPs inhibitors to test dorsal root ganglion (DRG) cell outgrowth. Results showed that when cultured DRG neurons are exposed to peptide inhibitors of MMPs, significantly lower neurite outgrowth is observed, being this inhibition dependent on the type of inhibitor and its concentration (Sarig-Nadir *et al.*, 2010).

Given the confirmed role of MMPs in regeneration events, MMPs-driven proteolysis has been extensively scrutinized *in vitro*, namely in studies aiming to engineer "biomaterial nerve guidance conduits (NGCs)" as delivery systems for MMPs, with the purpose of generating a permissive environment in mammals CNS.

However, the proteolytic pathways are not only restricted to ECM environment and other intracellular proteases have been implicated in axonal regeneration events. Calpain-mediated proteolysis has also been proven to have a fundamental role during neuronal growth-cone formation and axon regeneration after injury (Spira *et al.*, 2001; reviewed in Gumy *et al.*, 2010). It is known that the transient elevation of intracellular calcium levels associated with membrane rupture, followed by the opening of voltage-gated calcium channels and ER calcium storage release (Gumy *et al.*, 2010) causes the activation of calcium dependent calpain (BOX 4.1). Upon activation, this protease starts to degrade the submembrane cytoskeletal protein, spectrin. This enables microtubule and actin filaments protrusion onto the growth cone membrane and also enhances the fusion of axoplasmic vesicles transported by motor proteins along microtubules (Gilter *et al.*, 1998). Other than the recreation of physical permissive growth cone cytoskeleton fluidity, calpain-mediated proteolytic events have also been associated with an important signaling event that involves the breakdown of the intermediate filament vimentin, whose proteolytic fragment interacts with phosphorylated transcription factor *Erk* (Perlson *et al.*, 2004) preventing its dephophosrylation during the retrograde importin-β1-mediated transport to the neuronal soma, were it exerts its function in modulating neuronal gene expression (Perlson *et al.*, 2005 and 2006).

In addition, the ubiquitin-proteasome system (UPS), known to be responsible for regulating protein degradation in all eukaryotic cells (Glickman *et al.*, 2002), has also been reported as a major player in regulating a multitude of processes and dynamics within the normal neuronal functions, such as gene expression, synaptic and spine functions, and neuronal degeneration by tagging and eliminating key proteins required for morphological and chemical neuroplasticity (for reviews on the UPS functions within nervous systems see Hedge *et al.*, 2008; Hedge *et al.*, 2009; and Klimaschewski, 2007) and also plays a main role during neural development (Franco *et al.*, 2010). In fact, Verma *et al*. (2005), showed that an impaired UPS resulted in poor regeneration of isolated growth cones in cultured rat sensory axons, which is in accordance with reports of an increase in ubiquitin mRNA after axotomy (Savedia *et al.*, 1994), suggesting an enhanced requirement for ubiquitin during axonal regeneration.

Nowadays it is also widely accepted that the UPS is necessary for growth cone formation. However, only few mechanisms have been proposed to explain how UPS mediates axon regeneration, which essentially describe its major role in degradation of cytoskeletal components, known to be a limiting step in regulating axonal regeneration (Lewcock *et al.*, 2007; Tursun *et al.*, 2005). Therefore, future studies aiming to elucidate how specific ubiquitination occurs after axotomy and how these events are spatially and temporally controlled are still sought.

BOX 4.2| Protein synthesis and degradation in a neuron

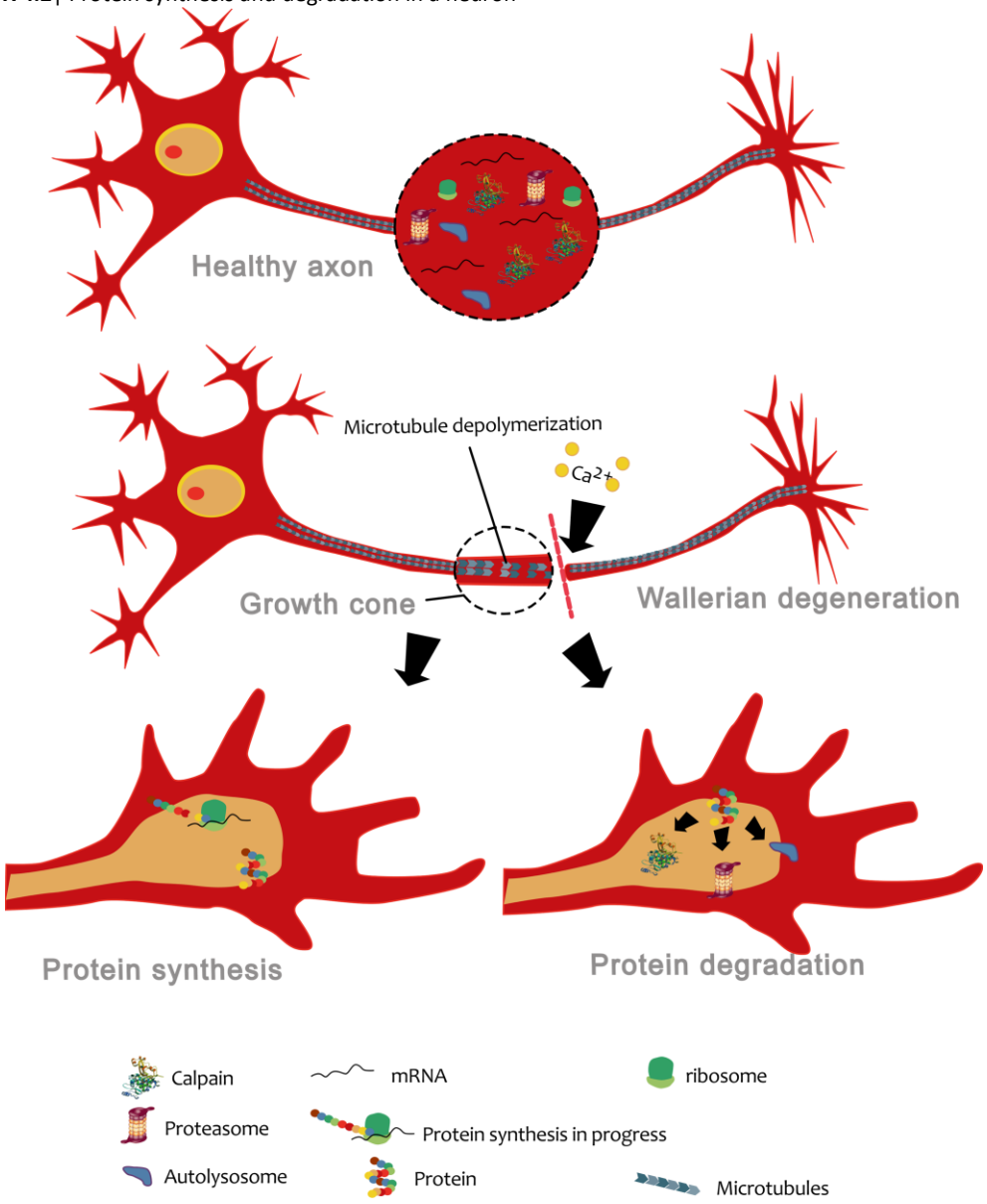

Inside a healthy axon a variety of protein synthesis and degradation machinery is present. As a result of transection, the axon is divided in two parts. The distal portion undergoes Wallerian degeneration and will subsequently be degraded. In the proximal portion, calcium enters the axon due to the disruption to the plasma membrane, as well as via voltage-gated calcium channels. Cytoskeletal structures such as microtubules and neurofilament undergo depolymerization and degradation. Later on, a terminal swelling appears at the tip of the proximal stump, as regeneration ensues. Microtubules and neurofilaments undergo re-polymerization. Protein synthesis and degradation occur simultaneously within the axon. Protein synthesis takes place via mechanism dependent on mTOR, ERK1/2 and PKA. Examples of protein synthesized locally after an injury include importin b1, vimentin, ribosomal protein L4, etc. Protein degradation may occur via calpain-dependent proteolysis (e.g. vimentin, spectrin) or ubiquitin-proteasome system, while the role of autophagy remains to be elucidated. (Figure adapted from Gumy *et al.*, 2010).

Changes in injured axons often occur without the contribution of transcriptional events in the cell body, partly due to the distance between the injury site and the axon nucleus. The currently increasing number of evidences emphasize the role of proteolysis (Spira *et al.*, 2001; reviewed in Gumy *et al.*, 2010 and Sun *et al.*, 2009), local axonal protein synthesis (Willis *et al.*, 2005; Yoo *et al.*, 2010; Donnelly *et al.*, 2010; Gumy *et al.*, 2010) (BOX 4.2), and also other important events of post-translational modifications such as, protein phosphorylation (Liu, 2001), ubiquitination (Franco *et al.*, 2010) and SUMOylation (Niekerk *et al.*, 2007; Martin *et al.*, 2007) during neuronal regeneration events. Taken together, these facts clearly highlight that deciphering how nervous system regenerate has become in part a post-genomic problem, which can partly be answered by proteomic approaches.

On the basis of their regenerative potential, proximity to Chordates and high genetic homology with humans (Consortium, 2006), echinoderms can become valuable new deuterostome models for the study of regeneration. Furthermore, the regenerative processes in echinoderms are more likely to be extended to mammals than those observed in other classical regeneration models phylogetically more distant from chordates, such as hydra or planarians. Nevertheless, it was only very recently that the first high throughput proteomic characterization of the starfish radial nerve cord was performed (Franco *et al.*, 2011; Chapter 2) showing a striking proteome homology between the echinoderm nervous system and the dorsal nerve cord of chordates, further highlighting the potential of echinoderms as models for neuroregeneration studies.

In this chapter we present an unprecedented proteomic characterization of *in vivo* impact of proteolytic events occurring during different stages of nervous system regeneration after arm tip amputation in a starfish species, *Marthasterias glacialis*. The signaling pathways being modulated through this post-translational modification event are also discussed.

A differential proteomic strategy was used in order to compare the radial nerve cords from injured starfish and their respective uninjured controls collected at 48h, 13 days and 10 weeks post arm tip ablation (*PAA*). The nerve tissues were then fractionated in soluble and membrane proteins enriched fractions and separated across several *pI* ranges 2D-DIGE gels. This approach led to the identification of 528 proteins, belonging to several pathways never before assigned to echinoderms, and that are known to be key effectors of regeneration in other model organisms. In addition, several proteins never reported as associated to regeneration events were also found, constituting interesting targets for future studies. Finally, a high number of proteins were identified with an apparent molecular mass above the expected. This suggests that the pathways involved in regeneration events are further being modulated by other post-translational modifications.

Altogether, the results highlight echinoderms as important model organisms that can help to elucidate the role of the several proteolytic pathways activated upon injury, and also the roles of their specific substrates as important signaling molecules whose functions need to be further validated in the future.

4.2. MATERIALS AND METHODS

4.2.1. Experimental groups and regeneration induction

Starfish collected as previously described (Chapter 2) were visually inspected and only selected for the experiments if no previous signs of regeneration were present, such as different-sized arms or arms with epidermal or pigmentation defects. Starfish were then divided in 6 groups, 3 control groups and 3 regenerating groups, each composed of 6 animals. Regeneration was induced by amputation of 2 arm tips per starfish (Figure 4.1) and both control and regenerating groups were kept throughout the course of the experiments in the exact same conditions.

4.2.2. Collection of wound healing (WH) radial nerve cords

Wound healing (WH) was studied in two time events, 48h and 13 days post arm tip ablation. Altogether, 12 regenerating and 12 non-regenerating starfish were used for the experiments, from which two radial nerve cords were collected per starfish. This was achieved by extracting only the first centimeter from the arm tip

upwards, in order to restrict our analysis to tissue adjacent to the injury plane (Figure 4.1). The collected tissues were immediately immersed in an ice cold solution of phosphate buffer saline (PBS) supplemented with protease, kinase and phosphatase inhibitors (Complete antiprotease kit; 4µM cantharidin; 4µM staurosporine and 1 mM sodium orthovanadate), flash frozen in liquid N_2 and conserved at -80°C until further use.

4.2.2. Collection of the re-growing (RG) radial nerve cords

Ten weeks after injury, a completely differentiated arm tip had regenerated, having the same appearance of uninjured arms and with approximately 7-10 mm in length (Figure 4.2.E). Only the regenerated part of the radial nerve cords were carefully excised and processed as explained above. Again, two regenerated radial nerve cords were extracted per starfish, and a total of 6 regenerating and 6 non-regenerating starfish were used in the experiments.

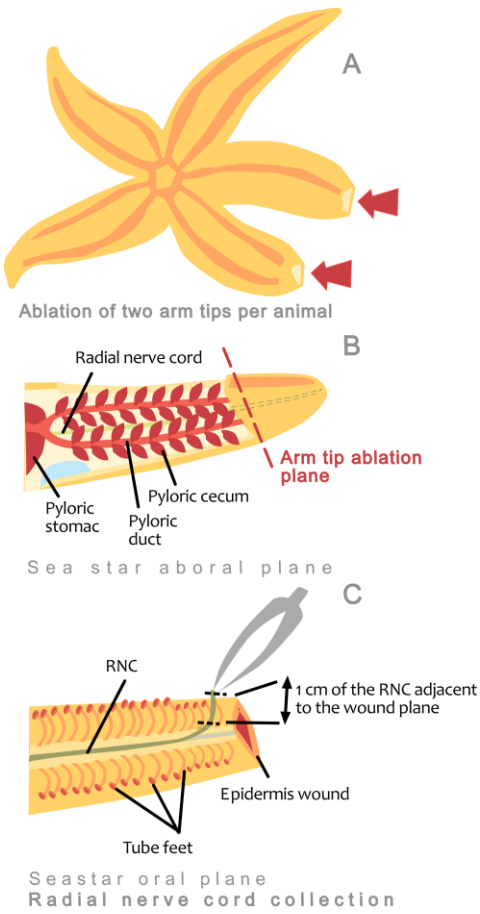

Figure 4.1: Illustration of starfish arm tip amputation (A, B) and radial nerve cord collection (C).

The new re-grown radial nerve cords were carefully excised and processed as explained above.

4.2.3. Radial nerve cord soluble and membrane enriched fraction preparation

For protein extraction, the collected nerve tissues were homogenized using an automated frozen disruption procedure, and further fractionated into a soluble and membrane protein enriched fractions, has previously described in Chapter 2.

4.2.4. Difference gel electrophoresis (DIGE)

4.2.4.1. Protein labeling

The prepared enriched protein fractions were resuspended in DIGE labeling buffer [7M urea, 2M thiourea, 1M Tris buffer, 4% CHAPS, Complete antiprotease kit (Sigma), pH 8.5] and gently shaken (4°C) to achieve complete solubilization of protein extracts. The *pH* was carefully re-adjusted to 8.5 using NaOH solutions from 100mM to 1mM. The total protein concentration was determined using the 2D Quant Kit ™ (GE Healthcare). Both protein enriched fractions were then labeled with Cyanine 3 or 5 (Cy3, Cy5) fluorescent dyes (GE Healthcare) according to manufacturer instructions (400pmol CyDye to 50 µg of total protein). To ensure that all labeling reactions took place in simultaneous, CyDyes were added to the tube caps, and then put in contact with the samples by a simultaneous quick spin down of all the reaction tubes. Labeling reaction was performed for 25 min on ice and in the dark. After this, 10 nmol of lysine (1µl of a 10mM solution) were added to each reaction tube cap and, after 5 min, the labeling reactions were simultaneously quenched by a quick spin down of the tubes, which were then kept on ice for another 10 min. The same procedure was applied to the internal standard, a pool of all samples (control and regenerating groups), which was then labeled with Cy2 fluorescent dye (GE Healthcare). The internal standard was used on all gels

to ease image matching and cross-gel statistical analysis. Prior to sample multiplexing, equal volumes of sample buffer (8M urea; 130mM DTE; 4% CHAPS and 1% (v/v) of the correspondent *pH* range ampholytes) were added to each of the labeled protein samples. Then, rehydration buffer (8M urea; 13mM DTE; 4% CHAPS and 0.5% (v/v) of the correspondent pH range ampholytes) was added up to a final volume of 450µL prior to isoelectric focusing (IEF). Each strip was actively rehydrated overnight at low voltage (30V) with 120µg of the multiplexed radial nerve cord soluble protein extracts (equal amount of Cy3 and Cy5 labeled samples and the internal standard) or, with 150µg of the radial nerve cord membrane protein extracts (equal amount of Cy3 and Cy5 labeled samples and internal standard). The 6 biological replicates per group were multiplexed randomly and fluorescent dye was swapped within the groups in order to prevent preferential labeling and bias results in gel image analysis.

4.2.4.2. Protein separation and image acquisition

For protein separation, a series of complementary *pH* range 24cm IEF strips were used. The optimized IEF protocols for each of the used strips are presented in Table 4.1. Prior to SDS-PAGE, the strips were equilibrated in a two-step process with a buffer (50mM Tris-HCl *pH* 8.8, 6M urea, 30 % (v/v) glycerol, 2 % (w/v) SDS, 0.002 % (w/v) bromophenol blue) containing first 2 % (w/v) DTE and then 4 % (w/v) iodoacetamide. Protein separation in the second dimension was performed in 24 cm SDS-PAGE gels (12.5 % (w/v) acrylamide). Electrophoresis was carried out at 38 mA/gel in the running buffer (25 mM Tris, pH 8.8; 192 mM glycine, and 0.2 % (w/v) SDS) until the bromophenol blue reached the bottom of the gel.

All gels were scanned using the Fujifilm FLA-5100 Fluorescent Image Analyzer (GE Healthcare). The Cy3 images were scanned using a 532nm laser and a 580nm band pass (BP) emission filter; Cy5 images were scanned using a 633nm laser and a 670nm BP emission filter and; the internal standard (Cy2) gels were scanned using the 457nm laser and the 610nm BP emission filter. All gels were scanned at 100 µm pixel size.

4.2.4.3. Gel image and statistical analysis

All gel images were exported into Progenesis SameSpots, v. 3.1 (Nonlinear Dynamics), where quantitative and statistical analysis of protein spots was performed. These were preceded by automatic and subsequent manual editing, alignment and matching of the gel images. For protein quantification, protein volumes (an integration of optical density and area) were measured as a percentage of the total volume of all detected spots and then *log* transformed to obtain a normalized distribution. Three types of statistical analysis were performed: ***1)*** a Power Analysis to evaluate if the number of biological replicates used were sufficient to account for the inter-individual variability, ***2)*** a Principle Component Analysis (PCA) to verify the distribution of the analyzed experimental groups (WH: 48h, 13 days; RG: 10 weeks post-arm tip ablation and the corresponding controls); and ***3)*** an analysis of variance (ANOVA) for all spots in the PCA groups in order to detect significant variations by setting the threshold to a p-value<0.05.

4.2.4.4. Preparative gels

High protein load 24cm 2DE preparative gels were run in duplicate for the WH and RG DIGE experiments. Each 2DE gel contained either 600µg of total protein with a pool of all control samples or, 400µg total protein with a pool of all regenerating samples (see Table 1 for IEF conditions used). The 2DE gels were fixed and then post-stained with colloidal Coomassie (CCB) (Neuhoff, 1988). The CCB stained gels were scanned using the Fujifilm FLA-5100 Fluorescent Image Analyzer (GE Healthcare) using the red laser without an emission filter. The subsequent gel image was exported into Progenesis SameSpots and matched with the DIGE gel images. Spots of interest were selected and manually excised from the preparative gels either in pools of

Table 4.1: IEF optimized conditions for the 2DE protein separation of the radial nerve cord soluble and membrane enriched fractions. Immobiline DryStrips (GE Healthcare) with lengths of 24 cm and several *pH* ranges (3-10*L*; 3-5.6*NL*; 5.3-6-5*L*) were used and the IEF conditions were thoroughly optimized in order to allow complete focusing of the proteins in the different *pH*-ranges use.

Preparative gels

pH range	**3-10 *L***	**3-5.6 *NL***	**5.3-6.5 *L***
Ampholytes *pH* range; mixture used and final concentration % (v/v)	*pH* range 3-10*L*; 1%	*pH* range 3.5-5.0*L*; 0.75% + *pH* range 3-10 *NL*; 0.25%	*pH* range 5.5-6.7*L*; 0.75% + *pH* range 3-10*L*; 0.25%
Total protein loaded (µg)	450-600	450-600	450-600

IEF program

Voltage (v)	Voltage mode	Time (h:min)	V.h
150	S&H	4:00	600
500	S&H	2:30	1250
1000	G	6:00	4500
3500	G	1:30	3375
3500	S&H	2:00	7000
8000	G	3:00	17250
8000	S&H	8:00	64000
Total		27:00	97975

Voltage (v)	Voltage mode	Time (h:min)	V.h
150	S&H	4:00	600
500	S&H	2:30	1250
1000	G	6:00	4500
3500	G	1:30	3375
3500	S&H	2:00	7000
8000	G	3:00	17250
8000	S&H	8:00	64000
Total		27:00	97975

Voltage (v)	Voltage mode	Time (h:min)	V.h
150	S&H	0:30	75
250	S&H	3:00	750
3500	G	3:00	5625
3500	S&H	32:26	113550
Total		38:56	120000

Analytical gels (DIGE)

Ampholytes *pH* range; mixture used and final concentration % (v/v)	*pH* range 3-10*L*; 0.5%	*pH* range 3.5-5.0*L*; 0.375% + *pH* range 3-10 *NL*; 0.125%	*pH* range 5.5-6.7*L*; 0.375% + *pH* range 3-10*L*; 0.125%
Total protein loaded (µg)	120-150	120-150	120-150

IEF program

Voltage (v)	Voltage mode	Time (h:min)	V.h
150	S&H	0:40	100
250	S&H	3:00	750
1000	G	3:00	1875
1000	S&H	3:00	3000
4000	G	3:00	7500
4000	S&H	3:00	12000
8000	G	3:00	18000
8000	S&H	8:21	66800
Total		27:00	110000

Voltage (v)	Voltage mode	Time (h:min)	V.h
150	S&H	0:40	100
250	S&H	3:00	750
1000	G	3:00	1875
1000	S&H	3:00	3000
4000	G	3:00	7500
4000	S&H	3:00	12000
8000	G	3:00	18000
8000	S&H	8:21	66800
Total		27:00	110000

Voltage (v)	Voltage mode	Time (h:min)	V.h
150	S&H	0:30	75
250	S&H	3:00	750
3500	G	3:00	5625
3500	S&H	32:26	113550
Total		38:56	120000

matched spots, if the spot of interest was of low abundance, or individually, if it was an intensely stained spot.

4.2.5. Protein identification, BLASTp searches and gene ontology annotation[4]

Protein identification was performed using two different search algorithms, MOWSE (MASCOT) and Paragon (ProteinPilot) and the three different protein sequence databases (For details see BOX 4.3 and 4.4).

In order to integrate and compare the protein identification results generated by the two search algorithms and three protein sequence databases, the new software tool COMPID was used (Lietzén, 2010). Two types of report were then generated, each containing the information of all the peptides and proteins common and unique to each search algorithm. Proteins were considered common if having at least one peptide with a strictly equal amino acid sequence, with the exception of the isobaric amino acids I and L, and Q and K. Since this tool was designed to compare protein identification data derived from LC-MS/MS experiments, only MS/MS data were used for the comparison.

Similarly to what was described in previous chapters, most of the identified proteins were homologous to *Strongylocentrotus purpuratus* proteins. Since the sparse information on Gene Ontology categories (GO) of *S. purpuratus* proteins impaired the success of data interpretation, a protein-protein BLAST (BLASTp) search was performed through BLAST2GO java application (http://www.blast2go.de). This enabled to perform GO annotation of the identified proteins in the starfish radial nerve cord by using GO categories of the best hit derived from the BLASTp results (BLASTp minimal Expectation value set to < $1x10^{-3}$).

BOX 4.3| Protein search parameters

MASCOT (version 2.2; Matrix Science, Boston, MA): Searches were performed in the MS/MS ion search mode and the parameters were set as follows: minimum mass accuracy of 30 ppm for the parent ions, an error of 0.3 Da for the fragments, one missed cleavage in peptide masses, and Cys carbamidomethylation and Met oxidation as fixed and variable amino acid modifications, respectively. Peptides were only considered if the ion score indicated extensive homology ($p<0.05$).

ProteinPilot (Protein Pilot software version 3.0, revision 114732; Applied Biosystems, USA): Searches with ProteinPilot software were performed without taxonomic restrictions and search parameters were set as follows: enzyme, trypsin; Cys alkylation, iodoacetamide; special factor, gel-based ID; and ID focus, biological modification and amino acid substitution. The false discovery rate (FDR) was determined using PSPEP algorithm from ProteinPilot search engine, using a concatenated database joined with the reversed decoy database. Peptides were only considered if their confidence was above 95% and proteins were selected if the FDR<1%.

BOX 4.4| Protein sequence databases used

[A] Purple sea urchin *Strongylocentrotus purpuratus* predicted protein database (42.420 entries; December 2006; ftp://ftp.ncbi.nih.gov/genomes/Strongylocentrotus_purpuratus/protein) joined together with
[B] Uniprot/SwissProt database (release 2011_01; 566.840 sequences; 203.332.110 residues);
[C] non-redundant protein database Uniref100 (release 2011_01; 11.659.891 clusters).

[4] *IMPORTANT NOTE*: *In-gel* digestion of the excised protein spots, tryptic peptides purification/concentration/separation and mass spectrometry (MALDI-TOF/TOF) procedures were performed as described in CHAPTER 2 of this thesis.

4.3. RESULTS

In order to study two distinct stages of starfish arm regeneration, three different time points were selected. To study wound healing events, tissues were collected at 48h and 13 days post-arm tip ablation (*PAA*) and, to study the re-growth phase (*RG*), tissues were collected 10 weeks *PAA*. Soon after 10-15h *PAA*, a contraction of the tissues surrounding the injury plane was observed, stopping the leakage of body fluids. At 48h *PAA*, the connective tissue began to accumulate at the wound edges, bridging the gap created by arm tip amputation (Figure 4.2C). At approximately two weeks after injury (13 days), the wound is completely sealed, however it is still not possible to observe traces of a re-growing arm (Figure 4.2D). In starfish, the regeneration process is mainly morphallactic, involving the dedifferentiation and transdifferentiation of the cells adjacent to the injury site, being, therefore, slower and more complex than in other echinoderm classes such as ophiuroids, in which regeneration occurs through epimorphosis (undifferentiated blastema) (Hernroth *et al.*, 2010).

At ten weeks post-arm tip ablation, it is possible to observe a completely formed and differentiated arm, although of smaller proportions (7-10 mm in length) in comparison with uninjured starfish arms (Figure 4.2E). Similarly, the radial nerve cord is fully regenerated, showing only a difference in thickness when comparing with the same tissue in the zone preceding the injury plane.

In order to increase the number of proteins to be resolved in 2DE, two strategies were used. First, the collected nerve tissues from both regenerating and non-regenerating starfish were pre-fractionated into a soluble and membrane proteins enriched fractions. This was done by automatic frozen disruption (Butt *et al.*, 2005), in order to minimize potential artifacts and to simultaneously improve protein extraction yield by increasing tissue surface area. Secondly, the obtained enriched protein fractions were separated using a set of complementary low range IEF pH strips (3-5.6*NL* and 5.3-6.5*L*) which greatly complemented the results obtained with broader *pH* strips (3-10*L*) (Table 4.2).

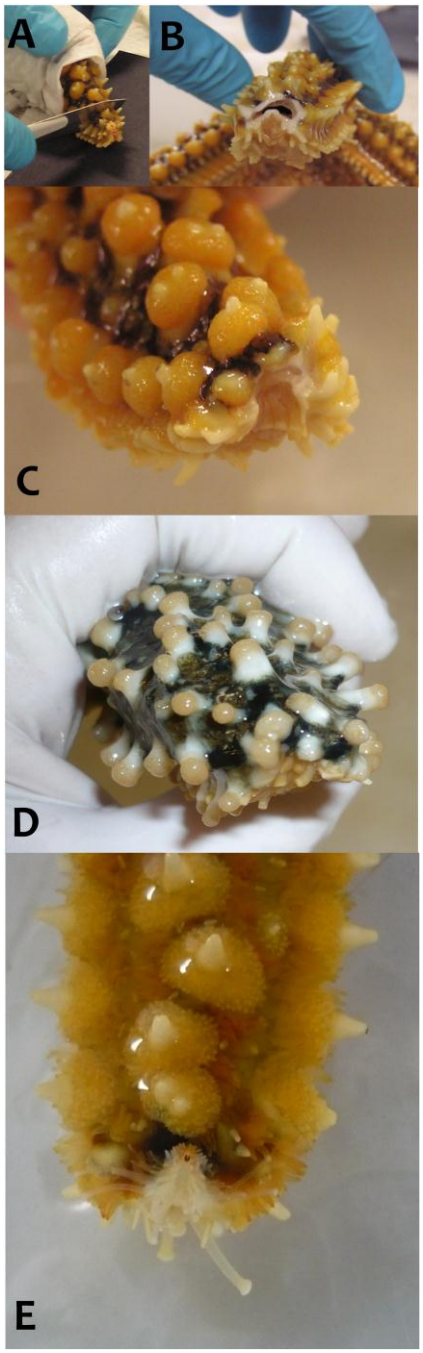

Figure 4.2: Several stages of *Marthasterias glacialis* arm regeneration events. **A|** Induction of regeneration by arm tip ablation; **B|** Wound aspect immediately after amputation; **C|** 48h *PAA*; **D|** 13 days *PAA* and **E|** 10 weeks *PAA*.

		WH			RG
		3-10*L*	**3-5.6*NL***	**5.3-6.5*L***	**3-10*L***
Soluble fraction	Number of resolved spots	1215	886	724	1548
	Number of spots with significant variation in the relative spot volume	197	156	239	149
	Number of excised spots	185	*	*	149
Membrane fraction	Number of resolved spots	830	*Np*[#]	857	1269
	Number of spots with significant variation in the relative spot volume	90	*Np*[#]	60	53
	Number of excised spots	85	*Np*[#]	*	52

Table 4.2: Description of the amount of spots resolved/with significant variation/excised per IEF strip used to separate both radial nerve cord enriched protein fractions (soluble and membrane) of the two different regeneration events studied (WH and RG). *NP*[#] not preformed; *no spots excised.

Several statistical analyses were performed on the obtained DIGE gels within Progenesis SameSpots. A power analysis revealed that the number of biological replicates used in the experiments (6 animals per group) was adequate to account for the inter-individual variability. In addition, the Principle Component Analysis of individual DIGE gels showed a clear separation of control and experimental groups. However, the gels from the samples collected at 48h and 13 days *PAA* showed close correlation and clustered together, for both soluble and membrane enriched fractions. For this reason, the analysis of variance was performed between controls and only two injured groups, wound healing (WH) (including 48h and 13 days *PAA* and the respective controls), and re-growing radial nerve cords (RG) (10 weeks *PAA* and the respective controls). This analysis detected a total of 592 and 150 spots with significant volume variation (p<0.05 and fold>1.5), respectively, in the soluble and membrane fractions of WH RNC DIGE gels in comparison with controls. However, due to limitations in the total amount of protein extracted from the collected nerve tissues, the preparative gels used for protein identification were only performed using pH strips 3-10*L*. This resulted in the excision of 185 and 85 spots from the WH soluble and membrane fractions, respectively.

For RG RNC, 149 and 53 spots from the soluble and membrane fractions, respectively, had a significant change (p<0.05 and fold>1.2) in the relative spot volumes when comparing with the respective controls. From the correspondent RG preparative gels (3-10*L*), 149 and 52 spots were excised for protein identification, from the soluble and membrane fractions (Table 4.2).

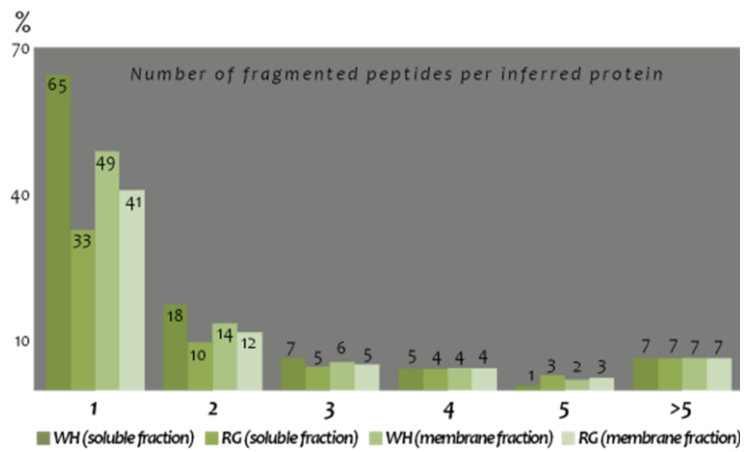

Figure 4.3: Number fragmented peptides per inferred protein in both enriched fractions (soluble and membrane) of the assayed time points of starfish arm tip regeneration. ***WH***, wound healing (48h and 13 days post-arm tip ablation); ***RG*** (10 weeks post-arm tip ablation).

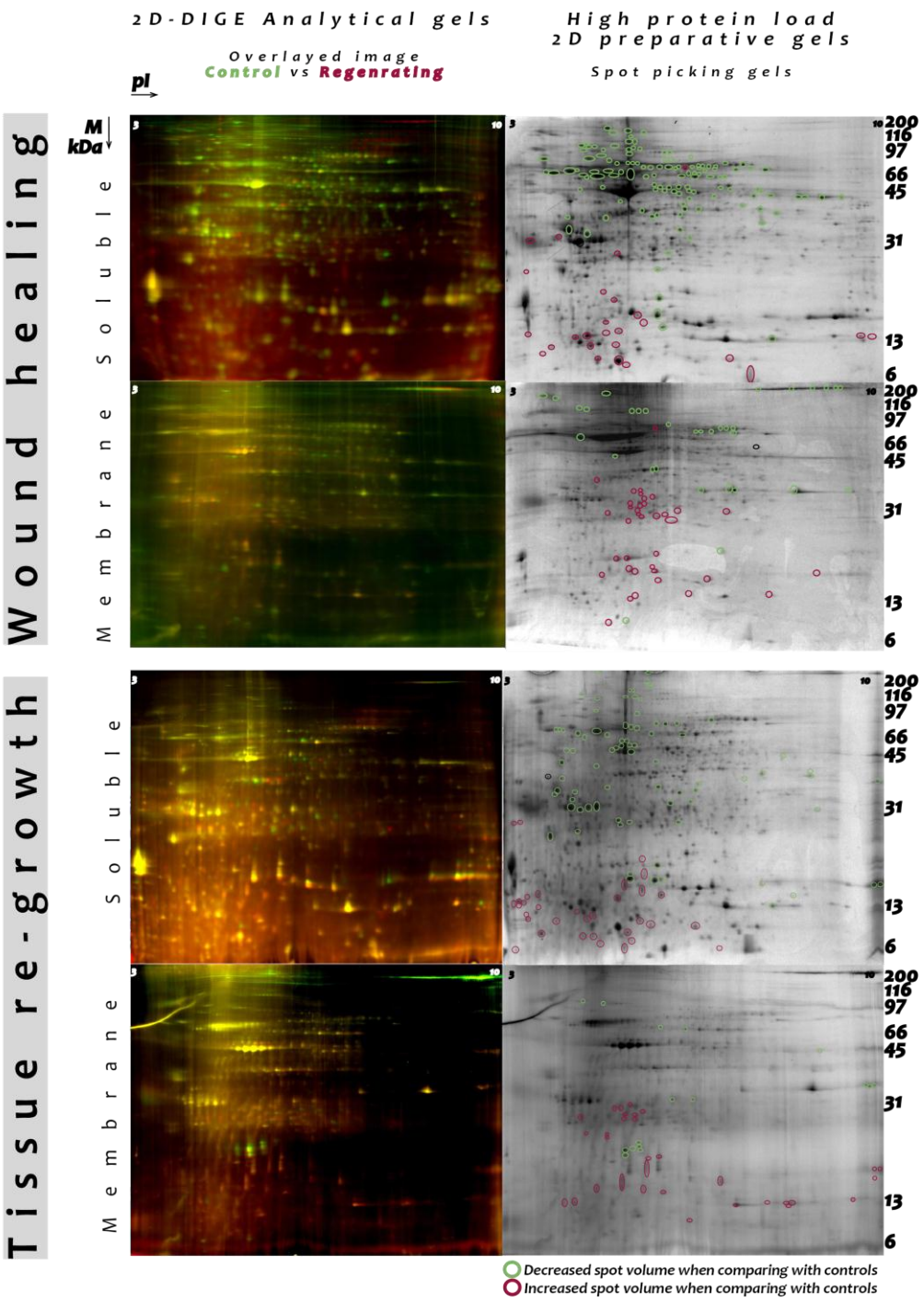

Figure 4.4: DIGE (left) and preparative gels (right) of the wound healing and re-growing starfish radial nerve cords. In the DIGE overlayed image of the controls *vs* regenerating radial nerve cords it is possible to see that in the high mass region of the gel the spots show higher volumes in the control group (green spots) and in the low mass region of the gel the regenerating gels show higher volumes in the regenerating group (red spots). On the preparative gels, spots that were picked for protein ID are marked with green circles (up-regulated proteins in controls) and red circles (up-regulated proteins in regenerating RNC).

Table 4.3 Number of MS/MS spectra successfully assigned to peptide sequences and unidentified good quality MS/MS spectra in both enriched fraction (soluble and membrane) of the assayed time points of starfish arm tip regeneration. ***WH***, wound healing (48h and 13 days post-arm tip ablation); ***RG*** (10 weeks post-arm tip ablation).

	Protein fractions	Number of MS/MS spectra	Protein databases	Identified MS/MS spectra	Unidentified MS/MS with good peak intensity and distribution along *m/z* range
WH	Soluble	2819	UniProt+S. *purpuratus*	400	2152
			Uniref100	461	2098
	Membrane	1334	UniProt+S. *purpuratus*	161	926
			Uniref100	147	937
RG	Soluble	2295	UniProt+S. *purpuratus*	376	1208
			Uniref100	404	1210
	Membrane	780	UniProt+S. *purpuratus*	241	344
			Uniref100	240	345

After in-gel digestion of the excised spots and analysis by MALDI-TOF/TOF, the obtained spectra were processed with two protein identification search algorithms and three protein sequence databases (in order to achieve both complementary and confirmatory protein identification results (Supplementary tables 4.1 and 4.3). This strategy was chosen because it was previously used with success to characterize the proteomes of starfish radial nerve cord (Chapter 2) and coelomocytes (Chapter 3). Among the excised spots from the soluble and membrane fractions of the WH group, 281 ***different*** proteins were inferred (207 and 74 ***different*** proteins in the soluble and membrane fractions, respectively (Supplementary table 4.2). For the RG group, a total of 247 ***different*** proteins were inferred (184 and 63 ***different*** proteins in the soluble and membrane fractions, respectively) (Supplementary table 4.4).

However, the low number of MS/MS spectra with an assigned peptide sequence (approximately 15% and 32% for WH and RG, respectively), reveals the need for the sequencing of a starfish species genome (see Table 4.3). Furthermore, from both nerve subcellular fractions of the several assayed times, a considerable amount of inferred proteins derived from a single peptide identification (p<0.05) (Supplementary tables 4.1 and 4.3; Figure 4.3). Another possible hypothesis for the low identification yield could be related with the existence of different post-translation modifications. In fact, several of the identified proteins had an apparent molecular mass (M) above the predicted by its sequence (Supplementary table 4.2 and 4.4; Figure 4.5), concomitantly with a shift in the *pI* apparent values. This effect has already been described in several 2DE studies aiming to understand protein dynamics in regenerating neurons (Jiménez *et al.*, 2005; Perlson *et al.*, 2004).

In the DIGE overlayed image of the soluble and membrane fractions from both WH and RG RNC with

Table 4.4: Criteria used to establish mass shift categories of the identified proteins according to the electrophoretic mobility of 2DE molecular markers.

2DE gel mass range (kDa) according to molecular markers	Error margin allowed in terms of the ***electrophoretic mobility*** of 2 adjacent molecular markers	Error margin in terms of kDa
200-116	±1/2	±40
116-97	±1/2	±13
97-66	±1/3	±13
66-45	±1/2	±13
45-31	±1/3	±5
31-14	±1/6	±4
14-6	±1/4	±4

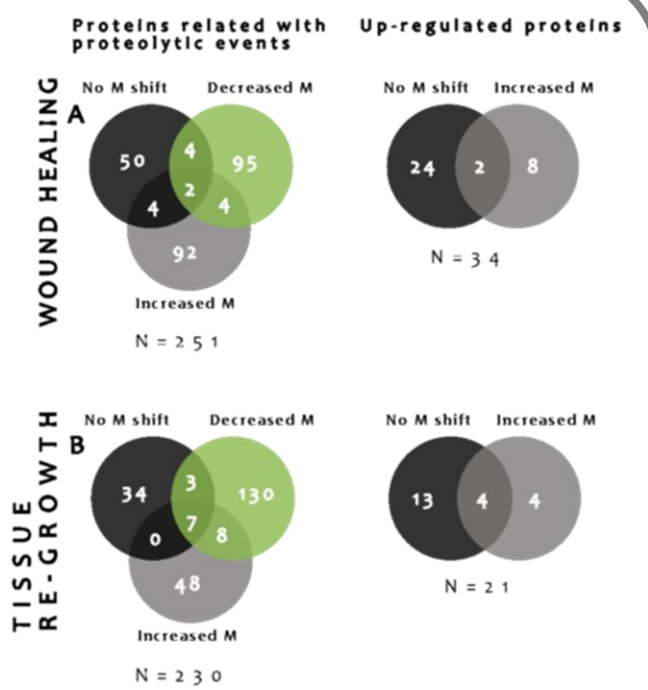

Figure 4.5: Number of identified proteins categorized in terms of molecular mass shifts in both soluble and membrane fractions during radial nerve cord wound healing (A) and re-growth (B) events.

their respective controls (Figure 4.4) it is possible to observe that the high molecular mass (M) region of the controls gels shows a considerable amount of spots with significant superior spot volumes. This effect is also observed in the regenerating RNC DIGE gels however, in low M region. The low M protein spots are generally more abundant in the regenerating RNC DIGE gels. This 2DE pattern is characteristic of proteolytic events occurring in the biological process.

In order to understand how proteins and pathways are being modulated through proteolytic events in the radial nerve cord WH and RG events, the predicted M (M_{pred}) of the identified proteins was compared with the apparent M (M_{apar}) based on the spot(s) position in the 2DE gels (Supplementary tables 4.1 and 4.3). For protein spots localized in the 2DE mass region (M) of 200-116 kDa, proteins were considered as having no mass change if the observed shift was inferior to 40 kDa; if the spots were localized in the 116-45 kDa region, the established margin was of 13 kDa; for the M region of 45-31 kDa, 5 kDa margin was permitted and finally, for 31-6 kDa M region, a 4 kDa shift was allowed (Table 4.4). According to this evaluation, the identified proteins in the regenerating (WH and RG) groups were further sub-divided in three categories:

1) ***Proteins with decreased M***: if the $M_{apar} < M_{pred}$,

2) ***Proteins with no M change***: if the $M_{apar} \approx M_{pred}$;

3) ***Proteins with increased M:*** if the $M_{apar} > M_{pred}$.

Identified proteins were further categorized as being ***fragments***; ***proteolysis substrates/down-regulated*** and ***up-regulated*** by adding to the above described categories for mass shift, the respective variation of the relative spot volumes between the control (CNT) and the regenerating (WH/RG) groups as described below:

Fragments: if presenting a decreased mass and if the correspondent relative spot volume in the WH/RG group was superior to the CNT group;

Proteolysis substrates/down regulated: All mass shift categories that presented a correspondent relative spot volume in the WH/RG group inferior to the CNT group, as there is no possible way to distinguish proteins that are being down regulated or are just being degraded through proteolytic pathways;

Up regulated proteins: If presenting an increased or equal mass and the relative spot volume in the WH/RG group is higher than in the CNT group (the only subset of proteins that could not be explained by any proteolytic events).

In Figure 4.5 are represented the number of proteins included in each category (related with proteolytic events or up-regulated) with the correspondent mass shifts (No mass shift, increased mass and decreased mass) for the WH and RG events.

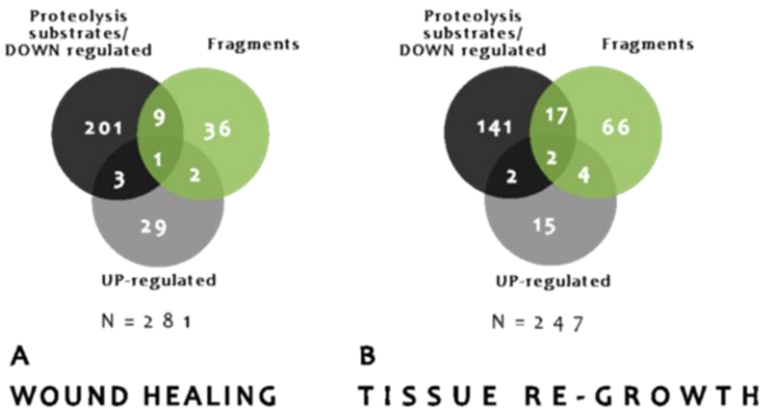

Figure 4.6: Protein distribution according to their injury relation in both soluble and membrane fractions (UP-regulated; Proteolysis substrate/DOWN-regulated or Proteolysis fragment) for WH (A) and RG (B) radial nerve cord events.

In the WH RNC, a total of 195 spots across soluble and membrane fractions were found to have significantly different relative spot volumes in comparison with the correspondent controls. In the WH RNC soluble fraction, 94% of the identified proteins were related to proteolytic/down regulated events (81% of the proteins were considered as proteolysis substrates/down-regulated; and 17% were fragments of the identified proteins). Only 7% of the identified protein spots could be assigned to up-regulated proteins (Table 4.5; Supplementary table 4.2). In the RNC membrane fraction, a lesser extent of the identified proteins were involved in the proteolytic pathways (78% of which, 45 proteins were categorized as proteolysis substrates and 12 as being fragments). The remaining proteins were considered to be up-regulated (27%) (Supplementary table 4.2).

In the RNC RG stage, the regenerated RNCs were compared with the correspondent controls and a total of 202 spots throughout both subcellular fractions were found to have significant changes in terms of relative spot volumes (Table 4.2). Nevertheless, still a high number of proteins were either identified as proteolysis substrates/down-regulated or as fragments (177 proteins in the soluble fraction and 53 proteins in the membrane fraction), highlighting the importance of proteolytic pathways that persist throughout RNC re-growth stage, although in lower levels. Also, similarly to the results obtained in the WH events, only 5% of the proteins were up-regulated in the soluble fraction of the RG RNC and 19% in the membrane fraction of the RG RNC (Supplementary table 4.4).

In several cases, the same protein was identified in multiple spots excised from substantially different positions on the 2DE gels, and consequently the same protein was found in the different established categories (Figure 4.6). This ubiquitous distribution of some proteins, such as actin, throughout the 2DE gels is probably due to several cleavage events, and in some cases probably by different proteolytic pathways. This observation of existence of the same protein in various *M* forms was also previously reported in a similar study using 2DE proteomics to study injury effects on mollusk neurons (Perlson *et al.*, 2003; Perlson *et al.*, 2004); which was the case for actin, tubulin, ATP synthase, phosphoglycerate kinase, HSP70, arginine kinase, enolase an actin modulator (arp2/3), results that are all in agreement to molecular mass shift also found in the injured starfish radial nerve cord.

Table 4.5

List of some of the identified proteins associated with *Marthasterias glacialis* radial nerve cord wound healing (48 and 13 days *PAA*) and re-growth (10 weeks *PAA*) events in both soluble and membrane enriched fractions. * Hypothetical/uncharacterized proteins that had a significant hit on the *BLASTp* searches. The name of the *BLASTp* search best hit is here presented. The complete lists of identified proteins are available in Supplementary tables 4.2 and 4.4 for WH and RG, respectively, with the correspondent information on the performed *BLASTp* searches.

Protein name	Accession number	General function	RNC fraction	Regeneration stage	Spot(s)	Predicted mass (kDa)	Apparent mass on the 2DE (kDa)	Mass shift	Injury relation category			Number of fragmented peptides
									Up-regulated	Proteolysis substrate or down-regulated	Fragment	
30S ribosomal protein S21	Q04T16	RNA interaction or translation regulator	S	WH	530	8	97	↑		●		1
30S ribosomal protein S8	sp|B2GDV5	RNA interaction or translation regulator	S	RG	4122	15	17	=		●		1
40S ribosomal protein S21	Q6AZJ9	RNA interaction or translation regulator	M	WH	3804	9	8	=	●			1
40S ribosomal protein S21	sp|Q6AZJ9	RNA interaction or translation regulator	S	RG	5370	9	9	=	●			1
50S ribosomal protein	sp|A0R8J2	RNA interaction or translation regulator	S	RG	848; 982; 1786; 2211; 4570; 4712; 5335; 5573; 5590; 6142	20	8-13; 45-119	↓/↑		●	●	1
54S ribosomal protein L4, mitochondrial	sp|A5DH98	RNA interaction or translation regulator	S	RG	6076	35	17	↓		●		1
Actin	P07828	cytoskeleton dynamics	S	WH	65; 149; 155; 430; 511; 523; 622; 964; 1282; 1290; 1622; 1623; 1631; 1637; 1640; 1653; 1660; 1661; 1668; 1690; 1697; 3951; 4092; 4109; 4149; 4169; 4338; 4444; 4574	31-42	9-14; 50-284	↑/=/↓		●	●	>15
Actin	B0FBP2	cytoskeleton dynamics	M	WH	1792; 2200; 2329; 2486; 2520; 2554; 2646; 2692; 2837; 2848; 2894; 3197; 3449; 3583; 3662; 3665; 4012	31-42	9-13; 20-55	=/↓	●	●	●	>15
Actin	sp|P07828	Cytoskeleton dynamics	M	RG	1311; 2004; 2085; 2118; 2203; 2223; 2224; 2307; 2345; 2357; 2417; 2433; 2593; 2620; 2630; 2732; 2738; 2748; 2750; 2796; 2966; 3047; 3125; 3130; 3140; 3142; 3157; 3163;	42	13-64	↑/↓		●	●	>12

Protein name	Accession number	General function	RNC fraction	Regeneration stage	Spot(s)	Predicted mass (kDa)	Apparent mass on the 2DE (kDa)	Mass shift	Injury relation category			Number of fragmented peptides
									Up-regulated	Proteolysis substrate or down-regulated	Fragment	
					3174; 3737; 3747; 3748; 3766; 3768							
Actin	gi|115918029	Cytoskeleton dynamics	S	RG	952; 1656; 2047; 4306; 5167; 1865; 5100; 1655; 920	42	10-15; 56-97	↑/↓		●	●	>8
Actin CylIb Cytoskeletal	gi|115918029	Cytoskeleton dynamics	M	RG	2657; 2681; 3079; 3147	42	13-22	↓		●		>12
Actin-related protein 2/3 complex subunit 5	C3Z4W4	Cytoskeleton dynamics	M	WH	3172	17	20	=	●			1
Allograft inflammatory factor	Q0H8V2	Calcium related/cytoskeleton dynamics	S	RG	4047	17	17	=	●			1
Alpha-actinin-1	sp|Q2PFV7	Cytoskeleton dynamics	S	RG	4802	103	12	↓			●	1
Ankyrin	B2KC90	Growth cone and axon guidance/ cytoskeleton dynamics	S	RG	1657	39	70	↑		●		1
ATP-binding cassette sub-family A member 7	sp|Q7TNJ2	Transport/cytoskeleton dynamics/lipid metabolism and transport	S	RG	4673	238	13	↓		●		1
Axonemal 84 kDa protein	Q8T880	Transport	S	WH	2752	84	31	↓		●		1
Beta-G spectrin (CRE-UNC-70 protein)	UniRef100_E3LPH0	Calpain activity evidences/growth cone and axon guidance/developmental/cytoskeleton dynamics	S	RG	6033; 6149	272	33-41	↓		●		2
BH2562 protein	Q9K9T3	Hypothetical/unkown	S	WH	4338; 4894	27	11, 48	↑/↓		●	●	2
Calmodulin	P69097	Kinase or kinase regulators/calcium related	S	WH	4207; 4269; 4373	17	10, 11, 12	↓			●	3
Calmodulin	Q32VZ5	Kinase or kinase regulators/calcium related/apoptosis/developmental/cytoskeleton dynamics	S	RG	3177; 4431; 4481; 4495; 4516; 4570; 4576; 4662; 4802; 4840; 4953; 4966	15-17	11-30	↑/=/↓	●		●	>3
Calreticulin	Q8IS63	Calcium related	S	WH	842	47	87	↑		●		9

Protein name	Accession number	General function	RNC fraction	Regeneration stage	Spot(s)	Predicted mass (kDa)	Apparent mass on the 2DE (kDa)	Mass shift	Injury relation category			Number of fragmented peptides
									Up-regulated	Proteolysis substrate or down-regulated	Fragment	
Cat eye syndrome critical region protein 2	115918080	Transport/apoptosis	S	WH	1690; 1713	202	54	↓		●		2
Cdc42 small GTPase	D0EVY0	Kinase or kinase regulators/growth cone and axon guidance/cytoskeleton dynamics	M	WH	3022	21	25	=	●			2
cGMP-dependent protein kinase, isozyme	E0W2T9	Kinase or kinase regulators	M	RG	2681; 2732	121	20-21	↓		●		2
Chaperone protein htpG	sp|P0A6Z3	Folding/Neuroprotection	S	RG	976	71	94	↑		●		10
Chaperonin containing TCP1, subunit 5 (epsilon)	P80316	Transport/Folding	S	WH	1157	60	75	↑		●		3
Cysteinyl-tRNA synthetase	Q0BKI3	RNA interaction or translation regulator	S	WH	2735	53	31	↓			●	1
Cytochrome P450 19A1 (Fragments)	sp|P79699	Neuroprotection	S	RG	1792	37	66	↑		●		1
Cytosol aminopeptidase	sp|Q2IX74	Endopeptidases or proteases	M	RG	3749	52	38	↓		●		1
Dihydropteridine reductase (Fragment)	UniRef100_D5LPS8	Neuroprotection	M	RG	2203	16	31	↑	●			1
dihydropyrimidinase, partial	115969215	Developmental	S	WH	1110; 1120; 1123; 1384	71-76	66-67	=/↓		●		4
Dihydropyrimidinase, partial	Q5DF26	Developmental	M	WH	1003; 1050; 1056	62	77	↑		●		5
Dyp-type peroxidase family protein	UniRef100_D2B1J7	Neuroprotection	M	RG	2966	49	16	↓			●	1
EF hand domain containing 2 (swiprosin-1)	B0K066	Calcium related/developmental	S	WH	3020	80	27	↓			●	3
EF-hand domain-containing protein D2 (swiprosin-1)	sp|Q4FZY0	Calcium related/apoptosis/developmental	S	RG	6157	27	29	=		●		6

Protein name	Accession number	General function	RNC fraction	Regeneration stage	Spot(s)	Predicted mass (kDa)	Apparent mass on the 2DE (kDa)	Mass shift	Injury relation category			Number of fragmented peptides
									Up-regulated	Proteolysis substrate or down-regulated	Fragment	
Elongation factor G 2	O83464	RNA interaction or translation regulator/cytoskeleton dynamics	S	WH	4897	76	41	↓		●		1
Eukaryotic translation initiation factor 5A-1	C1C496	RNA interaction or translation regulator/apoptosis	M	WH	3245	17	18	=	●			1
F-actin capping protein beta subunit, putative	B7Q243	Transport/developmental/cytoskeleton dynamics	S	WH	2200	40	43	=		●		
F-actin capping protein beta subunit, putative	B7Q243	Transport/developmental/cytoskeleton dynamics	M	WH	2287	40	40	=	●			
Ferritin	Q3HM65	Neuroprotection	M	WH	3197; 3172	20	20	=	●			>8
Ferritin	Q3HM65	Neuroprotection	M	RG	2657; 2681; 2732; 2738; 3737	20	20-22	=		●		>8
Fibronectin-binding protein	UniRef100_B1QW40	ECM interaction/ Transport/developmental	S	RG	6107	68	33	↓		●		1
FK506-binding protein	Q966Y4	Apoptosis	S	WH	4391	12	10	=	●			3
Gelsolin	B6RB97	Developmental/ Cytoskeleton dynamics	S	RG	6140; 6048	23, 41	59	↑		●		4
Glutathione peroxidase, partial	gi|115926010	Neuroprotection	S	RG	3258	21	28	↑		●		4
Glutathione S-transferase 3	sp|O16116	Neuroprotection	S	RG	3334; 3370	24	27	=		●		2
Heat shock 70kDa protein 9B (mortalin-2)	D8RYR3	Kinase or kinase regulators/neuroprotection	S	WH	788; 4885	71	79, 89	↑		●		>17
Heat shock cognate 71 kDa protein; Chaperone protein dnaK	A1BET8	Neuroprotection	S	WH	788; 843; 851; 959; 964	69	84, 89	↑		●		>17
Heat shock protein	C1H4I6	Transcription regulator/factor/neuroprotection	M	WH	3583	79	11	↓		●		1
Heat shock	D2GZA5	Ups/developmental	S	WH	622; 501; 509	83	94, 99	=/↑		●		>9

Protein name	Accession number	General function	RNC fraction	Regeneration stage	Spot(s)	Predicted mass (kDa)	Apparent mass on the 2DE (kDa)	Mass shift	Injury relation category			Number of fragmented peptides
									Up-regulated	Proteolysis substrate or down-regulated	Fragment	
protein 90												
heat shock protein gp96	Q868Z7	RNA interaction or translation regulator/transport/apoptosis/calcium related	M	WH	594	92	94	=		●		>9
Inositol phosphosphingolipids phospholipase C	C0NSF4	Cytoskeleton dynamics	S	WH	3358	53	23	↓		●		1
IQ motif containing GTPase activating protein 2	UniRef100_UPI0000F2C63C	Cytoskeleton dynamics	S	RG	2382	445	49	↓		●		1
Lamin	Q9XZN7	Calpain activity evidences/cytoskeleton dynamics	M	WH	954	51	81	↑		●		3
Leucine-rich repeat transmembrane neuronal protein 1	A1A4H9	Ups/growth cone and axon guidance/developmental	M	WH	2407; 2388	59	37	↓		●		2
Leucine-rich repeat transmembrane neuronal protein 1	sp|A1A4H9	Growth cone and axon guidance/developmental	M	RG	3749	59	38	↓		●		1
Lin2 protein	P94882	Transcription regulator/factor	S	WH	1166; 1206	16	72-74	↑	●	●		2
Lymphoid-restricted membrane protein	sp|Q12912	Transport	S	RG	5335; 5573	69	8; 9	↓			●	1
Lymphoid-restricted membrane protein	sp|Q12912	Transport	M	RG	3125	69	13	↓			●	2
Lysozyme C	sp|P00698	Neuroprotection	S	RG	4431; 4495; 4576; 4662	14	13; 14	=	●			>6
Lysozyme C	sp|P00698	Neuroprotection	M	RG	2960; 3125; 3757;2862	14	13-17	=	●			>4
Methionyl-tRNA synthetase	Q48LT7	RNA interaction or translation regulator	S	WH	423; 430	75	101	↑		●		2

Protein name	Accession number	General function	RNC fraction	Regeneration stage	Spot(s)	Predicted mass (kDa)	Apparent mass on the 2DE (kDa)	Mass shift	Injury relation category			Number of fragmented peptides
									Up-regulated	Proteolysis substrate or down-regulated	Fragment	
Novel protein similar to eukaryotic translation initiation factor 5A (Eif5a, zgc:77429)	UniRef100_Q7ZUP4	RNA interaction or translation regulator/apoptosis	M	RG	2781	17	19	=	●			1
Nuclear transcription factor Y subunit B-2	Q5QMG3	Transcription regulator/factor	S	WH	1713; 1716	19	53-54	↑		●		2
Nucleolar protein 58	sp|A6ZPE5	RNA interaction or translation regulator	S	RG	2382	57	49	=		●		1
O-sialoglycoprotein endopeptidase	B2GAG0	Endopeptidases or proteases	M	WH	3197	37	20	↓			●	1
Outer membrane protein	C2G0T1	Transport	S	WH	2126; 2352	114	39; 43	↓		●		2
Outer membrane usher protein psaC	Q56983	Transport	S	WH	65; 423	89	101; 284	↑/=		●		2
Oxidoreductase, short chain dehydrogenase/reductase family	D7HVA7; Q48NP0	Neuroprotection	S	RG	6033	28	33	=		●		1
Peptidyl-prolyl cis-trans isomerase	UniRef100_A0F006	Kinase or kinase regulators/transcription regulator/folding	S	RG	4040; 4052	17	18-20	=/↓		●		4
Peptidyl-prolyl cis-trans isomerase (Fragment)	UniRef100_A0F006	Kinase or kinase regulators/transcription regulator/folding	M	RG	3757; 2862	17	16	=	●			3
Peroxidase	Q1VZP2	Neuroprotection	S	RG	3258	24	28	=		●		1
Peroxiredoxin	C4WSM1	Neuroprotection/developmental	M	WH	2936; 4012; 4016	22	26	=	●			>6
Peroxiredoxin in rubredoxin operon	sp|P23161	Neuroprotection	M	RG	2748	20	26	↑	●			1
Peroxiredoxin-1	P0CB50	Developmental/neuroprotection	S	WH	3258	22	23	=		●		5
Peroxiredoxin-6	B0WMP0	Neuroprotection	M	WH	2862	24	28	=	●			1

Protein name	Accession number	General function	RNC fraction	Regeneration stage	Spot(s)	Predicted mass (kDa)	Apparent mass on the 2DE (kDa)	Mass shift	Injury relation category			Number of fragmented peptides
									Up-regulated	Proteolysis substrate or down-regulated	Fragment	
phosphoinositide dependent kinase-1	UPI000192786B	Kinase or kinase regulators/cytoskeletn dynamics	S	WH	4333	88	11	↓			●	1
Polyribonucleotide nucleotidyltransferase	sp|C1DTW6	RNA interaction or translation regulator	S	RG	3177	79	30	↓			●	1
Polyubiquitin	P62976	Kinase or kinase regulators/RNA interaction or translation regulator/transcription regulator-factor/UPS	S	WH	4850	9	7	=	●			2
Prefoldin subunit alpha	Q6LX82	Neuroprotection	S	WH	1162	16	74	↑		●		1
Pre-mRNA cleavage factor	A7URJ4	RNA interaction or translation regulator	S	RG	6062	16	33	↑		●		1
Pre-mRNA-processing ATP-dependent RNA helicase PRP5	sp|Q6FML5	RNA interaction or translation regulator	S	RG	5583; 5522	92	8; 9	↓			●	2
Proteasome subunit alpha	O59219	UPS	S	WH	4109	29	12	↓			●	1
Proteasome subunit beta type	Q1HPR0	UPS	M	WH	2817	23	29	↑	●			1
Protein grpE	Q14LB5	Neuroprotection	S	WH	1623	24	57	↑		●		1
Putative ankyrin repeat protein L675	Q5UNU1	Growth cone and axon guidance	S	WH	662	54	93	↑		●		1
ras homolog gene family, member A	UPI0001C65337	Kinase or kinase regulators/RNA interaction or translation regulator/transcription regulator/factor/transport/calcium related/apoptosis/developmental/neuroprotection	S	WH	3098	21	25	=		●		1
Ras-related	Q2TA29	Transport//cytoskeleto	M	WH	2692; 2731; 2759; 2837	24	28-31	=/↑	●			8

Protein name	Accession number	General function	RNC fraction	Regeneration stage	Spot(s)	Predicted mass (kDa)	Apparent mass on the 2DE (kDa)	Mass shift	Injury relation category			Number of fragmented peptides
									Up-regulated	Proteolysis substrate or down-regulated	Fragment	
protein Rab-11A		n dynamics										
Ras-related protein Rab-11A	sp|Q2TA29	Transport/cytoskeleton dynamics	M	RG	2357	24	28	=	●			1
Ras-related protein Rab-15	sp|Q1RMR4	Transport/cytoskeleton dynamics	M	RG	2307; 2345; 2748; 3766	21-25	26-29	↑/=	●			4
Ras-related protein Rab-6A	A0CE65	Transport/cytoskeleton dynamics	M	WH	3313; 2848; 2837; 2759; 2817; 2894	23-25	16-30	↑/=/↓	●		●	
Ras-related protein Rab-7a	sp|Q3T0F5	Transport/cytoskeleton dynamics	M	RG	2417	24	27	=	●			1
Regulatory protein Crp	D8J4J6	Transcription regulator	S	RG	1786; 4431	28	14; 66	↑/↓		●	●	2
Regulatory protein Crp	D8J4J8	Transcription regulator	S	RG	6142	18	45	↑		●		1
Regulatory protein Crp	D8J4J7	Transcription regulator	S	RG	5504	63	9	↓			●	1
Rho1 GTPase	115963593	Kinase or kinase regulators/RNA interaction or translation regulator/transcription regulator/factor/transport/calcium related/apoptosis/developmental/neuroprotection/cytoskeleton dynamics	S	WH	3098	23	25	=		●		3
Rho-type GTPase-activating protein 2	Q10164	Cytoskeleton dynamics	S	WH	103; 557	144	200; 95	↑/↓		●	●	3
RNA binding motif (Fragment)	Q13377	RNA interaction or translation regulator	S	RG	6103	56	39	↓		●		2
RNA ligase	E3KDA7	RNA interaction or translation regulator	S	WH	1147; 1159; 1165; 1166	107	74-75	↓		●		4
RNA polymerase sigma factor sigI	E0U2K8	Transcription regulator/factor/neuroprotection	M	WH	2445	29	36	↑		●		1
Serine/threonine-protein kinase ATM	sp|Q9M3G7	Kinase or kinase regulators/transcription regulator/developmental/neuroprotection	S	RG	6030	435	32	↓		●		1

Protein name	Accession number	General function	RNC fraction	Regeneration stage	Spot(s)	Predicted mass (kDa)	Apparent mass on the 2DE (kDa)	Mass shift	Injury relation category			Number of fragmented peptides
									Up-regulated	Proteolysis substrate or down-regulated	Fragment	
Severin	Q24800	Cytoskeleton dynamics	S	WH	4880	42	43	=		●		1
Signal transduction histidine kinase	C5SFK7	Kinase or kinase regulators	S	WH	634	37	93	↑		●		2
Signal transduction histidine kinase	C5SFK7	Kinase or kinase regulators	M	WH	523; 530	37	97	↑		●		1
Spectrin	115920116	Calpain activity evidences/growth cone and axon guidance/developmental/cytoskeleton dynamics	M	WH	235; 659	279	92; 162	↓		●		6
Spectrin	UPI00015B61A3	Calpain activity evidences/cytoskeleton dynamics	S	RG	971; 3760	279	21; 94	↓		●	●	2
Spectrin alpha chain	115954248	Calpain activity evidences/growth cone and axon guidance/developmental/cytoskeleton dynamics	S	WH	103; 217; 541; 551; 557; 4884	279	43-200	↓		●	●	>7
Spectrin beta chain	B0WDS4	Calpain activity evidences/cytoskeleton dynamics/lipid metabolism and transport	S	RG	4969; 5202	266	10; 11	↓			●	2
spectrin Beta-G	Q9U9J8	Calpain activity evidences/growth cone and axon guidance/developmental/cytoskeleton dynamics	S	WH	541; 551; 730	267-272	93-97	↓		●	●	3
spectrin beta-like	UPI0001D39591	Calpain activity evidences/growth cone and axon guidance/developmental/cytoskeleton dynamics	S	WH	730	272	93	↓			●	1
START domain-	A9ZT01	Cytoskeleton	S	WH	1153; 1269; 1286; 1660	43	55; 70; 75	↑		●		>7

Protein name	Accession number	General function	RNC fraction	Regeneration stage	Spot(s)	Predicted mass (kDa)	Apparent mass on the 2DE (kDa)	Mass shift	Injury relation category			Number of fragmented peptides
									Up-regulated	Proteolysis substrate or down-regulated	Fragment	
containing protein		dynamics/developmental										
START domain-containing protein (Fragment)	A9ZT01	Developmental/cytoskeleton dynamics	S	RG	1657; 1668; 1678	43	69; 70	↑		●		>4
Synaptosomal-associated protein 25	sp|P36976	Transport/growth cone and axon guidance/calcium related/cytoskeleton dynamics	M	RG	2118	24	33	↑		●		1
Transcription factor Sox-12	sp|Q8AXQ4	Transcription regulator/apoptosis/developmental	S	RG	5225	27	10	↓			●	1
Transcriptional activator Rgg/GadR/MutR	D0AHM2	Transcription regulator	S	RG	2546; 5583	39	8; 47	=/↓		●	●	2
Transcriptional regulator, LacI family	Q03ZF8	Transcription regulator/factor	S	WH	65	35	284	↑		●		1
tRNA (guanine-N(1)-)-methyltransferase	Q4WXA1	RNA interaction or translation regulator	S	WH	1108; 1109; 1110; 1120; 172	44	109; 77	↑		●		4
tRNA pseudouridine synthase A	D9WR76	RNA interaction or translation regulator	S	WH	2735	31	31	=	●			1
Tubulin alpha chain	P53372	Cytoskeleton dynamics	S	WH	1138; 1301; 1153; 1282; 1290; 4207; 4574; 1300	28; 50	76	↑/↓		●	●	>16
Tubulin alpha-1D chain	Q2HJ86	Cytoskeleton dynamics	M	WH	3022	50	25	↓			●	>9
Tubulin beta chain	P11833	Cytoskeleton dynamics	S	WH	1300	50	69	↑		●		>15
Tubulin beta-2C chain	Q3MHM5	Cytoskeleton dynamics	M	WH	3810	50	8	↓		●		3
Tubulin-alpha	Q2HJB8	Cytoskeleton dynamics	M	WH	3497; 4012; 2894	50	13; 26; 27	↓			●	>3
two component LuxR family transcriptional regulator	UPI0001DD0746	Transcription regulator/factor	M	WH	161; 142; 146; 162	24	200	↑		●		4
Two-component	D7JXA2	Kinase or kinase	S	WH	4744	156	8	↓			●	1

Protein name	Accession number	General function	RNC fraction	Regeneration stage	Spot(s)	Predicted mass (kDa)	Apparent mass on the 2DE (kDa)	Mass shift	Injury relation category			Number of fragmented peptides
									Up-regulated	Proteolysis substrate or down-regulated	Fragment	
system sensor histidine kinase/response regulator hybrid		regulators/transcription regulator/factor										
ubiquitin C, partial	UPI0001926211	Transcription regulator/factor/ups/apoptosis/growth cone and axon guidance	S	WH	4850	9	7	=	●			**3**
Ubiquitin family protein	A8IS91	Transcription regulator/factor/ups/apoptosis/growth cone and axon guidance	S	WH	4574	9	9	=	●			1
Ubiquitin/actin fusion protein	gi|115918029	UPS	S	RG	654; 853; 857; 1867; 1971; 1994; 2041; 2051; 2069; 2382; 3760; 4047; 4385; 4588; 4901; 4966; 4969; 5088; 5198; 5217; 5522; 5583; 6042; 6048; 6091; 6112; 6140	42	8-21; 49-63; 116-187	↑/=/↓		●	●	>15
Ubiquitin-conjugating enzyme	sp|Q1RMX2	UPS	S	RG	4306; 4198	16-17	15-16	=		●		2
villin 2	UPI0000D8B3D9	cytoskeleton dynamics	S	WH	818; 1031; 1032	68	82-88	↑		●		3
Villin-1	Q29261	cytoskeleton dynamics	S	WH	577	15	95	↑		●		1
von Hippel-Lindau binding protein 1-like	UPI0001CBB031	Neuroprotection	S	WH	3020	21	27	↑	●			1
V-type proton ATPase catalytic subunit A	C3XZE0	Calcium related/neuroprotection	S	RG	5088; 6130	68	11; 80	↑/↓			●	5
*Similar to 26S protease regulatory subunit	115942106	RNA interaction or translation regulator/transcription regulator/factor/ups	M	WH	1588	45	144	↑		●		3
*similar to ankyrin repeat protein	A2FHV3	Growth cone and axon guidance	S	WH	1269; 1286	72	70	=		●		2
*similar to Dihydropyrimidin	UPI0001925E76	Developmental	M	WH	1056	32	77	↑		●		1

Protein name	Accession number	General function	RNC fraction	Regeneration stage	Spot(s)	Predicted mass (kDa)	Apparent mass on the 2DE (kDa)	Mass shift	Injury relation category			Number of fragmented peptides
									Up-regulated	Proteolysis substrate or down-regulated	Fragment	
ase												
*similar to Dihydropyrimidinase	UPI0001925E76	Developmental	S	WH	1110	32	77	↑		●		1
*similar to fibronectin type III domain-containing protein	A8F5G5	ECM interaction/ Transport/developmental	S	RG	2656	174	40	↓		●		**1**
*similar to LacI family transcription regulator	C0A988	Transcription regulator	S	RG	2934	41	34	↓		●		1
*similar to luminal binding protein	C5YNI7	Neuroprotection	S	WH	788	16	89	↑		●		1
*similar to peroxiredoxin V protein	B3RM02	Neuroprotection	S	RG	3993; 6076	20	17-18	=		●		4
*similar to Rhs family protein	UniRef100_A7VY20	Kinase or kinase regulators/Neuroprotection	S	RG	1842	275	64	↓		●		1
*similar to ubiquitin specific peptidase 36	B7PMA2	UPS	S	WH	1159; 1165	127	74-75	↓		●		2

4.4. DISCUSSION

4.4.1. Proteolysis as a post-translational modification

Post-translation modifications such as phosphorylation are well established signaling events in neuronal injury, and for this reason it is not surprising to find indications of these processes in the regenerating starfish radial nerve cord, although never described before in echinoderms. On the other hand, the occurrence of proteolytic events in such great extent suggests that the starfish RNC regeneration depends on the occurrence of such processes simultaneously with protein synthesis.

Proteases are known to hydrolyze proteins peptide bonds, representing an important and irreversible post-translational modification responsible for the activation or inactivation of protein substrates or even affect protein localization (Domselaar *et al.*, 2010). Due to these enzymes ubiquity, it is postulated that every protein at some point in its life cycle is affected by proteolysis (Doucet *et al.*, 2008), and hence proteases are responsible for sculpting whole proteomes. Proteolysis ranges from the dramatic degradation-to-completion, to processing single specific cleavages within a protein, including the almost imperceptible trimming of a few N- or C-terminal residues (Doucet *et al.*, 2008). Biologically, proteolytic processing can be highly relevant: the removal of just two to four residues can convert a chemokine from a receptor agonist to an antagonist and hence abruptly change the cell migration patterns of immune and cancer cells (Gutierrez-Fernandez *et al.*, 2008).

BOX 4.5: GTPases and the growth cone: the motor of axonal regeneration and growth.

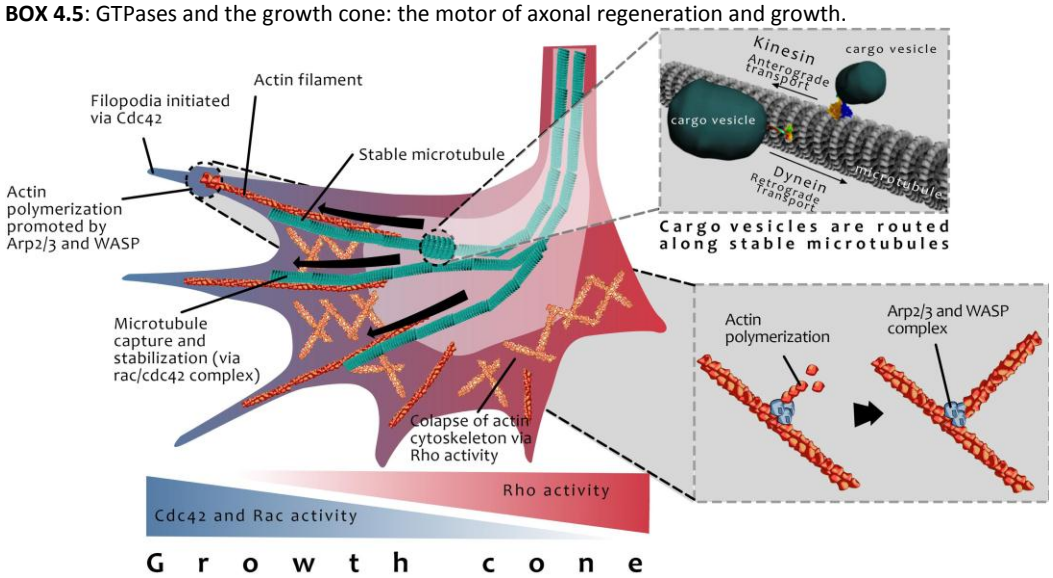

Neurons extend axons towards appropriate targets in the regenerating nervous systems via growth cones, the motile structures at axonal tips. The Rho family of GTPases, including Cdc42, Rac and Rho, regulate the dynamics of actin microfilaments and microtubules, and have been implicated in growth cone steering by molecular gradients (Giniger, 2002). Cdc42 activation in growth cones stimulates formation of dynamic, finger-like filopodia (Kozma *et al.,* 1997) comprising bundles of actin microfilaments. In addition to their roles in modulating microfilaments, Rho GTPases affect microtubules, which then affect neuronal growth (Andersen, 2004). This illustration represents a hypothetical mechanism by which Rho GTPases mediate growth cone steering. The concentrations of active Rac and Cdc42 (red) are relatively high on the right side of the growth cone promoting filopodia formation, but Rho activity (blue) is relatively low on that side. Conversely, active Rho is relatively high on the left side and active Rac and Cdc42 are low resulting on filopodial collapse, forming lamellipodia instead (Figure based on Rajnicek *et al.*, 2006).

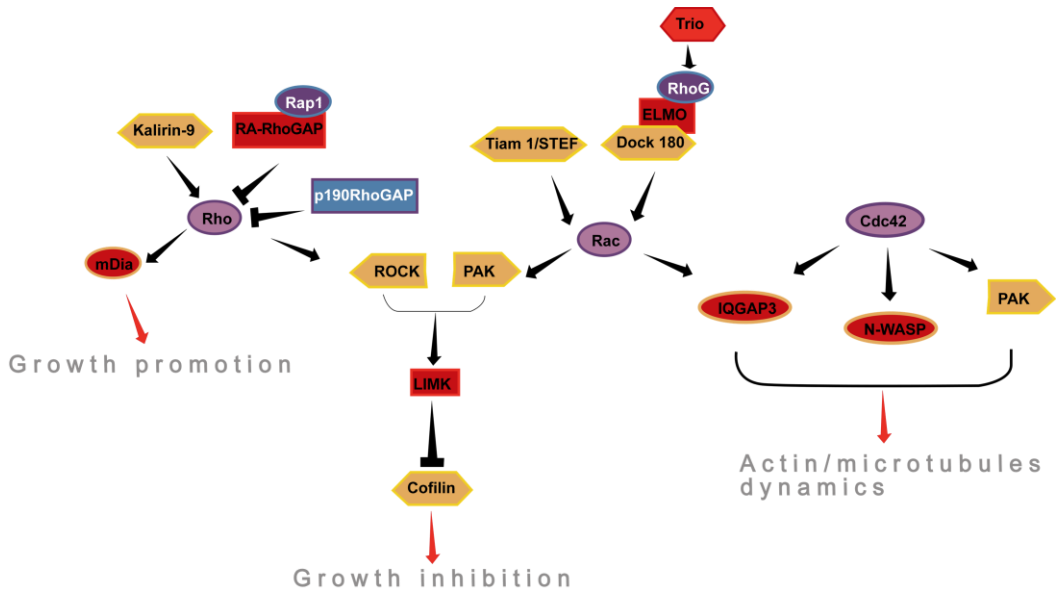

Figure 4.7: Rho GTPases in axon growth. Rho can either promote or inhibit axon extension depending on the type of effector (mDIA or ROCK, respectively). The Rap-1 activated RA-RhoGAP or p190RhoGAP *inactivate* Rho to promote axon growth. On the other hand, the Rho-specific GEF domain of Kalirin-9 *activates* Rho to promote axon growth. Both ROCK and PAK can inhibit the actin-depolymerizing factor cofilin through LIM kinase (LIMK). The balance of dephosphorylated (active) and phosphorylated (inactive) cofilin appears to be crucial for axon extension. Several GEFs like Tiam1, STEF and Dock180 may act upstream of Rac to regulate actin and microtubule dynamics. Cdc42 can also control the actin and microtubule cytoskeletons during axon growth via some of its effectors like IQGAP3, PAK, and N-WASP. (Figure based on Hall *et al.*, 2011). *GEFs*, Guanine nucleotide exchange factors; *GAPs*, GTPase-activating proteins.

The high number of genes that encode proteases across all organisms[5] justifies the importance of their role in many cellular processes such as in immunity (Domselaar *et al.*, 2010), blood clotting (Niessen *et al.*, 2011) and wound healing (Page-McGaw *et al.*, 2007).

Like all post-translational modifications, if proteolysis is not considered in proteomic analysis, then considerable metadata will be lost, and the functional annotation of proteome components will be misguided or at worst, **wrong**.

Even though proteolytic pathways are recognized for their role both in normal (Hegde, 2010) and regenerating neurons (Gumy *et al*., 2010), this subject has been given quite less consideration than protein synthesis.

During arm-tip wound healing events, a great involvement of the proteolytic pathways is expected, leading to major ECM reorganizations necessary for tissue remodeling, a process that has already been described to occur during intestine regeneration of a sea cucumber specie (Quiñones *et al.*, 2002). Within a regenerating nervous system, the proteolytic pathways are also expected to be involved soon after injury, affecting especially cytoskeleton proteins in order to promote the correct formation of axonal growth cones (Ambron, 1996).

Herein we describe the pathways that were found to be regulated through proteolysis, and even though greater emphasis is given to the proteolytic pathways and their protein substrates. The few proteins that were identified as up-regulated during starfish radial nerve cord regeneration events are also discussed.

[5] The human genome encodes over 569 proteolytic enzymes or homologues, constituting the second largest enzyme family and thus indicating the importance of this class of proteins (Puente *et al.,* 2003).

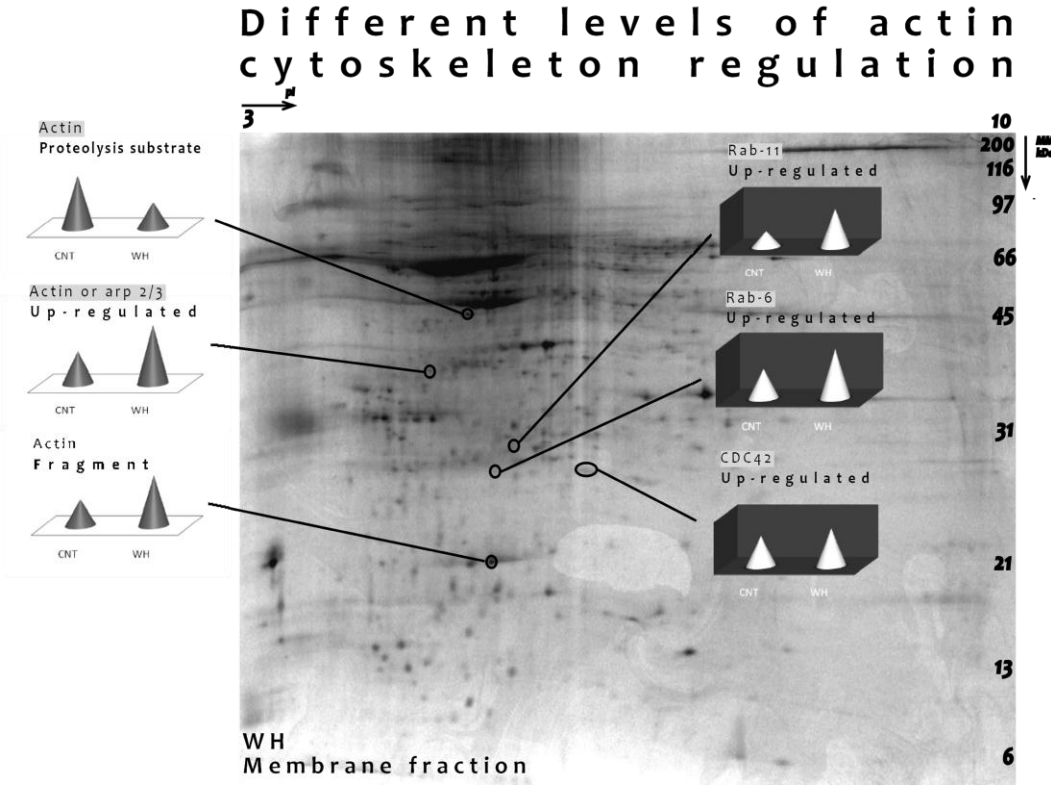

Figure 4.8: Several different levels of actin modulation within radial nerve cord wound-healing events: *de novo* synthesis (up-regulated); proteolysis (identified as a proteolysis substrate and as a fragment) and several actin regulatory proteins identified as being up-regulated, such as Cdc42; Rab-11; Rab-6 and Arp2/3. (Wound healing and the respective control spot volumes are represented in the cone charts).

A detailed description of the identified proteins and their related functions within neuronal regeneration events is here presented as a hypotheses-generating work, aiming to clarify the signaling functions of the newly generated protein fragments. The list of identified proteins in RNC WH and RG events with the corresponding annotations for generalized function and injury related category can be found in a summarized form in Table 4.5, or with the complete set of information in the Supplementary tables 4.2 and 4.4.

4.4.2. Cytoskeleton dynamics is modulated through de novo protein synthesis and proteolysis in the regenerating radial nerve cord

4.4.2.1. Actin and microtubules regulating proteins

Neural regeneration, axon guidance and growth, requires spatial and dynamic reorganization of the cytoskeleton. The growth cone, a highly motile cellular compartment at the tips of growing axons, is composed of a center region filled with organelles and microtubules and a peripheral, highly dynamic, actin-rich region containing lamellipodia and filopodia

(Lowery *et al.*, 2009). Highly tuned actin filament organization within the growth cone dictates the permissive protrusion of newly formed microtubules influencing the axon growth (Stiess *et al.*, 2011). The actin turnover dynamics is regulated by actin nucleating, severing, branching and bundling proteins. The Rho-GTPases Cdc42, Rac and Rho, are key regulators of the cytoskeleton, and therefore are also implicated in these processes (reviewed in Hall *et al.*, 2011) (BOX 4.5) driving many of the required morphological changes during axogenesis and axonal regeneration. These Ras superfamily[6] small GTPases coordinate multiple signal transduction pathways with **precise spatial control** by acting as molecular switches, changing between an inactive, GDP-bound state and an active GTP-bound state, which further interact with specific effectors to propagate downstream signaling events which include ***1)*** dynamic assembly/disassembly and reorganization of the actin and microtubule cytoskeleton, ***2)*** the interaction of the growing axon with other cells and extracellular matrix, ***3)*** the delivery of lipids and proteins to the axon through the exocytic machinery and, ***4)*** the internalization of membrane proteins at the leading edge of the growth cone through endocytosis (reviewed in Hall *et al.*, 2011).

Initially it was thought that the regulation of axon morphogenesis and regeneration by the GTPases could simply be explained by the antagonistic effects of Rac and Rho on the actin cytoskeleton. Nowadays, studies carried out in tissue cultures and animal models show a much more complex scenario that involves multiple small GTPases each acting locally to promote discrete downstream signaling events, sometimes antagonists, sometimes synergetic (Hall, 2011) (Figure 4.7).

Dynamic cytoskeleton remodeling events are also vital for cells at the injury site to undergo a morphallactic process and achieve functional re-growth of the lost tissues. Since this cellular strategy causes loss of tissue specificity in which terminally differentiated cells become undifferentiated (*i.e.*, dedifferentiation) and then again to re-differentiate into a cell of a different lineage (*i.e.*, transdifferentiation), it is expected that highly coordinated cytoskeleton rearrangements take place for such a dramatic cell morphology change.

Several actin and microtubules regulators were found to be up-regulated in WH RNC of the starfish namely, **Rab-11A**, **Rab-6**, **F-actin capping protein beta subunit**, the small **GTPase Cdc42** and **actin-related protein 2/3 complex subunit 5 (arp 2/3)**. The last two proteins, are known to be key effectors of the *Wiskott-Aldrich syndrome protein (WASP) family verprolin-homologous protein (WAVE)* pathway, which induces cytoskeletal changes by promoting actin polymerization by direct interaction with arp 2/3 complex and profilin promoting axon growth (Takenawa *et al.*, 2001) by regulating filopodia formation (Nobes *et al.*, 1995) (BOX 4.5). It was further proved by Garvalov and colleagues (2007) using Cdc42-null neurons that this GTPase acts upstream of a local actin depolymerizing activity, which is required for initial axon formation and hence, it is expected the up-regulation of these proteins during starfish RNC regeneration events. Conversely to arp 2/3 or Cdc42, increased Rho activity prevents neurite initiation and induces neurite retraction (Kouchi *et al.*, 2010) (BOX 4.5). The inactivation of Rho appears to be regulated by several mechanisms; namely by the Rho GTPase-activating protein, which enhances the intrinsic rate of GTP hydrolysis of Rho, suppressing Rho activity during neurite formation. **Rho-type GTPase-activating protein 2** and **Rho1 GTPase** were also identified in the WH RNC in three different protein forms: **1)** the *Rho-type GTPase-activating protein 2* was identified with an apparent *M* above the expected and also, as a proteolytic fragment, indicating that this protein is being targeted to proteolysis probably through the ubiquitin/proteasome pathway, which is in agreement with previous reports relating the down-regulation of Rho activity due to targeted degradation mediated by the UPS system (Wang *et al.*, 2003); **2)** *Rho1 GTPase* was identified in spots with the expected *M*, however having a reduced spot volume relatively to controls, caused either by a down-regulation or targeted proteolysis.

Not surprisingly, **actin** itself was identified in a multitude of different 2DE spots and consequently was one of the proteins that appeared to be regulated at three different levels (Figure 4.8): by an increase in protein levels (up-regulation) in WH RNC, indicating

[6] The Ras superfamily of small GTPases can be subdivided in six families: Rho, Ras, Rab, Arf, Sar and Ran (reviewed in Hall, 2011).

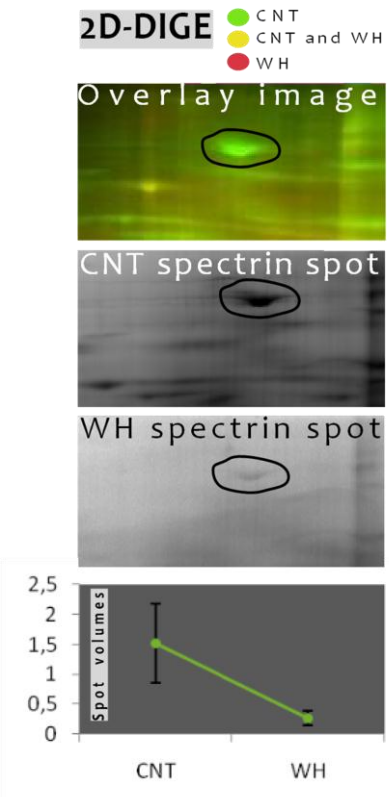

Figure 4.9: The 200 kDa spot identified as spectrin (a known calpain substrate) shows that this protein is a proteolysis substrate during radial nerve cord wound healing events.

that in this early stage of regeneration actin is being *de novo* synthesized; and by targeted proteolysis in both WH and RG RNC (identified as fragment and as proteolysis substrate). This suggests that the several actin forms are extremely dynamic and precisely controlled by different pathways. **Rab-6A** is also an example of modulation at different levels, being identified in WH RNC with different apparent *M* (increased, no change and decreased) and, as being up-regulated or a fragment (Supplementary table 4.2).

Furthermore, actin binding proteins, such as **villin** and **severin**, were also identified in WH RNC. These are known to promote the bundling, nucleation, capping and severing of actin filaments. Both proteins were identified as proteolytic fragment or down-regulated, thus suggesting that proteolysis might regulate the activity of these actin binding proteins to promote actin filaments polymerization or depolymerization in WH starfish RNC. Several proteolytic fragments of **calmodulin** were also identified in the WH RNC, a protein known to regulate actin-based motility and to participate in the signaling pathways used to steer growth cones (Seung Kim *et al.*, 2001).

Similarly to WH, several GTPases were also identified in the RG RNC. Among these are the GTPases **Rab-11A**, **Rab-15** and **Rab-7A** that were identified in several different spots and up-regulated. Several other proteins involved in actin and microtubule regulation were identified in the RG nerve namely, **IQ motif containing GTPase activating protein** (proteolysis substrate/down-regulated) and the **ATP-binding cassette sub-family A member 7** (proteolysis substrate/down-regulated), both involved in the Cdc42 protein signal transduction events (McCallum *et al.*, 1996). **Profilin**, an actin-binding protein involved in restructuring of actin cytoskeleton, was only identified in RG RNC as being up-regulated and also as a proteolysis substrate. Once more, these facts suggest that *de novo* protein synthesis and proteolytic pathways regulate actin dynamics, resulting in cytoskeleton changes associated with growth cone extension/retraction or, cellular transdifferentiation processes. Also involved in actin filament formation is the **allograft inflammatory factor** (Autieri *et al.*, 2003), which was also up-regulated in the RG RNC. This protein might be promoting actin polymerization towards the formation of microfilaments from the newly synthesized actin monomers, while other cytoskeleton proteins are being cleaved, as expected, according to the explained above. Other actin bundling proteins were also identified namely, **alpha-actinin-1** (proteolytic fragment), **gelsolin** (proteolytic fragment/down regulated), and **calmodulin** (up-regulated and proteolytic fragment).

These results seem to indicate that the several pathways that govern cytoskeleton dynamics are oriented towards neuronal re-growth as soon as 48h post-arm tip ablation. Nevertheless, it has to be considered that the majority of protein regulation at the post-translational level is extremely dependent on the physical location where the target proteins need to exert their actions, or be inactivated/eliminated. Hence, opposite modifications may be occurring in different

axonal locations, creating an endeavor task to interpret the function of a particular protein in a particular "proteolytic" state. For this reason, most of the results henceforward will be discussed in terms of being regulated or not, by proteolytic pathways, for whose the particular function of the regulation still remains to be clarified.

4.4.2.2. Calpain protease remains active throughout the course of regeneration

One of the proposed functions for calpain mediated cytoskeleton rearrangements relies in the proteolytic cleavage of spectrin, the protein that through its binding partner ankyrin, connects many integral membrane proteins to the actin cytoskeleton (Bennett *et al.*, 2001). This process was suggested to facilitate membrane fusion of axoplasmic vesicles, helping the construction of the growth cone or extension of the axon (Spira *et al.*, 2001). Calpain has been previously identified in the starfish radial nerve cord proteome characterization (Franco *et al.*, 2011; Chapter 2) and several fragments of **spectrin like proteins** (Figure 4.9), and its binding partner **ankyrin** (Garbe *et al.*, 2007; Otsuka *et al.*, 2002), were now identified in the WH RNC, indicating calpain involvement during starfish RNC wound healing events.

In the RG RNC DIGE gels, seven different protein spots, ranking from 94 to 11 kDa, were also identified with **spectrin** (6 spots) and **ankyrin** (1 spot), which seems to indicate that calpain mediated proteolysis is not only present in the initial WH stages, but it seems also to be critical for nerve re-growth. It is also possible that, the axon guidance function of spectrin may be attributed only to the fragments generated by the subsequent proteolytic events, since spectrin is ubiquitously distributed in cells and therefore might not always be exerting its function as a guidance molecule. Spectrin is also known to bind to the actin related protein subunit of the motor transport protein dynein (Holleran *et al.*, 2001). Hence, the on-going proteolytic events that persisted throughout RNC RG may be shaping the tracks of the vesicular transport within starfish nerve regeneration events. In fact, the supply and concentration of vesicles at restricted sites along the injured axon are known to be one of the critical steps

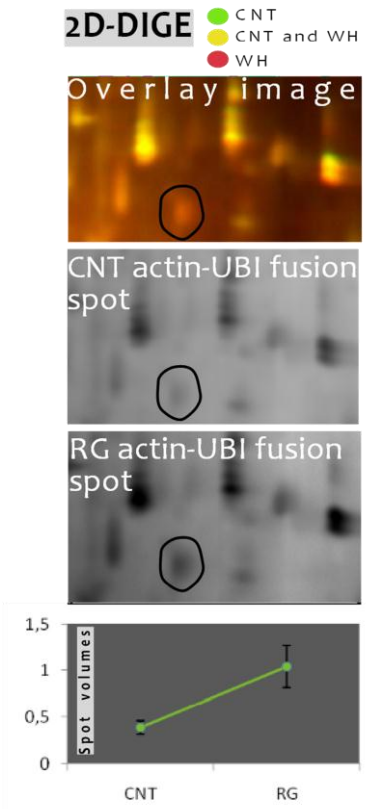

Figure 4.10: Actin-ubiquitin protein fusion showing a higher relative spot volume in the RG radial nerve cords when comparing with the correspondent controls.

which enable subsequent nerve fiber elongation after growth cone formation (Erez *et al.*, 2007).

Since at the RG stage the axonal membranes are properly sealed, the intracellular calcium levels are restored and thus, other pathways may be responsible for calpain activation and regulation during nerve elongation. This might involve other calcium regulating proteins or additional post-translational modifications. In fact, several proteins known to regulate intracellular levels of calcium were identified in RG RNC which include **V-type proton ATPase catalytic subunit A** (proteolysis substrate/down regulated and fragment), and several calcium binding proteins such as **calmodulin**.

4.4.2.3. Ubiquitin proteasome system (UPS) is actively involved in regulating protein levels throughout the radial nerve cord regeneration events

Another key intervenient in the proteolytic events necessary for cytoskeleton remodeling is the ubiquitin-proteasome system (UPS). The current hypothesis on the UPS role within regeneration events is related with the targeted degradation of cytoskeletal components and microtubule rearrangements (Lewcock *et al.*, 2007).

Several components of the UPS system were identified in the WH RNC: the **proteasome subunit alpha** (as a proteolysis substrate/down regulated or as a fragment) and **beta** (as up-regulated); three different spots were identified with **ubiquitin like molecules** and all up-regulated, which correlates with the recycling of ubiquitin via UPS; the **26S protease regulatory subunit** (which was identified with an increased mass and as a proteolysis substrate/down regulated); and a **ubiquitin specific peptidase 36** (proteolysis substrate/down regulated). The latter belongs to the large family of deubiquitinating proteases that in addition to ubiquitin recycling are involved in processing of ubiquitin precursors; proofreading of protein ubiquitination and in disassembly of inhibitory ubiquitin chains (Reyes *et al.*, 2009).

Additionally, both **actin** and **tubulin** were identified as proteolysis substrates or as fragments, most probably by the UPS proteolytic pathways.

Furthermore, several proteins were identified with apparent *M* above the expected along with the identification of the respective proteolytic fragments. This might indicate that these proteins are being conjugated with ubiquitin for targeted proteolysis by the proteasome system. Some examples occurring in WH RNC are: the **hypothetical protein BH2562**, and **Rho-type GTPase-activating protein 2**, all identified with an increase apparent *M* and as fragments.

Moreover, similarly to WH RNC, during RG events a multitude of spots were identified as being either actin or tubulin with considerable different *M*, decreased spot volumes in comparison with controls and also as fragments. For 23 protein spots, proteolytic fragments of an **ubiquitin/actin fusion protein** were identified (Figure 4.10); reinforcing the hypothesis that cytoskeleton degradation towards radial nerve cord re-growth is being regulated by several protein degradation pathways. This was further strengthened by the identification of an **ubiquitin-conjugating enzyme** (proteolysis fragment or down-regulated), which was not identified in WH RNC gels.

4.4.2.4. Metalloproteinases also contribute to the functional regeneration of starfish radial nerve cord

Matrix metalloproteinases (MMPs) are known to perform a crucial role in the degradation of extracellular matrix fibrillar proteins that accumulate soon after nervous system injury, thus creating a growth permissive environment. The involvement of MMPs driven proteolysis has been reported in embryogenesis and tissue regeneration throughout several animal clades. Echinoderms are no exception, since MMPs have been reported to be crucial in sea urchin embryogenesis (Wessel *et al.*, 1987) and during sea cucumber intestine regeneration (Quiñones *et al.*, 2002). Herein we also found several proteins homologous to known metalloproteinases, which seem to be involved in the regeneration events of starfish radial nerve cord. In all cases, MMPs were found to be associated to proteolytic events (identified as proteolysis substrates or as fragments) such as, the **O-sialoglycoprotein endopeptidase** identified in WH events and, the **cytosol aminopeptidase** identified in RG RNC. The MMPs identified in starfish RNC were found to be associated to proteolytic events. Since MMPs are synthesized with a signal peptide that is cleaved during the secretory pathway, this might justify a cleavage mediated-activation of these proteases during RNC regeneration events. Correspondingly, several fragments of MMPs known substrates were identified in the regenerating RNC such as, **lamin** in the WH events and a **protein homologous to fibronectin** in the RG RNC.

4.4.3. Vesicular transport

Small GTPases, besides being key effectors in the regulation of cytoskeleton and microtubule dynamics, are also known to be involved in the delivery of proteins and lipids to the axon, through the exocytic machinery (anterograde transport), as well as in the

internalization of membrane and proteins at the leading edge of the axon, by endocytosis (retrograde transport) (Hall *et al.*, 2010). Therefore, the previously mentioned GTPases, identified in WH and RG RNC gels can also be involved in axonal vesicular transport.

Other example of a vesicle-mediated transmembrane transport related protein is the **outer membrane protein**, identified in WH and RG RNC as being associated to proteolytic events.

Furthermore, the **synaptosomal-associated protein 25** (SNAP-25) was also identified with a decreased spot volume however, only in RG RNC. SNAP-25 is known to associate with proteins involved in vesicle docking and membrane fusion, also previously described to be regulated by proteolytic events (Glogowska *et al.*, 2008). SNAP-25 cleavage inhibits growth cone extension (Morihara *et al.*, 1999), and its mRNA has been reported to be enriched in embryonic axons (Gumy *et al.*, 2011). Other proteins involved in vesicle targeting and fusion were also identified namely, **lymphoid-restricted membrane protein**, identified as a fragment in both soluble and membrane fractions of RG RNC.

4.4.4. Other axon guidance and growth cone regulator proteins modulated by proteolysis

During re-growth of the axons post axotomy, the growth cone navigates a series of choice points to find the appropriate targets. These guidance decisions are shaped by a balance of attractive and repulsive cues found in the extracellular environment, that can act locally or at a distance (Tessier *et al.*, 1996). The question of how guidance receptors and their downstream effectors are targeted to, and distributed within functional domains of the growth cone plasma membrane, remains unanswered, even though it consists of an important key to understand the mechanisms of axon path finding.

Several proteins with known functions in axon guidance were identified and seem to maintain their function throughout both regeneration stages (WH and RG). This is the case for: the **leucine-rich repeat transmembrane neuronal protein 1**, which has been previously reported to participate in axon guidance by acting as midline repellent for commissural axons through the Robo (Roundabout) receptor (Battye *et al*., 1999; Brose *et al.*, 1999); and the **EF-hand domain-containing protein D2** (swiprosin-1), a protein that regulates the formation of neuron projection development.

In opposition, several proteins were only identified in one of the studied regeneration stages, highlighting a shift in the axon guidance molecules needed for RNC WH and RG events. This is the case for **dihydropyrimidinase** (increased mass and categorized as proteolysis substrate), which was identified in several different spots only in WH events, and is known to be involved in the semaphorins signaling pathway, necessary for cytoskeleton remodeling (Quinn *et al.*, 1999).

4.4.5. Protein synthesis machinery and RNA transport

Translation of mRNAs in injured axons provides a locally renewable source of proteins at sites that may be thousands of micrometers apart from the neuronal cell body, and hence, are essential for the rapid initiation of regenerative responses. For this reason it is not surprising to identify several ribosomal proteins in the WH RNC, namely **40S ribosomal protein S21** (up-regulated) and **30S ribosomal protein S21** (proteolytic fragment). In addition, the **elongation factor G 2** was also identified (proteolytic fragment) as well as the **ras homolog gene family, member A** and **Rho1 GTPase**, both regulators of translation, also identified as proteolysis substrates.

However, several ribosomal proteins were still altered (in terms of spot volume) in RG RNC namely, the **40S ribosomal protein S21** (up-regulated); **30S ribosomal protein S8**, **50S ribosomal protein and 54S ribosomal protein L4**, identified as proteolysis substrate or as fragments; and a protein similar to **eukaryotic translation initiation factor 5A**, identified as being up-regulated.

Several proteins that assist the folding process of *de novo* synthesized proteins were also identified in the WH RNC, namely, **calreticulin**. This protein interacts with nascent proteins in the endoplasmic reticulum along with protein **disulfide-isomerase A3** (Oliver *et al.*, 1999), which was also identified in WH RNC. Several other folding assistant proteins were identified namely, **chaperonin containing TCP1 subunit 5 (epsilon)**,

several **heat shock proteins**, **prefoldin subunit alpha**, **protein grpE** and **luminal binding protein**. All these folding assistants presented a decreased spot volume during WH due to down-regulation or proteolytic cleavage. The only up-regulated proteins with chaperone functions identified in the WH RNC were **von Hippel-Lindau binding protein 1-like** and a **putative FK506-binding protein**, the last being known to stabilize newly synthesized proteins by preventing its proteasomal degradation (Jascur *et al.*, 2005).

The number of proteins that act as folding assistants was substantially reduced in the RG RNC when compared with the WH events, being limited to the identification of a **chaperone protein htpG** (proteolysis substrate/down-regulated) and a **peptidyl-prolyl cis-trans isomerase** (up-regulated).

These observations further suggest that proteolysis might also control local protein *de novo* synthesis machinery in starfish radial nerve cord.

RNA localization is a highly regulated process that requires mechanisms for selecting which mRNAs to target for transport in distal neuronal processes. The mRNAs encoding axonally synthetized proteins must be delivered to the axonal compartment to enable local translational regulation, a strategy used by neurons to modulate protein levels in distal processes upon stimulus (reviewed in Yoo *et al.*, 2010 and Donnelly *et al.*, 2010). mRNAs to be transported are complexed with multiple proteins to form a ribonucleoprotein (RNP), that either engages with microtubule motor proteins for long range transport along the axon or, with microfilaments for short distances. However, knowledge of what RNPs are needed for localization, how their activity is regulated, and what sequence structures are recognized, is rather sparse. Several proteins that are involved in RNA modification and RNA binding were identified in WH RNC events such as, **tRNA pseudouridine synthase A** (up-regulated); **tRNA (guanine-N(1)-)-methyltransferase**, **RNA polymerase sigma factor sigI**, **RNA ligase**, **methionyl-tRNA synthetase**, identified as proteolysis substrates/down-regulated, and other cases like the **cysteinyl-tRNA synthetase** identified as proteolytic fragments. In the RG events also several proteins that are involved in RNA modification were identified, these include: the **nucleolar protein 58** (proteolysis substrates/down-regulated), a protein that is necessary for the formation of the large protein complexes that aggregate to RNA (RNP complexes) and enable its transport by engaging with motor proteins or microtubules; **polyribonucleotide nucleotidyltransferase**, involved in RNA degradation and identified as a fragment; **pre-mRNA cleavage factor** (proteolysis substrates/down-regulated); **pre-mRNA-processing ATP-dependent RNA helicase PRP5** (fragment); and **RNA binding motif** (proteolysis substrates/down-regulated) among others.

Once more, proteolysis seems to be having an important but yet, unknown role in RNA regulation during radial nerve cord regeneration events. Further studies in echinoderm species are needed to understand the dynamics of mRNA axonal transport during regeneration.

4.4.6. Kinases and transcription factors

Axonal injury induces local activation and retrograde transport of several mitogen-activated protein kinases (MAPK), including Erk (Perlson *et al.*, 2005) and the c-Jun N-terminal kinase (JNK) (Cavalli *et al.*, 2005). These activated kinases, in particular, JNK and Erk then interact with the motor proteins dynein/dynactin, engaging in the neuronal retrograde transport system back to the neuron body, where they exert their functions as injury signals. However the transport of such signals is a complex process since many of these kinases are activated by reversible phosphorylation, thus further protection against phosphatases is needed throughout the journey to the neuronal body. As previously stated, activated Erk interacts with the calpain proteolytic fragment of vimentin, which further protects it from dephosphorylation before reaching the cell body (Perlson *et al.*, 2006). **Cdc42** is one of the intervenients of the JNK cascade identified as being up-regulated in the WH RNC events. In addition, a fragment of a protein homologous to the dynein motor protein was also found in the WH RNC, the **axonemal 84 kDa protein**. Several other kinases without previous relation with regeneration processes were also identified, namely **two-component system sensor histidine kinase/response regulator hybrid**, **signal transduction histidine kinase** among others.

Similarly, a number of kinases were also identified in the RG RNC, *i.e.*, **cGMP-dependent protein kinase** (proteolysis substrates/down-regulated); **Rhs family protein** (proteolysis substrates/down-regulated) and **serine/threonine-protein kinase ATM** (proteolysis substrate/down-regulated), along with several others. Although the relation with proteolytic events is not clear, it can be a way to modulate these particular kinases and hence the correspondent downstream events.

Axonal injury also activates several transcription factors that are also translocated back to the nucleus (Abe, 2008). Several transcription factors were identified in the WH RNC, such as the **Cat eye syndrome critical region protein 2** (Cecr2) (proteolysis substrates/down-regulated), which is particularly interesting given its predominant expression in neural tissues during neurulation, as well as in the intermediate zone of the spinal cord, suggesting that it may play a role in neuronal development (Chen *et al.*, 2010). However, this study is the first to associate Cecr2 to neuronal regeneration events. Also in WH RNC the **transcriptional regulator LacI family**, **two component LuxR family transcriptional regulator, lin2 protein** (up-regulated and proteolysis substrates/down-regulated) and **nuclear transcription factor Y subunit B-2** were all identified with apparent masses above the expected suggesting possible post-translation modifications.

A number of transcription factors were also identified in the re-growing nerve, such as: the **LacI family transcription regulator** (proteolysis substrates/down-regulated), also identified in WH events, but with a *M* above the expected; the **regulatory protein Crp** (identified in 4 different 2DE spots both as proteolysis substrates/down-regulated and as a fragment); the **transcription factor Sox-12** (fragment), already described as being elevated in the DRG cell body after injury (Tanabe *et al.*, 2003) and also known to be involved in the *Wnt* signaling pathway, which also regulates axon path finding, axon remodeling, dendrite morphogenesis and synapse formation (Ciani *et al.*, 2005); and the **transcriptional activator Rgg/GadR/MutR** (proteolysis substrates).

4.4.7. Lipid signaling

The turnover of phosphoinositides is also implicated in neurite formation and extension (Arimura, 2007). Generation of phosphatidylinositol 4,5-bisphosphate (PI(4,5)P2)3 as well as phosphatidylinositol 3,4,5-trisphosphate seems to regulate neurite retraction in a growth factor-dependent manner, and several Rho family proteins are involved in the phosphoinositide signaling network in response to stimuli (Santarius *et al.*, 2006). Phospholipase C (PLC) is a key enzyme in phosphoinositide metabolism and is involved in the generation of two second messengers, namely diacylglycerol (DAG) and inositol 1,4,5-trisphosphate (IP3). Recently it was further shown that an isoform of PLC is an essential regulator of neuritogenesis, by suppression of the Rho signaling pathway via the down-regulation of RhoA level (Kouchi *et al.*, 2011). Both **phosphoinositide dependent kinase-1** and **inositol phosphosphingolipids phospholipase C** (proteolysis substrate/down-regulated) were found in WH RNC suggesting that proteolytic events might be a part of the described pathway regulation.

The phosphoinositide dependent kinase-1 is also involved in upstream activation of cap-dependent protein translation, by regulating the activity of ribosomal S6 kinase and eukaryotic initiation factor 4E binding protein (reviewed in Liu *et al.*, 2011). A similar initiation factor, the **eukaryotic translation initiation factor 5A-1**, was found to be up-regulated in WH RNC events.

Several fragments from a **START domain-containing protein**, a protein similar to a phosphatidylcholine transfer protein, were also identified in both regeneration stages of *Marthasterias glacialis* RNC (WH and RG). This START protein is known to be ubiquitously distributed during neuronal development of the starfish larvae *Asterina pectinifera* (Murabe *et al.*, 2008). Although its function seems to be related with phosphatidylcholine transfer through the identification of conserved domains, its relation with regeneration remains unknown, being possibly related with the supply of lipids for the new axoplasmic membranes. Clearly it is regulated through proteolysis, and most probably via UPS, since it was identified in both WH and

RG RNC with an apparent *M* above the expected and as proteolysis substrate/down-regulated.

4.4.8. Neuroprotective proteins

During the regeneration events, it is critical that molecules with protective functions are present, which was shown to be the case in regenerating RNC. Several antioxidant proteins were up-regulated in the WH and RG events namely, **ferritin**, a protein that has been described as an important molecule to control the levels of oxygen reactive species in astrocytes (Regan *et al.*, 2002); and **peroxiredoxin** like proteins, which were previously reported to be oxidized in the mouse model of axonal degeneration, indicating that axonal integrity is related to the control of oxidative stress (Mi *et al.*, 2005).

Several proteins responsible for controlling the cellular oxidation state, managing of reactive oxygen species among other functions, were identified only in RG events, such as **dihydropteridine reductase** and **lysozyme C**, both being up-regulated. The up-regulation of lysozyme has been previously reported in distal stumps of post-injured sciatic nerve (Kubo *et al.*, 2002). Other proteins with similar functions were found also to be modulated by proteolytic events such as, **cytochrome P450 19A1**; **glutathione peroxidase**; **glutathione *S*-transferase 3**; **oxidoreductase, short chain dehydrogenase/reductase family** and **peroxidase** among others.

4.5. CONCLUDING REMARKS

Neuronal regeneration results from a balance between protein *de novo* synthesis and protein catabolic pathways, however the last has received considerable less attention (Gumy *et al.*, 2010).

The use of *in vitro* neuronal models already allowed an exceptional understanding of the proteolytic pathways within neuronal regeneration events; however, this knowledge is deprived of the complexity of a natural biological system. To understand the vast number of protein substrates and the proteolytic impacts on whole neuronal tissue proteomes during regenerative events, these problems need to be addressed *in vivo*. The use of *in vivo* model systems has already been recognized as the way to further elucidate the effects of this post-translational regulatory mechanism, which will be determinant to decipher the signaling pathways regulated through proteolytic events (Page-McCaw *et al.*, 2007). However, such studies are not yet available, specially using the non-bias set of proteomic/mass spectrometry experimental approaches. These last have already been recognized as powerful tools to study proteolytic events on whole tissues (Doucett *et al.*, 2009), as demonstrated the recently published degradome of blood and plasma coagulation reactions (Niessen, 2011).

In the current study we examine the differential proteomes of two different stages of echinoderm radial nerve cord regeneration: wound healing (48h-13 days *PAA*) and tissue re-growth (10 weeks *PAA*), aiming to understand which are the activated molecular pathways in each stage and how they are modulated.

Several proteins with previously described functions in nerve regeneration events were identified in this proteomic study. However, the majority of them seem to be modulated through proteolytic events. For this reason, a greater emphasis is given to the proteolytic pathways, since clearly they play a major role in modulating and controlling starfish radial nerve cord proteomes during regeneration events. Furthermore, the observed abundance of protein fragments may be an indication of their role as necessary signaling molecules, which will modulate the regenerative pathways leading to the starfish successful nervous system regeneration.

Altogether, the results here presented, highlight echinoderms as important neuroregeneration models, which should be further explored since ***1)*** several of the identified proteins have a recognized role in regeneration in other model organisms, thus reinforcing its potential to aid our understanding of the phenomenon; ***2)*** many of the regeneration-related identified proteins constitute new assignments that should be further validated and tested for potential applications in vertebrate regeneration and ***3)*** new insights into proteolytic-driven regulation of neuronal regeneration are given, emphasizing the importance of investing in metadegradomics studies.

4.6. ACKNOWLEDGMENTS

This work was supported by Fundação para a Ciência e Tecnologia through a PhD grant to Catarina Franco (SFRH/BD/29799/2006), a research contract by the Ciência 2008 program to Romana Santos and a project grant (PTDC/MAR/104058/2008).

4.7. REFERENCES

Abe, N., Cavalli, V. (2008) Nerve injury signaling. Curr Opoin Neurobiol. 18, 276-283.

Agrawal, V., Johnson, S.A., Reing, J., Zhang, L., Tottey, S., Wang, G., Hirschi, K.K., Braunhut, S., Gudas, L. J., Badylak, S.F. (2010) Epimorphic regeneration approach to tissue replacement in adult mammals. PNAS. 107(8), 3351-3355.

Alvarado, A.S., Tsonis, P. A. (2006) Bridging the regeneration gap: genetic insights from diverse animal models. Nature reviews genetics. 7, 873-884.

Ambron, R.T., Walters, E.T. (1996) Priming events and retrograde injury signals. Mol Neurobiol. 13, 61-79.

Andersen, S. S. L. (2004). The search and prime hypothesis for growth cone turning. BioEssays 27, 86-90.

Arimura, N. and Kaibuchi, K. (2007) Neuronal polarity: from extracellular signals to intracellular mechanism. Nat Rev Neurosci. 8, 194-205.

Autieri, M.V., Kelemen, S.E., Wendt, K.W. (2003) AIF-1 is an actin-polymerizing and Rac1-activating protein that promotes vascular smooth muscle cell migration. Circ. Res. 92(10), 1107-1114.

Battye, R., Stevens, A., Jacobs, J.R. (1999) Axon repulsion from the midline of the Drosophila CNS requires slit function. Development. 126,2475–2481.

Bennett, V., Baines, A.J. (2001) Spectrin and Ankyrin-Based Pathways: Metazoan Inventions for Integrating Cells Into Tissues. Phyological reviews. 81, 1353-1392.

Brose, K., Bland, K.S., Wang, K.H., Arnott, D., Henzel, W., Goodman, C.S., Tessier-Lavigne, M., Kidd, T. (1999) Slit proteins bind Robo receptors and have an evolutionarily conserved role in repulsive axon guidance. Cell. 96, 795-806.

Butt, R. H.; Coorssen, J. R. Pre-extraction Sample Handling by Automated Frozen Disruption Significantly Improves Subsequent Proteomic Analyses. J Proteome Res. 2006, 5, 437-448.

Cavalli, V., Kujala, P., Klumperman, J., Goldstein, L.S. Sunday driver links axonal transport to damage signaling. J Cell Biol. 168, 775-787.

Chakraborty, G., Leach, T., Zanakis., M.F., Sturman, A., Ingoglia, N.A. (2006). Post-translational Protein Modification by Polyamines in Intact and Regenerating Nerves. Journal of Neurochemistry. 48, 669-675.

Chen, J., Morosan-Puopolo, G., Dai, F., Wang, J., Brand-Saberi, B. (2010) Molecular cloning of chicken Cecr2 and its expression during chicken embryo development. Int J Dev Biol. 54(5), 925-929.

Ciani, L., Salinas, P.C. (2005) WNTS in the vertebrate nervous system: from patterning to neuronal connectivity. Nature Reviews Neuroscience. 6, 351-362.

Consortium, Sea Urchin Sequencing. The genome of the sea urchin *Strongylocentrutus purpuratus*. Science. 2006, 10, 941-952.

Dheilly, N. M., Haynes, P.A., Bove, U., Nair, S.V., Raftos, D.A. Comparative proteomic analysis of a sea urchin (*Heliocidaris erythrogramma*) antibacterial response revealed the involvement of apextrin and calreticulin. Journal of Invertebrate Pathology. 2011, 106, 223-229.

Domselaar, R.V., AH de Poot, S., Bovenschen, N. (2010) Proteomic profiling of proteases: tools for granzyme proteomics. Expert Reviews Proteomics. 7(3), 347-359.

Donnelly, C.J., Fainzilber, M., Twiss, J.L. (2010) Subcellular communication through RNA transport and localized protein synthesis. Traffic. 11, 1498-1505.

Doucett, A., Butler, G.S., Rodrígez, D., Prudova, A., Overall, C.M. (2008) Metadegradomics. Molecular and cellular proteomics. 7, 1925-1951.

Erez, H., Malkinson, G., Prager-Khoutorsky, M., Zeeuw, C., Hoogenraad, C.C., Spira, M.E. (2007) Formation of microtubule-based traps controls the sorting and concentration of vesicles to restricted sites of regenerating neurons after axotomy. The Journal of Cell Biology. 176 (4), 497-507.

Franco, C., Santos, R., Coelho V. (2011A) Exploring the proteome of an echinoderm nervous system: 2-DE of the sea star radial nerve cord and the synaptosomal membranes subproteome. Proteomics. 11, 1359–1364.

Franco, C., Santos, R., Coelho V. (2011B) Proteome characterization of sea star coelomocytes - the innate immune effector cells of echinoderms. 11(17), 3587-3592.

Franco, M., Seyfried, N.T., Brand, A.H., Peng, J., Mayor, U. (2010) A novel strategy to isolate ubiquitin conjugates reveals wide role of ubiquitination during neural development. Molecular and cellular proteomics, 10, M110.002188.

Garbe, D.S., Das, A., Dubreuil, R.R., Bashaw, G.J. (2007) β-Spectrin functions independently of Ankyrin to regulate the establishment and maintenance of axon connections in the Drosophila embryonic CNS. Development. 134, 273-284.

Garvalov, B.K., Flynn, K.C., Neukirchen, D., Meyn, L., Teusch, N., Wu, X., Brakebusch, C., Bamburg, J.R., Bradke, F. (2007) Cdc42 regulates cofilin during the establishment of neural polarity. J Neurosci. 27, 13117-13129.

Gilter, D., Spira, M.E. (1998) Real time imaging of calcium-induced localized proteolytic activity after axotomy and its relation to growth cone formation. Neuron. 20, 1123-1135.

Giniger, E. (2002) How do Rho family GTPases direct axon growth and guidance? A proposal relating signalling pathways to growth cone mechanics. Differentiation 70, 385-396.

Glickman, M., Ciechanover, A. (2002) The ubiquitin-proteasome proteolytic pathway: destruction for the sake of construction. Physiol Rev. 82, 373-428.

Glogowska, A., Pyka, J., Kehlen, A., Los M., Perumal, P., Weber, E., Cheng, S.Y., Hoang-Vu, C., Klonisch, T. (2008) The cytoplasmic domain of proEGF negatively regulates motility and elastinolytic activity in thyroid carcinoma cells. Neoplasia. 10(10), 1120-1130.

Goll, D.E., Thompson, V.F., Li, H., Wei, W., Cong, J. (2003) The Calpain system. Physiol Rev. 83, 731-801.

Gross, J., Lapiere, C.M. (1962) Collagenolytic activity in amphibian tissues: a tissue culture assay. Proc Natl Acd Sci. 47, 1014-1022.

Gumy, L.F., Tan, C.L., Fawcett, J.W. (2010) The role of local protein synthesis and degradation in axon regeneration. Exp Neurol. 223, 28-37.

Gumy, L.F., Yeo, G.S.H, Tung, Y.C.L., Zivraj, K.H., Willis, D., Coppola, G., Lam, B.Y.H., Twiss, J.L., Holt, C.E., Fawcett, J.W. (2011) Trancriptome analysis of embryonic and adult sensory axons reveals changes in mRNA repertoire localization. RNA. 17, 85-98.

Gutierrez-Fernandez, A., Fueyo, A., Folgueras, A.R., Garabaya, C., Pennington, C.J., Pilgrim , S., Edwards, D.R., Holliday, D.L., Jones, J.L., Span, P.N., Sweep, F.C., Puente, X.S., López—Otín, C. (2008) Matrix metalloproteinases-8 functions as a metastasis suppressor through modulation of tumor cell adhesion and invasion. Caner Res. 68, 2755-2763.

Hall, A., Lalli, G. (2010) Rho and Ras GTPases in axon growth, guidance, and branching. Cold Spring Harbor perspectives in biology. 2:a001818.

Hegde, A.N. (2010) Proteolysis and Synaptic plasticity. In J. David Sweatt (Ed.), Molecular Mechanisms of memory. Vol 4 of Learning and Memory: A comprehensive reference, 4 vols. (J. Byrne Editor), 525-546.

Hellal, F., Hurtado, A., Ruschel, J., Flynn, K.C., Laskowski, C.J., Umlauf, M., Kapitein, L.C., Strikis, D., Lemmon, V., Bixby, J., Hoogenraad, C.C., Bradke, F. (2011) Microtubule stabilization reduces scarring and causes axon regeneration after spinal cord injury. Science. 331, 928-931.

Hernroth, B., Farahani, F., Brunborg, G., Dupont, S., Gejmek, A., Sköld, H.N. (2010) Possibility of mixed progenitor in sea star arm regeneration. Journal of Experimental Zoology Part B – Molecular and Developmental Evolution. 314B, 1-12.

Holleran, E.A., Ligon, L.A., Tokito, M., Stankewich, M.C., Morrow, J.S., Holzbaur, E.L. (2001) Beta III spectrin binds to the Arp1 subunit of dynactin. J Biol Chem. 276(39), 36598-36605.

Hur, E.M., Yang, I.H., Kim, D.H., Byun, J., Saijilafu, Xu, W.L., Nicovich, P.R., Cheong, R., Levchenko, A., Thakor, N., Zhou, F.Q. (2011) Engineering neuronal growth cones to promote axon regeneration over inhibitory molecules. PNAS. 108 (22), 5057-5062.

Jascur, T., Brickner, H., Salles-Passador, I., Barbier, V., El Khissiin, A., Smith, B., Fotedar, R., Fotedar, A. (2005) Regulation of p21(WAF1/CIP1) stability by WISp39, a Hsp90 binding TPR protein. Mol Cell. 17(2), 237-249.

Jiménez, C.R., Stam, F.J., Li, K.W., Gouwenberg, Y., Hornshaw, M.P., De Winter, F., Verhaagen, J., Smit, A.B. (2005) Proteomics of the injured rat sciatic nerve reveals protein expression dynamics during regeneration. Molecular and cellular proteomics. 4, 120-132.

Klimaschewski, L. (2007) Ubiquitination and Proteasomal Protein Degradation in Neurons. In: Handbook of Neurochemistry and Molecular Neurobiology. Eds. Lajtha, A., Banik, N. Springer, US. 653-662.

Kouchi, Z., Igarashi, T., Shibayama, N., Inanobe, S., Sakurai, K., Yamaguchi, H., Fukuda, T., Yanagi, S., Nakamura, Y., Fukami, K. (2011) Phopholipase Cδ3 regulates RhoA/Rho Kinase Signaling and neurite outgrowth. Journal of Biological Chemistry, 286, 8459-8471.

Kozma, R., Sarner, S., Ahmed, S. and Lim, L. (1997) Rho family GTPases and neuronal growth cone remodelling, relationship between increased complexity induced by Cdc42Hs, Rac1, and acetylcholine and collapse induced by RhoA and lysophosphatidic acid. Mol. Cell. Biol. 17, 1201-1211.

Kubo, T., Yamashita, T., Yamaguchi A., Hosokawa, K., Tohyama, M. (2002) Analysis of genes induced in peripheral nerve after axotomy using cDNA microarrays. Journal of neurochemistry. 82, 1129-1136.

Lee, R., Kermani, P., Teng, K.K., Hempstead, B.L. (2001) Regulation of cell survival by secreted proneurotrophins. Science. 294, 1945-1948.

Lewcock, J.W., Genoud, N., Lettieri, K., Pfaff, S.L. (2007) The ubiquitin ligase Phr1 regulates axon outgrowth through modulation of microtubule dynamics. Neuron. 56, 604-620.

Lietzén. N., Natri, L., Nevalainen, O., Salmi, J., Nyman, T.A. (2010) Compid: A new software tool to integrate and compare MS/MS based protein identification results from MASCOT and Paragon. Journal of Proteome Research. 9, 6795-6800.

Liu, K., Tedeschi, A., Kyungsuk, P., He, Z. (2011) Neuronal intrinsic mechanisms of axon regeneration. Ann Rev Neurosci. 34, 129-150.

Liu, R.Y., Snider, W.D. (2001) Different signalling pathways mediate regenerative versus developmental sensory axon growth. Journal Neuroscience Res. 68, 1-6.

Llorens, F., Gil, V., del Río, J.A. (2011) Emerging functions of myelin-associated protein during development, neuronal plasticity, and neurodegeneration. The FASEB journal. 25, 463-475.

Lowery, L.A., Vactor, D.V. (2009) The trip of the tip: understanding the growth cone machienery. Nature reviews Molecular Cell Biology. 10, 332-343.

Mandic, A., Viktorsson, K., Strandberg, L., Heiden, T., Hansson, J., Linder, S., Shoshan, M.C. (2002) Calpain-mediated Bid cleavage and calpain-independent Bak modulation: two separate pathways in cisplatin-induced apoptosis. Mol Cell Biol. 22, 3003-3013.

Mann, K., Poutka, A. J.; Mann, M. The sea urchin (*Strongylocentrotus purpuratus*) test and spine proteomes. Proteome Science. 2008, 6, epub.

Mannello, F., Tonti, G., Papa, S. (2005) Are matrix metalloproteinases the missing link? Invertebrate Survival Journal. 2(1), 69-74.

Martin, S., Wilkinson, K.A., Nishimune, A., Henley, J.M. (2007) Emerging extranuclear roles of protein SUMOylation in neuronal function and dysfunction. Nature Neuroscience Reviews. 8, 948, 959.

Mashanov, V.S., Zueva, O.R., Heinzeller, T. (2008) Regeneration of the radial nerve cord in a holothurians: a promising new model for studying post-traumatic recovery in the adult nervous system. Tissue and Cell. 40, 351-372.

McCallum, S.J., Wu, W.J., Cerione, R.A. (1996) Identification of a putative effector for Cdc42Hs with high sequence similarity to the RasGAP-related protein IQGAP1 and a Cdc42Hs binding partner with similarity to IQGAP2. J Biol Chem. 271(36), 21732-21737.

Mi, W., Beirowski, B., Gillingwater, T.H., Adalbert, R., Wagner, D., Grumme, D., Osaka, H., Conforti, L., Arnhold, S., Addicks, K., Wada, K., Ribchester, R.R., Coleman, M.P. (2005) The slow Wallerian degeneration gene, WldS, inhibits axonal spheroid pathology in gracile axonal dystrophy mice. Brain. 128, 405-416.

Miguel-Ruiz, J.S., Maldonado-Soto, A.R., García-Arrarás, J.E. (2009) Regeneration of the radial nerve cord in the sea cucumber *Holothuria glaberrima*. BMC Dev Biol.9: 3.

Mohien, C.U., Hartler, J., Breitwieser, F., Rix, U., Rix, L.R., Winter, G.E., Bennet, K.L., Superti-Furga, G., Trajanoski, Z., Colinge, J. (2010) MASPECTRAS2: and integration and analysis platform for proteomic data. Proteomics. 10, 2719-2722.

Morihara, T., Mizoguchi, A., Takahashi, M., Kozaki, S., Tsujihara, T., Kawano, S., Shirasu, M., Ohmukai, T., Kitada, M., Kimura, K., Okajima, S., Tamai, K., Hirasawa, Y., Ide, C. (1999) Distribution of synaptosomal-associated protein 25 in nerve growth cones and reduction of neurite outgrowth by botulinum neurotoxin A without altering growth cone morphology in dorsal root ganglion neurons and PC-12 cells. Neuroscience. 91(2), 695-706.

Murabe, N., Hatoyama, H., Hase, S., Komatsu, M., Burke, R., Kaneko, H., Nakajima, Y. (2008) Neural architecture of the Brachiolaria larva of the starfish, *Asterina pectinifera*. The journal of comparative neurology. 509, 271-282.

Nakagawa, T., Yuan, J. (2000) Cross-talk between two cysteine protease families. Activation of caspase-12 by calpain in apoptosis. J. Cell Biol. 150, 887-894.

Neuhoff, V., Harold, N., Ehrhardt, W. Improved staining of proteins in polyacrylamide gels including isoelectric focusing gels with clear background at nanogram sensitivity using Coomassie Brilliant Blue G-250 and R-250. Electrophoresis. 1988, 9, 255-262.

Niekerk, E.A., Willis, D.E., Chang, J.H., Reumann, K., Heise, T., Twiss, J.L. (2007) Sumoylation in axons triggers retrograde transport of the RNA-binding protein La. PNAS. 104(31), 12913-12918.

Niessen, S., Hoover, H., Gale, A.J. (2011) Proteomic analysis of the coagulation reaction in plasma and whole blood using PROTOMAP. Proteomics. 11, 2377-2388.

Nobes, C.D., Hall, A. (1995) Rho, Rac and Cdc42 GTPases regulate the assembly of multi-molecular focal complexes associated with actin stress fibbers, lamellipodia and filopodia. Cell. 81, 53-62.

Oliver, J.D., Roderick, H.L., Llewellyn, D.H., High, S. (1999) ERp57 functions as a subunit of specific complexes formed with the ER lectins calreticulin and calnexin. Mol. Biol. Cell. 10(8),2573-2582.

Orrenius, S., Zhivotovky, B., Nicotera, P. (2003) Regulation of cell death: the calcium-apoptosis link. Nature Reviews. 4, 552-565.

Otsuka, A.J., Boontrakulpoontawee, P., Rebeiz, N., Domanus, M., Otsuka, D., Velamparampil, N., Chan, S., Wyngaerde, M.V, Campagna, Cox, A.S. (2002) Novel UNC-44 AO13 Ankyrin Is Required for Axonal Guidance in C. elegans, Contains Six Highly Repetitive STEP Blocks Separated by Seven Potential Transmembrane Domains, and Is Localized to Neuronal Processes and the Periphery of Neural Cell Bodies. J Neurobiol. 50, 333-349.

Page-McGaw, A., Ewald, A.J., Werb, Z. (2007) Matrix metalloproteinases and the regulation of tissueremodelling. Nat. Rev. Mol. Cell. Biol. 8(3), 221-233.

Perlson, E., Hanz, S., Ben-Yaakov, B., Segal-Ruder, Y., Seger, R., Fainziber, M. (2005) Vimentin-dependent special translocation of an activated MAP kinase in inured nerve. Neuron. 34, 715-726.

Perlson, E., Hanz, S., Medzihradszky, K.F., Burlingame, A.L., Fainzilber, M. (2003) From Snails to Sciatic Nerve: Retrograde Injury Signaling from Axon to Soma in Lesioned Neurons. Inc. J Neurobiol. 58: 287–294.

Perlson, E., Medzihradszky, K.F., Darula, Z., Munno, D.W., Syed, N.I., Burlingame, A.L., Fainzilber, M. (2004) Differential Proteomics Reveals Multiple Components in Retrogradely Transported Axoplasm After Nerve Injury. Molecular and cellular proteomics. 3, 510-520.

Perlson, E., Michaelevski, I., Kowalsman, N., Ben-Yaakov, K., Shaked, M., Seger, R., Eisenstein, M., Fainzilber, M. (2006) Vimentin binding to phophorylated Erk sterically hinders enzymatic dephosphorylation of the kinase. J. Mol. Biol. 364, 938-944.

Pizzi, M.A., Crowe, M.J. (2007) Matrix metalloproteinases and proteoglycans in axonal regeneration. Experimental neurology. 204, 496-511.

Puente, X.S., Sanchez, L.M., Overall, C.M., Lopez-Otin, C. (2003) Human and mouse proteases: a comparative genomic approach. Nat. Rev. Genet. 4, 544-558.

Quinn, C.C., Gray, G.E., Hockfield, S. (1999) A family of proteins implicated in axon guidance and outgrowth. J. Neurobiol. 41, 158-164.

Quiñones, J.L., Rosa, R., Ruiz, D.L., Garcia-Arrarás, J.E. (2002) Extracellular matrix remodeling and metalloproteinase involvment during intestine regeneration in the sea urchin cucumber *Holothuria glaberrima*. Developmental Biology. 250, 181-197.

Rajnicek, A.M., Foubister, L.E., McCaig, C.D. (2006) Growth cone steering by a physiological electric field requires dynamic microtubules, microfilaments and Rac-mediated filopodial asymmetry. J Cell Sci 119, 1736-1745.

Regan, R.F., Kumar, N., Gao, F., Guo, Y. (2002) Ferritin induction protects cortical astrocytes from heme-mediated oxidative injury. Neuroscience 113 (4), 985-994.

Reyes Turcu, F.E., Ventii, K.H., Wilkinson, K.D. (2009) Activity and Cellular Roles of Ubiquitin-Specific Deubiquitinating Enzymes. Annual Review of Biochemistry. 78, 363-397.

Santarius, M., Lee, C. H., and Anderson, R. A. (2006) Supervised membrane swimming: small G-protein lifeguards regulate PIPK signalling and monitor intracellular PtdIns(4,5)P2 pools. Biochem. J. 398, 1–13.

Sarig-Nadir, O., Seliktar, D. (2010) The role of matrix metalloproteinases in regulating neuronal and nonneuronal cell invasion into PEGylated fibrinogen hydrogels. Biomaterials. 31, 6411-6416.

Savedia, S., Kierman, J.A. (1994) Increased production of ubiquitin mRNA in motor neurons after axotomy. Neuropathol Appl Neurobiol. 20, 577-586.

Schwab, M.E. (2004) Nogo and axon regeneration. Curr Opin Neurobiol. 14, 118-124.

Sewell, M. A., Eriksen, S.; Middleditch, M. J. Identification of protein components from the mature ovary of the sea urchin *Evechinus chloroticus* (Echinodermata: Echinoidea). Proteomics. 2008, 8, 2531-2542.

Shapiro, S.D. (1998) Matrix metalloproteinase degradation of extracellular matrix: biological consequences. Curr Opin Cell B. 10, 602-608.

Silver, J., Miller, J.H. (2004) Regeneration beyond the glial scar. Nature reviews. 5, 146-156.

Spira, M.E., Oren, R., Dormann, A., Ilouz N., Lev, S. (2001) Calcium, protease activation, and cytoskeleton remodeling underlie growth cone formation and neuronal regeneration. Cell Mol Neurobiol. 21, 591-604.

Stiess, M., Bradke, F. (2011) Neuronal polarization: The cytoskeleton leads the way. Developmental Neurobiology. 71, 430-444.

Streuli, C. (1999) Extracellular matrix remodeling and cellular differentiation. Curr Opin Cell Biol. 11, 634-640.

Sun, F., Cavalli, V. (2009) Neuroproteomics approaches to decipher neuronal regeneration and degeneration. Molecular and cellular proteomics. 9, 963-975.

Takenawa, T., Miki, H. (2001) WASP and WAVE family proteins: key molecules for rapid rearrangement of cortical actin filaments and cell movement. J Cell Sci. 114, 1801–1809.

Tanabe, K., Bonilla, I., Winkles, J.A., Strittmatter, S.M. (2003) Fibroblast growth factor-inducible-14 is induced in axoto mized neurons and promotes neurite outgrowth. J. Neurosc. 23, 9675-9686.

Tang, B.L. (2003) Inhibitors of neuronal regeneration: mediators and signaling mechanisms. Neurochem. Int. 42(3), 189-203.

Tessier-Lavigne, M., Goodman, C. S. (1996). The molecular biology of axon guidance. Science 274, 1123-1133.

Tursun, B., Schluter, A., Peters, M.A., Viehweger, B., Ostendorff, H.P., Soosairajah, J., Drung, A., Bossenz, M., Johnsen, S.A., Schweizer, M., Bernard, O., Bach, I. (2005) The ubiquitin ligase Rnf6 regulates local LIM kinase 1 levels in axonal growth cones. Genes Dev. 19, 2307-2319.

Verma, P., Chierzi, S., Codd, A.M., Campbell, D.S., Meyer, R.L., Holt, C.E., Fawcett, J.W. (2005) Axonal protein synthesis and degradation necessary for efficient growth cone regeneration. J. Neurosci. 25, 331-342.

Wang H.R., Zhang Y., Ozdamar B., Ogunjimi, A.A., Alexandrova E., Thomsen G. H., Wrana J.L. (2003) Regulation of Cell Polarity and Protrusion Formation by Targeting RhoA for Degradation. Science. 302, 1775-1779.

Wessel, G.M., McClay, D.R. (1987) Gastrulation in the sea urchin embryo requires the deposition of crosslinked collagen within the extracellular matrix. Dev. Biol. 121, 149-165.

Willis, D., Li, K.W., Zheng, J.Q., Chang, J.H., Smit, A., Kelly, T., Merianda, T., Sylvester, J., Minnen, J.V., Twiss, J.L. Differential transport and local translation of cytoskeletal, injury-response, and neudegeneration proteins mRNAs in axons. The Journal of Neuroscience. 26, 778-791.

Wood, D.E., Newcomb, E.W. (1999) Caspase-dependent activation of calpain during drug induced apoptosis. J. Chem. Biol. 274, 8309-8315.

Yiu, G., He, Z. (2006) Glial inhibition of CNS axon regeneration. Nature reviews-Neuroscience. 7, 617-627.

Yoo, S., Niekerk, E.A., Merianda, T.T., Twiss, J.L. (2010) Dynamics of axonal mRNA transport and implications for peripheral nerve regeneration. Experimental Neurol. 223, 19-27.

You-Seung Kim, Y., Furman, S., Sink, H., VanBerkum, M.F.A. (2001) Calmodulin and profilin coregulate axon outgrowth in Drosophila. Develop Neurobiol. 47, 26-38.

CHAPTER 5

PRELIMINARY VIEW OF PROTEIN PHOSPHORYLATION DYNAMICS IN STARFISH RADIAL NERVE CORD WOUND HEALING EVENTS

CATARINA FERRAZ FRANCO[1], RENATA SOARES[1], ELISABETE PIRES[1], ROMANA SANTOS[1,2], ANA VARELA COELHO[1]

1: Instituto de Tecnologia Química e Biológica, Universidade Nova de Lisboa, Oeiras, Portugal;

2: Unidade de Investigação em Ciências Orais e Biomédicas, Faculdade de Medicina Dentária, Universidade de Lisboa, Portugal.

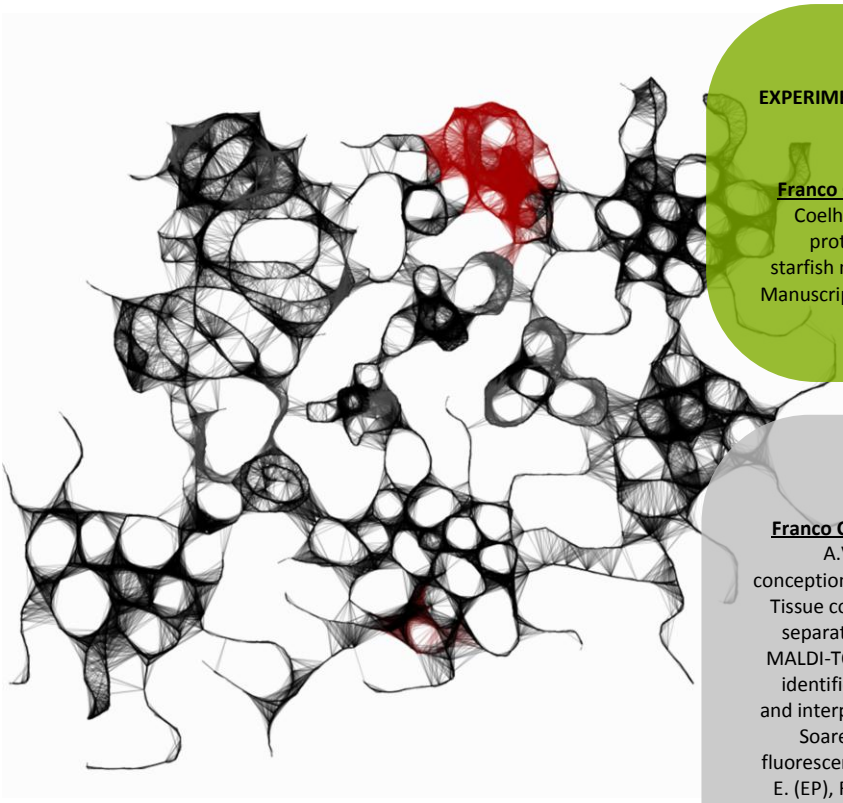

Image: "It starts with a signal".

PUBLICATIONS CONTAINING EXPERIMENTAL DATA PRESENTED IN THIS CHAPTER

Franco C., Soares, R., Pires, E., Santos R., Coelho A.V. (2011) Preliminary view of protein phosphorylation dynamics in starfish nerve cord wound healing events Manuscript drafted. Journal to be defined.

AUTHORS CONTRIBUTION

Franco C. (CF), Santos R. (RS) and Coelho A.V (AVC) were responsible for the conception and design of the experiments. Tissue collection, optimization of protein separation protocols, 2DE experiments, MALDI-TOF/TOF data acquisition, protein identification, annotation, data analysis and interpretation were performed by **CF**. Soares, R (ReS) and CF performed the fluorescent gel staining procedures. Pires, E. (EP), ReS and CF applied samples onto MALDI plate.

CF drafted the manuscript and RS, ReS and AVC revised them critically.

CHAPTER 5

PRELIMINARY VIEW OF PROTEIN PHOSPHORYLATION DYNAMICS IN STARFISH RADIAL NERVE CORD WOUND HEALING EVENTS

Supplementary material containing experimental data described in this chapter*

Supplementary table 5.1: Excel file containing 4 spreadsheets. ***Sheet 1*** displays an annotated 2DE image of the identified spots. ***Sheet 2*** contains a list of all the peptides identified per 2DE spot; the correspondent inferred proteins and also a list of all the predicted phosphopeptides according to the experimental intact peptide masses. In ***Sheet 3*** it is presented the **relative phosphorylation ratios** of the Pro-Q Diamond spots and also the correspondent GO annotation of the identified proteins. ***Sheet 4***, contains a non-redundant protein list and also *BLASTp* results for the uncharacterized proteins identified. Also, the phosphorylation prediction and its role in regulating protein function is described according to the literature.

* Please see enclosed CD to access the supplementary material

SUMMARY| RADIAL NERVE CORD PROTEIN PHOSPHORYLATION DYNAMICS DURING STARFISH ARM TIP WOUND HEALING EVENTS

Echinoderms, as invertebrate deuterostomes, have an amazing neuronal intrinsic growth capability, which can be triggered at any time point during the animal lifespan, leading to a successful functional tissue re-growth. This trait is well known to be in opposition to their mammal close phylogenic relatives, which have completely lost their ability to regenerate their central nervous system. Although this intrinsic echinoderm trait is of a promising nature, only recently this complex jigsaw has started to be assembled. In this study, we used a 2DE gel based phosphoproteomics approach to investigate injury related changes in the phosphorylation of proteins from a soluble fraction of the injured starfish radial nerve cord collected 48h and 13 days following arm tip ablation. Over 500 spots were resolved in 3.0-5.6 *NL* pH strips of which 190 and approximately 140 spots had a phosphoprotein signal in the control and injury experimental groups, respectively. A total of 47 different proteins were identified with MALDI-TOF/TOF, many presenting an injury correlated phosphorylation dynamics. Altogether, several intervenients of important injury signaling pathways, which seem to be modulated through phosphorylation, were identified for the first time during starfish radial nerve cord early regeneration events. These include cytoskeleton re-organization towards the formation of the neuronal growth cones; membrane rearrangements, actin filaments and microtubules dynamics; mRNA binding and transport; lipid signaling; Notch pathway; and neuropeptide processing.

5.1. INTRODUCTION

Neuronal functional regeneration is highly dependent on the ability of injured neurons to interpret and rapidly respond to several environmental cues, in order to elicit the proper neurite[7] outgrowth intrinsic mechanisms (Benowitz *et al.*, 2007; Rossi *et al.*, 2007). Depending on the type of neuron or on the organism species, the axon length can be extended up to several times the size of the neuronal soma. For this reason, it is not surprising that the initial stage of the injury mediated response is intimately related with the modification or activation of proteins at the injury site. These will then travel back to nucleus to promote further changes in the transcription and translation patterns (positive injury signals) or, will commence the proper activity modulation towards the necessary re-organization of the wounded area (Ambron *et al.*, 1996). Indeed, the current understanding of axonal regeneration events emphasizes the role of proteolysis (Gumy *et al.*, 2010), local axonal protein synthesis (Willis *et al.*, 2005) and a broad range of post-translational modifications (Nierkerk *et al.*, 2007; Hong *et al.*, 2009). Axonal local activation and transport of several kinases is now known to play a very important role in relaying the injury information to the neuron body. Injury induces local activation of several mitogen-activated protein kinases (MAPK) (reviewed in Abe, 2008), in particular Erk

[7] The term ***neurite*** refers to any projection of the neuron cell body, which can be either an *axon* or a *dentrite*.

(Perlson *et al.*, 2007) and c-Jun N-terminal kinase (JNK) (Cavalli *et al.*, 2005) which are also mediated by reversible phosphorylation. These kinases and other activated signals, which include various phosphoproteins, engage retrograde transport mechanisms based on dynein-mediated trafficking, promoting the increased production of several molecules, including transcription factors, cytoskeletal proteins, cell adhesion and axon guidance molecules, and trophic factors and receptors (Rossi *et al.*, 2007). Phosphoproteomics approaches have been successful in implicating several proteins whose function or fate is modulated through phosphorylation. Work done by Michaelevski and colleagues (2010) led to the identification of over 600 different phosphoproteins involved in the neuronal retrograde injury response. Several of the identified phosphoproteins had functions related with signal transduction, guanosine triphosphate activity (GTPase), microtubule-related transport and metabolism pathways. Again, using a phosphoproteomics approach, Wang and colleagues (2011) found evidences of a compartmentalized Erk activation/deactivation cytoskeletal switch that governs neurite growth and retraction. Erk and MAPK pathways were further implicated to be upstream of the activation of an HSP27 through phosphorylation events, which was further proven to be involved in the Glial-cell-line-derived neurotrophic factor (GDNF) induced neurite outgrowth (Hong *et al.*, 2009). Neurotrophic activities of insulin-like growth factor (IGF-1) are initiated also by specific kinase-dependent signaling cascades, that further induces other signaling cascades such as, the phosphorylation of phosphatidyl inositol 3-kinase (PI3-K/Cdc42), essential for determination of neuronal polarity (Sosa *et al.*, 2006). Cascades of phosphorylation/dephosphorylation are also implicated in cytoskeleton dynamics within growth cone motility and axon guidance during regeneration (Dent *et al.*, 2003; Geddis *et al.*, 2003).

Echinoderms, as invertebrate deuterostomes, have an amazing neuronal intrinsic growth capability, which can be triggered at any time point during the animal lifespan, leading to a successful tissue re-growth. Being chordates close relatives, it is inevitable to question which traits echinoderms maintained active throughout evolution that enable such a remarkable functional recovery of injured neuronal tissues. At present, this very intriguing question still remains unanswered, however several studies either using transcriptome approaches (Ortiz-Pineda *et al.*, 2009), individual gene candidates (Suárez-Castillo *et al.*, 2004; Bannister *et al.*, 2008), or proteomics (Chapter 4) have started to assemble some pieces of this complex jigsaw.

To complement the current knowledge on the cellular pathways actively involved in starfish radial nerve cord early regeneration events (Chapter 4), a characterization of protein phosphorylation dynamics in two distinct time points of wound healing was performed, as an effort to understand how this post-translational modification might be modulating the intervenients of the diverse signaling events of this complex, yet amazing, echinoderms functional nervous system re-growth capability.

Soluble proteins extracted from the starfish radial nerve cords (RNC) collected at 48h and 13 days post arm tip ablation, were subjected to 2DE and phosphoprotein detection using a specific fluorescent stain, Pro-Q diamond. 129 spots showed an injury related protein phosphorylation dynamics, with several phosphoprotein spots being exclusively present in controls or injured nerves or, showing significantly different phosphorylation ratios. Also, 81 protein spots were found to be equally phosphorylated in all experimental groups including the respective controls. Among the proteins found to be modulated by phosphorylation in this study, some are particularly relevant, namely: ***1)*** calpain, a serine protease which appears to be phosphorylated exclusively in starfish injured RNC, indicating that this PTM might be responsible for the modulation of its proteolytic activity (Goll *et al.*, 2003) under the influence of calcium intracellular levels; ***2)*** spectrin, calpain preferred substrate was found to be dephosphorylated in starfish injured nerves (48h and 13 days *PAA*), thus increasing its vulnerability towards calpain mediated degradation (Nicolas, 2002), a regenerative event that triggers membrane cytoskeleton rearrangements towards the formation of the growth cone; ***3)*** Notch homologue, which was dephosphorylated in injured RNC, thus acting as a possible inductor of cell differentiation during RNC regeneration (Inglés-Esteve *et al.*, 2001); ***4)*** re-

organization of the cytoskeleton and regulation of filaments and microtubules dynamics through phosphorylation; ***5)*** phosphorylation of a START domain containing protein, an important lipid signaling intervenient (Leung *et al.*, 2005) during neuronal regeneration, and finally, ***6)*** dephosphorylation induced activation of a neuroendocrine convertase that might be involved in the maturation of signaling neuropeptides (Lee *et al.*, 2006) during RNC regeneration events.

5.2. MATERIALS AND METHODS

5.2.1. Experimental groups and regeneration induction

Starfish were collected as previously described in Chapter 2, and then divided in 4 groups, 2 control and 2 regenerating groups, each composed by 6 animals. Regeneration was induced by amputation of 2 arm tips per starfish as previously described (Chapter 4) and both control and regenerating groups were kept throughout the course of the experiments in the exact same conditions. In this chapter only the wound healing stage was studied, by collecting starfish RNC in two time events, 48h and 13 days post arm tip ablation (*PAA*). The radial nerve cords were extracted as described in Chapter 4 and, immediately immersed in an ice cold solution of PBS containing protease, kinase and phosphatase inhibitors (Complete antiprotease kit; 4µM cantharidin; 4µM staurosporine and 1 mM sodium orthovanadate), flash frozen in liquid N_2 and stored at -80°C until further use.

5.2.2. Radial nerve cord soluble proteins enriched fraction preparation

For protein extraction, the collected control and injured RNCs were disrupted using the automated frozen disruption procedure as previously described (Butt *et al.*, 2006). The homogenized tissues were then fractionated in a soluble protein enriched fraction as previously described in Chapter 2 and 4. The obtained fractions from each animal groups (48h and 13 days *PAA* and the respective controls) were pooled together (Control RNC: pool of 12 biological replicates; 48h *PAA*: pool of 6 biological replicates; 13 days *PAA*: pool of 6 biological replicates) and protein concentrations were analyzed in triplicate with 2D Quant kit (GE Healthcare). The injured animals and control pooled samples were then divided in aliquots (60 µg each) and stored at -80°C.

5.2.3. Two-dimensional gel electrophoresis

To each protein aliquot (60 µg total protein) rehydration buffer was added in order to make up the volume to 125 µL prior to isoelectric focusing (IEF) [Rehydration buffer: 8M urea; 13mM DTE; 4% CHAPS and 0.75% (v/v) 3.5-5.0 ampholytes (GE Healthcare) and 0.25% (v/v) 3-10 *NL* ampholytes (GE Healthcare)]. Each 7cm Immobiline DryStrip with a non-linear *pH* gradient from 3-5.6 (GE Healthcare) was actively rehydrated overnight at low voltage (30V) with the correspondent samples (4 technical replicates per group). IEF was carried out on an IPGphor II system (GE Healthcare) with the following running conditions: focusing at 150 V for 75 V.h, 300 V for 300 V.h, 45 min linear gradient until 1000 V, 1h30 min linear gradient until 3000 V and finally 3000 V for a total of 13 kVh. As soon as 1st dimension was completed, the strips from IEF were equilibrated in a two-step process with a buffer (50mM Tris-HCl pH 8.8, 6 M urea, 30 % (v/v) glycerol, 2 % (w/v) SDS, 0.002 % (w/v) bromophenol blue) containing either 2 % (w/v) DTE or 4 % (w/v) iodoacetamide. Protein separation in the 2nd dimension was performed in a Mini-PROTEAN Tetra system (Bio-Rad) using 7 cm SDS-PAGE gels (12.5 % (w/v) acrylamide); electrophoresis was carried out at 100V in the running buffer (25 mM Tris, pH 8.8; 192 mM glycine, and 0.1 % (w/v) SDS).

Gels were immediately stained with Pro-Q Diamond phosphoprotein gel fluorescent stain according to manufacturer's instructions (Invitrogen) in order to reveal phosphoprotein expression. Then, the gels were scanned using a Fujifilm FLA-5100 Fluorescent Image Analyzer (GE Healthcare) using a 532nm laser and a 580nm band pass (BP) emission filter. Gels were subsequently stained with SYPRO Ruby total protein fluorescent stain according to manufacturer's instructions (Invitrogen) and rescanned using the 457nm laser and the 610nm BP emission filter.

5.2.4. Gel image analysis and relative protein phosphorylation ratios

All gel images were exported into Progenesis SameSpots, version v.3.3 (Nonlinear Dynamics). Following automatic and subsequent manual editing, aligning and matching of the gel images in pairs, Pro-Q Diamond/Sypro Ruby, spots were only selected if they were present consistently in all 4 technical replicates of each group. The Progenesis SameSpots normalized spot volumes were used to quantify the amount of protein (Sypro Ruby staining) and total amount of protein phosphorylation (Pro-Q diamond staining) per spot.

The relative amount of phosphorylation, ***relative phosphorylation ratio***, for all Pro-Q spots was determined in order to relate the amount of phosphorylation to the amount of protein in each gel spot:

$$Relative\ phosphorylation\ ratio = {Spot\ volume\ Pro-Q}/{Spot\ volume\ Sypro\ Ruby}$$

Unpaired Student´s *t*-tests were used to compare relative phosphorylation ratios between matched spots of control and injured samples.

For spots showing a significant change in the relative amount of protein phosphorylation following radial nerve cord injury ($p<0.05$), the correspondent fold changes were further determined using the ratio between the ***Injured RNC relative phosphorylation ratio*** and the ***Control RNC relative phosphorylation ratio***. For the spots showing increased phosphorylation signals, the inverse ratio was used to determine the fold change. Since phosphorylation dynamics are much more discrete than protein differential expression, all fold changes were considered, in opposition to the conventional cutoff used in differential proteome analysis.

5.2.5. Spot picking, in-gel digestion and MALDI-TOF/TOF analysis

After gel image analysis, the 7cm gels were stained with colloidal Coomassie (CCB) (Neuhoff *et al.*, 1988). The CCB stained gels were again scanned using the Fujifilm FLA-5100 Fluorescent Image Analyzer using the red laser but without an emission filter. The subsequent gel images were exported into Progenesis SameSpots and matched to the images generated from previous analysis. All spots showing a phosphoprotein signal either in controls and in injured animal groups or, showing a significant change in the relative amount of protein phosphorylation, were manually excised from the four 2DE gel technical replicates and pooled for posterior *in-gel* digestion. *In-gel* digestion of the excised protein spots, tryptic peptides

BOX 5.1| Protein identification software's and used parameters

MASCOT (version 2.2; Matrix Science, Boston, MA) Searches using MASCOT were performed using combined analysis of the intact masses of the tryptic peptides (MS) and tandem mass data (MS/MS). Search parameters were set as follows: minimum mass accuracy of 30 ppm for the parent ions, an error of 0.3 Da for the fragments, one missed cleavage in peptide masses, and carbamidomethylation of Cys and oxidation of Met; phosphorylation of serine (S) threonine (T) and tyrosine (Y), as fixed and variable amino acid modifications, respectively. Peptides were only considered if the ion score indicated extensive homology ($p<0.05$). Proteins were considered if having one peptide with extensive homology.

ProteinPilot (Protein Pilot software version 3.0, revision 114732; Applied Biosystems, USA). Searches with ProteinPilot software were performed without taxonomic restrictions and search parameters were set as follows: enzyme, trypsin; Cys alkylation, iodoacetamide; special factor, gel-based ID; and ID focus, biological modification and amino acid substitution. The false discovery rate (FDR) was determined using PSPEP algorithm from ProteinPilot search engine, using concatenated database joined with the reversed decoy database. Peptides were only considered having a confidence above 95% and proteins were selected if a FDR<1%.

BOX 5.2| Protein sequence databases used

[A] Purple sea urchin *Strongylocentrotus purpuratus* predicted database (42.420 entries; December 2006; ftp://ftp.ncbi.nih.gov/genomes/StrongylocentrotuS_purpuratus/protein;

[B] Uniprot/SwissProt database (release 2011_01; 566.840 sequences; 203.332.110 residues);

[C] Non-redundant protein database Uniref100 (release 2011_01; 11.659.891 clusters).

purification/concentration/separation and mass spectrometry (MALDI-TOF/TOF) procedures were performed as described in Chapter 2.

5.2.6. Protein identification, BLASTp searches and GO annotation

Protein identification was performed using two different search algorithms (BOX 5.1) and three different protein databases (BOX 5.2) similarly to the described procedures on previous chapters. Since most of the identified proteins were homologous to *Strongylocentrotus purpuratus* proteins, these were further submitted to protein-protein BLAST searches (BLASTp) using Basic Local Alignment Search tool available at NCBI web site (http://blast.ncbi.nlm.nih.gov/) through BLAST2GO java application (http://www.blast2go.de). Automated GO annotation was then performed using the GO categories of the best hit derived from the BLASTp results (BLASTp minimal Expectation value set to $<1x10^{-3}$).

5.3. RESULTS

In the previous chapter 4, several kinases, phosphatases and proteins, which are known to be regulated through phosphorylation events, were identified as key effectors of the signaling pathways that lead to the regeneration of the starfish radial nerve cord. However at present, nothing is known on how protein post-translation modifications (PTMs), such as phosphorylation, are tailoring echinoderm intrinsic neuronal growth capabilities. The present work aims to give a first glimpse on the protein phosphorylation dynamics during starfish radial nerve cord wound healing events, by using a 2D differential phosphoproteomics approach to analyze the radial nerve cord soluble proteins enriched fraction, in combination with MALDI-TOF/TOF MS.

Even though the initial stages of regeneration, 48h and 13 days post-arm tip ablation, did not show a significant difference in terms of differential protein expression (Chapter 4), we aimed to evaluate the differences in the phosphorylation dynamics between these two different time points, since this PTM is known to be associated with the fast response elicited upon injury (Ambron *et al.*, 1996) and accordingly, significant changes were found in the phosphorylated proteins in these two wound healing time events. Furthermore, since RNC from both control groups were grouped together in the principal component analysis previously performed; the 12 biological replicates were pooled together to form only one control RNC sample.

For a preliminary view of the phosphoproteome, the radial nerve cord soluble protein fraction was separated in a 3-10 *pH* range IEF strip and the 2DE gels were post-stained with a fluorescent stain that specific for phosphoproteins (Pro-Q Diamond, Invitrogen). The phosphoproteins were found to be mainly localized at the acidic region of the IEF strip (Figure 5.1), and for this reason the subsequent experiments were performed using 7 cm 3-5.6 *NL pH* range zoom strips to improve protein resolution and optimize phosphoprotein detection. Using this narrower *pH* range strip resulted in the detection of 554 total protein spots (stained with Sypro Ruby) of which 190, 142 and 124 spots were phosphorylated (stained with Pro-Q diamond) respectively in control, 48h and 13 days post arm tip ablation experimental groups. Only protein spots detected in all technical replicates per experimental group were considered, in order to guard against spot differences due to gel-to-gel variation.

After gel image analysis, 81 of the detected phosphorylated spots were commonly matched in all 2DE gels from the three experimental groups, whereas, 72 were found to be exclusively phosphorylated in controls and 8 of them were exclusively phosphorylated in the wound healing RNC. The remaining 37 spots common between controls and the injured groups (48h and/or 13 days) showed a significant change in protein phosphorylation ratios.

All the phosphorylated spots that were successfully matched with protein spots in the colloidal Coomassie stained gels (110 spots), despite its reduced sensitivity in comparison with the fluorescent Sypro Ruby Stain, were manually excised and processed for protein identification. The relative phosphorylation ratio per protein spot was estimated by dividing Pro-Q and the Sypro Ruby normalized spot volumes, as suggested by the manufacturer (Invitrogen) (see Supplementary table 5.1 for the phosphorylation ratios per Pro-Q Diamond spot). The obtained results were compared using a

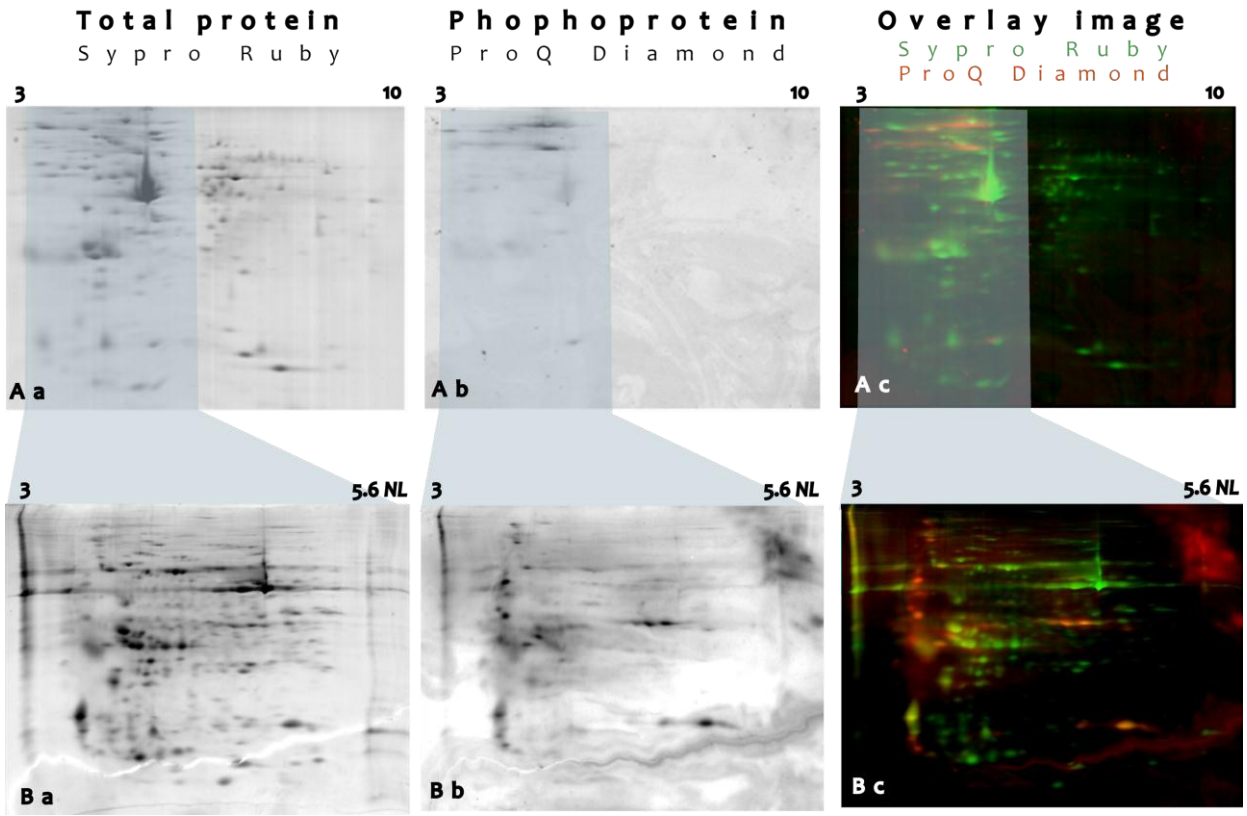

Figure 5.1: Control RNC soluble proteins enriched fraction detected with the total protein fluorescent stain Sypro Ruby (Invitrogen) (Aa; Ba) and phosphoproteins detected with the fluorescent stain Pro-Q Diamond (Ab; Bb). Proteins were resolved either on a 3 to 10 (Aa-Ac) or on 3 to 5.6 *NL* (Ba-Bc) *pH* range strips for the 1st dimension of the 7cm 2DE gels.

Table 5.1: Proteins exclusively phosphorylated in control RNC

Protein identity	Accession number	Protein General function	2DE Spot(s) number	Relative phosphorylation ratio#	How phosphorylation affects protein function
Actin, cytoplasmic	sp|P12716|ACTC_PISOC	Cytoskeleton dynamics	155	0,42±0,077	Actin filaments polymerization are regulated by calcium and protein kinase C (Job *et al.*, 1998)
Chaperone protein htpG	sp|B0BVI6|HTPG_RICRO	Neuroprotection/UPS/developmental	77	0,77±0,213	Hsp90 phosphorylation is linked to its chaperoning function (Zhao *et al.*, 2001)
GAF domain-related protein	O96195	Unknown/other	261	0,68±0,093	-
Gelsolin	gi|115961140; gi|115891439	Cytoskeleton dynamics/developmental	155	0,42±0,077	Gelsolin phosphorylation regulates actin polymerization (De Corte *et al.*, 1997)
Heat shock protein 5	Q7SZD3	Folding	80	0,33±0,111	Phosphorylation of heat-shock proteins alters its substrate binding characteristics (Peake *et al.*, 1998)
Lymphoid-restricted membrane protein	sp|Q12912|LRMP_HUMAN	Vesicle targeting and fusion	550	2,13±0,823	-
Moesin	sp|Q2HJ49|MOES_BOVIN	Cytoskeleton dynamics	77	0,77±0,213	Rho-kinase regulates moesin phosphorylation downstream of Rho in vivo and that the phosphorylation of moesin by Rho-kinase plays a crucial role in the formation of microvilli-like structures (Oshiro *et al.*, 1998)
Notch homolog	gi|115941626|ref|XP_001187416.1|	Developmental/regeneration/activated by proteolysis	32	1,10± 0,259	Notch phosphorylation modulates intracellular signal transduction through the Notch pathway (Inglés-Esteve *et al.*, 2001)
Putative uncharacterized protein (no significant hit on BLASTp search)	A8IIA9	Other	62 550	2,53±0,745 2,13±0,823	-
Regulatory protein Crp	D8J4J6	Transcription regulation	107 550	0,84±0,125 2,13±0,823	-
Spectrin	gi|115920116|ref|XP_785949.2|	Axon guidance/developmental/cytoskeleton dynamics	5	0,36±0,077	Tyrosine Phosphorylation Regulates Alpha II Spectrin Cleavage by Calpain; Phosphorylation of this residue decreases spectrin sensitivity to calpain in vitro (Nicolas *et al.*, 2002)
Transcriptional activator protein Pur-alpha	C1BSV9	Transcription regulation	253	1,30±0,260	-
Transporter, AcrB/AcrD/AcrF family protein	A3X4U4	Transport	261	0,68±0,094	-

Table 5.2: Proteins exclusively phosphorylated at 48h *PAA*

Protein identity	Accession number	Protein General function	2DE Spot(s) number	Relative phosphorylation ratio#	How phosphorylation affects protein function
Actin	sp|P18601|ACT2_ARTSX; sp|P07837|ACT2_BOMMO	Cytoskeleton dynamics	188	1,61±0,639	Actin filaments polymerization are regulated by calcium and protein kinase C (Job *et al.*, 1998)
Arginyl-tRNA synthetase	sp|Q8EWT9|RBFA_MYCPE	RNA interaction or translation regulator	359	0,64±0,28	-
GPN-loop GTPase 2	sp|Q4R579|GPN2_MACFA	RNA interaction or translation regulator	359	0,64±0,28	-
Calmodulin	gi|115960363; gi|115728588	Calcium/development/cytoskeleton dynamics/synaptic transmission/phosphatase	466	1,73± 0,33	Calmodulin phosphorylation regulates interaction with binding partners (Leclerc *et al.*, 1999)

Table 5.3: Proteins exclusively phosphorylated at 13 days *PAA*

Protein identity	Accession number	Protein General function	2DE Spot(s) number	Relative phosphorylation ratio#	How phosphorylation affects protein function
Alpha-tubulin	A8NY93	Cytoskeleton dynamics	489	0,90±0,30	Phosphorylation of alpha-tubulin carboxyl-terminal tyrosine prevents its incorporation into microtubules (Wandosel,*et al.*, 1997)
Calmodulin	sp|A8CEP3|CALM_SACJA	Calcium/development/cytoskeleton dynamics/synaptic transmission/phosphatase	489	0,90±0,30	Calmodulin phosphorylation regulates interaction with binding partners (Leclerc *et al.*, 1999)

Table 5.4: Proteins exclusively phosphorylated in both injured groups (48h and 13 days *PAA*)

Protein identity	Accession number	Protein General function	2DE Spot(s) number	Relative phosphorylation ratio#		How phosphorylation affects protein function
				48h *PAA*	13 days *PAA*	
Actin	Q7Z9F9	Cytoskeleton dynamics	519	0,51±0,10	0,45±0,13	Actin filaments polymerization are regulated by calcium and protein kinase C (Job *et al.*, 1998)
Beta-tubulin	UniRef100_Q7YZK4		519	0,51±0,10	0,45±0,13	
Calpain-like protease 1	sp|Q03792|RIM13_YEAST	Cytoskeleton dynamics/signaling/retrograde transport	316	0,51±0,12	0,34±0,78	Calpain dephosphorylation inactivates its action. Phosphorylation may have a primarily structural role and may target calpain to signal transduction functions (Goll *et al.*, 2003)
Gelsolin	B6RB97	Cytoskeleton dynamics/developmental	157	0,37±0,16	0,25±0,06	Gelsolin phosphorylation regulates actin polymerization (De Corte *et al.*, 1997)
Actin	Q7Z9F9	Cytoskeleton dynamics	635 424 631	0,11±0,055 0,68±0,361 0,10±0,031	0,07±0,009 0,75±0,326 0,07±0,006	Actin filaments polymerization are regulated by calcium and protein kinase C (Job *et al.*, 1998)
DNA polymerase IV	sp|P58965|DPO4_THETN	Neuroprotection/other	311	0,48±0,076	0,28±0,101	Phosphorylation of DNA polymerase is needed for efficient recovery from UV damage (Göhler *et al.*, 2011)
*Similar to Beta-xylosidase	C0A986	Unknown	311	0,48±0,076	0,28±0,101	-

Table 5.5: Proteins exclusively phosphorylated in control RNC and at 48h *PAA*

Protein identity	Accession number	Protein General function	2DE Spot(s) number	Relative phosphorylation ratio#		How phosphorylation affects protein function
				Control RNC	48 h *PAA*	
Actin	UniRef100_B4ZFM7	Cytoskeleton dynamics	193 473	0,39±0,08 1,12±0,34	0,70±0,17 1,00±0,37	Actin filaments polymerization are regulated by calcium and protein kinase C (Job *et al.*, 1998)
Calmodulin	UniRef100_P62184	Calcium/development/cytoskeleton dynamics/synaptic transmission/phosphatase	473 506	1,12±0,34 1,50±0,36	1,00±0,37 1,10±0,61	Calmodulin phosphorylation regulates interaction with binding partners (Leclerc *et al.*, 1999)
Cortactin (Cttn protein)	B3DLZ9	Cytoskeleton dynamics/Endocytosis/Growth cone/WASP pathway	75	0,80±0,18	1,26±0,50	Phosphorylated by Erk and Src (Daly, 2004; Tehrani *et al.*, 2007; Martin *et al.*, 2006; Cosen-Binker *et al.*, 2006)
Endoplasmin	B0W5Z4	Neuroprotection/UPS/developmental	455	1,33±0,69	1,37±0,24	Hsp90 phosphorylation is linked to its chaperoning function (Zhao *et al.*, 2001)
Protein CAF130 (no significant hit in BLASTp search)	sp|P53280|CF130_YEAST	Transcription regulation	352	1,28±0,32	0,83±0,21	-
*Transcription initiation factor	D2VJV9	Transcription regulation	352	1,28±0,32	0,83±0,20	-
Transporter, AcrB/AcrD/AcrF family protein	A3X4U4	Transport	259	0,68±0,14	0,61±0,24	-

Table 5.6: Proteins phosphorylated in all experimental groups (Control, 48h and 13 days *PAA*)

Protein identity	Accession number	Protein General function	2DE Spot(s) number	Relative phosphorylation ratio# Control RNC	48h *PAA*	13 days *PAA*	How phosphorylation affects protein function
Actin	UniRef100_B4ZFM7	Cytoskeleton dynamics	189 152	0,91±0,33 0,58±0,29	2,79±0,91 0,72±0,18	2,16±1,58 0,50±0,05	Actin filaments polymerization are regulated by calcium and protein kinase C (Job *et al.*, 1998)
Alpha-tubulin	A0AAM5	Cytoskeleton dynamics	310	1,59±0,19	1,71±0,39	1,47±0,16	Phosphorylation of alpha-tubulin carboxyl-terminal tyrosine prevents its incorporation into microtubules (Wandosel *et al.*, 1997)
Beta-tubulin	UniRef100_Q7YZK4	Cytoskeleton dynamics	128 143 146 144 161a	0,44±0,06 0,18±0,02 0,48±0,05 0,27±0,03 3,54±1,38	0,68±0,22 0,33±0,14 0,91±0,33 0,54±0,24 2,92±0,91	0,42±0,08 0,20±0,06 0,52±0,34 0,33±0,12 2,22±0,91	-
Calmodulin	B0WM51	Calcium/development/cytoskeleton dynamics/synaptic transmission/phosphatase	442 479	1,42±0,29 1,56±0,32	1,47±0,12 1,79±0,19	1,33±0,36 1,47±0,15	Calmodulin phosphorylation regulates interaction with binding partners (Leclerc *et al.*, 1999)
*similar to Dvl-associating protein	A0CL27	Regeneration (*wnt* signaling pathway)	273	0,89±0,06	1,54±0,56	1,15±0,55	-
Heat shock 70-related protein 4	sp|P12077|HSP74_LEIMA	Folding	116	0,62±0,09	0,86±0,35	0,57±0,26	Phosphorylation of heat-shock 70 protein at threonine 175 alters its substrate binding characteristics (Peake *et al.*, 1998)
* similar to tubulin, alpha 2 isoform 2	UPI0001CB954A	Cytoskeleton dynamics		0,89±0,06	1,54±0,56	1,15±0,55	Phosphorylation of alpha-tubulin carboxyl-terminal tyrosine prevents its incorporation into microtubules (Wandosel *et al.*, 1997)
*similar to Transcription elongation factor B	gi|115629401|ref|XP_001175953.1|	Ubiquitin conjugation pathway/RNA interaction or translation regulator	412	0,81±0,11	1,02±0,29	0,83±0,30	-

polypeptide 2							
*similar to glyceraldehydephosphate dehydrogenase isoform 1	gi|115738231; gi|115693294	Apoptosis/neuroprotection/energy metabolism	273	0,89±0,06	1,54±0,56	1,15±0,55	Phosphorylation catalyzed by specific protein kinases can constitute one of the mechanisms for the regulation of glycolysis and gluconeogenesis (Ashmarina *et al.*, 1988).
*similar to Unc119c	gi|115706054|ref|XP_001179317.1|	Synaptic transmission/visual perception/nervous system development	263b	0,80±0,11	0,86±0,19	0,89±0,23	-
Protein argonaute 11	sp|Q10F39|AGO11_ORYSJ	RNA interaction or translation regulator	250	0,72±0,11	0,78±0,24	0,63±0,06	Phosphorylation of human Argonaute proteins affects small RNA binding (Šatkauskas *et al.*, 2007)
Putative membrane protein ycf1	sp|Q0G9Q4|YCF1_DAUCA	Other	310	1,59±0,19	1,71±0,39	1,47±0,16	-
Putative uncharacterized protein (no significant hits in BLASTp search)	Q0UHY8	Other	250	0,72±0,11	0,78±0,24	0,63±0,06	-
START domain-containing protein	A9ZT01	Cytoskeleton dynamics/developmental	146 310	0,48±0,05 1,59±0,19	0,91±0,33 1,71±0,39	0,52±0,34 1,47±0,16	-
Translationally-controlled tumor protein homolog	sp|Q5MGM6|TCTP_LONON	Regulation of growth/calcium binding	343	0,44±0,03	0,52±0,08	0,47±0,08	-
*similar to axonemal dynein light chain domain-containing protein	E2RQ45	Motor protein/intracellular transport	280a	1,25±0,15	1,39±0,30	1,11±0,18	Phosphorylation of dynein regulates the velocity of in vitro microtubule translocation (Wang *et al.*, 1998; Hamasaki, 1999)
4-hydroxythreonine-4-phosphate dehydrogenase 2	A8S2W2	Other	373	0,26±0,22	0,36±0,12	0,36±0,02	-
Actin	Q7Z9F9	Cytoskeleton dynamics	177	0,26±0,24	0,39±0,10	0,31±0,02	Actin filaments polymerization are regulated by calcium and protein kinase C (Job *et al.*, 1998)

DNA polymerase IV	sp|P58965|DPO 4_THETN	Neuroprotection/other	626	0,15±0,009	0,18±0,030	0,16±0,032	Phosphorylation of DNA polymerase is needed for efficient recovery from UV damage
*similar to Beta-xylosidase	C0A986	Other	312	0,35±0,044	0,60±0,072	0,51±0,137	-
DEAD-box family RNA helicase	D0UKI0	RNA interaction or translation regulator	312	0,35±0,044	0,60±0,072	0,51±0,137	-

Table 5.7: Differently phosphorylated proteins in the injured groups

Injured RNC	Protein identity	Accession number	Protein General function	2DE Spot(s) number	Fold	*p* value	How phosphorylation affects protein function
48h *PAA*	Actin	UniRef100_B4ZFM7	Cytoskeleton dynamics	182 125	+1,42 +3,76	0,003 0,034	
	Alpha-tubulin	B0B5G4	Cytoskeleton dynamics	139 125 129	+2,84 +3,76 +2,27	0,003 0,003 0,02	Phosphorylation of alpha-tubulin carboxyl-terminal tyrosine prevents its incorporation into microtubules (Wandosel *et al.*, 1997)
	Beta-tubulin	UniRef100_Q7YZK4	Cytoskeleton dynamics	139	+2,84	0,003	
	*similar to ADP-ribosylation factor 1	A2XN99	Vesicular transport/protein transport/retrograde vesicle-mediated transport	360	+1,93	0,039	-
	* similar to ankyrin 2,3/unc44	A2FHV3	Growth cone and axon guidance	131	+1,9	0,036	Ankyrin phosphorylation is important for regulating the affinity of ankyrin for specific proteins, including spectrin (Mohler *et al.*, 2002)
	START domain-containing protein	A9ZT01	Cytoskeleton dynamics/developmental	131 139	+1,9 +2,8	0,036 0,003	-
	Tubby-related protein 2	sp|P46686|TULP2_MOUSE	Visual perception/developmental /central nervous system differentiation/ spinal cord patterning	291b	+1,37	0,034	-
	Actin	sp|Q0PGG4|ACTB_BOSMU	Cytoskeleton dynamics	202	-1,57	0,0007	Actin filaments polymerization are regulated by calcium and protein kinase C (Job *et al.*, 1998)
	*similar to H/ACA ribonucleoprotein complex subunit 4	B4MRD6	RNA interaction or translation regulator/RNA transport	258	-1,52	0,0173	Phosphorylation regulates its transport function to the nucleus (Heiss *et al.*, 1999)
	Neuroendocrine	sp|Q5REC2|NEC2_PONA	Neuropeptide metabolism	69a	-1,39	0,0135	Neuroendocrine Protein 7B2 is inactivated

	convertase	B					by phosphorylation (Lee *et al.*, 2006)
	Putative cuticle protein	C0H6L1	Other	69a	-1,39	0,0135	-
	Putative uncharacterized protein (no significant hits on BLASTp search)	A8IIA9	Other	555	-1,78	0,0137	-
	*similar to Beta-xylosidase	C0A986	Other	69b	-1,39	0,0135	-
	Set	C4QDV5	Transcription regulation	202	-1,57	0,0007	-
	Tena/thi-4 family domain protein	D5DCC7	Other	69b	-1,39	0,0135	-
	Calmodulin	P02595	Calcium/development/cytoskeleton dynamics/synaptic transmission/phosphatase activity/kinase regulation	484	-1,72	0,02	Calmodulin phosphorylation regulates interaction with binding partners (Leclerc *et al.*, 1999)
13 days *PAA*	Calmodulin	P02595	Calcium/development/cytoskeleton dynamics/synaptic transmission/phosphatase activity/kinase regulation	484	-2,18	0,02	Calmodulin phosphorylation regulates interaction with binding partners (Leclerc *et al.*, 1999)
	Beta-tubulin	Q7YZK4	Cytoskeleton dynamics	140	-1,19	0,036	-

Mean value of 4 technical replicates +/- standard deviation;

*Hypothetical/Uncharacterized proteins with a significant hit on the *BLASTp* searches. The name of the first *BLASTp* hit is here presented. For the complete set of information see Supplementary table 5.1.

Student´s *t*-tests to determine which were the spots having a significant differential phosphorylation dynamics ($p<0.05$) within **control *vs* 48h *PAA*** and **control *vs* 13 days *PAA*** experimental groups. Several spots, 32 and 17, at 48h and 13 days PAA, respectively, showed an injury correlated phosphorylation variation, demonstrating that protein phosphorylation events are critical to the initial stages of the regenerative responses in wound healing RNC.

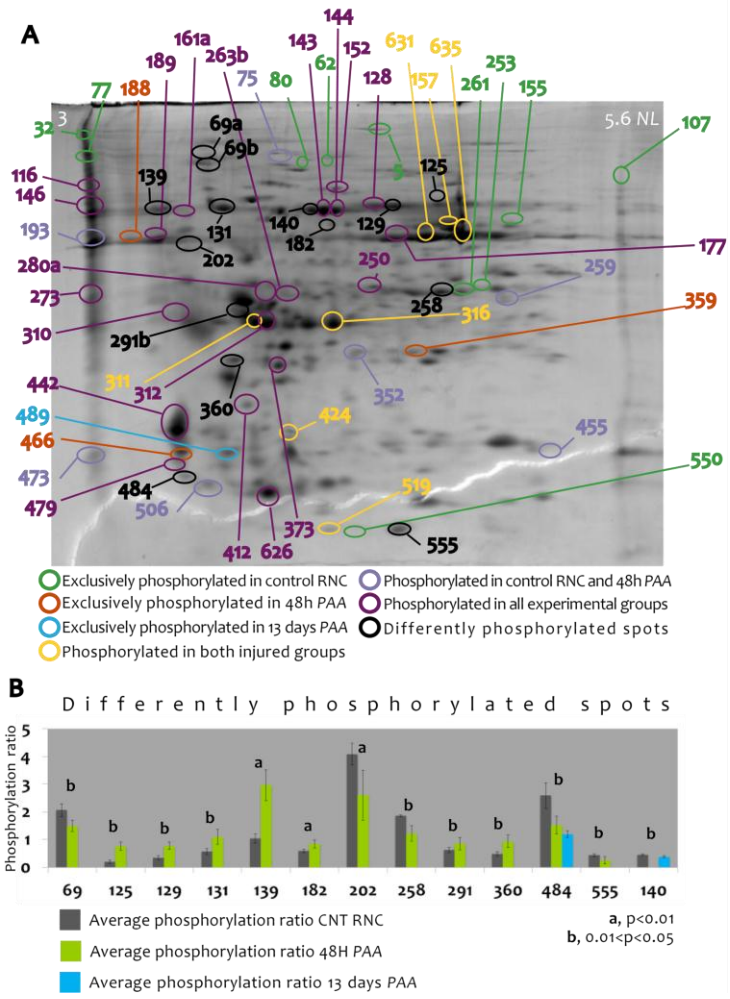

Figure 5.2: (A) Annotated 2DE (3-5.6 *NL*) with the spots referred on Tables 5.1-5.7. **(B)** Phosphorylation ratios of the 2DE spots that showed an injury correlated phosphorylation variation (Table 5.7).

Among the 110 spots manually excised for protein identification, 62 were successfully assigned to protein identities derived from two search engines through several confirmatory and complementary searches against three different protein databases. Several protein redundancies were found among the gel spots similarly to what was previously described in Chapter 4, and were likely due to the several proteolytic events known to be occurring in the injury signaling pathways; protein isoforms or the occurrence of several different post-translation modifications other than phosphorylation (i.e., ubiquitination and SUMOylation). According to the spots distribution along the different experimental groups, their relative phosphorylation ratios and the statistical analysis, the identified proteins were categorized as **exclusively phosphorylated in control RNC** (Table 5.1), **48h *PAA*** (Table 5.2) and **13 days *PAA*** (Table 5.3); **exclusively phosphorylated in both injured groups** (Table 5.4) or in **control RNC and 48h *PAA* group** (Table 5.5); **proteins phosphorylated in all experimental groups** (Table 5.6) and finally, **proteins that have an injury correlated phosphorylation significant variation when comparing with control RNC** (Table 5.7).

Careful data mining through GO annotation (Supplementary table 5.1) and pathway analysis based

on different references allowed to determine which were the regeneration related signaling pathways being modulated through phosphorylation, which is further described in the discussion section. In addition, the selected experimental approach generated a significant amount of valuable information on starfish RNC regeneration events, improving our understanding on the proteins that are being modulated through phosphorylation events. Nevertheless, these results do not dispense future confirmatory and complementary experiments to fully characterize protein phosphorylation sites through neutral loss data dependent mass spectrometry events (tandem MS^n mass spectrometry experiments).

5.4. DISCUSSION

The success of neuronal regeneration depends on a fast cascade of events that start at the wound site upon minutes after the injury, with the rapid retraction of the plasma membrane and, the formation of the growth cone just 40 minutes after axotomy (Ambron *et al.*, 1996). The elicited injury signals further engage axonal transport and travel back to the neuron nucleus in order to activate intrinsic neurite outgrowth mechanisms (Abe *et al.*, 2008). However, at present, still little is known about the kinetics of soluble proteins involved in axonal transport, namely whether they are transported individually or in a signaling complex or, which are the events responsible for the engagement within the molecular motor proteins. Several examples of the importance of protein phosphorylation events in the retrograde signaling were already described (reviewed in Ch´ng *et al.*, 2011), being generally accepted that local protein synthesis, proteolysis and protein post-translation modifications are implicated in the generation of the retrograde signaling ensemble as the primary events that will further enable neuronal regeneration (Sun *et al.*, 2010), thus reinforcing the importance of using proteomic approaches to study these signaling events.

In order to understand if protein phosphorylation events are equally critical to launch the proper regenerative response of the starfish radial nerve cord,

BOX 5.3: Cytoskeleton leads the way in neuronal outgrowth.

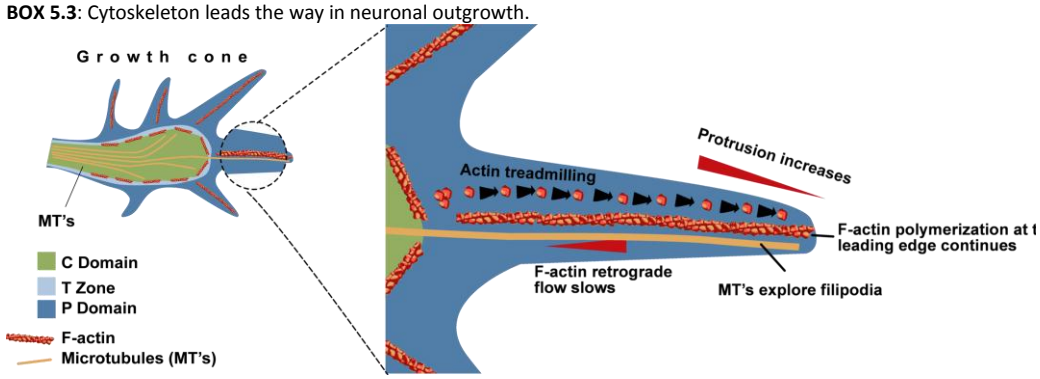

The growth cone machinery is maintained by both 1) filamentous (F)-actin treadmilling (in which F-actin is polymerized at the leading edge and severed at the transition (T) zone, with the subunits recycled back to the leading edge) and 2) F-actin retrograde flow (the continuous movement of F-actin from the leading edge towards the center of the growth cone). When retrograde flow and polymerization are balanced, no protrusion occurs. When filopodia encounters an adhesive substrate, growth cone receptors bind to the substrate and are coupled to F-actin through *clutch* proteins. This engages the clutch, anchoring F-actin with respect to the substrate and attenuating F-actin retrograde flow. Further F-actin polymerization pushes the membrane forward, which results in growth cone protrusion.
Peripheral (P) domain microtubules (MTs) explore filopodia along F-actin bundles and might act as guidance sensors. As a filopodium encounters a guidance cue, exploratory MTs might act as scaffolding for further signaling, and additional MTs are recruited to the region. Also actin has a role in determining MT localization in the growth cone. Actin arcs constrain and guide central (C) domain MTs, and F-actin bundles inhibit and guide P domain MTs. (Figure adapted from Lowery *et al.*, 2009).

a 2DE gel based approach and specific a phosphoprotein stain were combined to produce a preliminary evaluation of protein phosphorylation dynamics within starfish radial nerve cord early regeneration events, at 48h and 13 days post arm tip ablation. Additionally, all spots that revealed a phosphorylation signal were processed for identification, to further understand which proteins are being modulated through phosphorylation during the normal neuronal functions within the echinoderm nervous system. Altogether, from the 62 proteins identified by MALDI-TOF/TOF mass spectrometry, 47 are non-redundant proteins of which, 30 showed also an injury related phosphorylation dynamics during starfish radial nerve cord wound healing. Several of the identified proteins have already been described in different neuro-regeneration models as protein intervenients regulated through finely tuned phosphorylation/dephosphorylation events and are here described for the first time as belonging to the amazing echinoderm nervous tissue regeneration machinery.

5.4.1. Injured starfish radial nerve cord cytoskeleton dynamics is regulated through differential phosphorylation during wound healing signaling events

Several studies indicate that the actin and microtubule cytoskeletons are a final common target of many signaling cascades that influence the developing neuron. Regulation of polymer dynamics and transport are crucial for the proper growth cone motility. Cytoskeleton filaments (F-actin) and microtubules (tubulin) are the physical tracks for the motor protein driven cellular transport of soluble signaling molecules and vesicles, in the retrograde transport of positive injury signals or, anterograde transport of new molecules deriving from the neuron soma (reviewed in Ch'ng *et al.*, 2011). The growth cone undergoes a systematic maturation that is continuous during axon growth and includes filopodia and lamellipodia formation at the leading edge of the growth cone (BOX 5.3), followed by flow of the filopodia around the lateral aspects of the growth cone and subsequent retraction of filopodia at the base of the growth cone (reviewed in Dent *et al.*, 2003). The filopodia movements are driven by the flow of actin filaments and associated proteins. Studies using several protein kinase inhibitors and protein phosphatase activators resulted in a blocked growth cone formation after neurite transection (Geddis *et al.*, 2003) and thus have shown the importance of phosphorylation events required for the cytoskeleton rearrangements in an injured axon.

While cytoskeleton actin filaments polymerization have been shown to be regulated by calcium and protein kinase C (Job *et al.*, 1998), microtubule constitutive protein tubulin was shown to be the major *in vivo* substrate of the tyrosine-specific protein kinase $pp60^{c\text{-}scr}$ in nerve growth cone membranes (Matte *et al.*, 1990), being regulated through phosphorylation (Wandosel *et al.*, 1997). Further stabilization of microtubules is also regulated through filament interacting proteins (Microtubule associated proteins; MAP) (Gordon-Weeks, 1993) that were also identified in this study and will be also discussed below.

Within the starfish radial nerve cord wound healing events (48h and 13 days post-arm tip ablation) several spots showing different relative phosphorylation ratios were identified as actin and tubulin, suggesting that actin filaments and microtubules polymerization are also being regulated through phosphorylation events. Among the identified phosphorylated spots, 3 were identified as actin and showed a significant difference of the relative phosphorylation ratio between control and the 48h post-injury group, two spots (spots 182 and 125; Figure 5.2; Table 5.7) with an increase in the phosphorylation ratio of 1.4- and 3.8-fold, respectively, and one spot (spot 202; Figure 5.2; Table 5.7) with a 1.6-fold decrease in the phosphorylation ratio comparing with the control. In addition, 4 spots (spots 519, 635, 424, 631; Figure 5.2; Table 5.4) identified as actin were exclusively phosphorylated in both regenerating groups and 2 had an apparent molecular mass (*M*) inferior to the predicted *M*, indicating that they most probably are proteolysis products. Six different spots were identified as tubulin and had either an increased phosphorylation ratio (Table 5.7, Figure 5.2; 48h *PAA*: spots 139, 125, 129); decreased phosphorylation ratio (Table 5.7, Figure 5.2; 13 days *PAA*: spot 140) or were exclusively phosphorylated in the regenerating groups (Table 5.3: spot 489; Table 5.4: spot 519; Figure 5.2).

Spectrins are the central components of the membrane skeleton, forming an ubiquitous and complex spectrin-actin scaffold located under the lipid bilayer of metazoan animal cells (Bennett *et al.*, 2001). This spectrin-based skeleton is bound to various transmembrane proteins through two connecting proteins, ankyrin and protein 4.1. Spectrins are responsible for conferring resiliency and durability to the membrane itself, however they have also been assigned to several important signaling pathways such as membrane sorting, vesicle trafficking (Beck *et al.*, 1997), endocytosis (Kamal *et al.*, 1998) and neurite outgrowth (Hammarlund *et al.*, 2000). In the regeneration events of the starfish radial nerve cord, spectrin networks are cleaved by a calcium activated protease, calpain (Chapter 4), a process suggested to facilitate fusion of axoplasmic vesicles to the membrane, helping the construction of the growth cone or extension of the axon, also common with several neuro-regeneration models (reviewed in Gumy *et al.*, 2010; Spira *et al.*, 2001). Work done by Nicolas (2002) allowed the identification of a tyrosine residue (Y1176), located in the specific calpain cleavage site, that is phosphorylated and dephosphorylated *in vivo*. These authors have also proven that phosphorylation of the specific spectrin residue antagonizes calpain proteolytic activity. In our results, spectrin was only found to be phosphorylated in the control group (Table 5.1: spot 5; Figure 5.2), and several proteolytic fragments were previously identified during the regenerating events of the radial nerve cord (Chapter 4). These facts clearly highlight that spectrin phosphorylation prevents its proteolytic degradation in normal conditions; and that a dephosphorylation step associated with the cascade of injury signaling events is critical for calpain mediated proteolysis during echinoderm radial nerve cord regeneration (Figure 5.3). The spectrin binding partner ankyrin was also identified with a 2-fold increase in the relative phosphorylation ratio in the 48h *PAA* experimental group relatively to the control (Table 5.7: spot 360; Figure 5.2). Ankyrin phosphorylation has been suggested to be the key factor that regulates its affinity towards spectrin (Mohler *et al.*, 2002).

As previously described, calpain activation upon axonal injury is correlated with the intracellular increase of calcium levels, as result of the membrane physical disruption and also, by the release of internal calcium stored in the endoplasmic reticulum (Ch´ng *et al.*, 2011). However, calpain activity and its sensitivity to Ca^{2+} levels are also modulated by phosphorylation (Kuo *et al.*, 1994; Kovács *et al.*, 2008). The same authors also show evidence that calpain phosphorylation and activation is mediated through a pathway known to be activated in retrograde transport of injury signals, the ERK pathway, also reported to be responsible for the activation of calpain B in *Drosophila melanogaster* (Kovács *et al.*, 2008). In the starfish wound healing radial nerve cord events, calpain was exclusively phosphorylated in both regenerating groups (Table 5.4: spot 316; Figure 5.2), with no phosphorylation signal being detected in the control group, thus confirming that the cytoskeleton rearrangements' mediated by calpain proteolytic activity during echinoderm regeneration events are being modulated through phosphorylation.

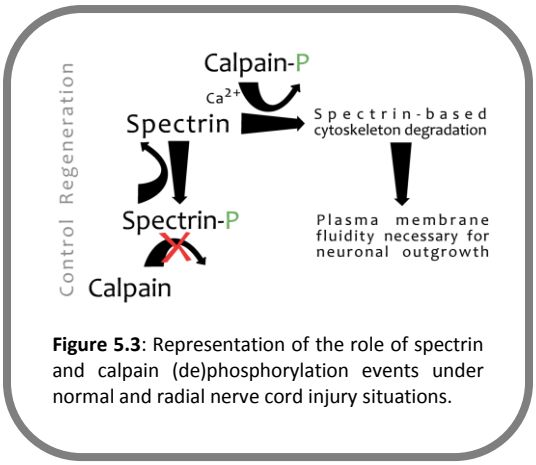

Figure 5.3: Representation of the role of spectrin and calpain (de)phosphorylation events under normal and radial nerve cord injury situations.

Several MAP proteins whose affinities towards actin and tubulin binding are known to be regulated through phosphorylation were also identified within starfish wound healing events. The MAP´s gelsolin, moesin and cortactin were also identified to be differently phosphorylated during starfish radial nerve cord wound healing events. Gelsolin severs assembled actin filaments in two, and caps the fast-growing plus end of a free or newly severed filament in a Ca^{2+}, *pH* and phospholipid dependent manner (Kwiatkowski, 1999; De Corte *et al.*, 1997). Although having five potential sites of phosphorylation, there is no consensus if any of these are phosphorylated *in vivo* (Pottiez *et al.*, 2010). Our results suggest that not only gelsolin is

phosphorylated *in vivo*, but also that this PTM might be regulating actin-severing dynamics, since 2 different gelsolin spots showing a phosphoprotein signal were identified in the starfish radial nerve cords, one being exclusive to the control group (Table 5.1: spot 155; Figure 5.2) and another exclusive to the regenerating groups (Table 5.4: spot 157; Figure 5.2). Moesin, a cross-linking protein between the plasma membrane and actin filaments, was also found to be phosphorylated in the control group (Table 5.1: spot 77; Figure 5.2). Although the role of moesin phosphorylation still needs to be clarified, it has been shown that the phosphorylation of moesin by Rho-kinase is thought to result in the inhibition of the head-to-tail suppression of moesin, leading to its activation (Matsui *et al.*, 1998), a process that results in the formation of microvilli-like structures (Oshiro *et al.*, 1998). In fact several members of the *WASP* pathway, where Rho-kinase is a key intervenient, have previously been identified as key effectors of the finely tuned actin filament organization within the starfish radial nerve cord regeneration (Chapter 4) and hence moesin constitutes one more key effector that may be involved in the formation of pseudopodia-like structures in the starfish neuronal growth cones upon injury. Cortactin, an actin filament-binding protein, substrate of multiple kinases, and a central element connecting signaling pathways with the restructuring cytoskeleton, was also identified in one spot (spot 75), showing a similar phosphorylation ratio in both control and 48h *PAA* groups (Table 5.5: spot 75; Figure 5.2). Like all the identified proteins, cortactin function within the starfish radial nerve regeneration had never been reported. However, it is known that when phosphorylated, cortactin recruits Arp2/3 complex proteins (previously identified as key effectors in the actin cytoskeleton remodeling during starfish radial nerve regeneration; Chapter 4) to the existing actin microfilaments, facilitating and stabilizing nucleation sites for actin branching (reviewed in Daly, 2004).

A START domain protein has already been identified as being involved in the regeneration events of the starfish *Marthasterias glacialis* (Chapter 4), and it is known to be ubiquitously distributed in the developing nervous system of the *Asterina pectinifera* starfish larvae (Murabe *et al.*, 2008). The human homologue START proteins have a well-conserved lipid binding domain and are involved in lipid signaling events (Alpy *et al.*, 2005), where they exert their action in suppression of cytoskeleton reorganization, cell growth, cell migration, and transformation (Leung *et al.*, 2005). Although the starfish START protein has several theoretical phosphorylation sites (14 phosphorylation sites with scores above 0.5, predicted by NetPhos 2.0 Server) its phosphorylation function was never before reported in echinoderms. In mammals, it is sought that phosphorylation events are responsible for targeting START proteins to specific donor or acceptor membranes and/or induce conformational changes to account for a rapid and efficient lipid transfer between membranes or other donor/acceptor molecules (Alpy *et al.*, 2005). In the present study, we have identified 4 different phosphorylated spots containing START domain protein, 2 of them had no significant changes in the relative ratio of phosphorylation among the three experimental groups (Table 5.6: spots 146 and 310; Figure 5.2), nonetheless the other 2 spots had over a 2-fold increase (1,9- and 2,8-fold increase, respectively, in the spots 131 and 139; Table 5.7; Figure 5.2) in the relative phosphorylation ratio in the 48h *PAA* experimental group, highlighting the importance that this protein might have in starfish RNC injury singling events.

With the increase of the intracellular calcium levels, calmodulin, a calcium binding protein, plays a major role in mediating the activation and modulation of several very important pathways during axonal regeneration events, which also include cytoskeleton re-organization. Calmodulin is also responsible for the activation of several kinases and phosphatases, such as myosin light-chain kinase (MLCK), CaM kinase II (CaMKII), protein phosphatase 2B, and calcineurin (Geddis *et al.*, 2003). In the previous chapter, it has been identified as one of the key intervenients in starfish radial nerve cord injury cascade events and concomitantly, in the present work several spots showing a phosphorylation signal were also identified as calmodulin. Within the calmodulin phosphorylated spots, several were common to the 3 experimental groups (Table 5.6: spots 442 and 479; Figure 5.2) or common between the control and 48h *PAA* (Table 5.5: spots 473 and 506; Figure 5.2), one was exclusive to each regenerating group (Table 5.2: spot

466; Table 5.3: spot 489; Figure 5.2), one spot showed a 1,72-fold decrease in the phosphorylation ratio within the 48h *PAA* group (Table 5.7: spot 484; Figure 5.2) and also a 2,2-fold decrease in the relative phosphorylation ratio within the 13 days *PAA* group (Table 5.7: spot 489; Figure 5.2). Calmodulin phosphorylation has been reported to modulate its interaction with binding partners (Leclerc *et al.*, 1999) and hence in echinoderm regenerating nervous system its function might also be to modulate the several Ca^{2+} driven signaling pathways where this protein is an important intervenient.

5.4.2. Key regeneration effectors are not differently expressed but show different phosphorylation ratios in the radial nerve cord wound healing events

Several proteins with known functions in the nervous system embryonic development, differentiation and growth have already been identified in the proteome of *M. glacialis* radial nerve cord (Chapter 2), nonetheless an injury correlated differential expression was not detected in the DIGE injured radial nerve cord experiments (Chapter 4). However, in this chapter, some of these proteins were found to have a significant variation in their relative phosphorylation ratio. This is in agreement with the currently accepted fact that the primary neuron injury signaling events are mainly based on post-translational modifications of pre-existing proteins, and/or localized protein *de novo* synthesis through axonal mRNA translation (Abe *et al.*, 2008), rather than differential genome expression. This cellular strategy compensates for the distance between the injury site and the neuron nucleus. In this study the identified Notch homologue was dephosphorylated in both regenerating groups, being only phosphorylated in the control group (Table 5.1: spot 32; Figure 5.2). Notch phosphorylation has been correlated with the inhibition of a cell differentiation signal in the 32D myeloid cell (Ingle´s-Esteve *et al.*, 2001) however; future studies are needed in order to understand the function of Notch dephosphorylation during radial nerve cord regeneration events. Two proteins with important functions in synaptic transmission, visual perception and maintenance of the nervous system architecture (Decourt *et al.*, 2005; Knobel *et al.*, 2001), namely, tubby-related protein 2 and an homologue of to the unc-119 B, were found to have different injury related phosphorylation. While tubby-related protein 2 showed a 1,4-fold increase in the relative phosphorylation ratio 48h post injury (spot 291b); the unc-119B homolog was equally phosphorylated in all experimental groups (Table 5.6: spot 263b; Figure 5.2). How the phosphorylation of tubby-related protein 2 is linked with general neuronal regeneration is still unknown, and hence future experiments using echinoderms as model organisms may further help to elucidate the functional modulation induced by this PTM in the newly regenerating radial nerve cord.

5.4.3. Transcription factors, RNA interacting proteins and intracellular transport mediators are also targets of phosphorylation in radial nerve cord early regeneration events

Downstream events are influenced by axotomy-activated kinases and include up-regulation or activation of several transcription factors (reviewed in Abe *et al.*, 2008), being also important regulators of the starfish radial nerve cord regenerative response (Chapter 4). In the present work several transcription factors that might be involved in the modulation of the proper gene expression to enable echinoderm nervous tissue functional re-growth were also found, showing an injury correlated phosphorylation such as, transcriptional activator protein Pur-alpha (Table 5.1: spot 253; Figure 5.2) and set protein, an homologue to TAF-Ibeta1 (Table 5.7: spot 202; Figure 5.2).

During axonal regeneration, mRNA transport and localized translation provide a renewable source of proteins in distal sites from the neuron nucleus. These events require a coordinated effort of several intervenients to target mRNA and regulate its individual translation. The transport of mRNA requires the formation of ribonucleoprotein complexes (RNP) that further engage the cellular transport systems (reviewed in Donnelly *et al.*, 2010). One of the proteins known to be constitutive of RNP complex, a dyskerin homologous protein (H/ACA ribonucleoprotein complex subunit 4) was found to have a 1,52-fold decrease in the relative phosphorylation ratio in the 48h *PAA* group (Table 5.7: spot 258; Figure 5.2). Although the particular role of this phosphorylation event is not known, it can be speculated that it might be modulating mRNA transport during the starfish radial nerve cord early regeneration

events. GPN-loop GTPase 2, another protein known to interact with RNA was only phosphorylated in the 48h *PAA* group (spot 359), and therefore its modulation might be an interesting target to study. Several other RNA interacting or binding proteins not showing injury related modifications were identified, such as a DEAD-box family RNA helicase (Table 5.6: spot 312; Figure 5.2), a protein known to complex with RNPs. In addition, an homologue of argonaute 11, was also found to be phosphorylated in all experimental groups (Table 5.6: spot 250; Figure 5.2). This protein has been described as responsible for controlling mRNA translation in growth cones through RNA interference (RNA*i*) (Šatkauskas *et al.*, 2007) and when phosphorylated it influences the small RNA binding capacity (Rüdel *et al.*, 2010). These evidences reinforce the importance of these proteins also for the normal starfish neuronal function.

During the local mRNA translation the co-localization of folding assistants is important to guarantee that the *de novo* synthesized proteins achieve their functional conformation to perpetrate their functions in the injury signaling events. Several chaperonine proteins were also up-regulated in the starfish radial nerve cord wound healing events and others were cleaved by proteolytic pathways (Chapter 4). It is known that heat shock proteins chaperoning functions are regulated through phosphorylation (Peake *et al.*, 1998; Zhao *et al.*, 2001), although their modulation mechanism in echinoderms still remains unknown. In the present work several gel spots from injured starfish radial nerve cord were identified as heat shock related proteins, being differently phosphorylated in comparison with the control groups. Among these are chaperone protein htpG and heat shock protein 5 which were found to be only phosphorylated in control group (Table 5.1: spots 77 and 80; Figure 5.2).

One important mechanism for nucleus-axon signaling involves the physical transport of signaling molecules from the site of injury back to the nucleus (retrograde transport) or in the opposite way, from the nucleus to injury site (anterograde transport). This type of signaling includes the transport of endosomes that further engage motor proteins like dynein, which travel along the uniformly aligned axonal microtubules (minus ends towards the neuronal body). An homologue of axonemal dynein light chain was found to be equally phosphorylated in all experimental groups (Table 5.6: spot 280a; Figure 5.2). In fact, dynein phosphorylation is known to determine the velocity of microtubule translocation (Hamasaki, 1999), highlighting the importance of dynein mediated transport in the radial nerve cord under normal conditions (*i.e.*, synaptic generated signals during neuronal plasticity), and also as part of the retrograde injury signaling events, never before characterized in an echinoderm. Other proteins related with retrograde vesicle-mediated transport were also found to be more phosphorylated at 48h following arm tip ablation, such as ADP-ribosylation factor (1,9-fold increase in the relative phosphorylation ratio, Table 5.7: spot 360; Figure 5.2), which might be specifically associated with the echinoderm injury responses.

5.4.4. Signaling neuropeptides produced through proteolytic events during injury response

Neuroendocrine convertases are members of the subtilisin family of serine proteases and are involved in the activation of precursor molecules by endoproteolytic cleavage at basic amino acid residues. Neuroendocrine Convertase-2 (NEC-2) is regarded as one of the important proteins involved in the maturation of many bioactive peptides (Muller *et al.*, 1999). It has been reported that NEC-2 and 7B2, its specific binding protein, are co-induced during neuronal differentiation (Jeannotte *et al.*, 1997), the last being inactivated by phosphorylation (Lee *et al.*, 2006). Although the direct relation between NEC-2 and phosphorylation events still remains to be clarified, in the present study an homologue of NEC-2 was identified (Table 5.7: spot 69a; Figure 5.2), showing a 1,38-fold decrease in the relative phosphorylation ratio, 48h after injury of the radial nerve cord. These results indicate that NEC-2 is probably inactivated by phosphorylation similarly to its binding partner, being probably actively involved in the maturation of important injury signaling neuropeptides.

5.5. CONCLUDING REMARKS

To study injury related protein phosphorylation dynamics during starfish radial nerve cord wound healing events, a 2DE gel based analysis was coupled

with a fluorescent stain tailored specifically for phosphoprotein detection. A fraction enriched in soluble radial nerve cord proteins was obtained after 48h and 13 days post arm tip ablation and separated in 7 cm length IEF 3.0-3.6 *NL* zoom strips. This strategy allowed the resolution of over 500 total protein spots, of which 180 had a phosphorylation signal, a considerable high number of detected phosphorylated spots when compared with similar studies (Chen *et al.*, 2010). Approximately 70% of the collected spots were successfully identified, resulting in the overall detection of 47 different proteins. Among the identified phosphorylated proteins, 30 of them showed an injury correlated phosphorylation, allowing an unprecedented glimpse over the time-dependent modulation of several injury related pathways in echinoderms regeneration events. However, this work is of preliminary nature, further impelling other confirmatory and complementary experimental approaches (*i.e.*, higher protein loads coupled with phosphopeptide enrichment and MS^n tandem experiments to unequivocally determine peptide phosphorylation sites). Nevertheless, several injury related pathways recently disclosured in echinoderm regeneration events (Chapter 4) were further confirmed and, additional information on the regulation of these pathways was obtained. In addition, proteins that were not implicated in an injury related differential protein expression pattern in the DIGE experiments (Chapter 4), were shown here to be regulated through phosphorylation/dephosphorylation events, such as the protease calpain and the neuroendocrine convertase 2. Therefore, the obtained results constitute an important first step towards the characterization of echinoderm injury signaling events modulated through protein post-translation, highlighting once more the potential of echinoderm as valuable animal models in regeneration studies.

5.6. ACKNOWLEDGMENTS

This work was supported by Fundação para a Ciência e Tecnologia through a PhD grant to Catarina Franco (SFRH/BD/29799/2006), a research contract by the Ciência 2008 program to Romana Santos and Renata Soares and a project grant (PTDC/MAR/104058/2008).

5.7. REFERENCES

Abe, N., Cavalli, V. (2008) Nerve injury signaling. Curr Opin Neurobiol. 18, 276-283.

Alpy, F., Tomasetto, C. (2005) Give lipids a START: the StAR-related lipid transfer (START) domain in mammals. J Cell Sci. 118, 2791-2801.

Ambron, R.T., Walters, E.T. (1996) Priming events and Retrograde Injury signals-A new perspective on the cellular and molecular biology of nerve regeneration. Molecular Neurobiology. 13, 61-79.

Ashmarina, L.I., Louzenko, S.E., Severin, S.E. Jr., Muronetz, V.I., Nagradova, N.K. (1988) Phosphorylation of D-glyceraldehyde-3-phosphate dehydrogenase by Ca^{2+}/calmodulin-dependent protein kinase II. FEBS Lett. 231, 413-416.

Bannister, R., McGonnell, I.M., Graham, A., Thorndyke, M.C., Beesley, P.W. (2008) Coelomic expression of a novel bone morphogenetic protein in regenerating arms of the brittle star *Amphiura filiformis*. Dev Genes Evol. 218(1), 33-38.

Beck, K. A., J. A. Buchanan, and W. J. Nelson (1997) Golgi membrane skeleton: identification, localization and oligomerization of a 195 kDa ankyrin isoform associated with the Golgi complex. J. Cell Sci. 110,1239-1249.

Bennett, V., and A. J. Baines (2001) Spectrin and ankyrin-based pathways: metazoan inventions for integrating cells into tissues. Physiol. Rev. 81,1353-1392.

Benowitz, L.I., Yin, Y. (2007) Combinatorial treatments for promoting axon regeneration in the CNS: Strategies for overcoming inhibitory signals and activating neurons' intrinsic growth state. Dev. Neurobiol. 67, 1148-1165.

Butt R. H.; Coorssen J. R. Pre-extraction Sample Handling by Automated Frozen Disruption Significantly Improves Subsequent Proteomic Analyses. J Proteome Res. 2006, 5, 437-448.

Cavalli, V., Kujala, P., Klumperman, J., Goldstein, L.S. (2005) Sunday driver links axonal transport to damage signalling. Journal of Cell Biology. 168, 775-787.

Ch´ng, T.H., Martin, KC. (2011) Synapse-to-nucleus signaling. Current Opinion in Neurobiology. 21, 1-8.

Chen, A., McEwen, M.L., Sun, S., Ravikumar, R., Springer, J.E. (2010) Proteomics and phosphoproteomic analysis of the soluble fraction following acute spinal cord contusion in rats. Journal of Neurotrauma. 27, 263-274.

Cosen-Binker, L.I., Kapus, A. (2006) Cortactin: the gray eminence of the cytoskeleton. Physiology (Bethesda). 21, 352-361.

Daly, R.J. (2004) Cortactin signalling and dynamic actin networks. Biochem. J. 382, 13-25.

De Corte, V., Gettemans, J., Vandekerckhove, J. (1997) Phosphatidylinositol 4,5-bisphosphate specifically stimulates PP60c-src catalyzed phosphorylation of gelsolin and related actin-binding proteins. FEBS Letters. 401, 191-196.

Decourt, B., Bouleau, Y., Dulon, D., Hafidi, A. (2005) Identification of differentially expressed genes in the developing mouse inferior *colliculus*. Developmental Brain Research. 159, 29-35.

Dent, E.W., Gertler, F.B. (2003) Cytoskeletal Dynamics and Transport in Growth Cone Motility and Axon Guidance. Neuron. 40, 209-227.

Donnelly, C., Fainzilber, M., Twiss, J.L. (2010) Subcellular communication through RNA transport and localized protein synthesis. Traffic. 11, 1498-1505.

Geddis, M.G., Rehder, V. (2003) The Phosphorylation State of Neuronal Processes Determines Growth Cone Formation After Neuronal Injury. Journal of Neuroscience Research. 74, 210-220.

Göhler, T., Sabbioneda, S., Green, C.M., Lehmann, A.R. (2011) ATR-mediated phosphorylation of DNA polymerase η is needed for efficient recovery from UV damage. J Cell Biol. 192(2), 219-227.

Goll, D.E., Thompson, V.F., Li, H., Wei, W., Cong, J. (2003) The calpain system. Physiol Rev. 83(3), 731-801.

Gordon-Weeks, P.R. (1993) Organization of microtubules in axonal growth cones: a role for microtubule-associated protein MAP 1B. Journal of Neurocytology. 22, 717-725.

Gumy, L.F., Tan, C.L., Fawcett, J.W. (2010) The role of local protein synthesis and degradation in axon regeneration. Exp Neurol. 223, 28-37.

Hamasaki, T. (1999) Regulation of outer-arm-dynein activity by phosphorylation and control of ciliary beat frequency. Protoplasma. 206, 241-244.

Hammarlund, M., W. S. Davis, Jorgensen, E. M. (2000) Mutations in beta-spectrin disrupt axon outgrowth and sarcomere structure. J. Cell Biol. 149, 931–942.

Heiss, N.S., Girod, A., Salowsky, R., Wiemann, S., Pepperkok, R., Poustka, A. (1999) Dyskerin localizes to the nucleolus and its mislocalization is unlikely to play a role in the pathogenesis of dyskeratosis congenita. Hum Mol Genet. 8(13), 2515-2524.

Hong, Z., Zhang, Q.Y., Liu, J., Wang, Z.Q., Zhang, Y., Xiao, Q., Lu, J., Zhou, H.Y., Chen, S.D. (2009) Phosphoproteome study reveals Hsp27 as a novel signaling molecule involved in GDNF-induced neurite outgrowth. Journal of Proteome Research. 8, 2768-2787.

Inglés-Esteve, J., Espinosa, L., Milner, L.A., Caelles, C., Bigas, A. (2001) Phosphorylation of Ser2078 Modulates the Notch2 Function in 32D Cell Differentiation. Journal of Biological Chemistry. 276, 44873-44880.

Jeannotte, R., Paquin, J., Petit-Turcotte, C., Day, R. (1997) Convertase PC2 and the neuroendocrine polypeptide 7B2 are co-induced and processed during neuronal differentiation of P19 embryonal carcinoma cells. DNA Cell Biol. 16, 1175-1187.

Job, C., Lagnado, L. (1998) Calcium and Protein Kinase C Regulate the Actin Cytoskeleton in the Synaptic Terminal of Retinal Bipolar Cells. The Journal of Cell Biology. 143, 1661-1672.

Kamal, A., Y. Ying, and R. G. Anderson (1998) Annexin VI-mediated loss of spectrin during coated pit budding is coupled to delivery of LDL to lysosomes. J. Cell Biol. 142, 937-947.

Knobel, K.M., Davis, W.S., Jorgensen, E.M., Bastiani, M.J. (2001) UNC-119 suppresses axon branching in *C. elegans*. 128, 4079-4092.

Kovács, L., Alexa, A., Klement, E., Kókai, E., Tantos, A., Gógl, G., Sperka, T., Medzihradszky, K.F., Tözsér, J., Dombrádi, V., Friedrich, P. (2008) Regulation of calpain B from *Drosophila melanogaster* by phosphorylation. The FEBS Journal. 276, 4959-4972.

Kuo, W.N., Ganesan, U., Davis, D.L., Walbey, D.L. (1994) Regulation of the phosphorylation of calpain II and its inhibitor. Molecular and Cellular Biochemistry. 136, 157-161.

Kwiatkowski, D.J. (1999) Functions of gelsolin: motility, signaling, apoptosis, cancer. Current Opinion in Cell Biology. 11, 103-108.

Leclerc, E., Corti, C., Schmid, H., Vetter, S., James, P., Carafoli, E. (1999) Serine/threonine phosphorylation of calmodulin modulates its interaction with the binding domains of target enzymes. Biochem. J. 344, 403-411.

Lee, S.N., Hwang, J.R., Lindberg, I. (2006) Neuroendocrine Protein 7B2 Can Be Inactivated by Phosphorylation within the Secretory Pathway. The Journal of Biological Chemistry. 281, 3312-3320.

Leung, T.H.Y., Ching, H.P., Yam, J.W.P., Wong, C.M., Yau, T.O., Jin, D.Y., Ng, I.O.L. (2005) Deleted in liver cancer 2 (DLC2) suppresses cell transformation by means of inhibition of RhoA activity. PNAS. 102, 15207-15212.

Lowery, L.A., Vactor, D.V. (2009) The trip of the tip: understanding the growth cone machienery. Nature Reviews Molecular Cell Biology. 10, 332-343.

Martin, K.H., Jeffery, E.D., Grigera, P.R., Shabanowitz, J., Hunt, D.F., Parsons, J.T. (2006) Cortactin phosphorylation sites mapped by mass spectrometry. J Cell Sci. 119, 2851-2853.

Matsui, T., Maeda, M., Doi, Y., Yonemura, S., Amano, M., Kaibuchi, K., Tsukita, S. (1998) Rho-kinase phosphorylates COOH-terminal threonines of ezrin/radixin/moesin (ERM) proteins and regulates their head-to-tail association. J Cell Biol 140, 647-657.

Matten, W.T., Aubry, M., West, J., Maness, P.F. (1990) Tubulin Is Phosphorylated at Tyrosine by pp60 $^{c\text{-}src}$ in Nerve Growth Cone Membranes. The Journal of Cell Biology. 111, 1959-1970.

Michaelevski, I., Segal-Ruder, Y., Rozenbaum, M., Medzihradszky, K.F., Shalem, O., Coppola, G., Horn-Saban, S., Ben-Yaakov, K., Dagan, S.Y., Rishal, I., Geschwind, D.H., Pilpel, Y., Burlingame, A.L., Fainzilber, M. (2010) Signaling to Transcription Networks in the Neuronal Retrograde Injury Response. Science Signaling. 3, ra53. [DOI: 10.1126/scisignal.2000952].

Mohler, P.J., Gramolini, A.O., Bennett, V. (2002) Ankyrins. Journal of Cell Science. 115, 1565-1566.

Muller, L., Lindberg, I. (1999) The cell biology of the prohormone convertases PC1 and PC2. Prog Nucleic Acid Res Mol Biol. 63, 69-108.

Murabe, N., Hatoyama, H., Hase, S., Komatsu, M., Burke, R.D., Kaneko, H., Nakajima, Y. (2008) Neural architecture of the Brachiolaria larvae of the starfish, *Asterina pectinifera*. The Journal of comparative Neurology. 509, 271-282.

Neuhoff, V., Harold, N., Ehrhardt, W. Improved staining of proteins in polyacrylamide gels including isoelectric focusing gels with clear background at nanogram sensitivity using Coomassie Brilliant Blue G-250 and R-250. Electrophoresis. 1988, 9, 255-262.

Nicolas, G., Fournier, C.M., Galand, C., Malbert-Colas, L., Bournier, O., Kroviarski, Y., Bourgeois, M., Camonis, J.H., Dhermy, D., Grandchamp, B., Lecomte, M.C. (2002) Tyrosine Phosphorylation Regulates Alpha II Spectrin Cleavage by Calpain. Molecular and Cellular Biology. 22, 3527-3536.

Nierkerk, E.A.V., Willis, D.E., Chang, J.H., Reumann, K., Heise, T., Twiss, J.L. (2007) Sumoylation in axons triggers retrograde transport of the RNA-binding protein La. PNAS. 31, 12913-12918.

Ortiz-Pineda, P.A., Ramírez-Gómez, F., Pérez-Ortiz, J., González-Díaz, S., Santiago-De Jesús, F., Hernández-Pasos, J., Valle-Avila, C.D., Rojas-Cartagena, C., Suárez-Castillo, E.C., Tossas, T., Méndez-Merced, A.T., Roig-López, J.L., Ortiz-Zuazaga, H., García-Arrarás, J.E. (2009) Gene expression profiling of intestinal regeneration in the sea cucumber. BMC Genomics. 10, 262.

Oshiro, N., Fukata, Y., Kaibuchi, K. (1998) Phosphorylation of Moesin by Rho-associated Kinase (Rho-kinase) Plays a Crucial Role in the Formation of Microvilli-like Structures. The Journal of Biological Chemistry. 273, 34663-34666.

Peake, P., Winter, N., Britton, W. (1998) Phosphorylation of Mycobacterium leprae heat-shock 70 protein at threonine 175 alters its substrate binding characteristics. Biochimica et Biophysica Acta. 1387, 387-394.

Perlson, E., Hanz, S., Ben-Yaakov, B., Segal-Ruder, Y., Seger, R., Fainziber, M. (2005) Vimentin-dependent special translocation of an activated MAP kinase in inured nerve. Neuron. 34, 715-726.

Pottiez, G., Haverland, N., Ciborowski, P. (2010) Mass spectrometric characterization of gelsolin isoforms. Rapid Commun. Mass Spectrom. 24, 2620-2624.

Rossi, F., Gianola, S., Corvetti, L. (2007) Regulation of intrinsic neuronal properties for axon growth and regeneration. Prog. Neurobiol. 81, 1-28.

Rüdel, S., Wang, Y., Lenobel, R., Körner, R., Hsiao, H.H., Urlaub, H., Patel, D., Meister, G. (2010) Phosphorylation of human Argonaute proteins affects small RNA binding. Nucleic Acids Research. 39, 2330-2343.

Šatkauskas, S., Bagnard, D. (2007) Local Protein Synthesis in Axonal Growth Cones. Cell Adhesion & Migration 1, 179-184.

Sosa L., Dupraz, S., Laurino, L., Bollati, F., Bisbal, M., Caceres, A., Pfenninger, K.H., Quioga, S. (2006) IGF- 1 receptor is essential for the establishment of hippocampal neuronal polarity. Nat Neuroscience. 9, 993-995.

Spira, M.E., Oren, R., Dormann, A., Ilouz, N., Lev, S. (2001) Calcium, protease activation, and cytoskeleton remodeling underlie growth cone formation and neuronal regeneration. Cellular and Molecular Neurobiology. 21, 591-604.

Suárez-Castillo, E.C., Medina-Ortíz, W.E., Roig-López, J.L., García-Arrarás, J.E. (2004) Ependymin, a gene involved in regeneration and neuroplasticity in vertebrates, is overexpressed during regeneration in the echinoderm Holothuria glaberrima. Gene. 334, 133-143.

Sun, F., Cavalli, V. (2010) Neuroproteomics approaches to decipher neuronal regeneration and degeneration. Molecular and cellular proteomics. 9, 963-975.

Tehrani, S., Tomasevic, N., Weed, S., Sakowicz, R., Cooper, J.A. (2007) Src phosphorylation of cortactin enhances actin assembly. Proc Natl Acad Sci U S A. 104(29), 11933-11938.

Wandosel, F., Serrano, L., Avila, J. (1997) Phosphorylation of a-Tubulin Carboxyl-terminal Tyrosine Prevents its Incorporation into Microtubules. The Journal of Biological Chemistry. 262, 8268-8273.

Wang, H., Satir, P. (1998) The 29 kDa light chain that regulates axonemal dynein activity binds to cytoplasmic dyneins. Cell Motil Cytoskeleton. 39, 1-8.

Wang., Y., Yang, F., Fu, Y., Huang, X., Wang, W., Jiang, X., Gritsenko, M.A., Zhao, R., Monore, M.E., Pertz, O.C., Purvine, S.O., Orton, D.J., Jacobs, J.M., Camp II, D.G., Smith, R.D., Klemke, R.L. (2011) Spatial phosphoprotein profiling reveals a compartmentalized Erk switch governing neurite growth and retraction. Journal of Biological Chemistry. doi:10.1074/jbc.M111.236133.

Willis, D., Li, K.W., Zheng, J.Q., Chang, J.H., Smit, A., Kellly, T., Merianda, T.T., Sylvester, J., Minnen, J.V., Twiss, J.L. (2005) Differential transport and local translation of cytoskeletal, injury-response, and neurodegeneration protein mRNAs in axons. The Journal of Neuroscience. 26, 778-791.

Zhao, W.G., Gilmore, R., Leone, G., Coffey, M.C., Weber, B., Lee, P.W.K. (2001) Hsp90 Phosphorylation Is Linked to Its Chaperoning Function. The Journal of Biological Chemistry. 276, 32822-32827.

CHAPTER 6

GENERAL DISCUSSION AND FUTURE PROSPECTS

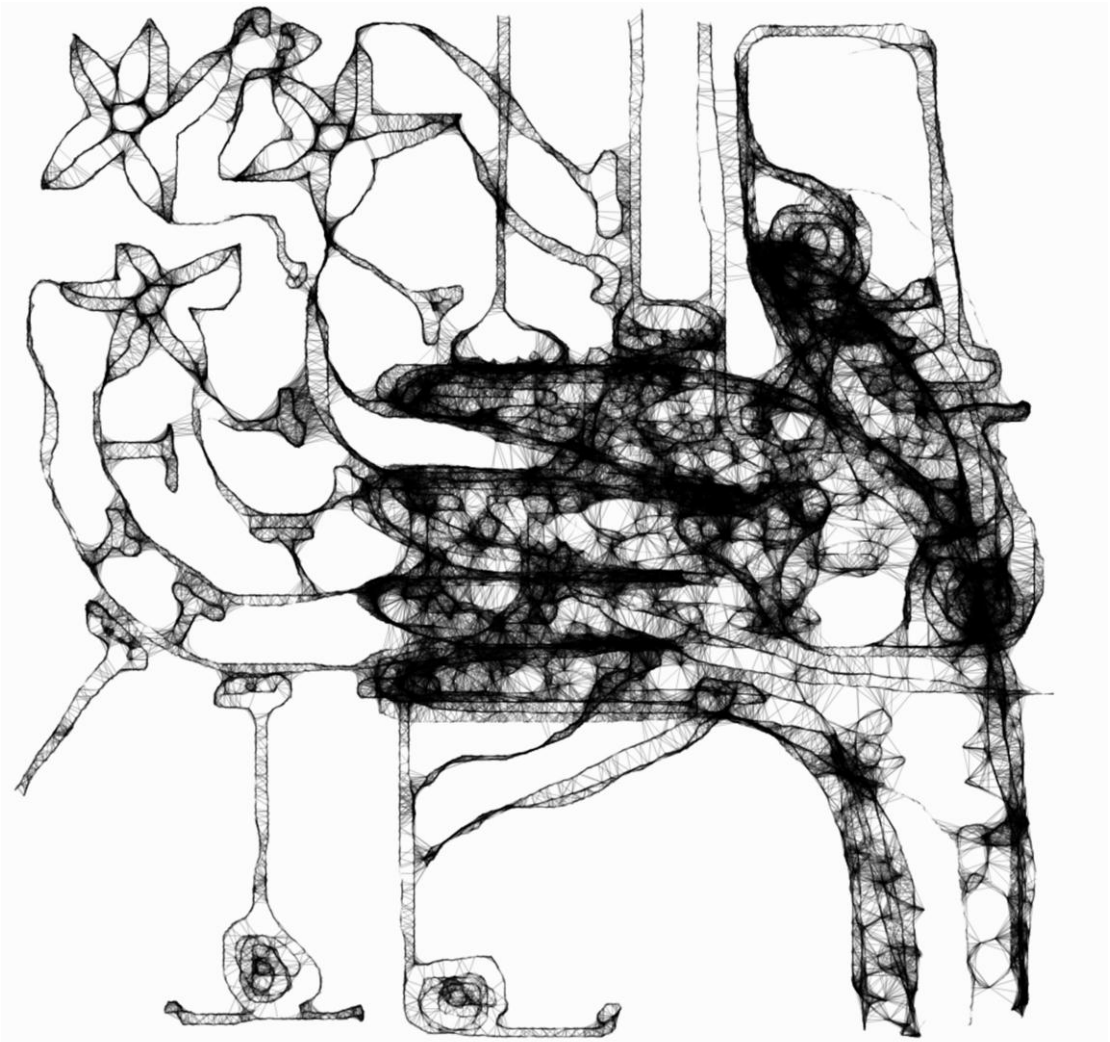

Image: "What have we learned?"

"Regeneration – the regrowth or repair of cells, tissues and organs – is widely but non-uniformly represented among animal phyla. Regenerative strategies include the rearrangement of pre-existing tissue, the use of adult somatic stem cells and the dedifferentiation and/or transdifferentiation of cells, with more than one mode possible to co-exist in different tissues of the same animal. As well as being a fascinating biological problem, regeneration has long attracted biomedical interest because of the potential of replacing old or damaged tissues with new ones." (Alvarado et al., 2006)

Since most of regenerative studies are aimed at biomedical applications, they are usually focused on research using stem cells *in vitro*. However, to gain a full understanding of regeneration, the related processes must be studied *in vivo*, in the context of complex interactions that take place in the different cell types involved. Within this perspective, model organisms that stand out for their amazing intrinsic regenerative abilities are essential for such *in vivo* interrogations, which can provide us with the necessary knowledge to eventually manipulate and control regenerative properties. However, in spite of the wide choice of potential models for studying regeneration, this phenomenon has been explored in detail only in few, vertebrates and invertebrates, such as amphibian urodeles and planarians, respectively (Alvarado *et al*., 2006). Nowadays, surprising gaps in the knowledge of many animal groups with striking regenerative capacities still persist, which is the case of echinoderms. At present only some pieces of this intriguing jigsaw have started to be assembled, using either transcriptomics (Rojas-Cartagena *et al.,* 2007; Ortiz-Pineda *et al*., 2009; Sun, 2011) or individual gene candidate approaches (Bannister *et al*., 2005; Patruno *et al*., 2002; Patruno *et al*., 2003; Thorndyke *et al*., 2001b; Ikuta *et al.*, 2011), and although proteomic approaches have proven to be very promising methodologies in the field of regeneration (Sun *et al*., 2010), so far no such studies were employed to further increase the knowledge on the molecular pathways behind echinoderms regenerative machinery. Within this context, *Marthasterias glacialis*, one of the most common starfish species in the Portuguese coast was selected as an animal model to understand tissue regeneration dynamics using a set of proteomic and mass spectrometry approaches.

After the necessary optimization of regeneration induction and collection of starfish tissues, the first set of regeneration experiments were conducted and, a gel based differential proteomics was employed to study proteome changes in the starfish radial nerve cords; the cell free coelomic fluid and coelomocytes. In two-dimensional electrophoresis, every sample represents a new challenge that needs careful optimization towards optimal resolution. Salt ions are one of the most common causes of interference during isoelectric focusing of proteins. Starfish tissues are known to have an elevated content of salts, 3% (w/v) when compared with 0.9% (w/v) content of vertebrate tissues. To compensate the high tissue salinity and avoid sample loss associated with the desalting procedures, the IEF programs were carefully adjusted. This involved several strategies such as, the use of custom made paper wicks placed between the electrodes and the *pH* strips, allowing the removal of salts during the first low voltage steps of the IEF program; and optimization of the different IEF voltage steps based on trial and error events according to sample conductivity.

Colloidal Coomassie stain (Neuhoff *et al*., 1988) was then used to detect and relatively quantify the resolved proteins of the referred proteomes. However, no significant protein expression changes were found between the regenerating groups and the respective controls. Nevertheless, the performed 2DE gels contained an unprecedented rich and valuable source of information which included approximately 403, 315 and 126 resolved protein spots of the radial nerve cord, the coelomocytes and the cell free coelomic fluid, respectively. The proteomic characterization of the referred tissues was then performed using the control 2DE gels. This strategy allowed also to evaluate the success of the homology-driven proteomic characterization of the different starfish analyzed tissues.

6.1. The starfish radial nerve cord proteome

Despite a thorough characterization of echinoderms nervous system morphology, so far, the only large scale molecular characterization performed relies on the genomic information derived from the sea urchin sequenced genome (Burke *et al.*, 2006). Although this set of information allowed an unprecedented glimpse into the echinoderms molecular neuro-architecture, genomic data does not reflect the proteins being expressed, which is the closest source of information to a real phenotype. This information together with protein post-translational modifications, which dictate every step in the life-cycle of a protein, can be retrieved using proteomic-mass spectrometry approaches. However, no such studies providing large-scale identification of echinoderm nervous system proteins were performed. For this reason, we aimed to contribute to withdraw echinoderm nervous system from one of the least studied metazoan category, by performing the first proteomic characterization of the intact nerve cord (2DE) and also of several different subcellular protein enriched fractions such as, soluble, membrane and synaptosomal membrane proteins.

Altogether, 905 proteins were identified across the several radial nerve cord protein fractions, allowing to identify several molecular pathways responsible for echinoderms nervous system functions. This first proteomic characterization also allowed to perceive that, although echinoderms present a neural organization that distinguishes them from other deuterostomes, at the proteome level, there is a remarkable homology. Furthermore, this set of information was also significant to highlight the importance of echinoderms as interesting and easy to manipulate animal models that despite possessing a simpler morphology, present a far more complex nervous system than initially thought. More importantly, the homology found with chordate spinal cord reinforced the possibility that echinoderm regeneration events are more likely to be extended to mammals than those observed in other classical models, such as hydra or planarians.

The proteomic characterization of the radial nerve cord was also important to determine the fractions to be studied in the regeneration experiments. A relevant increase on the number of identified proteins was achieved after performing the fractionation into soluble and membrane enriched fractions and, adding a peptide separation step (nano-LC) prior to mass spectrometry analysis. Henceforth, both soluble and membrane fractions were selected for the subsequent characterization of the radial nerve cord proteome dynamics during regeneration.

6.2. Coelomic fluid and coelomocytes proteomes

In contrast with the nervous system, echinoderms immune responses have been extensively studied, and guaranteed a Nobel Prize awarded to Metchinikoff in 1908 due to his pioneer demonstration of phagocytosis and encapsulation using starfish larvae immunocytes (Metchinikoff, 1891). Nevertheless, it is still possible to find contradicting opinions related with the type of immune responses that echinoderms elicit upon challenge.

Even though echinoderms immune responses have been extensively studied, so far, proteomic approaches were only very modestly applied to understand the molecular pathways responsible for the multitasks enrolled by these cells within echinoderm biology. For this reason, we performed the proteome characterization of the coelomocytes and the cell free coelomic fluid. This last is known to be very rich in proteins secreted by the coelomocytes and the surrounding tissues. Interestingly, distinct success rates of protein identification were obtained amongst the two analyzed proteomes, with 85% and 10% of the selected protein spots being identified in coelomocytes and cell free coelomic fluid proteomes, respectively.

The low success of protein identification of the coelomic fluid proteins highlights two main points:

1) **Coelomic fluid is rich in glycoproteins**; glycosylation is one of the most common protein post-translation modification of secreted proteins and since the bound oligosaccharide chains were not removed (digestion with glycosidases preceding trypsin digestion) prior to MALDI-TOF/TOF mass spectrometry it may have hindered protein identification, since most of the fragments in the MS/MS spectra correspond most likely to sugar losses due to this labile modification, thus resulting in sparse information of the peptide sequence (Mann *et al*., 2003). Also, the few CFF proteins inferred from *de novo* sequenced peptides are known glycoproteins, such as fibrinogen, lectin-like proteins and a glycosyltransferase, further confirming the "glycosylation hypothesis";

2) **The need to sequence other echinoderm species genomes**; the lectins identified in this study through peptide sequence inference from the tandem mass spectra (*de novo* sequencing), are known to belong to a very heterogeneous protein family, which has also been proven to be the case for echinoderms (Smith *et al*., 2011). Of the predicted *de novo* sequences, only two peptides were matched to echinonectin and echinoidin, the remaining of the predicted sequences either shared homology with lectins from other organisms or, had no homology match. This may derive from erroneous sequence inference (due to glycosylation) or, simply because starfish lectins may differ in sequence from the sea urchin genome predicted lectins. Similar cases can be observed when comparing the few starfish sequenced proteins, such as a START protein from the starfish *Asterina pectinifera* that shares only 40% homology with the sea urchin START protein.

Despite the low success of protein identification within CFF, both proteomes already allowed an unparalleled look into proteins being expressed at these echinoderm tissues. These comprehensive lists of proteins are of extreme importance as a ground-work that will lead to future studies, which might clarify the homology with vertebrate immune cells, *i.e*., with the identification of immunoglobulin-like proteins, or reveal the pathways responsible for coelomocytes functions during starfish regeneration events.

Nonetheless, in order to extend this proteomic characterization, new methodologies for the preparation of coelomocyte subcellular fractions, and the enrichment or depletion of low or abundant proteins will need to be developed. Furthermore, future differential proteomic experiments might help to understand how coelomocytes regulate their pathways during regeneration to create a growth permissive environment that enables the complete and functional regeneration of lost tissues.

Also of extreme importance would be to perform the coelomic fluid peptidome analysis, as the secreted/originated peptides might have important biological functions, such as mediating important cellular communication events, especially during arm regeneration events. During my PhD, I had the opportunity also to optimize protocols for the coelomic fluid peptidome analysis. These methods either included a step-wise peptide enrichment in microcolumns with different reverse phase materials prior to MALDI-TOF/TOF MS analysis or, using micro-LC ESI-linear ion trap analysis. Unfortunately, due to time constraints, such methods still remain to be applied to characterize and quantify the coelomic fluid peptidome during starfish arm regeneration events and are of extreme interest as future approaches.

6.3. The differential proteome of a regenerating radial nerve cord

Since the first set of proteomic experiments did not reveal significant changes between control and regenerating starfish tissues, a second approach was designed to increase both protein resolution and detection sensitivity. Consequently, the radial nerve cord was selected in detriment of the initial proposed set of tissues due to its obvious interest, since it is a nervous system with amazing intrinsic regeneration abilities. To increase protein separation and resolution, two new approaches were undertaken; ***1)*** the fractionation of the total radial nerve cord into soluble and membrane proteins and, ***2)*** the use of several *pH* range IEF strips (wide range, 3-10; acid *pH* ranges of 3-5.6NL and 5.3-6.5). Protein detection sensitivity was also dramatically increased by labeling samples with fluorescent Cyanine Dyes (DIGE approach). The introduction of an internal standard, as part of the typical DIGE experimental design, also improved the inherent gel-to-gel spot variations. The numbers of biological replicates used in the experiments were also increased to six animals, which according to power analysis was sufficient to account for biological variability. The combination of these new approaches allowed recovering from a *non*-significant statistical difference between control and regenerating radial nerve cords, to having 13% of the resolved protein spots with significant spot volume variations. However, the majority of the spots with significantly different volume variation had an expression profile related with their position in the 2DE gel: the spots in the high molecular mass (*M*) region of the gel appeared to be more abundant in the control radial nerve cords; and the spots in the low *M* of the 2DE gel were more abundant in the regenerating radial nerve cords. This trend in expression was immediately associated with proteolytic events somehow related with regeneration, which were regulating protein amounts at the injury site by complete proteolytic degradation or, by highly regulated proteolytic events, determinant for effective and fast regulation of protein functions in different neuronal spatial localizations.

Amongst the several pathways known to be key regulators of axonal regeneration, several of them were identified in this study also as regulators of neuronal regeneration in echinoderms. These include a vast number of Rho GTPases and actin and microtubule regulators that, according to the results obtained, seem to indicate that the several pathways that govern cytoskeleton dynamics are oriented towards neuronal re-growth as soon as 48h post-arm tip ablation. Several axon guidance molecules; RNA binding and transport; transcription factors; kinases; lipid signaling effectors were also identified. A number of proteins that control the oxidation state and share neuroprotective functions within other neuroregeneration animal models were also identified to be *de novo* synthesized in the regenerating starfish radial nerve cords and include ferritin, peroxiredoxin and lysozyme C.

6.4. Gel based proteomics shows the difference between mammals and invertebrate nerve injury models in terms of the proteolytic pathways activated

Curiously, when searching through the literature for similar proteolytic events related with *in vivo* nervous system regeneration or injury, two distinct situations were found, the occurrence or absence of proteolysis during nerve regeneration events depending on the studied animal model:

In mammal models of spinal cord injury, only one recent paper (Chen et al., 2010) reports that proteolysis may be enhanced in the injured spinal cord, due to the identification of a 20 kDa fragment of the neurofilament light chain together with the phosphorylation of ubiquitin carboxyl terminal hydrolase L1 in the injured spinal cord and the dephosphorylation of cathepsin, associated with its activation upon injury. Nevertheless, authors do not draw hypothesis on such observations. Several other similar papers using mammal's spinal cord injury models, and gel based approaches, do not mention nor observe proteolysis in such extent has the observed in the radial nerve cord of the regenerating starfish (Table 6.1). Intriguingly, protease activation in mammals' nervous system is often described as associated with different neuropathological disorders, and it is commonly suggested that protease inhibitors might be important therapeutic targets for such disorders as also for traumatic brain injury (Saatman *et al*., 2010).

However, it seems that invertebrate *in vivo* models, which are known for their intrinsic growth abilities, tell different stories. The mollusks have long attracted attention as animal models for regeneration studies due to their large neurons, capacity for functional regeneration and anatomical simplicity. Of particular interest is one study in which Eran Perlson and colleagues (Perlson *et al*., 2004) used differential 2DE approach to identify injury-correlated retrogradely transported proteins in nerves of the mollusk *Lymnaea*. In this study, the authors conclude that retrograde injury signaling may be mediated by soluble protein complexes arising from **cleavage** or **modification** of a wide variety of axonal proteins. This is the first *in vivo* report of a wide number of proteins cleaved by proteolysis during nerve regeneration processes, and also the first report of a wide number of proteins having apparent masses above expected, a fact suggested by the authors as a result of ubiquitination or cross-linking of protein species. In subsequent publications, using the same *Lymnaea* neurons in culture, the same authors additionally prove that a calpain generated proteolytic fragment of an intermediate filament sterically hinders the dephosphorylation of a positive injury signal (phosphorylated *Erk*) during its retrograde transport journey back to the cell body (Perlson *et al*., 2005; Perlson *et al*., 2006).

Table 6.1: Summary of the most important highlights of several studies using two-dimensional electrophoresis (2DE) to understand nervous system injury.

Reference	Animal model	Tissue	Protein fraction	2DE detection method	Resolution	Differently expressed proteins	Reference to proteolysis	Important notes
Kang *et al.*, 2006	rat	Spinal cord	Total protein fraction	Silver stain	947 spots	66 proteins (42 up-regulated; 24 down-regulated)	No	Most of the identified proteins migrated according to their theoretical *pI* and *M*; Some of the described rat spinal cord injury related up-regulated proteins are common with starfish injured radial nerve cord up-regulated proteins such as peroxiredoxin, which is correlated with wound healing response.
Jiménez *et al.*, 2005	rat	Sciatic nerve	Total protein fraction	Sypro-Ruby	1500 spots	121 proteins (74 up-regulated; 47 down-regulated)	No	pPCR analysis only confirmed some of the up-regulated proteins; mRNA levels of several down-regulated proteins did not show any change in the tissues, although proteins showed profound down-regulation. Authors propose that these proteins may be synthesized locally by Schwann cells, or alternatively, *de novo* synthesized within the regenerating axons by means of axonal mRNAs.
Yan *et al.*, 2010	rat	Spinal cord	Total protein fraction	Coomassie Brilliant Blue	Not described	51 proteins (categorized according to expression profiles clusters)	No	mRNA levels confirmed the expression of 6 different genes; No comment on the *M* of the identified proteins
Afjehi-Sadat *et al.*, 2010	rat	Spinal cord	Total protein fraction	Colloidal Coomassie Blue	319 spots	9	No	Authors report the occurrence of protein post-translational modifications induced by free oxygen radical attack on proteins indicating oxidative stress induced by spinal cord trauma.
Chen *et al.*, 2010 *Phophopr oteomic analysis	rat	Spinal cord	Soluble protein fraction	Sypro-Ruby	1500 Sypro-Ruby spots; 100 Pro-Q spots	26 proteins with different expression and phosphorylation ratios following acute spinal cord contusion	Yes	Authors report to have found several protein redundancies across different 2DE gel spots and attribute this effect to either proteolysis, post-translational modifications or protein isoforms; Authors further suggest that protein degradation pathways may be enhanced in spinal cord injury: cathepsin was found to be dephosphorylated after injury and; Ubiquitin carboxyl terminal hydrolase L1 significantly increased post injury.
Singh *et al.*, 2009	rat	Spinal cord	Crude synaptosoma l fraction	Silver stain	1500 spots	27 proteins (25 up-regulated; 2 down-regulated)	No	Only one differently expressed protein was successfully confirmed by western blot analysis which leads the authors recognize that nerve injury might modulate subcellular protein distribution. Authors also recognize that nerve injury might modulate protein functions, i.e., by post translational modifications; without affecting gene expression during injury.
Perlson *et al.*, 2004	Mollusk	Nerves	Soluble protein fraction and two membrane fractions	Silver stain	4000 spots across 8 different combinations of *pI* and *M* ranges	172 spots; Only 40 different proteins were successfully identified	Yes	Authors report the occurrence of different post-translational modifications such as *N*-terminal acetylation and glycosylation and sulfonation of threonine and serine residues. In addition authors also report the existence of several proteolytic cleavage fragments of the identified proteins or conversely variants with increased mass associated with injury.

6.5. Proteolysis occurs in regenerating neurons and fails in non-regenerating one: Insights from in vitro studies

The first reports that describe proteolytic events as being related with neuronal regeneration date back to the early 90's. In these *in vitro* studies it was observed a significant increase of N-terminal argynilation and ubiquitination of proteins in regenerating sciatic nerves (Jack *et al*., 1992). In opposition, in the optic nerve, which has a poor regenerative ability, N-argynilation failed to occur (Shyne-Athwal *et al*., 1988). It was only later that the proteasome machinery was first co-localized in the growth-cones of regenerating neurons (Campbell *et al*., 2001]. Recent studies where cultured neurons were treated with several proteasome inhibitors clearly demonstrated that axonal outgrowth in newly plated neurons is severely inhibited and that in established cultures, in which the axonal outgrowth is reduced in a dose dependent decrease (Klimascheweski *et al*., 2006). Moreover, all evidences point to the important role that UPS components perform in regenerating axons, nevertheless, nowadays still very few mechanisms have been proposed to explain how it actually takes place.

Similarly, treating cultured neurons with calpain inhibitors prevents growth cone formation if calpeptin is added before axotomy or, if added 5 min post-axotomy, there is the formation of a growth cone with expanding lamellipodia but at a much slower growth rate (Sahly *et al*., 2006). Clearly, protein catabolic pathways are determinant and indispensable during regeneration events, yet, have been given much less consideration than protein synthesis.

Our study joins the group of the sparse studies aiming to characterize the effect of the proteolytic pathways in the proteome of an *in vivo* regenerating nervous system. In the future, studies aiming to decipher which are the pathways specifically controlled by which proteolytic pathway will be important to validate several of the proposed hypotheses and, will ultimate help to clarify the mechanisms in which proteolysis is determinant. This knowledge might be important to further modulate the proteolytic pathways in non-regenerating-mammalian neurons, which clearly are inactivated/impaired when comparing with invertebrate models with high regeneration capacities.

In summary, we propose that several different pathways have protein intervenients modulated through proteolysis. Interestingly several of these pathways are already known to be key propellers of neuronal regeneration, further highlighting the importance of proteolytic events which hopefully, will be an incentive for future investments in research aiming to clarify the role of proteolysis as:

- A motor for generating injury signals that will modulate gene expression/cellular metabolism towards regeneration. To clarify these hypotheses, I strongly believe in a research line centered on the individual impact of the several proteolytic fragments generated during regeneration, involving characterization of peptides and their biological activities using *in vitro* cultures;

- These hypotheses will then need to be tested in *in vivo* models, and I believe that echinoderms, starfish in particular, can provide us with very interesting experimental approaches. For instance, by inhibiting proteolytic pathways in the wound area, which will allow testing the impact of individual proteolytic fragments and pathways, searching for a functional rescue of regeneration.

One strong validation of the importance of these hypotheses is the recently published paper (King *et al*., 2010) in which the authors examined the neuroprotective effect of fibronectin derived peptides, by placing a solution of fibronectin peptides into a rat spinal cord injury site. The treated animals showed a decrease in lesion size, apoptosis, and axonal damage within the first week post injury when comparing with the sham animals.

As demonstrated, future experiments are limitless and I strongly believe that they will lead to some interesting breakthroughs, especially in the field of degradomics behind regeneration events.

6.6. The preliminary analysis of the regenerating radial nerve cord phosphoproteome seems to confirm some of the previously proposed hypothesis

The last experimental set of my PhD involved a preliminary characterization of the phosphoproteome dynamics during regeneration events. Unfortunately, due to protein amount limitations, this analysis was limited only to the wound healing stages (48h and 13 days post-arm tip ablation), which was also interesting, since it is widely accepted that the role of post-translational modifications are determinant in the initial stages of regeneration.

To characterize the radial nerve cord phosphoproteome following arm tip ablation, a 2DE gel based proteomic approach together with specific phosphoprotein staining (Pro-Q diamond) was used. Although short length strips were used (7cm) it was possible to achieve the resolution of 554 protein spots in the *pH* range of 3-5.6 *NL*. Together with the Pro-Q Diamond, a total protein stain (Sypro Ruby) was also used in order to determine the phosphorylation ratio per protein spot. Altogether, the dynamics of protein phosphorylation seem to confirm several of the previously proposed hypotheses. For instance, calpain and its preferred substrate, spectrin, were found to be differently phosphorylated in the regenerating radial nerve cords, which correlates with calpain mediated cleavage of spectrin.

Also fascinating was the identification of several proteins that did not have a significantly altered spot volume in terms of total protein amount , but showed a significant variation in terms of phosphorylation dynamics which is correlated with the hypothesis that post-translational modifications are modulating the activities of certain proteins without the involvement of differential expression events. This was the case of a neuroendocrine convertase, a protein that is known to be involved in the maturation of neuropeptides. Neuropeptides are known to be discharged through stimulus-induced exocytosis of large dense-core vesicles with the plasma membrane (Zhao *et al*., 2011). These important signaling peptides can enroll several different functions (Strand *et al*., 1991), for instance in spinal cord, neuropeptides function as neurotransmitters conveying information about both acute pain and the chronic pain associated with nerve injury and inflammation, particularly in a subpopulation of neurons, known as nociceptors. Since neuropeptides distribution has been reported to vary during the neuronal regrowth process of the starfish *Asterias rubens* (Moss *et al*., 1998), these results suggest that neuropeptides might also have important regeneration-related functions and hence, future characterization and quantification of these bioactive peptides present in the radial nerve cord, in both normal and injury conditions, is also of extreme relevance.

Although the radial nerve cord phosphoproteome dynamics characterization confirmed some of previously suggested hypothesis, it is imperative to perform complementary experimental approaches, such as phosphopeptide enrichment and tandem MS^n experiments that will unequivocally determine peptide phosphorylation sites and thus confirm the attained results and, eventually increase the number of proteins that might be modulated through phosphorylation during radial nerve cord regeneration events.

7. SUMMARY OF CONCLUSIONS

7.1. Proteomic characterization of starfish tissues highlights the importance of echinoderms as relevant animal models

Using a gel based approach (1D and 2D electrophoresis) in combination with mass spectrometry; we performed the first proteomic characterization of the starfish *Marthasterias glacialis* radial nerve cord (Chapter 2), coelomocytes and cell free coelomic fluid (Chapter 3).

In **Chapter 2** it is described the first proteomic characterization of the radial nerve cord of an echinoderm. The initial proteomic characterization was performed using a total protein extract separated by 2DE. In an extra effort to identify radial nerve cord low abundant proteins, several different subcellular fractions separated by 1DE were also analyzed and include both soluble and membrane fractions and a synaptosomal membrane proteins enriched fraction. Altogether, 905 different proteins were identified for the first time in an echinoderm radial nerve cord. Although this proteomic characterization was important to perceive the functional complexity of these deuterostomes nervous system and to validate many of the proteins predicted in the sea urchin genome (Burke *et al*., 2006), the most important highlight relies on the corroboration of the use of echinoderms as important animal models. These deuterostomes of simpler morphology and easy manipulation, are here highlighted as promising animal models for the emerging field of neuroproteomics, especially due to their amazing ability to functionally regenerate their nervous system upon injury, whose knowledge might provide us with valuable insights on which pathways might be responsible for such trait, that later might even be transposed as targets to be studied in other model organisms, namely mammals.

In **Chapter 3**, the fundamental proteomic characterization of starfish tissues was extended to their immune effector cells, the coelomocytes, and to the cell-free coelomic fluid, the inner body fluid of the starfish. The identification of 358 proteins in the starfish coelomocytes allowed to infer several different pathways which justify the multiplicity of functions enrolled by these cells, such as clotting reactions, phagocytosis, encapsulation, nodule formation and secretion of antibacterial and antifungal proteins. These include several proteins responsible for cytoskeleton regulation, that substantiate the capacity of these cells to perform a rapid morphological transition; several proteins involved in diverse signaling events and also proteins that belong to *wnt* signaling pathway, which might play a role in the initial stages of regeneration, in which coelomocytes are also known to have important functions. The cell-free coelomic fluid clearly has a simpler proteome as observed in the number of resolved proteins in the 2DE, most of the identified proteins being related with antibacterial and immune functions. In addition, several peptides were successfully *de novo* sequenced and presented high homology with lectin like proteins, a heterogeneous group of glycoproteins that participate in immune response, either inducing bacterial agglutination or acting as opsonins to enhance phagocytosis by coelomocytes. Also several proteins with known antibacterial activity were also identified, such as lysozyme and enolase. A fibrinogen like protein was also identified, which is also involved in clotting reactions. Altogether this study represented the first high throughput proteomic characterization of echinoderm coelomic fluid circulating cells, the coelomocytes and of the secreted proteins to the coelomic fluid.

7.2. Echinoderms reveal new insights in the neuroregeneration events

In **Chapter 4** it is described the first proteomic based experiment to understand the functional regeneration ability of echinoderms nervous system. Using several different *pH* range strips and fluorescent detection by pre-labeling radial nerve cord protein subcellular fractions (soluble and membrane) with Cyanine Dyes

(DIGE) allowed a resolution of 7329 spots of which 944 showed injury correlated different regulation in the several analyzed regeneration events, wound healing (WH) - 48h, 13 days post arm tip ablation; and functional radial nerve cord re-growth (RG) - 10 weeks post arm tip ablation. Unexpectedly, in both wound healing and tissue re-growth regeneration stages, over 90% (260 proteins) and 64% (230 proteins) of the identified proteins, respectively, were identified as proteolytic cleavage fragments or conversely with variants with increased molecular mass that may represent ubiquitinated species. Although proteolytic pathways are widely accepted as having important roles in regeneration events, very few mechanisms have been proposed to elucidate such functions. With this work we propose that starfish radial nerve cord regeneration events implicate regulated proteolysis that modulate several distinct pathways such as cytoskeleton and microtubule regulators, axon guidance molecules. Although similar results were obtained in mollusk neurons (Perlson *et al*., 2004), the proposed hypothesis should be validated using different proteomic approaches such as PROTOMAP (Dix *et al*., 2008), and further complemented with *in vitro* or *in vivo* experiments.

The response of neurons to an injury relies on a fast cascade of events that will eventually initiate and modulate regeneration. For this reason it is not surprising that the initial stage of the injury mediated response has to be focused on modifying or activating proteins at the injury site and hence, protein post-translational modifications are irrevocably important for such response. In **Chapter 5** we described the preliminary characterization of radial nerve cord proteins phosphorylation dynamics during the early stages of arm regeneration. Altogether, 47 different proteins showing phosphoprotein signal with a specific phosphoprotein stain, were identified by MALDI-TOF/TOF mass spectrometry of which, 30 proteins showed an injury related phosphorylation dynamics during starfish radial nerve cord wound healing. The different pathways modulated through phosphorylation/dephosphorylation events are related to cytoskeleton re-organization towards the formation of the neuronal growth cones; membrane rearrangements; actin filaments and microtubules dynamics; mRNA binding and transport; lipid signaling; Notch pathway; calcium activated pathways regulated through calmodulin binding and neuropeptide processing.

"…in a fast bondage he bound Prometheus, the devious planner, whipping the painful bindings over a column at midpoint, and against him sent a long-winged eagle to feed on his liver, which was immortal; but whatever this long-winged bird ate during the day grew during the night again to perfection."

In: The Theogony (The birth of gods)

A poem by the ancient Greek poet Hesiod (8th-7th century BC) describing the punishment of Prometheus for the crime of stealing fire from Zeus and giving it to mortals.

Prometheus having his liver eaten by an eagle. Painting by Jacob Jordaens (1640).

The natural curiosity of mankind has always led him to question the ability of some species to fully regenerate lost body parts, or in case of humans, the mysterious reasons that allows some tissues/organs to retain this capacity, as here illustrated by the liver of Prometheus, a capacity also shared with common mortals, even though not accomplished overnight, as opposed to other tissues that have completely lost the ability to regenerate after trauma.

Nowadays, this curiosity has already led to amazing advances in regenerative medicine, using biologically inductive 3-dimentional scaffolds, either constituted by transplanted biological tissues (Gilbert, 2007) or extracellular matrix mimetic materials, which can support cell adhesion, differentiation, and proliferation and at the same time limit noxious immune responses (Ambrosio *et al*., 2010; Gonçalves *et al*., 2011; Martins *et al*., 2011). Despite the considerable advances, the more we learn about regeneration in any system, the more we realize how complex the phenomenon of regeneration really is. For instance, so far the complete regeneration of CNS components such as the spinal cord is yet to be reported. Even though stem cells were viewed as a panacea that can cure an amazing variety of illnesses, the complexity of the interactions and the regulatory systems, the variety of tissues and organs these cells differentiate into, has so far impaired the success of direct transplantation onto wound sites to restore missing or damaged tissues (Murry, 2004). For this reason, studying how invertebrate animal models or lower vertebrate deploy and regulate stem cells or rearrange the cells surrounding the wound towards tissue repair and regeneration is likely to provide us with answers on why these processes are not readily activated in mammals.

Consequently I strongly believe that echinoderms stand to provide us with important missing links and for this reason I finish this thesis by putting forth a table of future experiments (Table 8.1), which I consider will be the next steps towards understanding echinoderms wonderful regenerative abilities.

Table 8.1. Examples of future proteomic based experiments using echinoderms as regeneration models.

	Experiment	Hypothesis	Description	Challenges
Differential proteomes	Coelomocytes differential proteome characterization during starfish arm regeneration events	Determine which are the pathways responsible for the involvement of coelomocytes in early regeneration events	Gel based proteomic approach of several coelomocytes subcellular fractions (DIGE)	Coelomocytes subcellular fractionation optimization
	Cell free coelomic fluid differential proteome characterization during starfish arm regeneration events	Identify the secreted factors that might be mediating cell-to-cell communication events during regeneration	Gel based proteomic approach (DIGE)	Secreted proteins tend to be highly glycosylated. Optimization of protein identification is necessary.
PTMs in regeneration	High throughput phosphoproteomics of the radial nerve cord regeneration	Validate the preliminary results obtained and extend the phosphorylation dynamics characterization to other radial nerve cord subcellular fractions	Gel based proteomic approach or gel free MS^n approach to unequivocally identify phosphopeptides	The need to enrich in phosphopeptides
	Characterization of radial nerve cord *degradome* during regeneration	Validate the results from the DIGE experiments and characterize proteolytic fragments generated during regeneration	1DE gel based approach sliced according *M* with subsequent protein identification for the sequence coverage determination (Dix, 2008; PROTOMAP approach)	Sequence coverage evaluation may be compromised due to the lack of starfish genome information
***In vivo* experiments**	*In vivo* inhibition of proteolysis	Determine the effects of proteolytic pathways selective inhibition on the intrinsic regeneration ability of the starfish	Selective inhibition of the proteolytic pathways using specific inhibitors locally administrated on the wound site	Optimization of the local administration of the inhibitors (hydrogels; scaffolds) which need to be maintained in a aqueous environment without the risk of contaminating the water
	In vivo rescue of regeneration	Are the proteolytic fragments enough to rescue regeneration?	If regeneration is inhibited by the local administration of protease inhibitors, it would be interesting to try to rescue regeneration by individual administration of proteolytic fragments on site	Peptide enrichment and purification

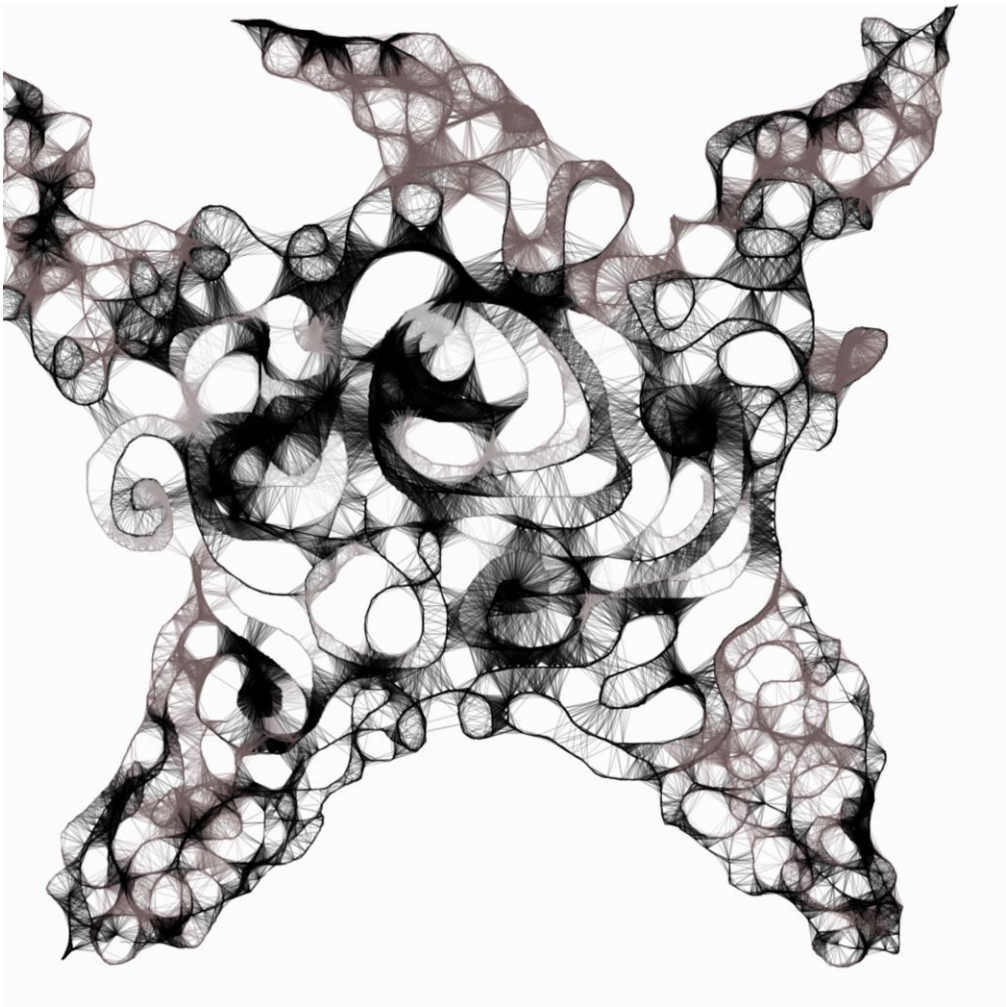

Image: "Starfish"

Abe, N., Cavalli, V. (2008) Nerve injury signaling. Curr Opoin Neurobiol. 18, 276-283.

Afjehi-Sadat, L., Brejnikow, M., Kang, S. U., Vishwanath, V., Walder, N., Herkner, K., Redl, H., Lubec, G. (2010) Differential protein levels and post-translational modifications in spinal cord injury of the rat. Journal of Proteome Research. 9, 1591-1597.

Agata, K., Saito, Y., Nakajima, E. (2007) Unifying the principles of regeneration I: Epimorphosis versus morphallaxis. Develop. Growth Differ. 49, 73-78.

Agata, K., Soejima, Y., Kato, K., Kobayashi, C., Umesono, Y., Watanabe, K. (1998) Structure of the planarian central nervous system (CNS) revealed by neuronal cell markers. Zool. Sci. 15, 433–440.

Al-Sharif, W. Z., Sunyer, J. O., Lambris, J. D., Smith, L. C. (1998) Sea urchin coelomocytes specifically express a homologue of the complement component C3. J. Immunol. 160, 2983.

Alvarado, A.S., Tsonis. (2006) Bridging the regeneration gap: genetic insights from diverse animal models. Nature Reviews Genetics. 7, 873-884.

Alvares, K., Dixit, S.N., Lux, E., Barss, J., Veis, A. (2007) The proteome of the developing tooth of the sea urchin, *Lytechinus variegatus*: mortalin is a constituent of the developing cell syncytium. J Exp Zool B Mol Dev Evol. 308(4), 357-370.

Ambrosio, F., Wolf, S., Delito, A., Fitzgerald, G.K., Badylak, S.F., Boninger, M.L., Russel, A.J. (2010) The emerging relashionship between regenerative medicine and physical therapeutics. Physical Therapy. 90, 1807-1814.

Andersson, L., Bohlin, L., Iorizzi, M., Riccio, R., Minale, L., Moreno-López, W. (1989). Biological activity of saponins and saponin-like compounds from starfish and brittlestars. Toxicon. 27(2),179−188.

Bannister, R., McGonnell, I.M., Graham, A., Thorndyke, M.C., Beesley, P.W. (2005) Afuni, a novel transforming growth factor-β gene is involved in arm regeneration by the brittle star *Amphiura filiformis*. Dev. Genes Evol. 215, 393-401.

Batts, L.E., Polk, D.B., Dubois, R.N., Kulessa, H. (2006) Bmp signaling is required for intestinal growth and morphogenesis. Dev. Dyn. 235, 1563-1570.

Baum, B., Settleman, J., Quinlan, M. P. (2008) Transitions between epithelial and mesenchymal states in development and disease. Semin. Cell Dev. Biol. 19, 294-308.

Bavington, C.D., Lever, R., Mulloy, B., Grundy, M.M., Page, C.P., Richardson, N.V., McKenzie, J.D. (2004) Anti-adhesive glycoproteins in echinoderm mucus secretions. Comp Biochem Physiol B Biochem Mol Biol. 139(4), 607-617.

Beauchemin, M., Noiseux, N., Tremblay, M., Savard, P. (1994) Expression of Hox A11 in the limb and the regeneration blastema of adult newt. Int. J. Dev. Biol. 38, 641-649.

Beck, C. W., Christen, B., Slack, J. M. (2003) Molecular pathways needed for regeneration of spinal cord and muscle in a vertebrate. Dev. Cell 5, 429–439.

Beck, C.W., Christen, B., Barker, D., Slack, J.M. (2006) Temporal requirement for bone morphogenetic proteins in regeneration of the tail and limb of Xenopus tadpoles. Mech. Dev. 123, 674-688.

Beck, G., Habicht, G.S. (1991) Primitive cytokines: harbingers of vertebrate defense. Immunol. Today. 12, 1980-183.

Beck, G., O´Brian, R.F., Habicht, G.S. (1989) Invertebrate cytokines: the phylogenic emergence of interleukin-1. Bioessays, 11, 62-67.

Blair, J.E., Hedges, S. (2005) Molecular phylogeny and divergence times of deuterostome animals. Mol. Biol. Evol. 22, 75-84.

Bonasoro, F., Ferro, P., Di Benedetto, C., Sugni, M., Mozzi, D., Carnevali, M.D.C. (2004) Regenerative potencial of echinoid test. In: Heinzeller, T. & Nebelsick L.H (eds.) Echinoderms: Munchen, Taylor & Francis Groups, London. 97-103.

Brillouet, C., Leclerc, M., Panijel, J., Binaghi, R. (1981) In vitro effect of various mitogens on starfish (*Asterias rubens*) axial organ cells. Cell Immunol. 57(1), 136-44.

Brockes, J.P. (1997) Amphibian Limb Regeneration: Rebuilding a Complex Structure. Science. 276, 81-87.

Broun, M., Sokol, S., Bode, H. R. (1999) Cngsc, a homologue of goosecoid, participates in the patterning of the head, and is expressed in the organizer region of Hydra. Development 126, 5245–5254.

Bryant, D. M., Stow, J. L. (2004) The ins and outs of E-cadherin trafficking. Trends Cell Biol. 14, 427-434.

Buchli, A. D., Schwab, M. E. (2005) Inhibition of Nogo: a key strategy to increase regeneration, plasticity and functional recovery of the lesioned central nervous system. Ann. Med. 37, 556–567.

Buonanno, A., Fischbach, G.D. (2001) Neuregulin and ErbB receptor signaling pathways in the nervous system. Curr. Opin. Neurobiol. 11, 287-296.

Burke, R.D., Angerer, L.M., Elphick, M.R:, Humphrey, G.W., Yaguchi, S., Kiyama, T., Liang, S., Mu, X., Agca, C., Klein, H.W., Brandhorst, B.P., Rowe, M., Wilson, K., Churcher, A.M., Taylor, J.S., Chen, N., Murray, G., Wang, D., Mellott, D., Olinski, R., Hallböök, F., Thorndyke, M.C. (2006) A genomic view of the sea urchin nervous system. Dev Biol. 300, 434-460.

Butt, R.H., Coorssen, J.R. (2005) Pre-extraction Sample Handling by Automated Frozen Disruption Significantly Improves Subsequent Proteomic Analyses. Journal of Proteome Research. 5, 437-448.

Byrne, M. (1994) Ophiuroidea. In: Harisson, F.W:, Chia, F.S: (eds) Microscopic anatomy of invertebrates. Vol. 14. Echinodermata. Wiley-Liss, New York. 247-344.

Cabrera-Serrano, A., García-Arrarás, J.E. (2004) RGD-Containing Peptides Inhibit Intestinal Regeneration in the Sea Cucumber *Holothuria glaberrima*. Developmental Dynamics 231, 171-178.

Camenisch, T. D., Schroeder, J. A., Bradley, J., Klewer, S. E., McDonald, J. A. (2002) Heart-valve mesenchyme formation is dependent on hyaluronan-augmented activation of ErbB2-ErbB3 receptors. Nat. Med. 8, 850-855.

Campbell, D.S., Holt, C.E. (2001) Chemotropic responses of retinal growth cones mediated by rapid local protein synthesis and degradation. Neuron. 32, 1013-1026.

Canicatti C, Roch P. (1989) Studies on *Holothuria polii* (Echinodermata) antibacterial proteins. I. Evidence for and activity of coelomocyte lysozyme. Experientia. 45(8), 756‑759.

Canicatti, C., Rizzo, A. (1991) A 220 kDa coelomocyte aggregating factor involved in *Holothuria polii* cellular clotting. Eur. J. Cell Biol. 56, 79-83.

Carlson, B. (2007) Principals of regenerative biology. Academic Press-Elsevier. USA.

Carnevali, M.D., Bonasoro, F. (2001) A microscopic overview of crinoid regeneration. Microsc. Res. Tech. 55, 403-426.

Carnevali, M.D., Lucca, E., Bonasoro, F. (1993) Mechanisms of arm regeneration in the feather star *Antedon mediterranea*: healing of wound and early stages of development. J. Exp. Zool. 267, 299-317.

Carnevali, M.D.C. (2006) Regeneration in echinoderms: repair, regrowth and cloning. Invert. Surv. J. 3, 64-76.

Carnevali, M.D.C., Bonasoro, F., Biale, A. (1997) Pattern of bromodeoxyuridine incorporation in the advanced stages of arm regeneration in the feather star *Antedon mediterranea*. Cell Tissue Res. 289, 363-374.

Carnevali, M.D.C., Thorndyke, M.C., Matranga, V. (2009) Regenerating echinoderms; a promise to understand stem cells potencial. In: Rinkevich, B., Matranga, V. (eds.) Stem cells in marine organisms. Heidelberg: Springer. 165-186.

Carroll, J. M., Luetteke, N. C., Lee, D. C., Watt, F. M. (1998) Role of integrins in mouse eyelid development: studies in normal embryos and embryos in which there is a failure of eyelid fusion. Mech. Dev. 78, 37-45.

Cavey, M.J.; Märkel, K. (1994) In F.W. Harrison and F.S. Chia (eds.). Microscopic anatomy of invertebrates. Vol 14:Echinodermata. Wiley-Liss, New York, 169-245.

Cebrià, F., Nakazawa, M., Mineta, K., Ikeo, K., Gojobori, T., Agata, K. (2002) Dissecting planarian central nervous system regeneration by the expression of neural-specific genes. Dev. Growth Differ. 44, 135–146.

Chen, A., McEwen, M.L., Sun, S., Ravikumar, R., Springer, J.E. (2010) Proteomic and phosphoproteomic analyses of the soluble fraction following acute spinal cord contusion in rats. Journal of neurotrauma. 27, 263-274.

Chera, S., de Rosa, R., Miljkovic-Licina, M., Dobretz, K., Ghila, L., Kaloulis, K., Galliot, B. (2006) Silencing of the hydra serine protease inhibitor Kazal1 gene mimics the human SPINK1 pancreatic phenotype. J. Cell Sci. 119, 846–857.

Chia, F.S.; Xing, J. (1996) Echinoderm coelomocytes. Zool. Stud. 35: 231-254.

Christofori, G. (2003) Changing neighbours, changing behaviour: cell adhesion molecule-mediated signalling during tumour progression. EMBO J. 22, 2318-2323.

Churchward, M.A., Butt, R.H., Lang, J.C., Hsu, K.K., Coorssen, J.R. (2007) Enhanced detergent extraction for analysis of membrane proteomes by two-dimensional gel electrophoresis. Proteome Science. 3(1), 5.

Ciruna, B., Rossant, J. (2001) FGF signaling regulates mesoderm cell fate specification and morphogenetic movement at the primitive streak. Dev. Cell. 1, 37-49.

Cobb, J.L.S (1995) The nervous systems of Echinodermata: recent results and new approaches. In: Breidbach, O., Kutsh, W. (eds). The nervous systems of invertebrates: an evolutionary and comparative approach. Birkhäuser, Basel, Boston, Berlin. 407-424.

Condic, M. L. (2001) Adult neuronal regeneration induced by transgenic integrin expression. J. Neurosci. 21, 4782–4788.

Consortium, Sea Urchin Sequencing. The genome of the sea urchin *Strongylocentrutus purpuratus*. Science. 2006, 10, 941-952.

Coteur, G., DeBecker, G., Warnau, M., Jangoux, M., Dubois, P. (2002) Differentiation of immune cells challenged by bacteria in the common European starfish, *Asterias rubens* (Echinodermata). Eur. J. Cell Biol. 81, 413-418.

Cuenot, L. (1948) Anatomie, ethologie et systematique des echinodermes. In Traité de Zoologie. Vol. XI. Edited by P.P. Grassé. Masson, Paris. 1–363.

de Craene, B., van Roy, F., Berx, G. (2005) Unraveling signalling cascades for the Snail family of transcription factors. Cell. Signal. 17, 535-547.

de Faria, M.T., da Silva, J.R. (2008) Innate immune response in the sea urchin *Echinometra lucunter* (Echinodermata). J. Invertebr. Pathol. 98: 58-62.

Delcommenne, M., Tan, C., Gray, V., Rue, L., Woodgett, J., Dedhar, S. (1998) Phosphoinositide-3-OH kinase dependent regulation of glycogen synthase kinase 3 and protein kinase B/AKT by the integrin-linked kinase. Proc. Natl. Acad. Sci. U.S.A. 95, 11211-11216.

Delmotte, F., Brillouet, C., Leclerc, M., Luquet, G., Kader, J.C. (1986) Purification of an antibody-like protein from the sea star *Asterias rubens* (L.) Eur J Immunol. 16(11), 1325-1330.

Deng, W., Lin, H. (2002) *miwi*, a murine homolog of piwi, encodes a cytoplasmic protein essential for spermatogenesis. Dev. Cell 2, 819–830.

Dheilly, N. M., Haynes, P.A., Bove, U., Nair, S.V., Raftos, D.A. (2011) Comparative proteomic analysis of a sea urchin (*Heliocidaris erythrogramma*) antibacterial response revealed the involvement of apextrin and calreticulin. Journal of Invertebrate Pathology. 106, 223-229.

Dheilly, N. M., Nair, S.V., Smith, L.C., Raftos, D.A. (2009) Highly Variable Immune-Response Proteins (185/333) from the Sea Urchin, *Strongylocentrotus purpuratus*: Proteomic Analysis Identifies Diversity within and between Individuals. The Journal of Immunology. 182, 2203-2212.

Dix, M.M., Simon, G.M., Cravatt, B.F. (2008) Global mapping of the topography and magnitude of proteolytic event in apoptosis. Cell. 134, 679-691.

Dohadwala, M., Yang, S.-C., Luo, J., Sharma, S., Batra, R. K., Huang, M., Lin, Y., Goodglick, L., Krysan, K., Fishbein, M.C., Hong, L., Lai, C., Cameron, R.B., Gemmill, R.M., Drabkin, H.A., Dubinett, S.M. (2006) Cyclooxygenase-2-dependent regulation of E-cadherin: prostaglandin E2 induces transcriptional repressors ZEB1 and Snail in non-small cell lung cancer. Cancer Res. 66, 5338-5345.

Dubois, P., Ameye, L. (2001) Regeneration of spines and pedicellariae in echinoderms: a review. Micr. Res. Tech. 55, 427-437.

Dunwoodie, S. L. (2009) The role of hypoxia in development of the mammalian embryo. Dev. Cell. 17, 755-773.

Duong, T. D., Erickson, C. A. (2004) MMP-2 plays an essential role in producing epithelial-mesenchymal transformations in the avian embryo. Dev. Dyn. 229, 42-53.

Dupont, S., Thorndyke, M.C. (2006) Growth or differentiation? Adaptive regeneration in the brittlestar *Amphiura filiformis*. J Exp Biol. 209, 3873-3881.

Dupont, S., Thorndyke, M.C. (2007): Bridging the regeneration gar: insights from echinoderm models. Nature reviews Genetics. Letter to Editor.

Echeverri, K., Tanaka, E. M. (2002) Ectoderm to mesoderm lineage switching during axolotl tail regeneration. Science 298, 1993–1996.

Egeblad, M., Werb, Z. (2002) New functions for the matrix metalloproteinases in cancer progression. Nat. Rev. Cancer. 2, 161-174.

Eliseikina, M.G., Magarlamov, T.Y. (2002) Coelomocyte morphology in the holothurians *Apostichopus japonicus* (Aspidochirota: Stichopodidae) and *Cucumaria japonica* (Dendrochirota: Cucumariidae). Russian J. Mar. Biol. 28: 197-202.

Endean, R. (1966) The coelomocytes and coelomic fluids. In: Boolootian RA (ed), Physiology of Echinodermata, Intersciences, New York.

Erickson, C. A. (1987). Behavior of neural crest cells on embryonic basal laminae. Dev. Biol. 120, 38-49.

Fenn, J. B., Mann, M.; Meng, C. K., Wong, S. F., Whitehouse, C. M. (1989) Electrospray ionization for mass spectrometry of large biomolecules. Science. 246 (4926), 64-71.

Ferreres, F., Pereira, D.M., Gil-Izquierdo, A., Valentão, P., Botelho, J., Mouga, T., Andrade, P.B. (2010) HPLC-PAD-atmospheric pressure chemical ionization-MS metabolite profiling of cytotoxic carotenoids from the echinoderm *Marthasterias glacialis* (spiny sea-star). J Sep Sci. 33(15), 2250-2257.

Franco, C.F., Santos, R., Coelho, A.V. (2011A) Exploring the proteome of an echinoderm nervous system: 2-DE of the sea star radial nerve cord and the synaptosomal membranes subproteome. Proteomics. 11(7), 1359-1364.

Franco, C.F., Santos, R., Coelho, A.V. (2011B) Proteome characterization of sea star coelomocytes - The innate immune effector cells of echinoderms. Proteomics. 11(17), 3587-3592.

Fujita, Y., Krause, G., Scheffner, M., Zechner, D., Leddy, H. E. M., Behrens, J., Sommer, T., Birchmeier, W. (2002) Hakai, a c-Cbl-like protein, ubiquitinates and induces endocytosis of the E-cadherin complex. Nat. Cell Biol. 4, 222-231.

Furber, K.L., Dean, K.T., Coorssen, J.R. (2010) Dissecting the mechanism of Ca^{2+}-triggered membrane fusion: probing protein function using thiol reactivity. Clin Exp Pharmacol Physiol. 37(2), 208-217.

García-Arrarás, J.E., Díaz-Miranda, L., Torres, I.I., File, S., Jiménez, L.B., Rivera-Bermudez, K., Arroyo, E.J., Cruz, W. (1999) Regeneration of the enteric nervous system in the sea cucumber *Holothuria glaberrima*. J Comp Neurol. 406(4), 461-475.

García-Arrarás, J.E., Dolmatov, I.Y. (2010) Echinoderms; potential model systems for studies on muscle regeneration. Curr Pharm Des. 16 (8), 942-955.

García-Arrarás, J.E., Torres-Avilan, I., Ortiz-Miranda, S. (1991) Cells in the intestinal system of holothurians (Echinodermata) express cholecytokinin-like immunoreactivity. Gen Comp. Endocrinol. 83, 233-242.

Gardiner, D.M., Bryant, S.V. (1996) Molecular mechanisms in the control of limb regeneration: the role of homeobox genes. Int. J. Dev. Biol. 40, 797-805.

Gauci, V.J., Wright, E.P., Coorssen, J.R. (2010) Quantitative proteomics: assessing the spectrum of in-gel protein detection methods. J Chem Biol. 4(1), 3-29.

Gilbert, T.W., Stewart-Akers, A.M., Simmons-Byrd, A., Badylak, S.F. Degradation and remodeling of small intestinal submucosa in canine Achilles tendon repair. J. Bone Joint Surg Am. 89, 621-630.

Glinski Z, Jarosz J. 2000. Immune phenomena in echinoderms. Archivum Immunologiae et Therapiae Experimentalis. 48, 189-193.

Goldfrab, A.J. (1909) The influence of the nervous system in regeneration. J. Exp. Zool. 7, 643-722.

Gonçalves, I.C., Martins, M.C., Barbosa, J.N., Oliveira, P., Barbosa, M.A., Ratner, B.D. (2011) Platelet and leukocyte adhesion to albumin binding self-assembled monolayers. J Mater Sci Mater Med. 22(9), 2053-2063.

Görg, A., Weiss, W., Dunn, M.J. (2004) Current two-dimensional electrophoresis technology for proteomics. Proteomics. 4, 3665-3685.

Grant, S.G., Marshall, M.C., Page, K.L., Cumiskey, M.A., Armstrong, J.D. (2005) Synapse proteomics of multiprotein complexes: en route from genes to nervous system diseases. Hum. Mol. Genet. 14, (suppl 2): 225-234.

Guder, C. Pinho, S., Nacak, T.G., Schmidt, H.A., Hobmayer, B., Niehrs, C., Holstein, T.W. (2006) An ancient Wnt-Dickkopf antagonism in Hydra. Development 133, 901–911.

Gurley, K.A., Rink, J.C., Sanchez Alvarado, A. (2008) Beta-catenin defines head versus tail identity during planarian regeneration and homeostasis. Science. 319(5861), 323-327.

Gustavson, M. D., Crawford, H. C., Fingleton, B., Matrisian, L. M. (2004) Tcf binding sequence and position determines b-catenin and Lef-1 responsiveness of MMP-7 promoters. Mol. Carcinog. 41, 125-139.

Hall, A., Giovanna, L. (2011) Rho and Ras GTPases in axon growth, guidance, and branching. Cold Spring Harbor Perspect Biol. 2, a001818.

Handberg-Thorsager, M., Fernandez, E., Salo, E. (2008) Stem cells and regeneration in planarians. Front Biosci. 13, 6374-6394.

Hao, E. Tyrberg, B., Itkin-Ansari, P., Lakey, J.R.T., Geron, I., Monosov, E.Z., Barcova, M., Mercola, M., Levine, F. (2006) β-cell differentiation from nonendocrine epithelial cells of the adult human pancreas. Nature Med. 12, 310–316.

Harada, M., Qin, Y., Takano, H., Minamino, T., Zou, Y., Toko, H., Ohtsuka, M., Matsuura, K., Sano, M., Nishi, J., Iwanaga, K., Akazawa, H., Kunieda, T., Zhu, W., Hasegawa, H., Kunisada, K., Nagai, T., Nakaya, H., Yamauchi-Takihara, K., Komuro, I. (2005) G-CSF prevents cardiac remodeling after myocardial infarction by activating the Jak-Stat pathway in cardiomyocytes. Nat. Med. 11, 305-311.

Harris, L.R., Churchward, M.A., Butt, R.H., Coorssen, J.R. (2007) Assessing Detection Methods for Gel-Based Proteomic Analyses. Journal of Proteome Research. 6, 1418-1425.

Hay, E. D. (2005) The mesenchymal cell, its role in the embryo, and the remarkable signaling mechanisms that create it. Dev. Dyn., 233, 706-720.

Hayashi, T., Asami, M., Higuchi, S., Shibata, N., Agata, K. (2006) Isolation of planarian X-ray-sensitive stem cells by fluorescence activated cell sorting (FACS). Dev. Growth Differ. 48, 371–380.

Hayashi, T., Mizuno, N., Takada, R., Takada, S., Kondoh, H. (2006) Determinative role of Wnt signals in dorsal iris-derived lens regeneration in newt eye. Mech Dev. 123(11), 793-800.

Henry, M.D., Campbell, K.P. (1996) Dystroglycan: an extracellular matrix receptor linked to the cytoskeleton. Curr. Opin. Cell Biol. 8, 625–631.

Henzel, W.J., Billeci, T.M., Stults, J.T., Wong, S.C., Grimley, C., Watanabe, C. (1993) Identifying proteins from two-dimensional gels by molecular mass searching of peptide fragments in protein sequence databases. Proc Natl Acad Sci U S A. 90(11), 5011-5015.

Hernroth, B., Farahani, F., Brunborg, G., Dupont, S., Dejmek, A., Sköld, H.N. (2010) Possibility of mixed progenitor cells in sea star arm regeneration. Journal of Experimental Zoology (Mol. Dev. Evol.). 314B, 1-11.

Hobmayer, B. Rentzsch, F., Kuhn, K., Happel, C.M., von Laue, C.C., Snyder, P., Rothbächer, U., Holstein, T.W. (2000) WNT signalling molecules act in axis formation in the diploblastic metazoan Hydra. Nature 407, 186–189.

Holm, K.; Dupont, S.; Sköld, H.; Stenius, A.; Thorndyke, M.; Hernroth, B. (2008) Induced cell proliferation in putative hematopietic tissues of the sea star, Asterias rubens. The Journal Exp Biol. 211: 2551-2558.

Holstein, T. W., Hobmayer, E., David, C. N. (1991) Pattern of epithelial cell cycling in hydra. Dev. Biol. 148, 602–611.

Hood, J. D., Cheresh, D. A. (2002) Role of integrins in cell invasion and migration. Nat. Rev. Cancer. 2, 91-100.

Huet, M. (1975) Le role du sytème nerveux au cours de la régénération du Brás chez une Etoile de mer: *Asterina gibbosa* Penn. (Echinoderme, Astéride). J. Embryol. Exp. Morph. 33(3), 535-552.

Ikuta, T. (2011) Evolution of Invertebrate Deuterostomes and Hox/ParaHox Genes. Genomics Proteomics Bioinformatics. 9(3), 77-96.

Irie, H. Y., Pearline, R. V., Grueneberg, D., Hsia, M., Ravichandran, P., Kothari, N., Natesan, S., Brugge, J.S. (2005) Distinct roles of Akt1 and Akt2 in regulating cell migration and epithelial-mesenchymal transition. J. Cell Biol. 171, 1023-1034.

Ito, M., Yang, Z., Andl, T., Cui, C., Kim, N., Millar, S.E., Cotsarelis, G. (2007) Wnt dependent *de novo* hair follicle regeneration in adult mouse skin after wounding. Nature. 447(7142), 316-320.

Jack, D.L., Chakraborty, G., Ingoglia, N.A. (1992) Ubiquitin is associated with aggregates of arginine modified proteins in injured nerves. Neuroreport. 3, 47-50.

Jadlowiec, J., Koch, H., Zhang, X., Campbell, P.G., Seyedain, M., Sfeir, C. (2004) Phosphophoryn regulates the gene expression and differentiation of NIH3T3, MC3T3-E1, and human mesenchymal stem cells via the integrin/MAPK signaling pathway. J. Biol. Chem. 279, 53323-53330.

James, P., Quadroni, M., Carafoli, E., Gonnet, G. (1993) Protein identification by mass profile fingerprinting. Biochem Biophys Res Commun. 195, 58–64.

Jefferies, R.P.S., Brown, N.A., Daley, P.E.J. (1996) The early phylogeny of chordates and echinoderms the origin of chordates left-right asymmetry and bilateral symmetry. Acta. Zool. 77, 101-122.

Jiménez, C.R., Stam, F.J., Li, K.W., Gouwenberg, Y., Hornshaw, M.P., Winter, F.D., Verhaagen, J., Smit, A.B. (2005) Proteomics of the injured rat sciatic nerve reveals protein expression dynamics during regeneration. Molecular and Cellular Proteomics. 4, 120-132.

Jung, H., Lee, K. P., Park, S. J., Park, J. H., Jang, Y. S., Choi, S. Y., Jung, J.G., Jo, K., Park, D.Y., Yoon, J.H., Park, J.H., Lim, D.S., Hong, G.R., Choi, C., Park, Y.K., Lee, J.W., Hong, H.J., Kim, S., Park, Y.W. (2007) TMPRSS4 promotes invasion, migration and metastasis of human tumor cells by facilitating an epithelial-mesenchymal transition. Oncogene. 27, 2635-2647.

Junqueira, M., Spirin, V., Santana Balbuena, T., Thomas, H., Adzhubei, I., Sunyaev, S., Shevchenko, A. (2008) Protein identification pipeline for the homology-driven proteomics. Journal of Proteomics. 71, 349-356.

Kaneshiro, E.; Karp, R. (1980) The ultrastructure of coelomocytes of the sea star *Dermasterias imbricata*. Biol. Bull. 159: 295-310.

Kang, S., K., So, H., H., Moon, Y.S., Kim, C.H. (2006) Proteomic analysis of injured spinal cord tissue proteins using 2-DE and MALDI-TOF MS. Proteomics. 6, 2797-2812.

Karas, M., Bachmann, D.; Hillenkamp, F. (1985) Influence of the Wavelength in High-Irradiance Ultraviolet Laser Desorption Mass Spectrometry of Organic Molecules. Anal. Chem. 57 (14), 2935-2939.

Karhadkar, S.S., Bova, G.S., Abdallah, N., Dhara, S., Gardner, D., Maitra, A., Isaacs, J.T., Berman, D.M., Beachy, P.A. (2004) Hedgehog signalling in prostate regeneration, neoplasia and metastasis. Nature 431, 707-712.

Kiffmeyer, W. R., Tomusk, E. V., Mescher, A. L. (1991) Axonal transport and release of transferrin in nerves of regenerating amphibian limbs. Dev. Biol. 147, 392–402.

Kim, J.B., Leucht, P., Lam, K., Luppen, C., Ten Berge, D., Nusse, R., Helms, J.A. (2007) Bone regeneration is regulated by wnt signaling. J Bone Miner Res. 22(12), 1913-1923.

King, H. (1898) Regeneration in *Asterias vulgaris*. Arch. Entw Mech. Org. 7, 351-363.

King, V.R., Hewazy, D., Alovskaya, A., Phillips, J.B., Brown, R.A., Priestley, J.V. (2010) The neuroprotective effects of fibronectin peptides following spinal cord injury in the rat. Neuroscience. 168, 523-530.

Klimascheweski, L., Hausott, B., Ingorokva, S., Pfaller, K. (2006). Constitutively expressed catalytic proteoasomal subunits are up-regulated during neuronal differentiation and required for axon initiation, elongation and maintenance. J. Neurochem. 96, 1708-1717.

Klimaschewski, L., Nindl, W., Feurle, J., Kavakebi, P., Kostron, H. (2004) Basic fibroblast growth factor isoforms promote axonal elongation and branching of adult sensory neurons *in vitro*. Neuroscience 126, 347–353.

Kobayashi, C., Kobayashi, S., Orii, H., Watanabe, K., Agata, K. (1998) Identification of two distinct muscles in the planarian *Dugesia japonica* by their expression of myosin heavy chain genes. Zool. Sci. 15, 855–863.

Kobayashi, C., Saito, Y., Ogawa, K., Agata, K. (2007) Wnt signaling is required for antero-posterior patterning of the planarian brain. Dev Biol. 306(2),714-724.

Koshikawa, N., Giannelli, G., Cirulli, V., Miyazaki, K., Quaranta, V. (2000) Role of cell surface metalloprotease MT1-MMP in epithelial cell migration over laminin-5. J. Cell Biol. 148, 615-624.

Kuwahara, R., Hatate, H., Yuki, T., Murata, H., Tanaka, R., Hama, Y. (2009) Antioxidant property of polyhydroxylated naphthoquinone pigments from shells of purple sea urchin *Anthocidaris crassispina*. LWT - Food Science and Technology. 42 (7), 1296-1300.

Laemmli, U.K. (1970) Cleavage of structural proteins during the assembly of the head of bacteriophage T4. Nature. 227, 680-685.

Leclerc, M. (2000) Human kappa-like expression in the axial organ of the sea star *Asterias rubens* (Echinoderma). Eur J Morphol. 38(3), 206-207.

Leclerc, M., Bajelan, M. (1992) Homologous antigen for T cell receptor in axial organ cells from the asteroid *Asteria rubens*. Cell Biol. 16, 487-490.

Leclerc, M., Dupont, S., Ortega-Martinez, O., Hernroth, B., Krezdorn, N., Rotter B. (2011) Evidence of Kappa genes in the sea star *Asterias rubens* (Echinodermata). Immunol Lett. 138(2), 197-198.

Lenhoff, S.G:, Lenhoff, H.M. (1744) Hydra and the birth of experimental biology. Abraham Trembley´s Memoirs concerning the natural Hystory of a type of freshwater polyp with arms shaped like horns. Boxwood Press. Pacific Grove, 1986.

Li, C., Haug, T., Styrvold, O.B., Jørgensen, T.Ø., Stensvåg, K. (2008) Strongylocins, novel antimicrobial peptides from the green sea urchin, *Strongylocentrotus droebachiensis*. Dev Comp Immunol. 32(12), 1430-1440.

Lichtenfeld, J., Viehweg, J., Schutzenmeister, J., Naumann, W.W. (1999) Reissener´s substance expressed as a transient pattern in vertebrate floor plate. Anat Embryol. 200, 161-174.

Lim, M.S., Elenitoba-Johnson, K.S.J (2004) Proteomics in pathology research. Laboratory Investigation. 84, 1227–1244.

Llorens, F., Gil, V., del Río, J.A. (2011) Emerging functions of myelin-associated protein during development, neuronal plasticity, and neurodegeneration. The FASEB journal. 25, 463-475.

Lu, Z., Ghosh, S., Wang, Z., Hunter, T. (2003) Downregulation of caveolin-1 function by EGF leads to the loss of E-cadherin, increased transcriptional activity of β-catenin, and enhanced tumor cell invasion. Cancer Cell. 4, 499-515.

Maeda, M., Johnson, K. R., Wheelock, M. J. (2005) Cadherin switching: essential for behavioral but not morphological changes during an epithelium-to-mesenchyme transition. J. Cell Sci. 118, 873-887.

Makino, S., Whitehead, G.G., Lien, C.L., Kim, S., Jhawar, P., Kono, A., Kawata, Y., Keating, M.T. (2005) Heat-shock protein 60 is required for blastema formation and maintenance during regeneration. Proc. Natl Acad. Sci. USA 102, 14599–14604.

Mann, K., Poutka, A. J.; Mann, M. (2008) The sea urchin (*Strongylocentrotus purpuratus*) test and spine proteomes. Proteome Science. 6, 22.

Mann, K., Poutka, A. J.; Mann, M. (2010) Phosphoproteomes of *Strongylocentrotus purpuratus* shell and tooth matrix: identification of a major acidic sea urchin tooth phosphoprotein, phosphodontin. Proteome Science. 8(1), 6.

Mann, M., Højrup, P., Roepstorff, P. (1993) Use of mass spectrometric molecular weight information to identify proteins in sequence databases. Biol Mass Spectrom. 22(6), 338-345.

Mann, M., Jensen, O.N. (2003) Proteomics analysis of post-translational modifitications. Nature Biotech. 21, 255-261.

Mann, M., Wilm, M. (1994) Error-tolerant identification of peptides in sequence databases by peptide sequence tags. Anal. Chem. 66 (24), 4390–4399.

Margadant, C., Sonnenberg, A. (2010) Integrin–TGF-β crosstalk in fibrosis, cancer and wound healing. EMBO reports. 11, 97–105.

Martini, R., Schachner, M. (1988) Immunoelectron microscopic localization of neural cell adhesion molecules (L1, N-CAM, and myelin-associated glycoprotein) in regenerating adult mouse sciatic nerve. J. Cell Biol. 106, 1735–1746.

Martins, M.C., Ochoa-Mendes, V., Ferreira, G., Barbosa, J.N., Curtin, S.A., Ratner, B.D., Barbosa, M.A. (2011) Interactions of leukocytes and platelets with poly(lysine/leucine) immobilized on tetraethylene glycol-terminated self-assembled monolayers. Acta Biomater. 7(5), 1949-1955.

Martin-Villar, E., Megias, D., Castel, S., Yurrita, M. M., Vilaro, S., Quintanilla, M. (2006). Podoplanin binds ERM proteins to activate RhoA and promote epithelial-mesenchymal transition. J. Cell Sci. 119, 4541-4553.

Mashanov, V.S., Zueva, O.R., Garcia-Arraras, J.E. (2010) Organization of glial cells in the adult sea cucumber central nervous system. Glia. 58, 1581-1593.

Mashanov, V.S., Zueva, O.R., Heinzeller, T. (2008) Regeneration of the radial nerve cord in a holothurian: A promising new model system for studying post-traumatic recovery in the adult nervous system. Tissue and Cell. 40, 351-372.

Mashanov, V.S., Zueva, O.R., Heinzeller, T., Aschauer, B., Naumann, H.H., Grondona, J.M., Cifuentes, M., Garcia-Arraras, J.E. (2009) The central nervous system of sea cucumbers (Echinodermata: Holothuroidea) shows positive immunostaining for a chordate glial secretion. Frontiers in Zoology. 6 (11).

Mashanov, V.S., Zueva, O.R., Heinzeller, T., Dolmatov, I.Y. (2006) Ultrastructure of the circumoral nerve ring and the radial nerve cords in holothurians (Echinodermata). Zoomorphology. 125, 27-38.

Mashanov, V.S., Zueva, O.R., Rojas-Catagena, C., Garcia-Arraras, J.E. (2010) Visceral regeneration in a sea cucumber involves extensive expression of survivin and mortalin homologs in the mesothelium. 10, 117.

Matranga, V., Pinsino, A., Celi, M., Natoli, A., Bonaventura, R., Schroder, H.C., Müller, W.E. (2005) Monitoring chemical and physical stress using sea urchin immune cells. Prog. Mol. Subcell. Biol. 39, 85-110.

McCaffrey, L. M., Macara, I. G. (2009) Widely conserved signaling pathways in the establishment of cell polarity. Cold Spring Harbor Perspect. Biol. 1, a001370.

McGuire, P. G., Alexander, S. M. (1993) Inhibition of urokinase synthesis and cell surface binding alters the motile behavior of embryonic endocardial-derived mesenchymal cells in vitro. Development. 118, 931-939.

Medici, D., Nawshad, A. (2010) Type I collagen promotes epithelial-mesenchymal transition through ILK dependent activation of NF-kB and LEF-1. Matrix Biol. 29, 161-165.

Mendez, M.G., Kojima, S.-I., Goldman, R.D. (2010) Vimentin induces changes in cell shape, motility, and adhesion during the epithelial to mesenchymal transition. FASEB J., 24, 1838-1851.

Metchnikoff, E. (1891) Lectures on the comparative pathology of inflammation: delivered at the Pasteur Institute in 1981: Kegan Paul, Trench, Trubner and Co. Ltd.; 1893.

Michalopoulos, G.K., DeFrances, M.C. (1997) Liver regeneration. Science 276, 60-66.

Miguel-Ruiz, J.E.S., Maldonado-Soto, A.R., García-Arrarás, J.E. (2009) Regeneration of the radial nerve cord in the sea cucumber *Holothuria glaberrima*. BMC Developmental Biology. 9(3).

Miljkovic, M., Mazet, F., Galliot, B. (2002) Cnidarian and bilaterian promoters can direct GFP expression in transfected hydra. Dev. Biol. 246, 377–390.

Millott, N. (1969) Injury and the axial organ of echinoids. Experientia. 25: 756-757.

Minale, L., Pizza, C., Riccio, R., Zollo, F., Pure Appl. Chem. 1982, 54, 935-950.

Mizuta, I., Ogasawara, N., Yoshikawa, H., Sakoyama, Y. (1996) Identification of homeobox genes expressed during the process of rat liver regeneration after partial hepatectomy. Biochem. Genet. 34, 1-15.

Mladenov, P.V., Bisgrove, B., ASotra, S., Burke, R.D. (1989) Mechanisms of arm-tip regeneration in the sea star, *Leptasterias hexactis*. Roux´s Arch Develop Biol. 198, 19-28.

Molina, M.D., Salo, E., Cebria, F. (2007) The BMP pathway is essential for re-specification and maintenance of the dorsoventral axis in regenerating and intact planarians. Dev. Biol. 311, 79-94.

Monaghan, J.R., Epp, L.G., Putta, S., Page, R.B., Walker, J.A., Beachy, C.K., Zhu, W., Pao, G.M., Verma, I.M., Hunter, T., Bryant, S.V., Gardiner, D.M., Harkins, T.T., Voss, S.R. (2009) Microarray and cDNA sequence analysis of transcription during nerve-dependent limb regeneration. BMC Biol. 7, 1.

Moreno-Bueno, G., Portillo, F., Cano, A. (2008) Transcriptional regulation of cell polarity in EMT and cancer. Oncogene. 27, 6958-6969.

Morrison, J. I., Loof, S., He, P., Simon, A. (2006) Salamander limb regeneration involves the activation of a multipotent skeletal muscle satellite cell population. J. Cell Biol. 172, 433–440.

Mortensen, T. (1927) Handbook of the echinoderms of the British Isles. Oxford. Oxford University Press.

Moss, C., Hunter, A.J., Thordyke, M.C. (1998) Patterns of bromodeoxyuridine incorporation and neuropeptides immunoreactivity during arm regeneration in the starfish *Asterias rubens*. Phil. Trans. R. Soc. Lond. 353, 421-436.

Mount, J.G., Muzylak, M., Allen, S., Althnaian, T., McGonnell, I.M., Price, J.S. (2006) Evidence that the canonical Wnt signalling pathway regulates deer antler regeneration. Dev Dyn. 235(5), 1390-1399.

Multerer, K.A:, Smith, L.C. (2004) Two cDNAs from the purple sea urchin, *Strongylocentrotus purpuratus*, encoding mosaic proteins with domaisn found in factor H, factor I and complement components C6 and C7. Immunogenetics. 56 (2), 89-106.

Muños-Chápuli, R., Carmona, R., Guadix, J.A., Macías, D., Pérez-Pomares, J.M. (2005) The origin of the endothelial cells: na evo-devo approach for the invertebrate/vertebrate transition of the circulatory system. Evol Dev. 7, 351-358.

Murry, C.E., Soonpaa, M.H., Reinecke, H., Nakajima, H., Nakajima, H.O., Rubart, M., Pasumarthi, K.B., Virag, J.I., Bartelmez, S.H., Poppa, V., Bradford, G., Dowell, J.D., Williams, D.A., Field, L.J. (2004) Haematopoietic stem cells do not transdifferentiate into cardiac myocytes in myocardial infarcts. Nature. 428, 664-668.

Nelson, W. J. (2009) Remodeling epithelial cell organization: transitions between front-rear and apical-basal polarity. Cold Spring Harbor Perspect. Biol. 1, a000513.

Neuhoff, V., Harold, N., Ehrhardt, W. Improved staining of proteins in polyacrylamide gels including isoelectric focusing gels with clear background at nanogram sensitivity using Coomassie Brilliant Blue G-250 and R-250. Electrophoresis. 1988, 9, 255-262.

Nielsen, C. (1995) Animal evolution: Interrelationships of animal phyla. Oxford Univ. Press, Oxford.

Ogawa, K., Kobayashi, C., Hayashi, T., Orii, H., Watanabe, K., Agata, K. (2002) Planarian FGFR homologues expressed in stem cells and cephalic ganglions. Dev. Growth Differ. 44, 191–204.

Okada, T.S. (1996) A brief history of regeneration research—For admiring Professor Niazi's discovery of the effect of vitamin A on regeneration. J. Biosci. 21 (3), 261-271.

Oppenheim, R.W. (1991) Cell death during development in the nervous system. Annu Rev Neurosci. 14, 453-501.

Ortiz-Pineda, P.A., Ramírez-Gómez, F., Pérez-Ortiz, J., González-Díaz, S., Santiago-De Jesús, F., Hernández- Pasos, J., Valle-Avila, C.D., Rojas-Cartagena, C., Suárez-Castillo, E.C., Tossas, K., Méndez-Merced, A.T., Roig- López, J.L., Ortiz-Zuazaga, Z., García-Arrarás, J.E. (2009) Gene expression profiling of intestinal regeneration in the sea cucumber. BMC Genomics. 10, 262.

Owens, P., Han, G.W., Li, A.G., Wang, X.J. (2008) The role of Smads in skin development. J. Invest. Dermatol. 128, 783-790.

Ozdamar, B., Bose, R., Barrios-Rodiles, M., Wang, H.-R., Zhang, Y., Wrana, J. L. (2005) Regulation of the polarity protein Par6 by TGFβ receptors controls epithelial cell plasticity. Science. 307, 1603-1609.

Pappin, D.J., Hojrup, P., Bleasby, A.J. (1993) Rapid identification of proteins by peptide-mass fingerprinting. Curr Biol. 3, 327-332.

Patruno, M., McGonnell, I., Graham, A., Beesley, P., Carnevali, M.D.C., Thorndyke, M. (2003) Anbmp2/4 is a new member of the transforming growth factor-beta superfamily isolated from a crinoid and involved in regeneration. Proc Biol Sci. 270(1522), :1341-1347.

Patruno, M., Smertenko, A., Carnevali, C.M.D., Bonasoro, F., Beesley, P.W., Thorndyke, M.C. (2002) Expression of transforming growth factor β-like molecules in normal and regeneration arms of the crinoids *Antedon mediterranea*: immunocytochemical and biochemical evidence. Proc. R. Soc. Lond. B. Biol. Sci. 270, 1341-1347.

Penn, P.E. (1979) Wound healing in the tropical intertidal asteroid, *Napanthia belcheri* (Perrier). Amer. Zool. 19, 1006.

Perlson, E., Hanz, S., Ben-Yaakov, B., Segal-Ruder, Y., Seger, R., Fainziber, M. (2005) Vimentin-dependent special translocation of an activated MAP kinase in inured nerve. Neuron. 34, 715-726.

Perlson, E., Medzihradszky, K.F., Darula, Z., Munno, D.W., Syed, N.I., Burlingame, A.L., Fainzilber, M. (2004) Differential Proteomics Reveals Multiple Components in Retrogradely Transported Axoplasm After Nerve Injury. Molecular and cellular proteomics. 3, 510-520.

Perlson, E., Michaelevski, I., Kowalsman, N., Ben-Yaakov, K., Shaked, M., Seger, R., Eisenstein, M., Fainzilber, M. (2006) Vimentin binding to phophorylated Erk sterically hinders enzymatic dephosphorylation of the kinase. J. Mol. Biol. 364, 938-944.

Peterson, R. T., Link, B. A., Dowling, J. E., Schreiber, S. L. (2000) Small molecule developmental screens reveal the logic and timing of vertebrate development. Proc. Natl Acad. Sci. USA 97, 12965–12969.

Pinsino, A., Thorndyke, M.C., Matranga, V. (2008) Coelomocytes and post-traumatic response in the common sea star *Asterias rubens*. Cell Stress Chaperones 12, 331-341.

Pinsino, A.; Thorndyke, M.; Matranga, V. (2007) Coelomocytes and post-traumatic response in the common sea star *Asterias rubens*. Cell stress & chaperones. 12: 331-341.

Prendergast, R., Suzuki, M. (1970) Invertebrate protein stimulating mediators of delayed hypersensitivity. Nature, 227, 277-279.

Quinones, J.L., Rosa, R., Ruiz, D.L., García-Arrarás, J.E. (2002) Extracellular Matrix Remodeling and Metalloproteinase Involvement during Intestine Regeneration in the Sea Cucumber *Holothuria glaberrima*. Developmental Biology 250, 181-197.

Ramírez-Gómez, F., Aponte-Rivera, F., Mendez-Castaner, L., Garcia-Arraras, J.E. (2010) Changes in holothurian coelomocyte populations following immune stimulation with different molecular patterns. Fish Shellfish Immunol. 29, 175-185.

Ramírez-Gómez, F., García-Arrás, J.E. (2010) Echinoderm Immunity. Inv. Surv. J. 7, 211-220.

Raya, A., Koth, C.M., Buscher, D., Kawakami, Y., Itoh, T., Raya, R.M., Sternik, G., Tsai, H.J., Rodriguez-Esteban, C., Izpisua-Belmonte, J.C. (2003) Activation of notch signaling pathway precedes heart regeneration in zebrafish. Proc. Nat. Acad. Sci. U. S. A. 100 (Suppl 1), 11889–11895.

Reddien, P. W., Bermange, A. L., Murfitt, K. J., Jennings, J. R., Sánchez Alvarado, A. (2005a) Identification of genes needed for regeneration, stem cell function, and tissue homeostasis by systematic gene perturbation in planaria. Dev. Cell 8, 635–649.

Reddien, P. W., Oviedo, N. J., Jennings, J. R., Jenkin, J. C., Sánchez Alvarado, A. (2005b) SMEDWI-2 is a PIWI-like protein that regulates planarian stem cells. Science 310, 1327–1330.

Reddien, P. W., Sánchez Alvarado, A. (2004) Fundamentals of Planarian Regeneration. Annu. Rev. Cell Dev. Biol. 20, 725–757.

Reddien, P.W., Bermange, A.L., Kicza, A.M., Alvarado, A.S. (2007) BMP signaling regulates the dorsal planarian midline and is needed for asymmetric regeneration. Development 134, 4043-4051.

Richardson, P. M., and Issa, V. M. (1984) Peripheral injury enhances central regeneration of primary sensory neurons. Nature 309, 791-793.

Rinkevich, Y., Matranga, V., Rinkevich, B. (2009) Stem cells in aquatic invertebrates: Common premises and emerging unique themes. In: Rinkevich, B., Matranga. V. (eds.) Stem Cells in Marine Organisms: Springer Publishers. 61‑104.

Rishal, I., Fainzilber, M. (2010) Retrograde signaling in axonal regeneration. Experimental Neurol. 223, 5-10.

Roberts, A. B., Tian, F., Byfield, S. D., Stuelten, C., Ooshima, A., Saika, S., Flanders, K.C. (2006) Smad3 is key to TGF-β mediated epithelial-to-mesenchymal transition, fibrosis, tumor suppression and metastasis. Cytokine Growth Factor. Rev. 17, 19-27.

Roch, P.H. (1996) A definition of cytolytic responses in invertebrates. Adv. Comp. Environ. Physiol. 23, 114-150.

Roepstorff, P.; Fohlman, J. (1984) Proposal for a common nomenclature for sequence ions in mass spectra of peptides. Letter to the editors. Biological Mass Spectrometry. 11, 601.

Rojas-Cartagena, C., Ortiz-Pineda, P., Ramirez-Gomez, F., Suarez-Castillo, E.C., Matos-Cruz, V., Rodriguez, C., Ortiz-Zuazaga, H., Garcia-Arraras, J.E. (2007) Distinct profiles of expressed sequence tags during intestinal regeneration in the sea cucumber *Holothuria glaberrima*. Physiol. Genomics 31, 203-215.

Roux, M.M., Radeke, M.J., Goel, M., Mushegian, A., Foltz, K.R. (2008) 2DE identification of proteins exhibiting turnover and phosphorylation dynamics during sea urchin egg activation. Dev Biol. 313(2), 630-647.

Ruan, K., Bao, S., Ouyang, G. (2009) The multifaceted role of periostin in tumorigenesis. Cell Mol. Life Sci. 66, 2219-2230.

Ruppert, E. e Barnes, R. Invertebrate Zoology. Sixth Edition. s.l. : Harcourt, Inc., 1994.

Saatman, K.E., Creed, J., Raghupath, R. (2010) Calpain as a Therapeutic Target in Traumatic Brain Injury. Neurotherapeutics. 7(1): 31-42.

Sahly, I., Khoutorsky, A., Erez, H., Prager-Khoutorsky, M., Spira, M.E. (2006) On-line confocal imaging of the events leading to structural dedifferentiation of an axonal segment into a growth cone after axotomy. J. Comp. Neurol. 84, 1763-1769.

Santiago, P., Roig-Lopez, J.L., Santiago, C., Garcia-Arraras, J.E., 2000. Serum amyloid A protein in an echinoderm: its primary structure and expression during intestinal regeneration in the sea cucumber *Holothuria glaberrima*. J. Exp. Zool. 288, 335-344.

Santos, R., Haesaerts, D., Jangoux, M., Flammang, P. (2005) The tube feet of sea urchins and sea stars contain functionally different mutable collagenous tissues. The Jounal of Experimental Biology. 208, 2277-2288.

Satoh, A., Cummings, G.M.C., Bryant, S.V., Gardiner, D.M. (2010) Neurotrophic regulation of fibroblast dedifferentiation during limb skeletal regeneration in the axolotl (*Ambystoma mexicanum*). Dev. Biol. 337, 444-457.

Savy, S. (1987) Activity pattern of the sea star, *Marthasterias glacialis* in Port-Cros Bay (France, Mediterranean Coast). Marine Ecology. 8, 97-106.

Schapiro, J. (1914) Über die Regenationserscheinungen verchiedener Seestern Arten. Arch. Entw Mech. Org. 38, 210-251.

Schummer, M., Scheurlen, I., Schaller, C. Galliot, B. (1992) HOM/HOX homeobox genes are present in hydra (*Chlorohydra viridissima*) and are differentially expressed during regeneration. EMBO J. 11, 1815–1823.

Schwab, M.E. (2004) Nogo and axon regeneration. Curr Opin Neurobiol. 14, 118-124.

Sewell, M. A., Eriksen, S.; Middleditch, M. J. (2008) Identification of protein components from the mature ovary of the sea urchin Evechinus chloroticus (Echinodermata: Echinoidea). Proteomics. 8, 2531-2542.

Shibata, N., Umesono, Y., Orii, H., Sakurai, T., Watanabe, K., Agata, K. 1999. Expression of vasa (vas)-related genes in germline cells and totipotent somatic stem cells of planarians. Dev. Biol. 206, 73–87.

Shyne-Athwal, S., Chakraborty, G., Gage, G., Ingoglia, N.A. (1988) Comparison of post-translational modification by amino acid addiction after crush injury to sciatic and optic nerves of rats. Exp. Neurol. 99, 281-295.

Silver, J., Miller, J.H. (2004) Regeneration beyond the glial scar. Nature reviews. 5, 146-156.

Singh, O.V., Yaster, M., Xu, J.T., Guan, Y., Guan, X., Dharmarajan, A. M., Raja, S., N., Zeitlin, P.L., Tao, Y-X. (2009) Proteome of synaptosome-associated proteins in spinal cord dorsal horn after peripheral nerve injury. Proteomics. 9, 1241-1253.

Smith JE (1966) The form and function of the nervous system. In Boolootian RA (ed) Echinoderm physiology. Wiley, New York. 503–512.

Smith, A., Avaron, F., Guay, D., Padhi, B.K., Akimenko, M.A. (2006) Inhibition of BMP signaling during zebrafish fin regeneration disrupts fin growth and scleroblast differentiation and function. Dev. Biol. 299, 438-454

Smith, C.L.; Shih, C.S.; Dachenhausen, G. (1998) Coelomocytes express SpBf, a homologue of factor B, the second component in the sea urchin complement system. The journal of immunology, 161: 6784-6793.

Smith, J. E. (1936) On the Nervous System of the Starfish *Marthasterias glacialis* (L.). Philosophical Transactions of the Royal Society of London. 227, 111-173.

Smith, J. E. (1965) Structure and function in the nervous systems of invertebrates. [ed.] T.H., Horridge, G.A. Bullock. W.H. Freeman and Co. 1519-1558.

Smith, L.C., Gosh, J., Buckley, K.M., Clow, L.A., Dheilly, N., Haug, T., Henson, J.H., Li, C., Man, L., Majeske, A, J., Matranga, V., Nair, S., Rast, J.P., Raftos, D.A., Roth, M., Sacchi, S., Schrankel, C.S., Stesvag, K. (2011) Echinoderm immunity. In: Invertebrate Immunuty. Söderhall, K. (eds). Springer Verlag.

Smith, L.C., Rast, J.P., Brockton, V., Terwilliger, D.P., Nair, S.V., Buckley, K., Majeske, A.J. (2006) The sea urchin immune system. Inv. Surv. J. 3, 25-39.

Smith, M.M., Smith, L.C., Cameron, R.A:, Urry, L.A. (2008) The Larval Stages of the Sea Urchin, *Strongylocentrotus purpuratus*. Jornal of morphology. 269,713–733.

Smith, V.J. (1981) The echinoderms. In: Ratcliffe, N.A., Rowley, A.T. (eds) Invertebrate blood cells. London. Academic Press. 514-561.

Snider, W.D., Zhou, F.Q., Zhong, J., Markus, A. (2002) Signaling the pathway to regeneration. Neuron, 35, 13-16.

Sobkow, L., Epperlein, H. H., Herklotz, S., Straube, W. L., Tanaka, E. M. (2006) A germline GFP transgenic axolotl and its use to track cell fate: dual origin of the fin mesenchyme during development and the fate of blood cells during regeneration. Dev. Biol. 290, 386–397.

Steen, H., Mann, M. (2004) The ABC´s (and XYZ's) of peptide sequencing. Nat Rev Mol Cell Biol. 5, 699-711.

Stepniak, E., Radice, G. L., Vasioukhin, V. (2009) Adhesive and signaling functions of cadherins and catenins in vertebrate development. Cold Spring Harbor Perspect. Biol., 1, a002949.

Stoick-Cooper, C.L., Weidinger, G., Riehle, K.J., Hubbert, C., Major, M.B., Fausto, N., Moon, R.T. (2007) Distinct Wnt signaling pathways have opposing roles in appendage regeneration. Development 134, 479-489.

Strand, F.L., Rose, K.J., Zuccarelli, L.A., Kume, J., Alves, S.E., Antonawich, F.J., Garrett, L.Y. (1991) Neuropeptides hormones as neurotrophic factors, Physiol. Rev. 71, 1017-1046.

Suàrez-Castillo, E.C., Medina-Ortiz, W.E., Roig-Lòpez, J.L., Garcia-Arraras, J.E. (2004) Ependymin, a gene involved in regeneration and neuroplasticity in vertebrates, is over expressed during regeneration in the echinoderm *Holothuria glaberrima*. Gene. 334, 133-143.´

Sullivan, N. J., Sasser, A. K., Axel, A. E., Vesuna, F., Raman, V., Ramirez, N., Oberyszyn, T.M., Hall, B.M. (2009) Interleukin-6 induces an epithelial-mesenchymal transition phenotype in human breast cancer cells. Oncogene. 28, 2940-2947.

Sun, F., Cavalli, V. (2010) Neuroproteomics approaches to decipher neuronal regeneration and degeneration. Molecular and Cellular Proteomics. 9, 963-975.

Sun, L., Chen, M., Yang, H., Wang, T., Liu, B., Shu, C., Gardiner, D.M. (2011) Large scale gene expression profiling during intestine and body wall regeneration in the sea cucumber *Apostichopus japonicas*. Comparative Biochemistry and Physiology. Part D. 6, 195-205.

Sun, X.Q., Zheng, F.X., Zhang, J.X. (2005) Evisceration and regeneration in the holothurian. Period. Ocean Univ. Chin. 35, 719-724.

Swamynathan, S.K. (2010) Kruppel-like factors: three fingers in control. Hum.Genomics 4, 263-270.

Tanney, D.C., Feng, L., Pollack , A.S., Lovett, D.H: (1998) Regulated expression of matrix metalloproteinase and TIMP in nephrogenesis. Dev. Dyn. 213, 121, 129.

Technau, U., Bode, H. R. (1999) HyBra1, a Brachyury homologue, acts during head formation in Hydra. Development 126, 999–1010.

Thiery, J.P., Sleeman, J.P. (2006) Complex networks orchestrate epithelial–mesenchymal transitions. Nature reviews Molecular cell Biology. 7, 131-142.

Thorndyke, M.C., Carnevali, M.D.C. (2001a) Regeneration neurohormones and growth factors in echinoderms. Can. J. Zool. 79, 1171-1208.

Thorndyke, M.C., Patruno, M., Chen, W.C., Beesley, P.W. (2001b) In: Brain stem cells. Miyan, J., Thorndyke, M., Beesley, P.W., Bannister, C. (eds) BIOS Scientific, Oxford. 107-120.

Thorndyke, M.C., Patruno, M., Moss, C., Beesley, P.W., Patruno, M. (2001c) Cellular and molecular bases of arm regeneration in brittlestars. In: Barker, M. (ed), Echinoderms 2000: New Zealand. Balkema, Rotterdam. 323-326.

Thornton, C.S., and M.T. Thornton. 1970. Recuperation of regeneration in denervated limbs of Ambystoma larvae. J Exp Zool. 173, 293–302.

Thummel, R., Ju, M., Sarras Jr., M.P., Godwin, A.R. (2007) Both Hoxc13 orthologs are functionally important for zebrafish tail fin regeneration. Dev. Genes Evol. 217, 413-420.

Timmerman, L. A., Grego-Bessa, J., Raya, A., Bertran, E., Perez-Pomares, J. M., Diez, J., Aranda, S., Palomo, S., McCormick, F., Izpisúa-Belmonte, J.C., de la Pompa, J.L. (2004). Notch promotes epithelial-mesenchymal transition during cardiac development and oncogenic transformation. Genes Dev. 18, 99-115.

Tingjun, F., Xianyuan, F., Yutang, D., Wenjie, S., Shaofeng, Z., Jiaxin, L. (2011) Patterns and cellular mechanisms of arm regeneration in adult starfish *Asterias rollestoni* Bell. J. Ocean Unv. China. 10(3), 255-262.

Tsonis, P. A. (2000) Regeneration in vertebrates. Dev. Biol. 221, 273–284.

Umesono, Y., Watanabe, K., Agata, K. (1997) A planarian orthopedia homolog is specifically expressed in the branch region of both the mature and regenerating brain. Dev. Growth Differ. 39, 723–727.

Valentine, J. (1926) Regeneration in *Linckia*. Carnegie Instn. Washington. 25, 257-258.

Valles, A., Boyer, B., Tarone, G., Thiery, J. (1996) Alpha 2 beta 1 integrin is required for the collagen and FGF-1 induced cell dispersion in a rat bladder carcinoma cell line. Cell Adhes. Commun. 4, 187-199.

Vanden Bossche, J.P.; Jangoux, M. (1976) Epithelial origin of starfish coelomocytes. Nature. 261, 227-228.

Verling, E., Crook, A.C., Narnes, D.K.A., Harrison, S.S.C. (2003) Structural dynamics of a sea-star (*Marthasterias glacialis*) population. J. Mar. Biol. Ass. U.K. 83, 583-592.

Viehweg, J., Naumann, W., Olsson, R. (1998) Secretory radial glia in the ectoneural system of the sea star *Asterias rubens* (Echinodermata). Acta Zool. 79, 119-131.

Vincent, T., Neve, E.P., Johnson, J.R., Kukalev, A., Rojo, F., Albanell, J., Pietras, K., Virtanen, I., Philipson, L., Leopold, P.L., Crystal, R.G., de Herreros, A.G., Moustakas, A., Pettersson, R.F., Fuxe, J. (2009) A SNAIL1-SMAD3/4 transcriptional repressor complex promotes TGF-beta mediated epithelial-mesenchymal transition. Nat Cell Biol. 11(8), 943-950.

Wanami, L. S., Chen, H.-Y., Peiró, S., García de Herreros, A., Bachelder, R. E. (2008) Vascular endothelial growth factor-A stimulates Snail expression in breast tumor cells: implications for tumor progression. Exp. Cell Res. 314, 2448-2453.

Wang, S.P., Wang, W.L., Chang, Y.L., Wu, C.T., Chao, Y.C., Kao, S.H., Yuan, A., Lin, C.W., Yang, S.C., Chan, W.K., Li, K.C, Hong, T.M., Yang, P.C. (2009) p53 controls cancer cell invasion by inducing the MDM2-mediated degradation of Slug. Nat. Cell Biol. 11, 694-704.

White, J. A., Boffa, M. B., Jones, B., Petkovich, M. (1994) A zebrafish retinoic acid receptor expressed in the regenerating caudal fin. Development 120, 1861–1872.

Wilkie, I.C. (2001) Autotomy as a prelude to regeneration in echinoderms. Microsc. Res. Tech. 55, 369-396.

Wilkins, M.R., Sanchez, J.C., Gooley, A.A., Appel, R.D., Humphrey-Smith, I., Hochstrasser, D.F., Williams, K.L. (1996) Progress with proteome projects: why all proteins expressed by a genome should be identified and how to do it. Biotechnology and Genetic Engineering Reviews. 13, 19-50.

Witte, H., Bradke, F. (2008) The role of cytoskeleton during neuronal polarization. Curr Opinion Neurobiology. 18, 479-487.

Wolpert, L., Hicklin, J., Hornbruch, A. (1971) Positional information and pattern regulation in regeneration of hydra. Symp. Soc. Exp. Biol. 25, 391-415.

Woods, I.G., Wilson, C., Friedlander, B., Chang, P., Reyes, D.K., Nix, R., Kelly, P.D., Chu, F., Postlethwait, J.H., Talbot, W.S. (2005) The zebrafish gene map defines ancestral vertebrate chromosomes. Genome Res. 15, 1307–1314.

Wu, L.W., Mayo, L.D., Dunbar, J.D., Kessler, K.M., Baerwald, M.R., Jaffe, E.A., Wang, D., Warren, R.S., Donner, D.B. (2000) Utilization of distinct signaling pathways by receptors for vascular endothelial cell growth factor and other mitogens in the induction of endothelial cell proliferation. J. Biol. Chem. 275, 5096-5103.

Wu, W.S. (2006) The signaling mechanism of ROS in tumor progression. Cancer Metastasis Rev. 25, 695-705.

Xiao, K., Oas, R. G., Chiasson, C. M., Kowalczyk, A. P. (2007) Role of p120-catenin in cadherin trafficking. Biochim. Biophys. Acta. 1773, 8-16.

Xing, K., Yang, H.S., Chen, M.Y. (2008) Morphological and ultrastructural characterization of the coelomocytes in *Apostichopus japonicus*. Aquat. Biol. 2, 85-92.

Yamashita, S., Miyagi, C., Fukada, T., Kagara, N., Che, Y.-S., Hirano, T. (2004) Zinc transporter LIVI controls epithelial-mesenchymal transition in zebrafish gastrula organizer. Nature. 429, 298-302.

Yan, X., Liu, J., Luo, Z., Ding, Q., Mao, X., Yan, M., Yang, S., Hu, X., Huang, J., Luo, Z. (2010) Proteomic profiling of proteins in rat spinal cord induced by contusion injury. Neurochemistry International. 56, 971-983.

Yates III, J.R. (2000) Mass spectrometry from genomics and proteomics. Trends in Genetics. 16, 5-8.

Yates, J.R., Speicher, S., Griffin, P.R., Hunkapiller, T. (1993) Peptide mass maps — a highly informative approach to protein identification. Anal Biochem. 214, 397-408.

Yi, J. Y., Shin, I., Arteaga, C. L. (2005) Type I transforming growth factor beta receptor binds to and activates phosphatidylinositol 3-kinase. J. Biol. Chem. 280, 10870-10876.

Yiu, G., He, Z. (2006) Glial inhibition of CNS axon regeneration. Nature reviews-Neuroscience. 7, 617-627.

Yokoyama, H., Ide, H., Tamura, K. (2001) FGF-10 stimulates limb regeneration ability in *Xenopus laevis*. Dev. Biol. 233, 72–79.

Yokoyama, H., Ogino, H., Stoick-Cooper, C.L., Grainger, R.M., Moon, R.T. (2007) Wnt/beta-catenin signaling has an essential role in the initiation of limb regeneration. Dev Biol, 306(1), 170-178.

Yoshida, M. Physiology of Echinoderms. [ed.] Boolootian R.A. s.l.: Interscience, 1966. pp. 435-464. Photosensitivity.

Yun, S.S., Thorndyke, M.C., Elphick, M.R. (2007) Identification of novel SALMFamide neuropeptides in the starfish *Marthasterias glacialis*. Comp Biochem Physiol A Mol Integr Physiol. 147(2), 536-542.

Zavadil, J., Bottinger, E. P. (2005) TGF-b and epithelial-to-mesenchymal transitions. Oncogene. 24, 5764-5774.

Zhao, B., Wang, H., Lu, Y., Hu, J., Bao, L., Zhang, X. (2011) Transport of receptors, receptor signaling complexes and ion channels via neuropeptide-secretory vesicles. Cell Research. 21, 741-753.

Zhou, B. P., Deng, J., Xia, W., Xu, J., Li, Y. M., Gunduz, M., Hung, M.C. (2004) Dual regulation of Snail by GSK-3β-mediated phosphorylation in control of epithelial-mesenchymal transition. Nat. Cell Biol. 6, 931-940.

Zhu, H., Bilgin, M., Snyder, M. (2003) Proteomics. Annual Review of Biochemistry. 72, 783-812.

Zon, L.I. (2008) Intrinsic and extrinsic control of haematopoietic stem-cell self-renewal. Nature 453, 306-313.

Zuk, A., Hay, E. D. (1994) Expression of β1 integrins changes during transformation of avian lens epithelium to mesenchyme in collagen gels. Dev. Dyn. 201, 378-393.

10. Appendix 1

Exploring the proteome of an echinoderm nervous system: 2DE of the sea star radial nerve cord and the synaptosomal membranes subproteome.

Franco CF, Santos R, Coelho AV.

Proteomics. 2011 Apr;11(7):1359-64.

D 61519

PROTEOMICS

7'11

www.proteomics-journal.com

Animal Proteomics
Bioinformatics
Biomedicine
Cell Biology
Microbiology
Plant Proteomics
Technology

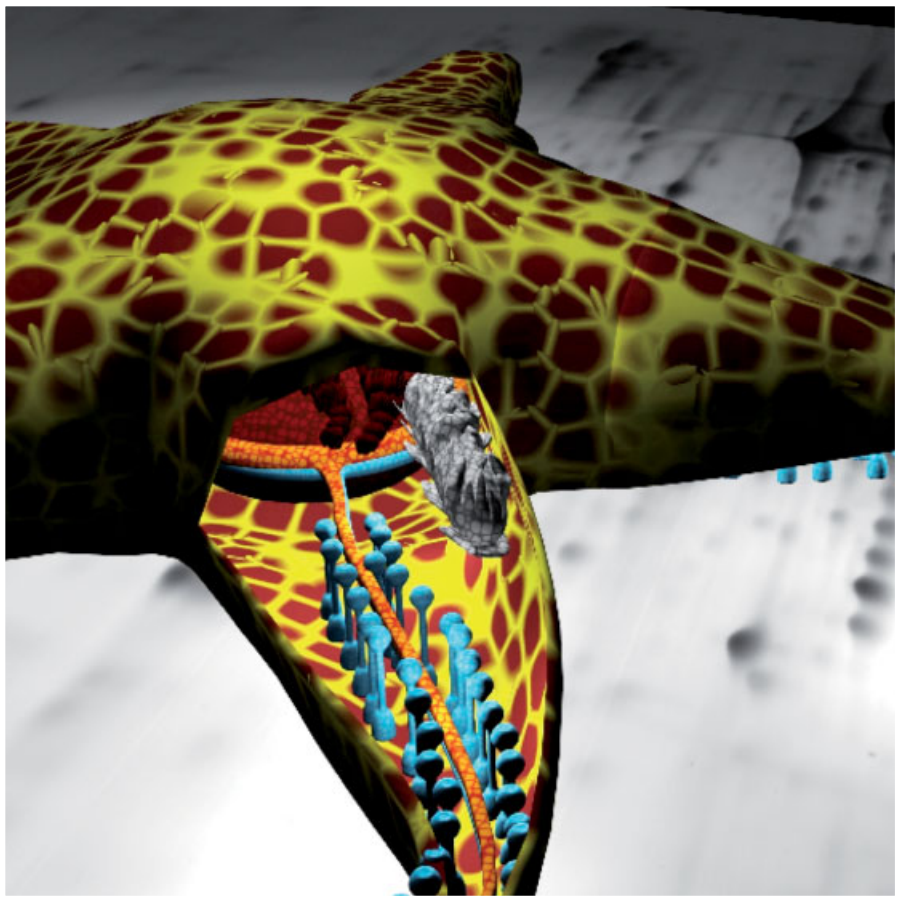

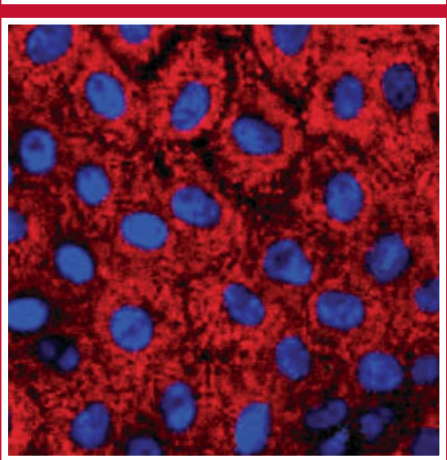

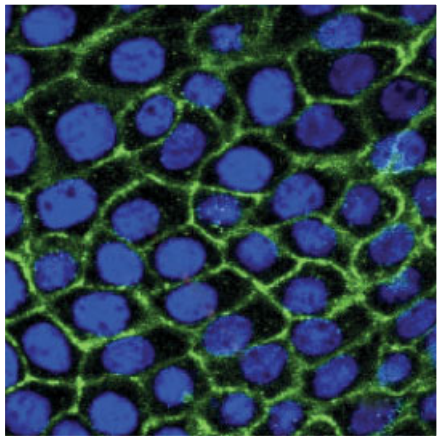

Endorsed as an Official Journal of HUPO
Human Proteome Organisation

WILEY-BLACKWELL

ISSN 1615-9853 · PROTC 11 (7) 1213–1370 (2011) · Vol. 11 · No. 7 · April 2011

DATASET BRIEF

Exploring the proteome of an echinoderm nervous system: 2-DE of the sea star radial nerve cord and the synaptosomal membranes subproteome

Catarina Ferraz Franco[1], *Romana Santos*[1,2] *and Ana Varela Coelho*[1]

[1] Instituto de Tecnologia Química e Biológica, Universidade Nova de Lisboa, Oeiras, Portugal
[2] Unidade de Investigação em Ciências Orais e Biomédicas, Faculdade de Medicina Dentária, Universidade de Lisboa, Portugal

Received: August 27, 2010
Revised: November 25, 2010
Accepted: December 29, 2010

We describe the first proteomic characterization of the radial nerve cord (RNC) of an echinoderm, the sea star *Marthasterias glacialis*. The combination of 2-DE with MS (MALDI-TOF/TOF) resulted in the identification of 286 proteins in the RNC. Additionally, 158 proteins were identified in the synaptosomal membranes enriched fraction after 1-DE separation. The 2-DE RNC reference map is available via the WORLD-2DPAGE Portal (http://www.expasy.ch/world-2dpage/) along with the associated protein identification data which are also available in the PRIDE database. The identified proteins constitute the first high-throughput evidence that seems to indicate that echinoderms nervous transmission relies primarily on chemical synapses which is similar to the synaptic activity in adult mammal's spinal cord. Furthermore, several homologous proteins known to participate in the regeneration events of other organisms were also identified, and thus can be used as targets for future studies aiming to understand the poorly uncharacterized regeneration capability of echinoderms. This ''echinoderm missing link'' is also a contribution to unravel the mystery of deuterostomian CNS evolution.

Keywords:
2-DE / Animal proteomics / MALDI-TOF/TOF / Radial nerve cord / Sea star / Synaptosomal membrane

The echinoderms (Phylum Echinodermata), as invertebrate deuterostomes, are one of the closest living relatives to vertebrates (Phylum Chordata), as they both belong to the superphylum Deuterostomia. Several reasons make these exceptionally well-adapted organisms very interesting animals to be studied: (i) their spectacular regenerative capability, including the nervous system [1–3]; (ii) their phylogenetic proximity to chordates (Fig. 1A) highlights them as alternative animal models for neurobiology which can contribute with a ''missing link'' of extreme importance to draw new theories on brain evolution.

Echinoderms present a neural organization that distinguishes them from other deuterostomes (chordates and hemichordates). In the adult echinoderm, the nervous system does not present a cephalized region, being composed by five radial nerve cords (RNCs) that derive from the circumoral nerve ring, a pentagonal nervous center that surrounds the mouth [4–6] (Fig. 1B). The integrity of the radial nerves and the circumoral nerve ring was shown to be essential for the reconstruction of their external body parts and internal organs [7].

Here, we present the first proteomic characterization of the RNC of an echinoderm, the sea star *Marthasterias glacialis*, as well of the synaptosomal membranes (SMs) subproteome. This first proteomic characterization of the nerve cord of an echinoderm is a significant step to

Correspondence: Dr. Ana Varela Coelho, Instituto de Tecnologia Química e Biológica, Universidade Nova de Lisboa, Av. da República – EAN, 2780-157 Oeiras, Portugal
E-mail: varela@itqb.unl.pt
Fax: +351-21441-1277

Abbreviations: RNC, radial nerve cord; **SM,** synaptosomal membrane enriched fraction; **SV,** synaptic vesicles

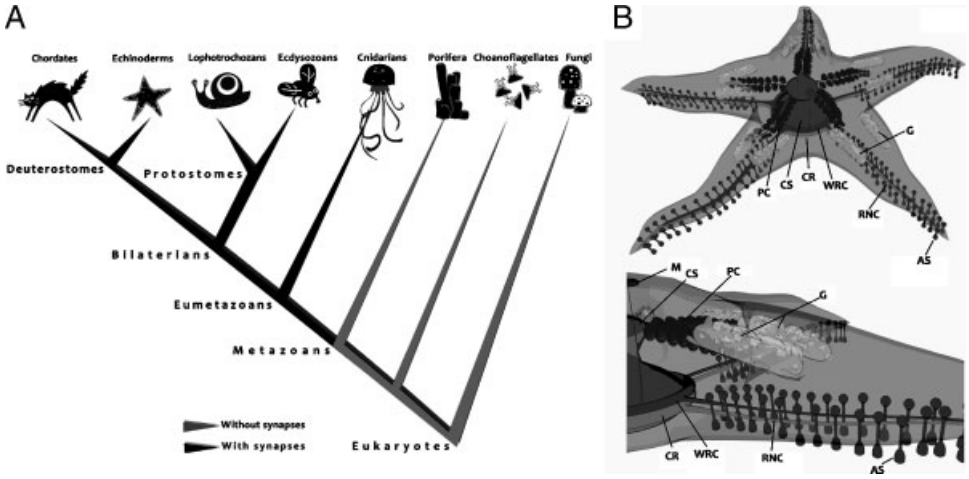

Figure 1. (A) Eukaryotes phylogeny. Phylogenic tree emphasizing the proximity between chordates and echinoderms. (B) Simplified diagrams of the anatomical organization of the sea star nervous system. Sea stars as all echinoderms have a radial symmetry, which means that each arm has an exact replica of all internal organs. Top: top view of an adult sea star (aboral side), and Down: lateral view of one sea star arm, show the organizational relationship between the nervous system and other internal organs. Nervous system: CR, circumoral nerve ring; RNC, radial nerve cord. Digestive system: CS, cardiac stomach; PC, pyloric caeca. Water vascular system: WRC, water ring canal; AS, ambulacrary system with tube feet; M, madreporite (controls entry of water into the water vascular system). Reproductive system: G, gonads.

withdraw them from the least studied metazoan nervous systems category and can be used as a starting point for future studies on neurobiology and organ regeneration and also to elucidate the role of this organism as a model animal, as the given results reveal an extensive homology between the echinoderm nervous system and the dorsal nerve cord of chordates.

Several adult specimens of the sea star *M. glacialis* (Linné, 1758) were collected at low tide on the west coast of Portugal (Estoril, Cascais) and kept at ''Vasco da Gama'' Aquarium (Dafundo, Oeiras) in open-circuit tanks with re-circulating seawater at 15°C and 33‰. They were fed ad libitum with a diet of mussels collected at the same site. Animals used for the experiments had similar sizes (21–26 cm measured between one arm tip and the most distant opposite one). Two RNCs were collected per animal as previously described [8].

Nerve cord proteome: For protein extraction, approximately 30 mg of the RNCs were homogenized with 100 μL of solubilization buffer (8 M urea, 2 M thiourea, 2% w/v CHAPS, 60 mM DTE) containing a complete protease inhibitor cocktail (Sigma, Portugal) and centrifuged at 10 000 × *g* for 15 min at 4°C to remove cellular debris. The protein concentration was determined using the 2D Quant Kit™ (GE Healthcare, Portugal). RNC protein extracts were subjected to 2-DE using an IPGphor system (GE Healthcare), 11 cm Immobiline pH 3–11 non linear DryStrip loaded with 400 μg total protein and 1% v/v of ampholytes in the rehydratation buffer (GE Healthcare) with a minor adaptation of the first dimension IEF program due to high salt content of sea star RNC (a total of 24 kV h starting with several step&hold constant voltages for 5 h and with a maximum end voltage of 4000 V). After a two-step equilibration of the strips for reduction and alkylation, the second dimension was performed in a Ettan DaltSix (GE Healthcare). The 24-cm gels containing two IEF strips were stained with Coomassie Blue Colloidal [9], scanned with LabScan (GE Healthcare) and analyzed with ImageMaster Platinum software (version 5.0; GE Healthcare). To characterize the nerve cord proteome of *M. glacialis*, ten 2-DE gels were run and a total of ten biological replicates were used. The spots selected for protein identification were present at least in half of the 2-DE gels and had a relative spot volume (%vol) above 0.05%.

SM proteome: The SM fraction was isolated as previously described [10, 11], with minor adaptations to sea star nervous tissue. Briefly, three RNCs (±40 mg) were homogenized in ice-cold TEVP buffer (10 mM Tris-HCl pH 7.4; 5 mM NaF; 1 mM Na_3VO_4; 1 mM EDTA; 1 mM EGTA) containing 320 mM sucrose and a complete protease inhibitor cocktail (Sigma). After large debris removal (1000 × *g* for 10 min) the obtained supernatant was centrifuged at 10 000 × *g* for 20 min in order to obtain a crude synaptosomal fraction which was subsequently lysed by hypo-osmotic shock and centrifuged at 25 000 × *g* for 30 min to pellet the SMs. For protein extraction, the SMs were solubilised in a buffer containing SDS (1%, w/v) and DTT (50 mM) and heated up to 60°C for 10 min to ensure complete solubilization of large protein complexes and then diluted to 0.5% w/v SDS and incubated in 1-DE sample buffer [12]. The SMs protein extract were loaded (25 μg total protein per lane) on 10% w/v acrylamide gels and stained with Coomassie Blue Colloidal [9]. Then, two gel lanes were excised for in-gel digestion.

The excised gel spots and bands were digested as previously described [13] and peptides were resuspended in 5% v/v formic acid (Supporting Information 1). Prior to MS analysis, tryptic peptides from the 2-DE gel spots were desalted and concentrated on chromatographic microcolumns using GELoader tips packed with POROS R2 (20 μm bead size) and the directly eluted onto the MALDI plate using 0.5 μL of 5 mg/mL α-CHCA in 50% v/v ACN with 2.5% v/v of formic acid. The tryptic peptides from the SM fraction gel bands, were subjected to an additional sequential stepwise elution from microcolumns packed with increasing hydrophobic material (POROS R2 (20 μm bead size), R3 (20 μm bead size) and activated charcoal) [14, 15] in order to overcome the limiting separating ability of 1-DE gels.

MS/MS was performed using a MALDI-TOF/TOF 4800 plus mass spectrometer (Applied Biosystems, Foster City, CA, USA). Raw data were generated by the 4000 Series Explorer Software v3.0 RC1 (Applied Biosystems) and contaminant m/z peaks resulting from trypsin autodigestion were excluded when generating the peptide mass list used for database search.

A detailed description of the protein identification workflow is given in Supporting Information 1. To overcome the lack of a complete sea star genome information, which impairs the success of protein identification, two different protein identification algorithms were used: PARAGON® provided with the ProteinPilot software (version 3.0, revision 114732; Applied Biosystems) and MOWSE® from MASCOT (version 2.2; Matrix Science, Boston, MA, USA), and three different protein sequence databases were used for protein identification. UniProt (Release 2010_06; 11 384 898 entries; European Bioinformatics Institute) joined with the purple sea urchin *Strongylocentrotus purpuratus* predicted protein database (42 420 entries; December 2006; ftp://ftp.ncbi.nih.gov/genomes/Strongylocentrotus_purpuratus/protein); and the non-redundant database Uniref100 (release 2010_06; 10 246 365 entries). Protein identification files derived from MASCOT were converted to mzML files using PRIDE Converter tool [16] and are available in the PRIDE database [17] under accession number 15331. Uncharacterized/unknown proteins and all *S. purpuratus* proteins were further submitted to protein-protein BLAST searches against Swiss-Prot database using Basic Local Alignment Search tool available at NCBI web site (http://blast.ncbi.nlm.nih.gov/). The false discovery rate (FDR) for each 2-DE spot and 1-DE band was determined using PSPEP algorithm from Protein Pilot search engine, using concatenated database joined with the reversed decoy database. Identified proteins were selected if a false discovery rate $<1\%$.

A mean value of 403 spots was detected per 2-DE gel of RNC (Fig. 2A) and after analysis a total of 339 spots were selected and processed for protein identification by MS (RNC 2-DE annotated reference gel available via the WORLD-2DPAGE Portal displaying also relevant information on all identified spots including protein identification data). Using the two identification algorithms and the selected protein databases, 286 spots were successfully identified (Supporting Information Tables ST1 and ST2) representing 84% of the selected spots. Searches using MASCOT resulted in the identification of 112 proteins in the UniProt/*S. purpuratus* databases and 126 proteins in the UniRef100 protein database (Supporting Information 1). Searches with ProteinPilot combining UniProt/*S. purpuratus* and UniRef100 databases produced 139 protein identifications. Altogether, approximately 200 non-redundant protein identifications were achieved (Supporting Information Table ST1). This high yield of protein identification was only possible using a protein identification workflow that comprised different databases and search algorithms (Supporting Information 1).

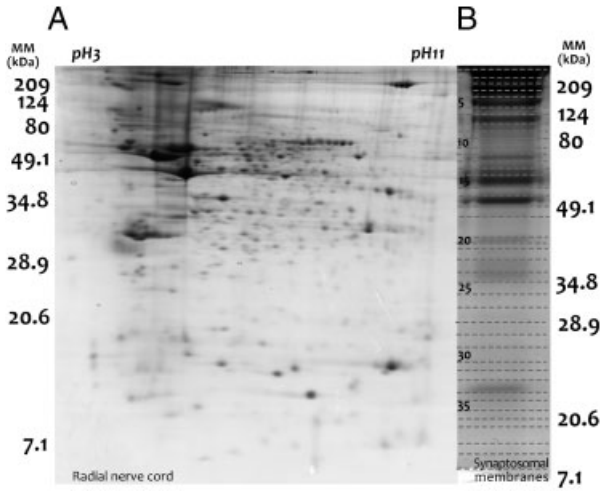

Figure 2. (A) 2-DE gel of the sea star *M. glacialis* RNC: Sea star nerve cord proteins were separated by p*I* using non-linear 3–11 11-cm IEF strips. For second dimension 12.5% SDS-PAGE gels were used to separate proteins according to their molecular masses. The complete annotated 2-DE gel image is present in Supporting Information Table ST2. (B) Synaptosomal-enriched fraction: 1-DE separation of the SM proteins using a 10% SDS-PAGE gel. The SM protein lanes were sliced for further processing as indicated in the figure (horizontal lines).

Since proteomic analysis of whole tissues is often unsuitable for the study of low-abundance proteins, a nerve subcellular fractionation was employed based on mammal nervous tissues protocols, in order to improve the proteomic characterization of sea star RNC through the enrichment in proteins specific of nerve physiological functions. Visible bands, mainly on the higher mass region of the gel, were excised for protein identification, while the remaining lane was sliced in order to identify, possible unstained low abundant proteins (Fig. 2B). The stepwise elution of the retained peptides using increments of ACN minimized the ion suppression effect and greatly increased the number of peptides detected by MALDI-TOF/TOF mass spectrometry. This fractionation resulted in the identification of 158

proteins, of which 38 are proteins that were not identified in the intact nerve (Supporting Information Tables ST3 and ST4).

Since a limited number of sea star proteins are deposited on the available protein sequence databases, the present study is a homology-driven proteomic characterization of *M. glacialis* RNC. STRAP software [18] was used to fully annotate the identified proteins using the UniProt gene ontology information. Three independent sets of ontology were used in the annotation: the biological function in which the protein participates (Fig. 3A), their subcellular location (Fig. 3B) and their molecular functions (Fig. 3C). However, since cellular pathways focus on physical and functional interactions between proteins rather than merely taking the gene-centric view of GO-based analyses, a pathway analysis using DAVID functional annotation tools (http://david.abcc.ncifcrf.gov/home.jsp) [19] was also performed and therefore a more comprehensive overview of the relevant functions enrolled by this tissue is also presented (Supporting Information Tables ST1 and ST3). The comparison of the subcellular localization and function of the identified synaptosomal proteins with the proteins identified in the intact nerve 2-DE gels showed that although the SM fractionation procedure was originally optimized for mammalian nerve tissues, it was also effective on echinoderms nerve tissues. As shown in Fig. 3A, among the identified proteins with known localization, approximately 15% of the proteins identified in the SM fraction are membrane-associated proteins, in contrast with the 6% found in the intact nerve cord. Nevertheless, some nuclear proteins (11%) persisted in the SM fraction. As for mitochondrial proteins they were totally absent in the SM fraction. In terms of biological functions (Fig. 3B), after the abundant constitutive proteins as expected due to the high cellular abundance of these classes [20] (cytoskeleton, 23%, and metabolic pathways, 6%), the majority of the identified proteins in the RNC are involved in synaptic vesicles (SVs) and protein transport (24%) or are G-protein modulators (15%). Proteins having a molecular transducing activity are also highly represented in the SM-enriched fraction with 12% as well as calcium binding proteins (10%). Proteasome proteins, which are known to regulate some pre-synaptic protein functions [21], were also found in the SM representing 6%.

The possible homology between the echinoderms nervous system and the chordate CNS is neither new nor

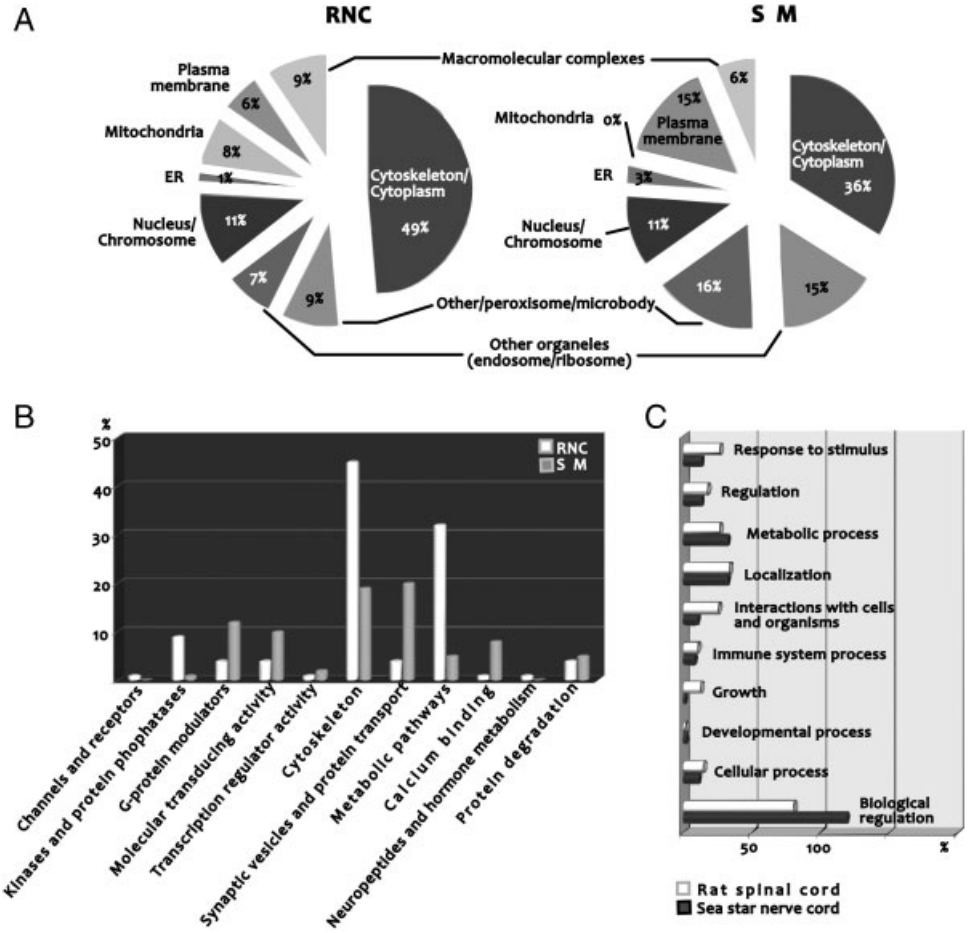

Figure 3. Gene ontology annotations of the identified sea star *M. glacialis* nerve cord proteins. Cellular localization (A) and biological function (B) of the identified proteins in the RNC (NC) and SMs-enriched fraction (SM). (C) Homology of rat spinal cord and sea star RNC proteins according to their biological function. Biological function distribution of the identified proteins in spinal cord of a vertebrate [25] and the RNC of an echinoderm, the sea star *M. glacialis*.

consensual [22–24]. It is still an issue of great debate since the major approaches to support these hypotheses rely mainly on information provided by comparative anatomy and morphological studies. In an effort to further clarify this persisting question, the biological functions of the identified proteins in sea star nervous system were compared with the described proteins from the spinal cord of a chordate [25]. In order to do so, all accession numbers of the rat spinal cord and sea star nervous tissue proteins were manually uploaded into STRAP software [18],] which was then used to annotate the identified proteins of both organisms according to gene ontology. This analysis revealed an important homology between the biological functions of the proteins described for rat and sea star nervous systems (Fig. 3C). Nevertheless, since this study is the first characterization of an echinoderm RNC proteome, more detailed and thorough studies should be performed before drawing new theories on CNS evolution.

A functional overview of the identified proteins in *M. glacialis* nervous system clearly highlights the functional complexity of echinoderms nervous system.

Synaptic transmission in echinoderms: Up to date no voltage-gated ion channels (VGIC) molecules have been described on echinoderms nervous tissues and our study is the first evidence that several of these channels, which are specially crucial in chemical synapses, are present. Evidence of membrane potentials generated by K^+; Ca^{2+} and Na^+ permeability is given, namely by the identification of a potassium channel, sodium/potassium-transporting ATPase and also several calcium-dependent proteins (e.g. Calmodulin; Calpain), showing evidence for calcium-based action potentials. Proteins responsible for the turnover of the neutransmitters glutamate and choline were also found. Several Rab GTPases, a multigene family that mediates targeting of intracellular vesicles to membranes, were also identified in the SM-enriched fraction (Supporting Information Table ST3). Among these is the Rab GDP dissociation inhibitor α, which in vertebrates is predominantly present in brain and neural/sensory tissues and Rab-3D, which is the major isoform that binds to SVs. The identified vesicle fusing ATPase is required for vesicle-mediated transport and is a cellular component of dendritic shaft and postsynaptic density. Electrical synapses (or neuronal gap junctions) are relatively simple compared to chemical ones and enable rapid impulse propagation [26]. However, these proteins appear to be encoded by distinct gene families unequally distributed among different animal phyla [27]. BLAST searches within the genome of the purple sea urchin failed to find representative genes of any of these proteins [28] and in agreement also no Gap junction proteins were identified in our study, which can be one more hint on the similarity between the RNC of echinoderms and spinal cord of chordates since the synaptic activity of adult mammal spinal cords relies essentially on chemical transmission. Other proteins involved in protein trafficking and transport among different compartments, as well as clathrin, one of the major proteins of SV, were also identified.

Neurogenesis and regeneration: One of the most interesting echinoderm capabilities is their amazing ability to fully regenerate body parts upon a traumatic injury, a natural trait also extended to their nervous system [1–3], a process that is at the present time far from being understood. Regeneration is seen at some point to be a recapitulation of the embryogenic pathways. Several proteins involved in neurogenesis with functions of axonal guidance, dentrite morphogenesis and neuron growth have been identified, namely calreticulin, dihydropyrimidinase and protein enabled. Proteins belonging to the *Wnt* signaling pathway, described as involved in the regeneration of the thickened wound epithelia in *Amphiura filiformis* [29], were also identified.

Sensory perception: Echinoderms lack evident light-sensitive organs; however, they respond to light, photoperiod and lunar cycles. Several proteins responsible for sensory perception were identified which further highlights the functional complexity of the echinoderm nervous system.

In summary, the many newly identified proteins in the nerve cord of *M. glacialis* are of extreme importance and highlight the potential of echinoderms as models to study CNS itself and its regeneration ability. The use of these animals as model systems, given their simpler morphology, easy manipulation, complex nervous system, can be a promising way to understand the molecular mechanisms involved in regeneration, which can then be transposed to find regeneration targets to be studied in other model organisms, namely mammals.

Protein identification data are available in the PRIDE database, accession number 15331.

This work was supported by Fundação para a Ciência e Tecnologia through a PhD grant to Catarina Franco (SFRH/BD/29799/2006), a research contract by the Ciência 2008 program to Romana Santos and a project grant (PTDC/MAR/104058/2008). We also acknowledge Dr. Patrick Flammang for scientific advice, Vasco da Gama Aquarium (Dafundo, Oeiras, Portugal), namely Dr. Fátima Gil and Miguel Cadete, for sea stars maintenance, Henrique Braga for the help with mussels collection and Dr. Renata Soares for paper revision.

The authors have declared no conflict of interest.

References

[1] Thorndyke, M. C., Patruno, M., Moos, C., Beesley, P., Cellular and molecular bases of arm regeneration in brittlestars, in: Barker, M. (Ed.) *Proceedings of the 10th International Echinoderm Conference*, Dunedin, 2000. AA Balkema, Rotterdam 2001, pp. 323–326.

[2] Thorndyke, M., Carnevali, C., Regeneration neurohormones and growth factors in echinoderms. *Can. J. Zool.* 2001, *79*, 1171–1208.

[3] Dupont, S., Thorndyke, M., Bridging the regeneration gap: insights from echinoderm models. *Nat. Rev. Genet.* 2007, *8*.

[4] Ruppert, E. E., Barnes, R. D., *Invertebrate Zoology*, 6th Edn, Saunders College Publishing, Philadelphia 1994.

[5] Smith, J. E., On the nervous system of the starfish *Marthasterias glacialis* (L.). *Philos. Trans. R. Soc. Lond.* 1936, *227*, 111–173.

[6] Smith, J. E., *Structure and Function in the Nervous Systems of Invertebrates*. T.H., Horridge, G.A. Bullock. W.H. Freeman and Co., San Francisco 1965, pp. 1519–1558.

[7] Carnevali, C., Bonasoro, F., Welsch, U., Thorndyke, M. C., Arm regeneration and growth factors in crinoids. Mooi, R., Telford, M. (Eds.), *Echinoderm*, Balkema, Rotterdam, 1998, pp. 145–150.

[8] Moss, C., Hunter, A., Thorndyke, M., Patterns of bromodeoxyuridine incorporation and neuropeptide immunoreactivity during arm regeneration in the starfish *Asterias rubens*. *Phil. Trans. R. Soc. Lond.* 1998, *353*, 421–436.

[9] Neuhoff, V., Harold, N., Ehrhardt, W., Improved staining of proteins in polyacrylamide gels including isoelectric focusing gels with clear background at nanogram sensitivity using Coomassie Brilliant Blue G-250 and R-250. *Electrophoresis* 1988, *9*, 255–262.

[10] Singh, O. V., Yaster, M., Xu, J., Guan, Y. et al., Proteome of synaptosome-associated proteins in spinal cord dorsal horn after peripheral nerve injury. *Proteomics* 2009, *9*, 1241–1253.

[11] Dunah, A. W., Standaert, D. G., Dopamine D1 receptor-dependent trafficking of striatal NMDA glutamate receptors to the postsynaptic membrane. *J. Neurosci.* 2001, *21*, 5546–5558.

[12] Laemmli, U. K., Cleavage of structural proteins during the assembly of the head of bacteriophage T4. *Nature* 1970, *227*, 680–685.

[13] Santos, R., Costa, G. C., Franco, C. F., Alves, P. G. et al., First insights into the biochemistry of the tube foot adhesive from the sea urchin *Parentrotus lividus* (Echinoidea, Echinodermata). *Mar. Biotechnol.* 2009, *11*, 686–698.

[14] Larsen, M. R., Cordwell, S. J., Roepstorff, P., Graphite powder as an alternative or supplement to reversed-phase material for desalting and concentration of peptide mixtures prior to matrix-assisted laser desorption/ionization-mass spectrometry. *Proteomics* 2002, *2*, 1277–1287.

[15] Gobon, J., Nordhoff, E., Migorodskaya, E., Ekman, R., Roepstorff, P., Sample purification and preparation technique based on nano-scale reversed-phase columns for the sensitive analysis of complex peptide mixtures by matrix-assisted laser desorption/ionization mass spectrometry. *J. Mass Spectrom.* 1999, *34*, 105–116.

[16] Barsnes, H., Vizcaino, J. A., Eidhammer, I., Martens, L., PRIDE converter: making proteomics data-sharing easy. *Nat. Biotechnol.* 2009, *27*, 598–599.

[17] Vizcaíno, J. A., Côté, R., Reisinger, F., Foster, J. M. et al., A guide to the Proteomics Identifications Database proteomics data repository. *Proteomics* 2009. *9*, 4276–4283.

[18] Bhatia, V. N., Perlman, D. H., Costello, C. E., McComb, M. E., Software tool for researching annotations of proteins: open-source protein annotation software with data visualization. *Anal. Chem.* 2009, *81*, 9819–9823.

[19] Da Wei Huang, D. W., Sherman, B. T., Lempicki, R. A., Systematic and integrative analysis of large genelists using DAVID bioinformatics resources. *Nat. Protoc.* 2009, *4*, 44–57.

[20] Petrak, J., Ivanek, R., Toman, O., Cmejla, R. et al., Déjà vu in proteomics. A hit parade of repeatedly identified differentially expressed proteins. *Proteomics* 2008, *8*, 1744–1749.

[21] Burré, J., Volknandt, W., The synaptic proteome. *J. Neurochem.* 2007, *101*, 1448–1462.

[22] Hagg, E. S., Echinoderm rudiments, rudimentary bilaterians, and the origin of the chordate CNS. *Evol. Dev.* 2005, *7:4*, 280–281.

[23] Nielsen, C., Homology of echinoderm radial nerve cords and the chordate neural tube?. *Evol. Dev.* 2006, *8:1*, 1–2.

[24] Hagg, E. S., Reply to Nielsen. *Evol. Dev.* 2005, *8:1*, 3–5.

[25] Gil-Dones, F., Alonso-Orgaz, S., Avila, G., Martin-Rojas, T. et al., Na optimal protocol to analyze the rat spinal cord proteome. *Biomark. Insights* 2009, *4*, 135–164.

[26] Zoidl, G., Dermietzel, R., On the search for the electrical synapse: a glimpse at the future. *Cell Tissue Res.* 2002, *310*, 137–142.

[27] Hervé, J. C., Phelan, P., Bruzzone, R., White, T. W., Connexins, innexins and pannexins: bridging the communication gap. *Biochim. Biophys. Acta* 2005, *1719*, 3–5.

[28] Burke, R. D., Angerer, L. M., Elphick, M. R., Humphrey, G. W. et al., A genomic view of the sea urchin nervous system. *Dev. Biol.* 2006, *300*, 434–460.

[29] Rychel, A. L., Swalla, B. J., Regeneration in Hemichordates and Echinoderms. In: Rinkevich, B., Matranga, V. (Eds.), *Stem Cells in Marine Organisms*. Springer, Netherlands, 2009, pp. 245–265.

Proteome characterization of sea star coelomocytes - The innate immune effector cells of echinoderms.

Franco CF, Santos R, Coelho AV.

Proteomics. 2011 Sep;11(17):3587-92.

DATASET BRIEF

Proteome characterization of sea star coelomocytes – The innate immune effector cells of echinoderms

Catarina F. Franco[1], Romana Santos[1,2] and Ana V. Coelho[1]

[1] Instituto de Tecnologia Química e Biológica, Universidade Nova de Lisboa, Oeiras, Portugal
[2] Unidade de Investigação em Ciências Orais e Biomédicas, Faculdade de Medicina Dentária, Universidade de Lisboa, Portugal

Received: November 22, 2010
Revised: April 19, 2011
Accepted: May 30, 2011

Sea star coelomic fluid is in contact with all internal organs, carrying signaling molecules and a large population of circulating cells, the coelomocytes. These cells, also known as echinoderm blood cells, are responsible for the innate immune responses and are also known to have an important role in the first stage of regeneration, i.e. wound closure, necessary to prevent disruption of the body fluid balance and to limit the invasion of pathogens. This study focuses on the proteome characterization of these multifunctional cells. The identification of 358 proteins was achieved using a combination of two techniques for protein separation (1-D SDS-PAGE followed by nanoLC and 2-D SDS-PAGE) and MALDI-TOF/TOF MS for protein identification. To our knowledge, the present report represents the first comprehensive list of sea star coelomocyte proteins, constituting an important database to validate many echinoderm-predicted proteins. Evidence for new pathways in these particular echinoderm cells are also described, and thus representing a valuable resource to stimulate future studies aiming to unravel the homology with vertebrate immune cells and particularly the origins of the immune system itself.

Keywords:
2-D SDS-PAGE / Animal proteomics / Coelomocytes / *Marthasterias glacialis* / nanoLC-MALDI-TOF/TOF MS / Sea star

Similarly to other invertebrates, echinoderms lack an acquired immune system and therefore do not express the lymphoid antibody producers' cell line responsible for the existence of immunoglobulins in vertebrates. Nevertheless, they have a very well-developed nonspecific and nonadaptive immune response that shows similarities to higher vertebrate innate immunity. This response is mediated by the circulatory cells that occupy the perivisceral coelomic cavities – coelomocytes, which are key players in clotting reactions, phagocytosis, oxygen transport, synthesis, and secretion of antibacterial and antifungal proteins [1–3] namely, hemolysins, agglutinins, and lectins [2, 4, 5].

Correspondence: Professor Ana V. Coelho, Instituto de Tecnologia Química e Biológica, Universidade Nova de Lisboa, Av. da República – EAN, 2780-157 Oeiras, Portugal
E-mail: varela@itqb.unl.pt
Fax: +351-21441-1277

Abbreviation: FDR, false discovery rate

Recently, the characterization of cDNA sequences from the purple sea urchin *Strongylocentrotus purpuratus* showed evidence for the homologies in the innate immune responses within the deuterostome lineage, which include echinoderms and vertebrates [6]. Sea urchins were shown to possess proteins homologous to the vertebrate C3 and factor B complement system components, called SpC3 and SpBf, respectively [6, 7]. These two proteins act together to promote opsonization of foreign cells and particles in sea urchins and subsequent destruction by the coelomocytes [7]. The level of complexity of echinoderm immune responses has been further demonstrated by the identification of several differentially expressed proteins in the coelomic fluid of sea urchins upon bacterial challenge, namely of proteins 185/333 which seem to be tailored to produce a pathogen-specific immune response and apextrin and calreticulin that seem to be involved in the sequestration or inactivation of bacteria [8–10].

In asteroids, coelomocytes have been reported to respond to trauma stress, having an important role in wound

closure, the first stage of regeneration. This is done by a rapid and massive accumulation of coelomocytes at the wound site, which plugs and heals the wound, helping to maintain homeostasis, thus preventing the loss of body fluids and limiting the invasion of pathogens [11–13]. At the molecular level, enhanced expression of profilin transcripts in coelomocytes has demonstrated the immune response of echinoderms to minimal injury [14].

Curiously, since the sequencing of the purple sea urchin, *S. purpuratus* genome, in 2006, [15], only a minority of the genome predicted proteins were validated by a few proteomic studies on echinoderms [8, 10, 16, 17], thus strengthening the need to verify and explore this rich source of information.

In the present study, several adult specimens of both genders of the sea star *Marthasterias glacialis* (Linné, 1758) were collected at low tide on the west coast of Portugal (Estoril, Cascais). Animals were transported to ''Vasco da Gama'' Aquarium (Dafundo, Oeiras) where they were kept in open-circuit tanks with recirculating seawater at 15°C and 33‰. They were fed ad libitum with a diet of mussels collected weekly at the same site. Animals used for the experiments had similar sizes, with radius ranging from 10 to 13 cm, measured from the largest arm to the centre of the oral disc.

To characterize the proteome of *M. glacialis* coelomocytes, the coelomic fluid of five sea stars was obtained by puncturing the animal epidermis at the arm tip with a needle and collecting the fluid by gravity into separate ice cold recipients, containing a protease inhibitor cocktail to prevent endogenous proteolysis. Then, low-speed centrifugation ($800 \times g$; 10 min; 4°C) was used to separate the circulating cells from the coelomic fluid.

The number of coelomocytes present in *M. glacialis* coelomic fluid was determined using a syringe with an anticoagulant to avoid clotting (1.2 mL paediatric syringes, S-Mono Vet Sarsted and 20Gx 1(1/2)' hypodermic needle, S-Mono Vet needle, Starsted). Cells were then counted using a Burker chamber, being comprised between 1 and 2×10^6 cell/mL which is in the range of the values reported for the sea star *Asterias rubens* [11].

For the proteomic experiments, pelleted coelomocytes were flash frozen in liquid N_2 and stored at −80°C until further processing. The deep frozen coelomocytes were then mechanically disrupted as described previously [18] and the resulting powder was resuspended in 1-D sample buffer [19] or 2-D solubilization buffer [20] (see Supporting Information 1 for a detailed description of all the procedures used). After cellular debris removal by a low-speed centrifugation ($1000 \times g$; 20 min, 4°C), the total protein concentration was determined using the 2D Quant Kit™ (GE Healthcare).

For 1-DE protein separation, 12.5% w/v acrylamide gels were loaded with 25 μg total protein per lane and stained with Colloidal Coomassie [21]. Then, gel lanes were sliced for in-gel digestion as shown in Fig. 1A.

Coelomocyte protein extracts were also subjected to 2-DE separation using an IPGphor system (GE Healthcare), 11 cm Immobiline pH 3–11 nonlinear DryStrip loaded with 400 μg total protein and 1% v/v of ampholytes (GE Healthcare) in the rehydration buffer. IEF was carried out with a minor adaptation due to high salt content of sea star coelomocytes. After a two-step equilibration of the strips for reduction and alkylation, the second dimension was performed in an Ettan DaltSix (GE Healthcare). The 24 cm gels containing two IEF strips were stained with Colloidal Coomassie [21] (Fig. 1B), scanned with LabScan (GE Healthcare), and analyzed with Progenesis SameSpots v.3.3 (Nonlinear Dynamics, Newcastle Upon Tyne, UK). To characterize the proteome of *M. glacialis* coelomocytes, five 2-D gels were run, each with the coelomocytes protein extract from one sea star. The spots were only selected for protein identification if they were present consistently in all analyzed 2-D gels. The excised 2-D gel spots and 1-D gel bands were digested as described previously [20] and the tryptic peptides were resuspended in 5% v/v formic acid.

Peptides from the 1-D gel digested bands were further separated with Proxeon Easy-nano-LC (Proxeon Biosystems, Odense, Denmark) using a C18 reversed-phase EASY-Column (10 cm, 75 μm id; Proxeon Biosystems). The obtained fractions were mixed with a solution of 5 mg/mL CHCA in 50% v/v ACN, 2.5% v/v formic acid, and deposited

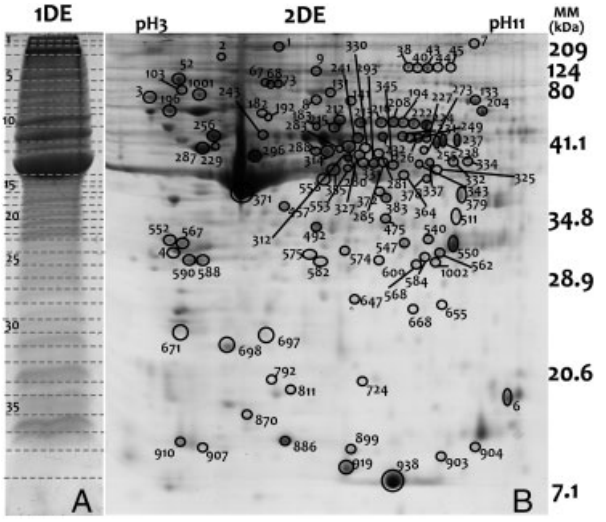

Figure 1. Gel separation of protein extract of the sea star *M. glacialis* coelomocytes by 1-D (A) and 2-D (B) electrophoresis. (A) Horizontal lines in the 1-D protein separation indicate the sections excised for in-gel tryptic digestion. See Supporting Information Material for the proteins identified in each band (Supporting Information Tables ST1 and ST3). (B) Black circles indicate spots with protein identification compliant with the specified criteria. The identified 2-D spots are annotated with numbers to facilitate a comprehensive reading of the Supporting Information material (Supporting Information Tables ST1 and ST2).

on a MALDI target plate using an online SunCollect automatic spotting system (SunChrom, Friedrichsdorf).

The tryptic digests from the 2-D gel spots were desalted and concentrated on chromatographic microcolumns using GELoader tips (Eppendorf) packed with POROS R2 (bead size, 20 μm) and directly eluted onto the MALDI plate using 0.5 μL of 5 mg/mL α-CHCA in 50% v/v ACN with 2.5% v/v formic acid.

Tandem MS was performed using a MALDI-TOF/TOF 4800 plus mass spectrometer (AB Sciex, USA). Raw data were generated by the 4000 Series Explorer Software v3.0 RC1 (AB Sciex) and contaminant *m/z* peaks resulting from trypsin autodigestion were excluded when generating the peptide mass list used for database search.

For the 2-D coelomocyte proteome characterization, in order to overcome the lack of a complete sea star genome information, which impairs the success of protein identification, two different protein identification algorithms were used: PARAGON® provided with the ProteinPilot software (version 3.0, revision 114732; AB Sciex) and MOWSE® from MASCOT (version 2.2; Matrix Science, Boston, MA, USA) and three different protein sequence databases were used for protein identification (Fig. 2). Protein identification files derived from MASCOT were converted to mzML files using PRIDE Converter tool [22] and are available in the PRIDE database [23] under accessions numbers 15332/15334.

For the nanoLC experiments regarding the tryptic digests from 1-D separation, peptides were identified using the algorithm PARAGON® provided with ProteinPilot software and the false discovery rate (FDR) was determined individually for each gel band using PSPEP algorithm supplied with this search engine, using the reversed and original database joined together. Identified proteins were selected if a FDR < 1%.

Protein clustering and parsimony analysis was performed using the MassSieve software [24] in order to reduce protein name redundancy. Protein isoforms were considered only if the unique peptide(s) were identified, and the lists of the identified proteins in both 1-D and 2-D experiments have all been compiled into the data set (Supporting Information Table ST1).

Sea star coelomocyte proteins identified as uncharacterized/unknown or homologous to *S. purpuratus* proteins were further submitted to protein–protein BLAST searches against Swiss-Prot database using the Basic Local Alignment Search tool available at NCBI website (http://blast.ncbi.nlm.nih.gov/). STRAP software [25] was used to fully annotate the identified proteins using the UniProt gene ontology information. Three independent sets of ontology were used in the annotation: the biological function in which the protein participates (Fig. 3A), their subcellular location (Fig. 3B) and their molecular functions (Fig. 3C). However, since cellular pathways focus on physical and functional interactions between proteins rather than merely taking the gene-centric view of GO-based analyses, a pathway analysis using DAVID functional annotation tools

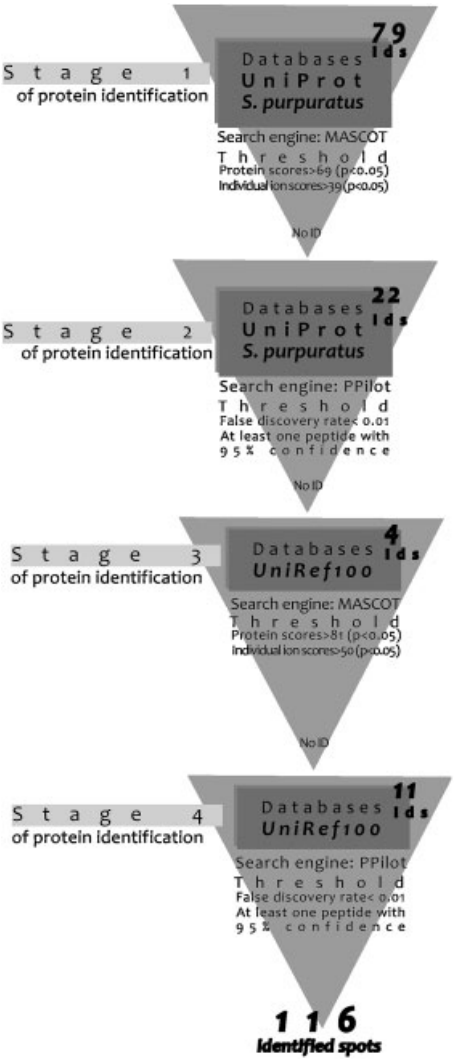

Figure 2. Coelomocytes 2-DE protein identification workflow. Schematic representation of the protein identification workflow using different search engines (MASCOT®, ProteinPilot®) and several protein databases : UniProt/Swiss-Prot (release 2010_04) joined together with the purple sea urchin *S. purpuratus* predicted database (42 420 entries; December 2006) and the nonredundant database Uniref100 (release 2010_06; 10 246 365 entries).

(http://david.abcc.ncifcrf.gov/home.jsp) [26] was also performed and a more comprehensive overview of the relevant functions enrolled by these cells is also presented (Supporting Information Table ST1).

The excised spots from the coelomocytes 2-D gels were processed for protein identification by MS and altogether, more than 85% of the selected spots were successfully identified (Supporting Information Table ST2) which was only possible using a protein identification workflow involving different databases and search algorithms. The coelomocytes reference 2-D map with the corresponding identified spots is shown in Fig. 1B, complemented by a

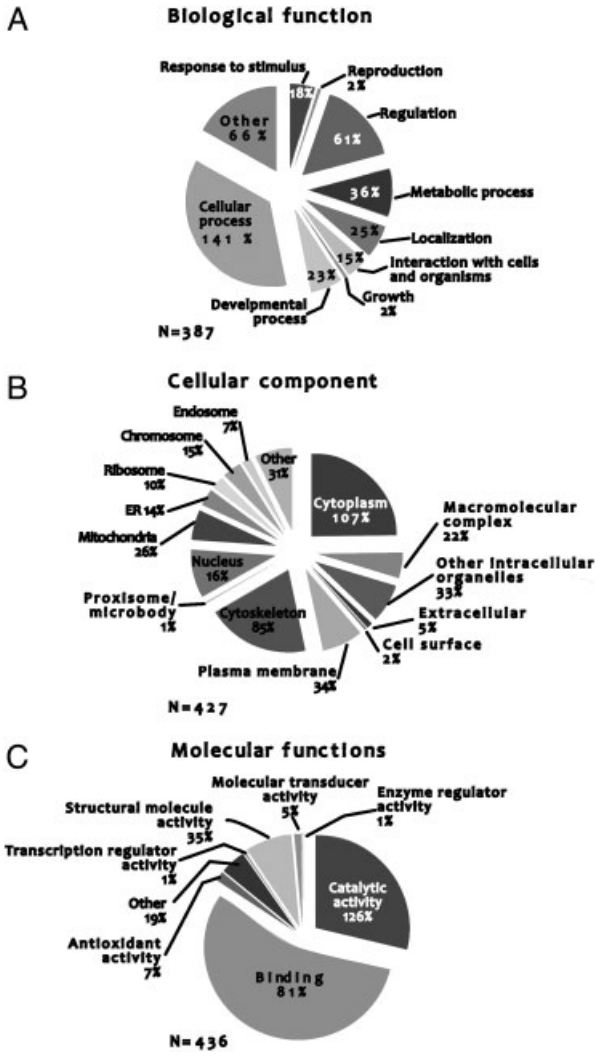

Figure 3. Gene ontology annotations of the identified sea star *M. glacialis* coelomocytes proteins. Biological functions (A) cellular component (B) and molecular functions (C).

detailed information on the number of identified proteins in each step of the described protein identification workflow shown in Fig. 2.

As in each 1-D band (Fig. 1A) there is a high probability of protein co-migration, an extra separation at the peptide level was also performed. This was achieved by injecting each band digest in a nano-flow HPLC coupled to a MALDI plate spotter. The peptides for each 1-D band were separated in one chromatographic run and the obtained 72 fractions per gel band were applied onto the MALDI sample plate. This approach, followed by database search using independent data for each band, allowed the identification of approximately six proteins per band from which were derived a total of 242 proteins with an estimated FDR of 1% (Supporting Information Table ST3).

The combination of two techniques for protein separation (1-D SDS-PAGE coupled with nanoLC and 2-D SDS-PAGE) followed by MALDI-TOF/TOF MS allowed the identification of 358 proteins, many constituting, to our knowledge, new assignments for echinoderm coelomocytes. Also, some of the identified proteins were present in more than one 2-D spot, indicating the presence of possible post-translational modifications or different protein isoforms that should be further investigated in order to obtain a more complete characterization of the coelomocytes proteome. Since only a few sea star proteins are deposited on the available protein sequence databases (1438 results for Asteroidea in UniProt of which only 58 are curated sequences), the present study is a homology-driven proteomic characterization. As expected, a high number of identified proteins were homologous with other echinoderm proteins deposited on the searched protein sequences databases (30%). However, several of the identified proteins from the sea star coelomocytes shared homology with proteins from other organisms (i.e. Chordata 34%; Nematode and Annelida 9%; Arthropoda 6%; Bacteria 6%), in some of the cases with only one identified peptide. This suggests the presence of novel forms of the proteins predicted in the sea urchin genome, which need to be further validated, and/or simply highlights the urgent need to increase the available information on genomes/proteomes of other echinoderm species.

A functional overview of the identified proteins in *M. glacialis* coelomocytes clearly highlights the multiple roles of these cells in the biology of echinoderms. The newly identified proteins provide preliminary evidence for several molecular pathways that have never been reported in coelomocytes of which some examples are described below:

Cytoskeleton regulation and cellular adhesion-related proteins: The phagocytic cell population (a dendritic-like coelomocyte phenotype) in *A. rubens* can perform a rapid morphological transition from petaloid to filipoidal shape [11]. In order for a cell to move and change shape, its cytoskeleton must undergo rearrangements that involve breaking down and reforming filaments. Two major pathways involved in these events are here revealed through several identified proteins. The first is the integrin signaling pathway, which is triggered when integrins in the cell membrane bind to extracellular matrix components causing downstream events such as actin reorganization and activation of MAPK and other signaling cascades [27]. The second pathway involves regulation by Rho GTPase, a family of key regulatory molecules that link surface receptors to the organization of the actin cytoskeleton. Also, several proteins which play a role in the regulation of cell adhesion and cytoskeleton organization were found: profilin, (already reported as being associated with changes in cell shape in the sea urchin coelomocytes [14]), ezrin; α-parvin, filamin A and C, several actin-binding and -capping proteins, clathrin-associated proteins and linker proteins.

Signaling, cellular regulation, and proliferation-related proteins: As coelomocytes secrete a number of regulating

factors into the coelomic fluid, the pathways that lie at the base of important biological events, like vesicular protein secretion mediated by G-protein receptor-activated pathways, were also represented through several identified proteins namely: clathrin heavy chain, AP-1 complex subunit μ, AP-2 complex subunit sigma, and ras-related protein Rab-11A. Moreover, several Ca^{2+}-binding proteins, such as calmodulin, calpain, calreticulin, and gelsolin were identified, indicating that like in other immune cell, calcium intracellular concentration is also an important second messenger in the signaling events [28] of echinoderm coelomocytes. Other regulatory proteins such as, cell division cycle and apoptosis regulator protein 1 LIM, senescent cell antigen-like-containing domain protein 2 and Rho-related GTP-binding protein RhoB were also found. Cell proliferation is tightly regulated by exposure to serum, growth factors, survival factors, and other cues from the cellular environment. This was shown to be the case also for coelomic fluid coelomocytes [1, 29, 30]. Several RAS family proteins and growth factors were also identified in this study, such as Ras-related proteins (e.g. Rab-10, Rab-6A, and Rab-7A) and the growth factor receptor-bound protein 2-B; LIM and senescent cell antigen-like-containing protein and the pre-B-cell colony-enhancing factor.

Regeneration-related proteins: Coelomocytes are involved in the very early stages of regeneration namely in the wound-healing phase [31], and the *wnt* genes have already been described as being involved in the formation of the thickened wound epithelia that is vital for regeneration in the echinoderm *Amphiura filiformis* [32]. Several proteins belonging to this pathway were also identified in the present study, namely, cAMP-dependent histone kinase and guanine nucleotide-binding protein subunit β-1.

Contrary to our expectations, no homologous proteins of the vertebrate complement system were identified. This suggests that to extend this proteomic characterization, new methodologies for the preparation of coelomocyte subcellular fractions, and the enrichment or depletion of low or abundant proteins will need to be developed. Nevertheless, the present study constitutes the first high-throughput proteomic characterization of echinoderm coelomic fluid-circulating cells, the coelomocytes. The newly identified coelomocyte proteins provide evidence for several unreported signaling pathways, eventually responsible for the diverse functions enrolled by these cells. Characterization of coelomocyte proteins post-translation modifications will further elucidate how the described pathways are being regulated. This comprehensive list of coelomocyte proteins is of extreme importance as a ground-work that will lead to future studies, which might clarify the homology with vertebrate immune cells or discover the pathways responsible for the coelomocytes functions during sea star regeneration events.

Protein identification files derived from MASCOT are available in the PRIDE database [23] under accession numbers 15332/15334.

This work was supported by Fundação para a Ciência e Tecnologia through a PhD grant to Catarina Franco (SFRH/BD/29799/2006), a research contract by the Ciência 2008 program to Romana Santos and a project grant (PTDC/MAR/104058/2008). The authors also acknowledge Vasco da Gama Aquarium (Dafundo, Oeiras, Portugal), namely Dr. Fátima Gil and Miguel Cadete, for sea stars maintenance. Acknowledgements are extended to Daniel Ettlin (Thermo UNICAM, Portugal) and Dr. Erik Verschuuren (Proxeon, Denmark) for providing the Nano-HPLC (Proxeon) and Gûnes Barka (SunChrom) for providing the automatic Spotter.

The authors have declared no conflict of interest.

References

[1] Cavey, M. J., Märkel, K. In: Harrison, F. W., Chia, F. S. (Eds.), *Microscopic Anatomy of Invertebrates. Echinodermata, vol. 14*, Wiley-Liss, New York 1994, pp. 169–245.

[2] Gross, P. S., Al-Sharif, W. Z., Clow, L. A., Smith, L. C., Echinoderm immunity and the evolution of the complement system. *Dev. Comp. Immunol.* 1999, *23*, 429–442.

[3] Haug, C. L. T., Stensvag, K., Antimicrobial peptides in echinoderms. *Invert. Surviv. J.* 2010, *7*, 132–140.

[4] Cervello, M., Arizza, V., Cammarata, M., Matranga, V., Parrinello, N., Properties of sea urchin coelomocytes agglutinins. *Italian J. Zool.* 1996, *63*, 353–356.

[5] Tahseen, Q., Coelomocytes: biology and possible immune functions in invertebrates with special remarkes on nematodes. *Int. J. Zool.* 2009, *2009*, 1–13.

[6] Al-Sharif, W. Z., Sunyer, J. O., Lambris, J. D., Smith, L. C., Sea urchin coelomocytes specifically express a homologue of the complement component C3. *J. Immunol.* 1998, *160*, 2983–2997.

[7] Smith, C. L., Shih, C. S., Dachenhausen, G., Coelomocytes express SpBf, a homologue of factor B, the second component in the sea urchin complement system. *J. Immunol.* 1998, *161*, 6784–6793.

[8] Dheilly, N. M., Nair, S. V., Smith, L. C., Raftos, D. A., Highly variable immune-response proteins (185/333) from the Sea Urchin, *Strongylocentrotus purpuratus*: proteomic analysis identifies diversity within and between individuals. *J. Immunol.* 2009, *182*, 2203–2212.

[9] Nair, S. V., Valle, H. D., Gross, P. S., Terwilliger, D. P., Smith, L. C., Macroarray analysis of coelomocyte gene expression in response to LPS in the sea urchin. Identification of unexpected immune diversity in an invertebrate. *Physiol. Genomics* 2005, *22*, 33–47.

[10] Dheilly, N. M., Haynes, P. A., Bove, U., Nair, S. V., Raftos, D. A., Comparative proteomic analysis of a sea urchin (*Heliocidaris erythrogramma*) antibacterial response revealed the involvement of apextrin and calreticulin. *J. Invert. Pathol.* 2011, *106*, 223–229.

[11] Pinsino, A., Thorndyke, M., Matranga, V., Coelomocytes and post-traumatic response in the common sea star *Asterias rubens*. *Cell Stress Chaperones* 2007, *12*, 331–341.

[12] Carnevali, C., Bonasoro, F., Microscopic overview of crinoid regeneration. *Microsc. Res. Tecnhiq.* 2001, *55*, 403–426.

[13] Holm, K., Dupont, S., Sköld, H., Stenius, A., Thorndyke, M., Hernroth, B., Induced cell proliferation in putative hematopietic tissues of the sea star, *Asterias rubens*. *J. Exp. Biol.* 2008, *211*, 2551–2558.

[14] Smith, L. C., Britten, R. J., Davidson, E. H., SpCoel1, a sea urchin profilin gene expressed specifically in coelomocytes in response to injury. *Mol. Biol. Cell.* 1992, *3*, 403–414.

[15] Consortium, Sea Urchin Sequencing. The genome of the sea urchin *Strongylocentrutus purpuratus*. *Science* 2006, *10*, 941–952.

[16] Mann, K., Poutka, A. J., Mann, M., The sea urchin (*Strongylocentrotus purpuratus*) test and spine proteomes. *Proteome Sci.* 2008, *6*, 22.

[17] Sewell, M. A., Eriksen, S., Middleditch, M. J., Identification of protein components from the mature ovary of the sea urchin *Evechinus chloroticus* (Echinodermata: Echinoidea). *Proteomics* 2008, *8*, 2531–2542.

[18] Butt, R. H., Coorssen, J. R., Pre-extraction sample handling by automated frozen disruption significantly improves subsequent proteomic analyses. *J. Proteome Res.* 2006, *5*, 437–448.

[19] Laemmli, U. K., Cleavage of structural proteins during the assembly of the head of bacteriophage T4. *Nature* 1970, *227*, 680–685.

[20] Franco, C., Santos, R., Coelho, V., Exploring the proteome of an echinoderm nervous system: 2-DE of the sea star radial nerve cord and the synaptosomal membranes subproteome. *Proteomics* 2011, *11*, 1359–1364.

[21] Neuhoff, V., Harold, N., Ehrhardt, W., Improved staining of proteins in polyacrylamide gels including isoelectric focusing gels with clear background at nanogram sensitivity using Coomassie Brilliant Blue G-250 and R-250. *Electrophoresis* 1988, *9*, 255–262.

[22] Barsnes, H., Vizcaino, J. A., Eidhammer, I., Martens, L., PRIDE converter: making proteomics data-sharing easy. *Nat. Biotechnol.* 2009, *27*, 598–599.

[23] Vizcaíno, J. A., Côté, R., Reisinger, F., Foster, J. M., et al., A guide to the Proteomics Identifications Database proteomics data repository. *Proteomics* 2009, *9*, 4276–4283.

[24] Slotta, D. J., McFarland, M. A., Markey, S. P., MassSieve: panning MS/MS peptide data for proteins. *Proteomics* 2010, *10*, 3035–3039.

[25] Bhatia, V. N., Perlman, D. H., Costello, C. E., McComb, M. E., Software tool for researching annotations of proteins: open-source protein annotation software with data visualization. *Anal. Chem.* 2009, *81*, 9819–9823.

[26] Da Wei Huang, D. W., Sherman, B. T., Lempicki, R. A., Systematic and integrative analysis of large genelists using DAVID bioinformatics resources. *Nat. Protoc.* 2009, *4*, 44–57.

[27] Yoo, Y., Guan, J.-L., Integrin signaling through focal adhesion kinase, in: LaFlamme, S. E., Kowalczyk, A. P. (Eds.), *Cell Junctions: Adhesion, Development, and Disease*. Wiley-VCH Verlag GmbH & Co. KGaA, Weinheim, Germany, 2008.

[28] Vig, M., Kinet, J. P., Calcium signaling in immune cells. *Nat. Immunol.* 2009, *10*, 21–27.

[29] Patruno, M., Thorndyke, M. C., Candia Carnevali, M. D., Bonasoro, F., Beesley, P. W., Growth factors, heat-shock proteins and regeneration in echinoderms. *J. Exp. Biol.* 2001, *204*, 843–848.

[30] Carnevali, C., Bonasoro, F., Welsch, U., Thorndyke, M. C., *Arm Regeneration and Growth Factors in Crinoids*, Mooi and Telford, San Francisco 1998, pp. 145–150.

[31] Coteur, G., DeBecker, G., Warnau, M., Jangoux, M., Dubois, P., Differentiation of immune cells challenged by bacteria in the common European starfish, *Asterias rubens* (Echinodermata). *Eur. J. Cell Biol.* 2002, *81*, 413–418.

[32] Dupont, S., Thorndyke, M., Bridging the regeneration gap: insights from echinoderm models. *Nat. Rev. Genetics* 2007, *8*, 1–4.

ITQB-UNL | Av. da República, 2780-157 Oeiras, Portugal
Tel (+351) 214 469 100 | Fax (+351) 214 411 277

www.itqb.unl.pt